vOX2- A potential immune regulatory protein involved in Kaposi's sarcoma-associated herpesvirus pathogenesis

Amanda Francine Brass

PhD

University of Edinburgh

2004

Declaration

I declare that this thesis has been composed by myself and has not been submitted for any other degree. The work described herein is my own except where otherwise indicated and all work of other authors is duly acknowledged.

Amanda Francine Brass
September, 2004

Laboratory for Clinical and Molecular Virology,
Department of Veterinary Pathology,
Royal (Dick) School of Veterinary Studies,
University of Edinburgh,
Summerhall Square,
Edinburgh, EH9 1QH

Acknowledgements

I would first like to thank my supervisors, Dr Simon Talbot and Dr Bernadette Dutia for their support and guidance throughout my studies. I thank Simon for always being there to help out and endless ideas of new experiments. I also wish to thank Bernadette for her sound advice and mastery of teaching even me (who is sometimes described as "*a bull in a china shop*"), delicate procedures. I must also acknowledge the help of Dr Susan Rhind, who taught me how decipher the countless histological images that I had to analyse.

A big thanks goes out to Jill, Lara, Maurice and Clem, the fellow-KSHV crew and the rest of the lab for all the appreciated help and practical expertise. I would also like to thank Billy, Christine and all the other members of staff lurking in the basement for their assistance during my many experiments with them.

Furthermore, I am immensely thankful for the support received from my family and friends near and far. Although not with me here in Edinburgh, Vanessa and Dennis have always been in my thoughts and encouraging me to persevere. A very special thanks to Charlie who has had to put up with all my ups and downs during the past few years, particularly the more turbulent past six months. I couldn't have made it without your encouragement and support – Thanks! Lastly, a massive thanks to Onnie for coffee breaks and making me just get on with it, in addition to not making home feel so far away.

Abstract

Kaposi's sarcoma-associated herpesvirus (KSHV), the newest member of the human herpesviruses, was first identified in 1994, and has been shown to be the etiological agent of Kaposi's Sarcoma (KS); a tumour most commonly associated with the onset of AIDS. KSHV is also involved in the development of other malignancies, including Multicentric Castleman's disease (MCD) and primary effusion lymphoma (PEL), both of which are B-cell lymphoproliferative disorders. The study of KSHV, as is the case with other herpesviruses from the *Gammaherpesvirinae* subfamily, is severely limited due to their species specificity and restricted growth *in vitro*. This has led to the increasing use of closely related murine gammaherpesviruses as a model system to study gammaherpesvirus pathogenesis.

A common feature of the gammaherpesviruses is their incorporation of cellular homologous genes during viral evolution, presumably aiding in viral replication and dissemination. One such gene found in KSHV is vOX2, which has homology with the human OX2 gene (hOX2, also recently termed CD200). There are also homologous genes found in mice (mCD200) and rats (rCD200). This membrane bound protein is expressed on a wide variety of cell types, excluding myeloid derived cells. Recent studies have indicated that CD200 plays an important regulatory role in macrophage and microglia activation, through its interaction with a receptor (CD200R) found to be expressed predominantly on macrophage and microglia.

Studies on the viral gene, vOX2, have indicated that this glycoprotein has a similar structure to the human CD200, an immunoglobulin superfamily gene, containing two extracellular domains, a single transmembrane region and a short cytoplasmic tail. In order to investigate the potential role of vOX2 in an *in vivo* system, a novel murid herpesvirus, murine gammaherpesvirus-76 (MHV-76), was utilised. MHV-76 is a natural deletion mutant of murine gammaherpesvirus-68 (MHV-68), lacking four unique genes and eight viral tRNA-like genes from the left end of the MHV-68 genome. This deletion has provided an opportunity to generate a recombinant MHV-76 virus expressing vOX2 (MHV76-vOX2) and a selectable

marker (EGFP-Hyg^R), thus allowing a functional study of vOX2 through the infection of mice. A control recombinant virus (MHV76-IRES) was also generated, which only expressed the selectable marker (EGFP-Hyg^R). The genomic structures of all recombinant viruses were verified by Southern blot analysis and the expression of the inserted genes was confirmed by northern blot analysis. The growth kinetics of MHV76-vOX2 and MHV76-IRES were compared with wild type MHV-76 in both an *in vitro* single-step and multi-step growth assay. The growth kinetics of the recombinant viruses was not significantly different from that of MHV-76.

In vivo studies have indicated that vOX2 has an effect on viral replication; a 10 to 100-fold increase in viral lung titres was observed in mice infected with MHV76-vOX2 compared to the control recombinant virus. Examination of lung sections showed that mice infected with the vOX2 recombinant virus elicited a strong influx of inflammatory cells, particularly peripheral mononucleocytes (PMN) and macrophages, resulting in perivascular and peribronchiolar inflammation. Unlike MHV-76, none of the recombinant viruses were able to establish latency in the spleen. Findings from infection of CD200 knock-out mice (C57BL/6 CD200$^{-/-}$) with MHV76-vOX2 support the possibility that vOX2 is playing an important immuno-regulatory role. These studies provide a starting point for further investigation of vOX2 and its potentially important role in KSHV pathogenesis.

Contents

List of Figures

List of Tables

Abbreviations

A	Adenosine
aa	Amino acid
AIDS	Acquired immunodeficiency syndrome
AlHV-1	Alcelaphine herpesvirus 1
AP	Alkaline phosphatase
APC	Antigen presenting cell
ATP	Adenosine triphosphate
BART	*Bam*HI A rightward transcripts
BCIP	5-bromo-4-chloro-3-indolyl phosphate
bcl-2	B-cell lymphoma/leukaemia 2
BHK	Baby hamster kidney
BHV-4	Bovine herpesvirus 4
BL	Burkitt's lymphoma
bp	Base pair
BSA	Bovine serum albumin
C	Cytidine
c	Prefix for cosmid DNA
CD	Cluster of differentiation
cDNA	Complementary DNA
CIA	Collagen-induced arthritis
CMV	Cytomegalovirus
CNS	Central Nervous System
CTL	Cytotoxic T lymphocyte
DAB	3,3' Diaminobenzidine
DMEM	Dulbecco's modified Eagle's medium
DNA	Deoxyribonucleic acid
DTT	Dithiothreitol
dATP	Deoxyadenosine triphosphate
dCTP	Deoxycytidine triphosphate
dGTP	Deoxyguanosine triphosphate

dNTP	Deoxynucleoside triphosphate
dTTP	Deoxythymidine triphosphate
dH_20	Distilled water
diH_20	De-ionised water (18 megohm)
ds	Double stranded
EAE	Experimental autoimmune encephalomyelitis
EBER	Epstein-Barr virus-encoded small RNA
EBNA	Epstein-Barr virus nuclear antigen
EBV	Epstein-Barr virus
E.coli	*Escherichia coli*
ECL	Enhanced chemiluminescence
EDTA	Ethylenediaminetetraacetic acid
EGFP	Enhanced green fluorescent protein
EHV-2	Equine herpesvirus 2
ER	Endoplasmic reticulum
FACS	Fluorescent activated cell sorting
FCS	Foetal calf serum
FITC	Fluorescein isothiocyanate
FLICE	FADD homologous ICE/CED-3-like protease
FLIP	FLICE-inhibitory protein
G	Guanosine
g or gp	Glycoprotein
GFP	Green fluorescent protein
G.I.	Gastrointestinal
GPCR	G protein-coupled receptor
GM-CSF	Granulocyte-macrophage colony stimulating factor
GMEM	Glasgow's modified Eagle's medium
GS	Glutathione sepharose
GST	Glutathione S-transferase
HBSS	Hank's buffered salt solution
HCMV	Human cytomegalovirus
HEPES	N'-[2-hydroxyethyl] piperazine-N'-[2-ethanesulphonic acid]

HHV	Human herpesvirus
His_6	Six consecutive histidine residues
HIV	Human immunodeficiency virus
HLA	Human leukocyte antigen
HSUR	Herpesvirus saimiri uRNA
HSV	Herpes simplex virus
HRP	Horseradish peroxidase
HVA	Herpesvirus ateles
HVS	Herpesvirus saimiri
ICAM	Intracellular adhesion molecules
IDO	Indo amine 2,3-dioxygenase
IE	Immediate early
IFN	Interferon
Ig	Immunoglobulin
IL	Interleukin
IM	Infectious mononucleosis
IPTG	Isopropyl-β-D-thiogalactopyranoside
IRES	Internal ribosomal entry site
kb	Kilobase
kDa	Kilodalton
KO	Knock-out
KS	Kaposi's sarcoma
KSHV	Kaposi's sarcoma associated herpesvirus
LANA	Latency associated nuclear antigen
LAT	Latency associated transcript
LB	Luria Bertani
LCL	Lymphoblastoid cell line
LCV	Lymphocryptovirus
LMP	Latent membrane protein
MCD	Multicentric Castleman's disease
MCF	Malignant catarrhal fever
MCS	Multiple cloning site

MG	Microglia
MHC	Major histocompatibility complex
MHV-68	Murine gammaherpesvirus 68
MHV-76	Murine gammaherpesvirus 76
MHV	Murine herpesvirus
MIP	Macrophage inhibitory protein
MLN	Mediastinal lymph node
MOG	Myelin oligodendrocyte glycoprotein
MOI	Multiplicity of infection
MOPS	3-[N-morpholino] propanesulphonic acid
MΦ	Macrophage
mRNA	Messenger RNA
MYX	Myxomavirus
NK	Natural killer
NBCS	Newborn calf serum
NBT	Nitro blue tetrazolium
NPC	Nasopharyngeal carcinoma
nt	Nucleotide
OD	Optical density
ORF	Open reading frame
Ori	Origin of replication
PAGE	Polyacrylamide gel electrophoresis
PBS	Phosphate buffered saline
PCR	Polymerase chain reaction
PEL	Primary effusion lymphoma
p.i.	Post-infection
PK	Protein kinase
PFU	Plaque forming unit
POD	Peroxidase
PTLD	Post-transplant lymphoproliferative disease
pv	Portal vein
RNA	Ribonucleic acid

RPMI	Rosewell Park Memorial Institute
RRV	Rhesus Rhadinovirus
RT	Room temperature
RT-PCR	Reverse transcriptase PCR
SDS	Sodium dodecyl sulphate
SSC	Standard saline citrate
STP	Saimiri transformation-associated protein
SV40	Simian vacuolating virus 40
T	Thymidine
TBE	Tris borate EDTA buffer
TBS	Tris buffered saline
TE	Tris EDTA buffer
TEMED	N, N, N',N'-tetraethylmethylenediamine
TIP	Tyrosine kinase interacting protein
TK	Thymidine kinase
TNF	Tumour necrosis factor
TPB	Tryptose phosphate broth
TRITC	Tetramethylrhodamine B isothiocyanate
U	Unit
U_L	Unique sequence of the long component of the genome
U_S	Unique sequence of the short component of the genome
UV	Ultraviolet light
v/v	Volume per volume
vbcl-2	Viral bcl-2 homologue
v-cyc	Viral cyclin D homologue
vFLIP	Viral FLICE-inhibitory protein homologue
vGPCR	Viral GPCR homologue
vIL	Viral interleukin homologue
vMIP	Viral macrophage inhibitory protein homologue
vOX2	Viral OX2 (CD200) homologue
vtRNA	Viral tRNA-like sequence
VZV	Varicella zoster virus

WT	Wild type
w/v	Weight per volume
YLDV	Yaba-like disease virus
X-gal	5-bromo-4-chloro-3-indolyl-β-D-galactoside

Chapter One: Introduction

1.1 *Herpesviridae*

Herpesviruses are highly disseminated in a wide range of organisms, including both vertebrates and invertebrates. At present there have been approximately 130 herpesviruses identified, however this is thought to be only a proportion of the number in existence with new members being discovered every year (Minson *et al.*, 2000). Herpesviruses are generally well adapted and ubiquitous within their host species, with over 90% of the human population infected with the Epstein Barr virus (EBV) and over 95% sero-positive for varicella-zoster virus (VZV). The ability of herpesviruses to establish latency and co-exist with the host organisms for life is the principal reason for its evolutionary success. In most circumstances, the virus remains dormant within the host, and in immunocompetent organisms rarely manifest into overt disease. However, a wide spectrum of diseases can result following infection of an alternative host species or due to a variety of external stimuli affecting the natural host, for example, immune suppression resulting from an organ transplant or infection with other viruses, exposure to UV or simply stress. This is illustrated when observing infection of an individual with varicella-zoster virus (VZV). Following primary infection which causes varicella, more commonly known as *chicken-pox*, VZV establishes lifelong latency in the dorsal root ganglia. Reactivation of the virus, commonly in elderly or immunocompromised individuals, leads to shedding of the virus, which may be asymptomatic but more commonly produces herpes zoster; a vesicular rash restricted to a dermatomal distribution, referred to as *shingles*. Acute reactivation of VZV can result in more severe acute pain that may progress to a chronic syndrome called *post-herpatic neuralgia* (PHN) (Arvin, 2001).

It is due to the ability of herpesviruses to maintain life long latency and the wide spectrum of diseases caused that has lead it to be the topic of much scientific research.

1.1.1 Characteristics of Herpesviruses

Traditionally, grouping of viruses in the family *Herpesviridae* was based on the architecture of the virion (Figure 1.1). The virion consists of a core containing a large linear double-stranded DNA enclosed within an icosadeltahedral capsid, approximately 100 to 110nm in diameter, comprised of 162 capsomeres. The nuclear capsid is surrounded by an amorphous tegument that is predominantly composed of viral proteins, and is enclosed by the viral envelope. The viral envelope is derived from the host cell membrane and incorporates numerous viral glycoprotein spikes that protrude from the surface where they play an important role in cell adhesion and virus entry.

Herpesvirus DNA genomes are linear and double stranded, however viral DNA circularises upon release from the capsid into the nucleus of infected cells and when in a latent form. Herpesvirus genomes range from 120 – 250kb, however variation between virion genome sizes of the same virus strain does occur. These differences are primarily due to the variation in copy number of reiterated terminal and internal repeat sequences, which can result in up to a 10kbp difference in genome length. Genome length can also vary due to spontaneous deletions, which has been known to occur in herpesviral strains of high-passage number, as observed in a laboratory strain of human cytomegalovirus, HCMV (Cha *et al.*, 1996). Herpesviruses can also be grouped on the basis of their arrangement of terminal and internal repeat sequences, illustrated in Figure 1.2.

All known herpesviruses share four major biological properties (Roizman and Pellett, 2001).

1. They possess several open reading frames (ORFs) that specify enzymes involved in nucleic acid metabolism (e.g. thymidine kinase), DNA synthesis (e.g. DNA polymerase), and protein processing (e.g. protein kinases).
2. Viral DNA synthesis and capsid assembly occurs in the nucleus.
3. Infected cells are destroyed following lytic replication (the production of infectious progeny).
4. All herpesviruses are able to remain latent in their natural host. During this latent stage, the viral genome forms a closed circular molecule, and only

limited subsets of viral genes are expressed. However, upon reactivation, the latent genome retains the capability to replicate and cause disease.

Although herpesviruses possesses several similarities in virion structure and some biological properties, such as the ability to establish latency, there are many differences in other aspects such as host range and disease pathogenesis. It is these differences that lead to dividing the herpesvirus family into subfamilies.

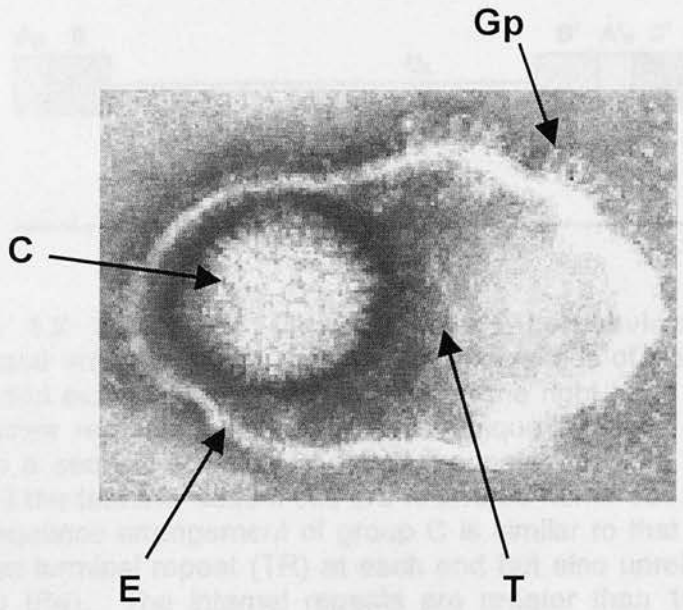

Figure 1.1 An electron micrograph image of a HSV-1 virion. The negatively stained virion shows the icosahedral capsid (**C**) surrounded by the tegument (**T**). The glycoprotein spikes (**Gp**) seen on the outer envelope (**E**) appears larger than normal due to being permeabilised during the staining process. Photograph taken by Linda Stannard and reproduced from the Big Picture Book of Viruses, available at http://www.virology.net/Big_Virology/BVDNAherpes.html

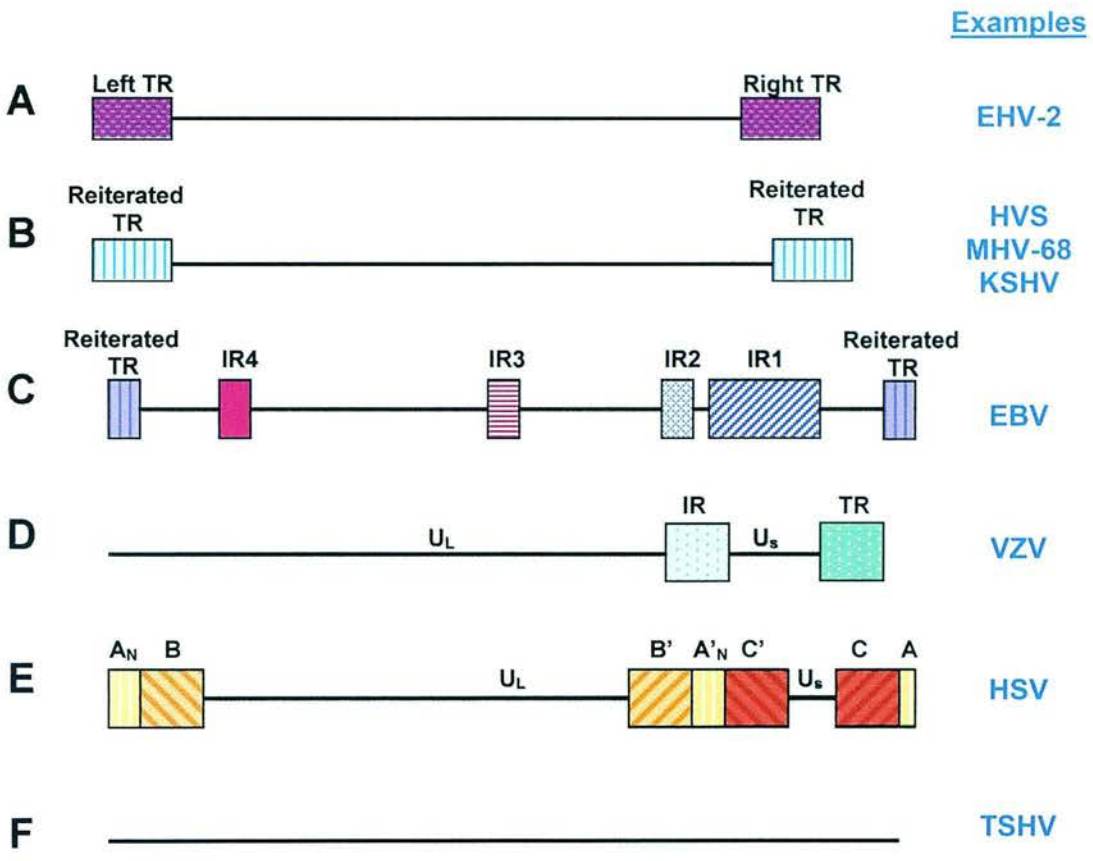

Figure 1.2 Schematic illustrations of herpesvirus family genomes sequence arrangements. There are six classes of genomes A, B, C, D, E and F and examples are given in blue on the right hand side. The horizontal black lines represent unique or quasi-unique regions. Viruses in group A contain a sequence which is directly repeated at both termini, where as in group B the terminal sequences are reiterated numerous times at both termini. The sequence arrangement of group C is similar to that of group B, in that it possess terminal repeat (TR) at each end but also unrelated internal repeats (IR1 to IR4). The internal repeats are greater than 100bp and divide the unique region of the genome into several well delineated sections. In group D **viruses the** repeat sequence at one terminus is repeated internally in an **inverted** orientation (IR). The genome in group E is comprised of one terminus containing N copies of sequence A that is next to sequence B. The other terminus has a single repeated sequence A next to sequence C. The A_N B and CA sequences are inserted in an inverted form internally (B'A_N'C'). The inverted internal sequences in groups D and E divide the genome into a long (U_L) and short (U_S) domain, which can invert relative to each other leading to the formation of two and four isomers of viral DNA, respectively. Group F viruses, such as tree shrew herpesvirus, TSHV, no repeat sequences have been identified. (Adapted from Roizman and Pellett, 2001).

1.1.2 Classification

Based on their biological properties, viruses in the *Herpesviridae* family were initially classified into three subfamilies; *Alphaherpesvirinae*, *Betaherpesvirinae* and *Gammaherpesvirinae* (see Table 1.1 for examples). Although, more recently, DNA sequence conservation is also taken into consideration with the identification of new viruses. A phylogenetic tree showing the relation of each herpesvirus sub-family is shown in Figure 1.3.

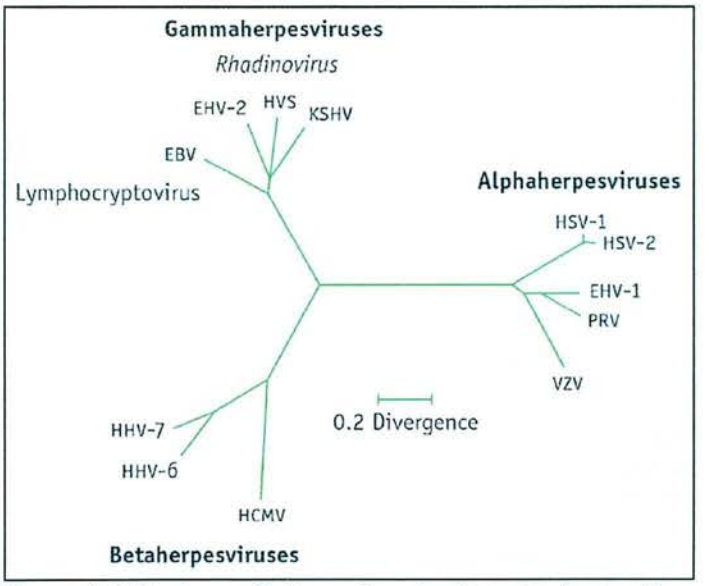

Figure 1.3 Phylogentic tree showing herpesvirus sub-families: Alapha-, Beta-, Gamma-herpesvirus.
(Image adapted from Talbot and Whitby, 1999)

1.1.2.1 The Alphaherpesvirus

Members of this subfamily characteristically have a variable host range, relatively short reproductive cycle, spread rapidly in culture, efficient destruction of infected cells, and capacity to establish latent infections, primarily in the sensory ganglia. There are several genera within this subfamily, including *Simplexvirus* (e.g. Herpes Simplex Virus-1, HSV-1), *Varicellovirus* (e.g.Varicella-zoster virus, VZV), *Marek's disease-like virus* and *Infectious laryngotracheitis-like virus*.

Table 1.1 Examples of herpesviruses and their associated diseases.

	Herpesvirus	Host	Disease(s)
Alphaherpesvirinae			
Simplexvirus	Herpes simplex virus-1	Human	Cold Sores, Keratitis
	Herpes simplex virus-2	Human	Genital lesions
	Bovine herpesvirus-1	Cow	Infectious rhinotracheitis, genital disease, abortions
Varicellovirus	Varicella zoster virus	Human	Chicken pox, shingles
	Equine herpesvirus-1	Horse	Abortion, neurological disease
	Porcine herpesvirus-1	Pigs	Aujeszky's disease
"Marek's disease-like viruses"	Marek's disease virus	Chicken	Marek's Disease
"ILTV-like viruses"	Infectious laryngotracheitis virus		
Betaherpesvirinae			
Cytomegalovirus	Human Cytomegalovirus	Human	Mononucleosis, Congenital deformities, Ocular disease
Muromegalovirus	Murine Cytomegalovirus	Mice	
Roseolovirus	Human herpesvirus-6	Human	Fever, Rash in infants
	Human herpesvirus-7	Human	
Gammaherpesvirinae			
Lymphocryptovirus	Epstein Barr virus	Human	Infectious mono-nucleosis, Burkitt's lymphoma, Nasopharyngeal carcinoma, PTLD, Hodgkin's disease
	Herpesvirus papio	Baboon	
	Herpesvirus pan	Chimpan-zee	
Rhadinovirus	Herpesvirus saimiri	Squirrel monkey	Fatal lymphoproliferative disease in cotton tail rabbit & new world monkeys e.g. marmosets
	Kaposi's sarcoma-associated herpesvirus	Human	Kaposi's sarcoma, Body cavity based lymphoma, Multicentric Castleman's disease
	Equine herpesvirus-2	Horse	? Respiratory illness
	Bovine herpesvirus-4	Cattle	? Conjunctivitis, mastitis
	Murine gamma-herpesvirus-68	Wood mouse	Lymphomas
	Rhesus monkey rhadinovirus	Rhesus monkey	Lymphoproliferative disease in immuno-suppressed host
	Herpesvirus aeteles	Spider monkey	Lymphomas in new world primates
	Alcelaphine herpesvirus-1	Wilde-beest	Malignant catarrhal fever in cattle, deer and other ruminants
	Ovine herpesvirus-2	Sheep	Malignant catarrhal fever in cattle, deer and other ruminants

1.1.2.2 The Betaherpesviruses

A large proportion of members in the Betaherpesvirus sub-family exhibit a restricted host range, long reproductive cycle and slow progression of infection in culture; infected cells often become enlarged (cytomegalia). Latency can be maintained in secretory glands, leukocytes, kidneys and other tissues. This sub-family contains the genera *Cytomegalovirus* (e.g. Human Cytomegalovirus, HCMV), *Muromegalovirus* (e.g. Murine Cytomegalovirus, MCMC) and *Roseolovirus* (e.g. Human Herpesvirus-6, HHV-6).

1.1.2.3 The Gammaherpesviruses

Unlike the other subfamilies, the members of the *Gammaherpesvirinae* are limited to the family or order to which the natural host belongs. Most members are able to replicate *in vitro* in lymphoblastoid cells, and some in epithelioid and fibroblastic cells. However viruses from this group are usually specific for either T or B-lymphocytes. Latent virus is commonly detectable in lymphoid tissue. There are two genera within this subfamily: *Lymphocryptovirus* (e.g. Epstein-Barr virus, EBV) and *Rhadinovirus* (e.g. Herpesvirus Saimiri, HVS, and Kaposi's Sarcoma-associated Herpesvirus, KSHV).

1.1.3 Herpesvirus Genes

The number of genes encoded by herpesviruses can vary from the smallest genome encoding 70, to the largest genome that encodes up to 200 genes. However, these numbers are likely to be underestimates due to alternative splicing, translational frameshifiting and the identification of new open reading frames (ORFs). Most herpesviruses transcripts are comprised of a single major ORF flanked by a 30-300bp 5' and 10-30bp 3' nontranslated sequence, a promoter/regulatory sequence upstream of a TATA box and a polyadenylation signal. The ORFs are typically located close to each other and often overlap, resulting in some regulatory sequences that are within the coding sequence of others. Transcription can occur in both directions with some ORFs being expressed that are situated entirely antisense to each other, such as HSV-1 $\gamma_1$34.5 and ORFs P and O (Lagunoff and Roizman, 1994).

The majority of herpesvirus genes are transcribed by RNA polymerase II and are not spliced. Nonetheless, every herpesvirus does have a small number of spliced genes, some of which are used to alter differential regulation of a gene during different stages of their life cycle. Some herpesviruses also encode noncoding RNAs, such as the EBERs of EBV and the tRNAs of the Murine Gammaherpesvirus-68 (MHV-68).

There are approximately 26 core genes found to be conserved within all subgroups from the herpesvirus family (Chee and Barrell, 1990). The conserved genes typically encode proteins involved in structural roles, such as the tegument, capsid and envelope, however some are also involved in DNA replication and nucleotide metabolism. Each of these genes are located within one of seven core gene blocks, which are conserved at the subfamily level. Most herpesviruses also possesses at least one gene of host orgin, with gammaherpesviruses encoding more cellular homologues than the other subgroups (Davison, 2002). These genes and other conserved genes within a subfamily may all play important roles in the virus' ability to infect and establish latency at a variety of levels ranging from inhibiting apoptosis to inducing or inhibiting host cell DNA replication, or immortalizing the host cell.

1.1.4 Herpesvirus Lifecycle

Following infection of a cell, there are two distinct routes a herpesvirus can undertake: lytic or latent. The lytic phase involves productive replication of the virus and release of the progeny with the ultimate destruction of the host cell. Whereas, latent infection results in the maintenance of the viral genome in a circular episomal form within the nucleus with limited expression of viral genes. The virus can maintain the latent state for long periods with no generation of progeny; in dividing cells the circular episome is amplified to give multiple copies per cell that are partitioned into daughter cells during mitosis (Sugden *et al.*, 1979). The viral genome retains the ability to undergo reactivation to a lytic form, usually triggered by a stimulus, however the precise mechanisms are not fully understood.

The majority of research has been performed on the α-herpesvirus prototype, HSV-1, and since many replication genes are conserved between herpesviruses the

general mechanisms can be applied to other herpesviruses. Therefore the following descriptions of the lytic stages of herpesvirus lifecycle will be primarily based on HSV-1, as reviewed by Roizman and Knipe (2001) and Whitley (2001). A schematic diagram of the infectious lifecycle of HSV-1 is outlined in Figure 1.4.

1.1.4.1 Lytic Replication

Initiation of viral infection commences with the attachment of the virus via its glycoproteins and the cell surface receptor, which in turn triggers fusion of the viral envelope with the plasma membrane. In the case of HSV-1, there are multiple attachment pathways including the interaction of viral glycoproteins gC and gB with cell surface-associated heparan sulphates (Shieh *et al.*, 1992). It is thought that the various pathways arose as a result of the different cell types that HSV-1 naturally infects (epithelial cells and neurons) and thus these receptors are partially responsible for determining tropism, pathogenicity and spread. Following the initial interaction, glycoprotein gD binds with one of several cellular co-receptors, including members of the tumour necrosis factor (TNF) receptor family and members of the immunoglobulin superfamily (IgSF) (Cocchi *et al.*, 1998; Montgomery *et al.*, 1996). The next stage is the fusion of the viral envelope with the host cell membrane, which is mediated by the viral glycoproteins gD, gB and gH/gL, a heterodimer. Most herpesviruses encode homologs to gB, gH and gL.

In contrast, EBV infection of B lymphocytes is mediated by binding of the EBV glycoproteins gp350/220 with the cellular receptor CD21 (Fingeroth *et al.*, 1984). EBV encodes a homologue of HSV gB, termed gp110, however it is not thought to have a similar function, as it does not localise on the viral envelope or cell surface (Gong *et al.*, 1987; Gong and Kieff, 1990). There are also homologues of gH (gp85) and gL (gp25) which form a complex; the gp85/gp25/gp42 complex is implicated in the penetration of EBV into the cell (Haddad and Hutt-Fletcher, 1989; Wang *et al.*, 1988).

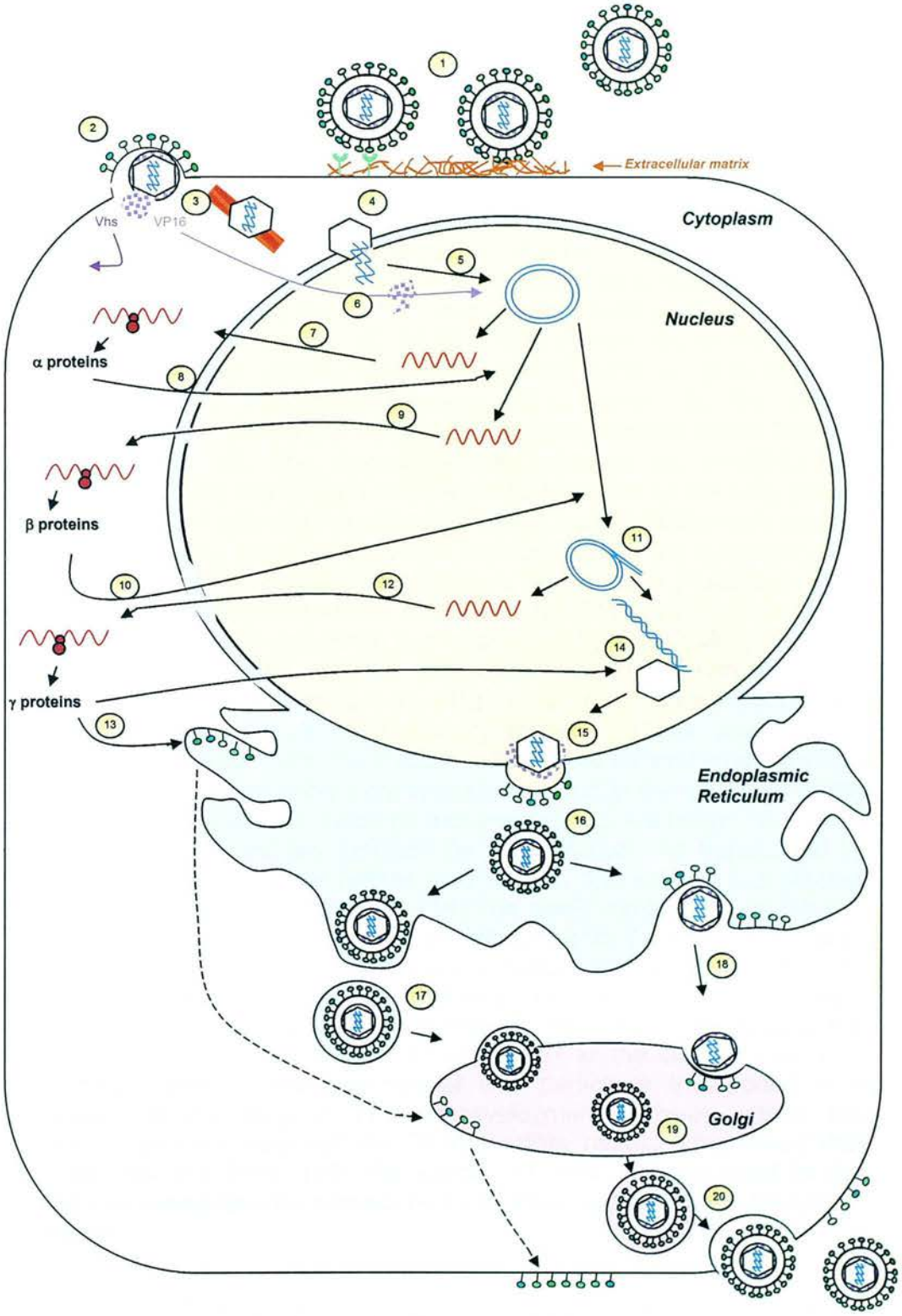

Figure 1.4 Lytic replication of HSV-1.
(Full legend on following page)

Figure 1.4 Lytic replication of HSV-1. Infection of a cell is initiated by (1) the binding of the virion to the extracellular matrix via the interaction of gB and gC with heparin sulphate and then gD with a cellular co-receptor. This is followed by (2) fusion of the viral envelope with the host cell membrane and uncoating of the virus, releasing the nucleocapsid and tegument proteins such as; VP16 and virion shutoff factor (Vhs). (3) The viral nucleocapsid attaches to microtubules and is transported to the nucleus where it (4) docks to a nuclear pore and releases the viral DNA. (5) Once in the nucleus the viral DNA immediately circularises. (6) VP16 is also transported to the nucleus where it interacts with the host transcriptional components to stimulate transcription of the immediate-early or α genes. (7) The mRNA transcripts are spliced and transported to the cytoplasm where they are translated. (8) The immediate-early proteins (α proteins) are transported into the nucleus to activate transcription of the early genes (β genes) and also regulate transcription of the immediate-early genes. (9) Early gene transcripts are also transported into the cytoplasm and translated. (10) The primary functions of the early proteins is DNA replication and production of substrates for DNA synthesis, and are present in both the cytoplasm and nucleus. (11) Viral DNA synthesis is initiated from viral origins of replication and produces long concatermeric DNA molecules. (12) Late or γ gene transcripts are generated and translated in the cytoplasm. These proteins are primarily involved in structural roles and required for viral assembly and egress. (13) Some of the γ proteins are involved in the formation of the virus envelope and are made on and inserted into the rough ER. These membrane proteins are modified by glycosylation and transported to the Golgi apparatus for further modification, and then to the plasma membrane of the infected cell. (14) The newly replicated viral DNA is packaged into the preformed capsids and (15) together with some tegument proteins, bud from the inner nuclear membrane into the ER, (16) acquiring an envelope containing precursors of viral envelope proteins. There are two schools of thought regarding the passage of the enveloped virus from the lumen of the ER to the cell surface; (17) luminal pathway, where enveloped viral particle is transported in a vesicle to the Golgi or (18) de-envelopment pathway, where the enveloped virus fuses with the ER from within, releasing the capsid that buds into the Golgi. (19) The enveloped virus is transported to the plasma membrane for release by exocytosis (20) into the extracellular space.

After fusion of HSV-1 to the cellular membrane, the virus is uncoated and the nucleocapsid is transported, by the microtubular network, to the nucleus where the viral DNA is released and immediately circularises (Mabit *et al.*, 2002). Tegument proteins are also liberated at this stage and are involved in several functions. Tegument protein VP16 augments basal level expression of genes and trans-activates the transcription of the immediate-early (IE) or α- viral genes by host cell RNA polymerase II, this in turn causes a cascade of gene trancription. In addition, VP16 is also an important structural protein of the virion (Whitley, 2001; Wysocka and Herr, 2003) and is involved in viral egress (Mossman *et al.*, 2000). The virion host shut-off (Vhs) protein causes non-specific degradation of mRNA and aids in determining levels and kinetics of viral and cellular gene expression. (Viral replication is relatively fast, approximately 8 hours, so is not as greatly affected by the destruction of mRNA compared to the host cell) (Everly *et al.*, 2002; Feng *et al.*, 2001).

IE genes were originally described as genes whose expression occurs in the absence of *de novo* protein synthesis, and in HSV-1 there are five genes: encoding for ICP0, ICP4, ICP22, ICP27 and ICP47. These genes are transcribed in the nucleus, spliced and then translated in the cytoplasm. Early genes (β genes) are differentiated from the IE genes by their requirement for protein synthesis for expression. ICP4 is involved in auto-regulation transcription of the early genes. The early genes are also translated in the cytoplasm and are involved in viral DNA replication, and include the major DNA binding protein (ICP8), thymidine kinase and DNA polymerase. The late genes, or γ genes, are not expressed until after the early proteins are generated, and require DNA replication for their expression. Late proteins primarily comprise the majority of the viral structural proteins required for viral assembly and egress. In addition, the late proteins also act as a self-regulatory control by down regulating transcription of both the immediate-early and early viral genes.

Replication of HSV-1 DNA requires seven gene products which include the viral DNA polymerase (U_L30) and processivity factor (U_L42), a single stranded DNA binding protein (U_L29), an origin-binding protein (U_L9), and a helicase-primase complex (U_L5, U_L8 and U_L52). Homologues of all of these gene products, except the origin-binding protein, have been identified in all three herpesvirus subfamilies.

Viral DNA synthesis occurs by a rolling circle mechanism (Garber *et al.*, 1993) that gives rise to head-to-tail concatamers of progeny viral DNA, which are cleaved into monomers. These monomers are then packaged into mature capsids within the nucleus (Deiss and Frenkel, 1986). Following encapsidation of viral DNA, the DNA-containing capsids transfer from the inner nuclear membrane into the lumen of the endoplasmic reticulum (ER) by budding. However, the subsequent route for viral envelopment and egress is not fully understood, with two proposed models. The luminal model, proposes that the enveloped virus in the ER is transported via exocytic vesicular transport to the Golgi where viral glycoproteins undergo final maturation, but the envelope has originated from the inner nuclear membrane. Vesicular movement to the cell surface then transports the mature virions to be released. The alternative theory is the de-envelopment model, in which the nucleocapsids lose their first envelope when fusing from the outer nuclear membrane-ER into the cytoplasm. The mature viral envelope is acquired when re-enveloped into the Golgi and then also trafficked by vesicular movement to the exterior of the cell. Several recent studies have found evidence to support the de-envelopment model. For example, the retention of the viral glycoproteins gH and gD in the ER prevents their incorporation into the viral envelope of the mature virions (Browne *et al.*, 1996; Skepper *et al.*, 2001; Whiteley *et al.*, 1999). In addition, differential ultracentrifugation found enveloped virions within the Golgi but not within other cellular compartments (Harley *et al.*, 2001). Ultrastructural studies have also suggested that this occurs with EBV as well as other alphaherpesviruses (Gong and Kieff, 1990; Granzow *et al.*, 2001).

1.2.1.2 Latency

Latency can be described as a state when the viral genome is maintained intact and genetically identical to an infectious particle, but without the highly regulated gene-expression cycle cascade. The ability to establish latency is a characteristic of all herpesviruses studied to date and any transcription that does occur is usually drastically reduced. Latency can be described as having three phases: establishment, maintenance and reactivation.

Establishment entails the entry of the virus into the appropriate cell; while at the same time suppresses viral gene expression, so as not to arouse the normal cytopathic results generated during productive infection. Following this, viral genomes need to persist and provide a reservoir of potential infectious particles in the event of reactivation. This is not a big issue for viruses such as HSV-1, which establishes latency in sensory neurons, as they are non-replicating cells and the virus can remain entirely dormant; thus requiring minimal viral gene expression. On the other hand, EBV establishes latency in dividing lymphatic cells and most transcription activity that occurs is in relation to ensuring the maintenance of viral genomes in dividing cells, immune evasion and ensuring that the infected cells do not undergo apoptosis.

Gene expression during latency is limited and not conserved across the subfamilies. As previously mentioned, HSV-1 latency could occur without gene expression, however there is production of a single transcript, termed the latency-associated transcript (LAT). The LAT mRNA is spliced and a number of small ORFs (O and P) have been detected (Lagunoff and Roizman, 1994). Studies on mutant viruses lacking LAT found increased levels of expression of the immediate-early, early and late genes when compared to the rescued or wild-type viruses (Garber *et al.*, 1997), therefore suggesting that LAT may be down-regulating expression of the lytic gene expression cycle. This idea is still unclear as more recent findings by Burton *et al.* (2003) seem to suggest otherwise. It has been demonstrated that expression of just the first 1.5kb of the 8.3kb-LAT-gene is able to inhibit apoptosis and enhance spontaneous reactivation of the virus (Jin *et al.*, 2003; Peng *et al.*, 2003). Alternatively, VZV establishes latency in trigeminal and dorsal root ganglia, and at least five ORFs (4, 21, 29, 62, 63) are transcribed during latent infection (Cohrs *et al.*, 1996; Kennedy *et al.*, 1990).

By comparison to the γ-herpesviruses, the molecular basis of the α- and β-herpesvirus latency is poorly understood. EBV latent gene expression involves the expression of several proteins and will be discussed further in the following section on EBV.

1.2 Gammaherpesviruses

The *Gammaherpesvirinae* sub-family includes several important human and animal pathogens, many of which have been studied extensively due to their association with transformation and oncogenesis. There are two genera in this sub-family: the *Lymphocrytovirus* (LCV), also known as *Gamma-1-herpesvirus* (γ1), and the *Rhadinovirus* (RDV), also known as *Gamma-2-herpesvirus* (γ2). EBV is the only human LCV, and KSHV is the only human RDV. Lymphocrytoviruses have only been identified in primate species, predominately in Old World primates, where many are endemic. More recently, new LCVs have been identified in New World primates, including the golden-handed tamarin, squirrel monkey and white-face saki (Cho *et al.*, 2001; de Thoisy *et al.*, 2003). The RDVs, on the other hand, are found in a range of species, including both primates and non-primates.

In addition to being the etiological agent of human diseases, gammaherpesviruses are known to also cause fatal diseases in animals. Several animal viruses, such as Equine herpesvirus-2 (EHV-2), Bovine herpesvirus-4 (BHV-4) and Alcelaphine herpesvirus-1 (AIHV-1) can cause a variety of diseases including, abortion, pneumonia, malignant catarrhal fever and even death. Understanding the pathogenesis of these viruses is not only beneficial to the farming of herd animals, zoos and game farms, but also human disease; primarily due to their use as animal models of human diseases.

Gamma-1-herpesvirus

1.2.1 Epstein-Barr Virus

The Epstein-Barr virus (EBV) is the prototypic *Lymphocryptovirus*, discovered in 1964 by Epstein, Achong and Barr from a lymphoblastoid cell line derived from an endemic Burkitt's lymphoma biopsy (Epstein *et al.*, 1965). EBV is ubiquitous in the human population, with over 90% of adults sero-positive for the virus. Like other gammaherpesviruses, EBV, has a restricted host range; humans are the natural host. Primary infection usually occurs in early childhood, resulting in an asymptomatic infection. However, when primary infection does not occur until

nearing adulthood a self-limiting lymphoproliferative illness, infectious mononucleosis (IM), can be the outcome. EBV is also associated with several tumours including Burkitt's lymphoma, nasopharyngeal carcinoma, post transplant lymphoproliferative disease, Hodgkin's disease and oral hairy leukoplakia, some of which will be discussed later in this chapter.

1.2.1.1 The EBV Genome

The EBV genome is a linear, double-stranded, 184 kbp DNA molecule, with 0.5kb reiterated repeats at both termini and several internal repeats. In 1984, the EBV genome was the first herpesvirus to be fully sequenced (Baer *et al.*, 1984), however the strain initially used had a 12kb deletion, which was later determined from another strain (Parker *et al.*, 1990).

1.2.1.2 EBV Infection

The most common route of transmission of EBV is from the intermittent shedding of virus in saliva from EBV positive adults. EBV can infect primary B lymphocytes *in vitro*, resulting in the conversion of cells into continuous proliferation long term lymphoblastoid cell lines (LCLs). Viral replication in LCLs is minimal, with only a small number of cells spontaneously undergoing lytic replication. There is no *in vitro* system available that is fully permissive for EBV replication. EBV replication can be induced in some semi-permissive LCLs or Burkitt's lymphoma (BL) cell lines, following treatment with a phorbol ester, TPA (12-*O*-tetradecanolyphorbol-13-acetate), to allow studies on lytic infection. EBV can also establish latent infection in other cell types, including T cell or natural killer (NK) cells, however the efficiency is low (Kanegane *et al.*, 1998; Shapiro *et al.*, 1982).

As briefly mentioned earlier, EBV initiates infection by the interaction of the most abundant viral surface protein, gp350/220, with CD21: the cell surface receptor for the C3d component of complement. Following this, the gp85 (gH)/ gp 25 (gL) and gp42 complex is involved in mediating the co-receptor interaction of gp42 with human leukocyte antigen (HLA) Class II molecules, expressed on the surface of B-lymphocytes. However, studies have indicated that gp42 is not utilised in this

manner for infection of epithelial cells, as these cells do not express HLA Class II, whereas, gp42 is essential for efficient B-lymphocyte infection (Molesworth *et al.*, 2000; Wang *et al.*, 1998b).

EBV infection in its natural host is most often found in its latent phase, however in order to spread and infect new hosts the virus must reactivate and produce infectious virions. This switch from latent to lytic replication is as yet uncharacterised; it is associated with the expression of two immediate-early viral genes, BZLF1 and BRLF1, producing ZEBRA and Rta, respectively. Production of ZEBRA and or Rta triggers expression of the other IE factors and can act individually or in synergy on downstream targets to activate a cascade of events in the lytic cycle (Ragoczy *et al.*, 1998).

1.2.1.3 Latent infection of EBV

The majority of studies on herpesvirus latency have been focused on EBV and its ability to establish latent infection in B-lymphocytes *in vitro*. During latency, EBV can only express a limited number of genes that include; six EBV nuclear antigens (EBNA) 1-6, two latent membrane proteins (LMP), two small non-polyadenylated RNAs (or EBERs) and highly spliced *Bam*A rightward transcripts (BARTs). Due to the complexity of EBV latency, and based on differential latent gene expression in EBV positive tumours and immortalized B-cell lines *in vitro*, EBV latency has been grouped into three types; Latency I, II and III (see Figure 1.5).

Latency I phenotype is displayed in Burkitt's lymphoma (BL) cells; these are characterised by the limited expression of EBNA-1, EBERs and BARTs. Hodgkin's lymphomas and NPC cells exhibit a transcription pattern described as Latency II, where EBNA1, EBERs and the latent membrane proteins, LMP1 and LMP2, are expressed. In contrast, Latency III, also described as the growth program, involves expression of all the major latent transcripts (EBNA1-6, LMP1, LMP2, EBERs and BARTs). Latent infection in immortalised LCLs *in vitro*, and immunoblastic lymphomas in transplant recipients displays this Latency III phenotype. The reasons for these different types of latency in EBV infection are still not fully understood, however, it is thought that EBV utilises these different latency programs in order to manipulate the normal biology of B-lymphocytes to gain access to and remain

quiescent within the long-lived memory B-cell compartment. It has been proposed that latency III is essential for the establishment of EBV, as it allows the latently infected B-cells to differentiate into resting memory B-cells (Thorley-Lawson and Babcock, 1999).

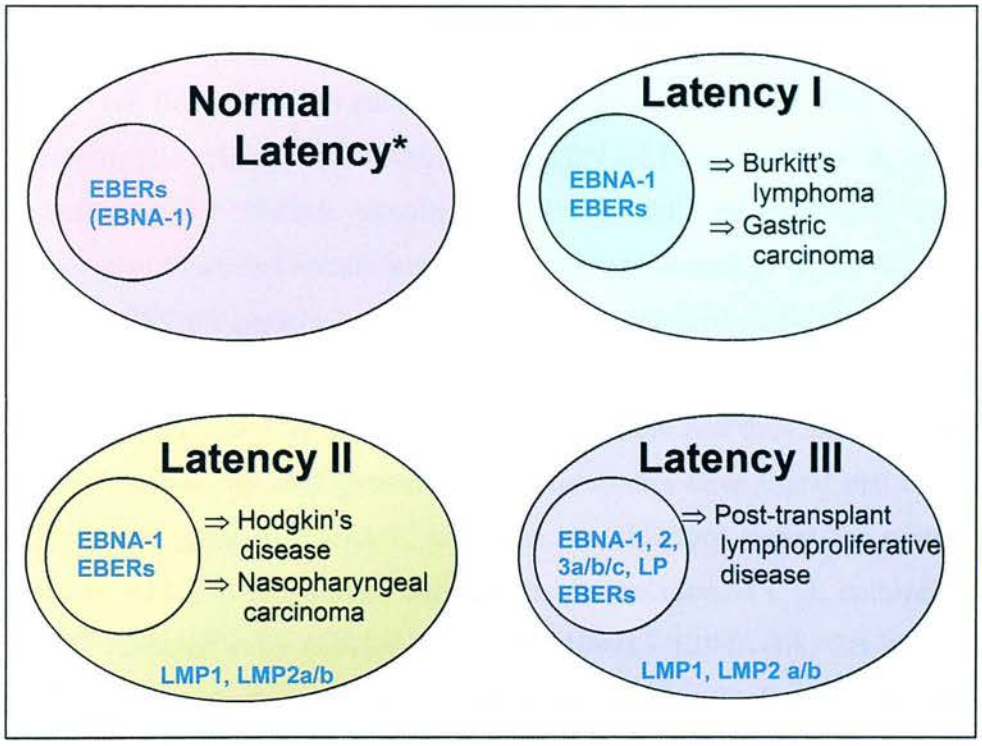

Figure 1.5 Patterns of disease association and EBV latent gene expression in normal EBV infection and during Latency I, II and III. EBERs, EBV encoded small RNAs; EBNA, EBV nuclear antigens; LP, leader protein; LMP, latent membrane protein. *Denotes this is the postulated phenotype of latency infected B cells in a normal EBV seropositive individual. It is unclear whether EBNA1 is consistently expressed (Tierney *et al.*, 1994).

1.2.1.3.1 EBV Latent Genes

EBV Nuclear Antigens (EBNAs)

The Wp promoter is utilised for transcription of the first EBV mRNAs, which are differentially spliced to encode EBNA-LP and EBNA-2. These two proteins up-regulate transcription from both viral and cellular promoters, including Wp and Cp, an activatible upstream surrogate promoter (Evans *et al.*, 1996; Woisetschlaeger *et al.*, 1991). For instance, EBNA-2 up-regulates the cellular encoded genes for CD23, CD21, *c-fgr* and *c-myc*, and viral genes for the other EBNAs, LMP1 and LMP2. EBNA-LP has been found to enhance EBNA-2 up-regulation of viral and cellular gene transcription (Harada and Kieff, 1997). EBNA-LP has also been demonstrated to be important for efficient growth of LCLs, as cells infected with EBNA-LP mutants display a reduced transformation phenotype (Mannick *et al.*, 1991).

The EBNA-1 protein is present in all EBV infected cells, regardless of the state of infection. EBNA-1 mediates binding of the EBV genome to the host chromosome via the oriP or latent origin of replication, and thus aids in replication and maintenance or the viral genome. Previous studies have found that the unique glycine-alanine repeat in EBNA-1, acts as a *cis*-inhibitory signal for proteasomal degradation, which in turn blocks endogenous presentation of CTL epitopes within these EBV infected cells (Levitskaya *et al.*, 1997). EBNA-3A, 3B and 3C are successively placed in the genome and are transcriptional regulators. They all have the ability to bind and stably associate with RBP-J*k*, and by competing for the site with EBNA-2, are able to limit the function of EBNA-2. EBNA-3A and EBNA-3C are essential for B-cell growth transformation; however, *in vitro* studies have found this not to be the case with EBNA-3B, which is dispensable (Thomkinson and Kieff, 1992).

Latent Membrane Proteins (LMP)

The first ORF of EBV encodes an important transforming protein, LMP1. LMP1 has been shown to have to ability to transform rodent fibroblasts and is essential for immortalisation of primary B-lymphocytes to a lymphoblastoid cell line (Wang *et al.*, 1985, 1998a). LMP1 has been demonstrated to mimic the B-lymphocyte activation antigen CD40, a member of the TNF receptor family

(Hatzivassiliou *et al.*, 1998; Kilger *et al.*, 1998). The LMP1 protein has six transmembrane domains and a 199 amino acid carboxy terminal cytoplasmic tail, which causes multimerization, the property that mimics ligand-induced CD40 receptor aggregation. This generates a constitutively active signal and a cascade of events including the activation of NF-κB and JNK, and induction of *bcl-2*, *bclx*, *mcl1* and *A20* gene expression (Damania *et al.*, 2000).

Two forms of LMP2 are expressed, LMP2A and LMP2B, which are both similar in structure; twelve transmembrane domains linked by loops and a short cytoplasmic C-terminus. LMP2A possesses an additional 119 amino acid cytoplasmic N-terminus, which when phosphorylated associates with the SH2 domain of the *Lyn*, *Fyn*, *Syk*, and *Csk* kinases, aiding in intracellular calcium mobilisation and cytokine production (Burkhardt *et al.*, 1992; Longnecker *et al.*, 1991; Scholle *et al.*, 1999). Although LMP2A is not an essential protein, it is involved in preventing reactivation to a lytic state, and thus plays a critical role in establishment and maintenance of latent infection. It has been suggested that LMP2B may be involved in regulation of LMP2A (Longnecker, 2000).

EBV-encoded RNAs (EBERs)

There are two non-translated RNAs encoded by EBV during latency; these are also the most abundant RNAs present. EBER-1 is transcribed by RNA polymerase III and II, whereas, EBER-2 is only transcribed by RNA polymerase III. Recent studies have found that EBERs can induce the secretion of IL-10, which might stimulate growth of infected B cells and suppress cytotoxic T cells (Kitagawa *et al.*, 2000). It also appears that the EBERs are able to mediate resistance to interferon-α-induced apoptosis in Burkitt's lymphoma cells (Nanbo *et al.*, 2002). Other studies have also suggested that expression of the EBERs may increase the tumorigenicity of Burkitt's lymphoma (Komano *et al.*, 1998, 1999).

1.2.1.4 EBV- associated Diseases

EBV infection is associated with a variety of diseases in immunocompetent individuals, such as infectious mononucleosis (IM), Burkitt's lymphoma (BL), nasopharyngeal carcinoma and Hodgkin's disease. However, EBV infection in immunosupressed individuals can also result in severe illnesses, including post-transplant lymphoproliferative disease (PTLD).

1.2.1.4.1 Infectious Mononucleosis

In more affluent societies, primary infection of EBV is often delayed until adolescence or adulthood, and is commonly associated with IM, also know as the "kissing disease" due to its route of transmission. IM symptoms can range from mild transient fever to several weeks of pharyngitis, lymphadenopathy, splenomegaly, hepatocellular dysfunction and general malaise. However, these disease symptoms are unlikely to be the direct result of viral replication; IM is believed to be an immunopathologic disease in which the symptoms are the result of pro-inflammatory cytokines, such as IL-1, IFN-γ and TNF-α. High levels of these pro-inflammatory cytokines are secreted by the large numbers of T-lymphocytes infiltrating various tissues throughout the body during IM (Niedobitek *et al.*, 1997; Verbeke *et al.*, 2000). IM is self-limiting and in most cases does not develop complications although, prolonged fatigue, hypersomnia and short-lived depressive disorder may occur after IM (Macsween and Crawford, 2003).

1.2.1.4.2 Burkitt's Lymphoma

Burkitt's Lymphoma (BL) was first described in children in equatorial Africa and New Guinea (Burkitt, 1962). In this endemic form of BL over 97% of cases are EBV positive, while the more rare sporadic form has only a 20-30% association with EBV. There is a third form, AIDS-associated BL, which has a higher incidence of BL than the endemic or sporadic BL of childhood; 30-40% of tumours from this group are EBV positive. BL malignancies are commonly presented at extranodal sites, most frequently in the jaw, but have also been found in the CNS and the

abdomen. In the absence of treatment, BL tumours can grow quickly and can result in death within several months.

All BL tumours display the same homogenous population of malignant cells that are morphologically similar to germinal centre B cells. Chromosomal translocations are present in BL cells where the *c-myc* oncogene on chromosome 8 is brought under the influence of the IgH enhancer on chromosome 14, or more rarely by the light-chain loci on chromosomes 2 or 22. This chromosomal translocation results in the constitutive expression of *c-myc* and uncontrolled cell proliferation. Mutations in the gene encoding the tumour suppressor p53 have also been detected in about a third of cases of BL (Gaidano *et al.*, 1997). Viral gene expression in BL cells is restricted to the pattern seen in type I latency; in addition to the EBERs and BARTs, only EBNA-1 is expressed. As previously mentioned the EBERs may play an important role in this tumour and it has recently been reported that EBER expression may be positively regulated by *c-myc* (Niller *et al.*, 2003).

1.2.1.4.3 Nasopharyngeal Carcinoma

Nasopharyngeal carcinoma (NPC) is a tumour derived from the epithelium of the nasopharyngeal surface and is seen throughout the world but varies in incidence and histological subtype. There are two classifications of NPC; those that are classified as keratinised have observable epithelial differentiation, whereas the non-keratinised NPC have undifferentiated epithelial cells. NPC has a high incidence among people from Southern China and Inuit races, where most tumours are of the non-keratinised type and preferentially affect middle aged men. Sporadic cases of both classes of NPC are seen in Europe and North America but these numbers are small in comparison to those seen in Southeast Asia. EBV has been identified in all cases of non-keratinised NPC and most cases of keratinised NPC in Southeast Asia, and approximately 30% of this class of tumours from Europe (Nicholls *et al.*, 1997).

NPC cells are believed to exhibit a latency II phenotype (see Figure 1.5), however LMP1 detection is variable and LMP2 protein expression has not been unequivocally demonstrated. Studies have also indicated that there are several co-factors that may have an impact on the pathogenesis of the disease and geographic distribution, such as genetic susceptibility (Lu *et al.*, 1990). Environmental factors

such as diet have also been indicated; consumption of traditional salt fish dishes that contain carcinogenic nitrosamines and herbal remedies containing tumour-promoting phorbol esters have been implicated as risk factors (Armstrong *et al.*, 1998; Hirayama and Ito, 1981; Zou *et al.*, 1994). Thus a number of environmental factors, dictated by diet or lifestyle, and a genetic predisposition may all contribute to NPC.

1.2.1.4.4 Post-transplant Lymphoproliferative Disease

Post-transplant lymphoproliferative disease (PTLD) is a life-threatening complication associated with organ transplantation and the treatment with immunosuppressive drugs to prevent graft rejection. EBV has been etiologically associated with PTLD by virtue of its presence in the majority of PTLD lesions. PTLD often develops in sites considered unusual for other lymphomas, such as the G.I. tract, CNS or the transplant organ (Penn and Porat, 1995; Thomas *et al.*, 1990). The incidence of PTLD is variable ranging from 1% to over 20%, which is primarily due to EBV status prior to the transplant and the type of organ transplanted; levels of immunosuppressive drugs vary depending on the organ e.g. heart and lung transplants require a higher dose than renal or liver transplants (Rickinson and Kieff, 2001). Over 50% of these cases are associated with primary EBV infection and the disease is understandably seen to be of higher risk to paediatric transplant recipients (Ho *et al.*, 1985).

PTLD arises as an opportunistic tumour in an environment where there is intense T-cell immune suppression, thus allowing the latently infected B-cells to survive and proliferate. Early lesions are often polyclonal, however later progress to a monoclonal lymphoma. EBV infected cells within the lymphomas exhibit a type III latency, as characterised by expression of all the latent proteins (Tanner and Alfieri, 2001). However, these EBV positive cells are only a small proportion of the cells within the tumour mass; CD4+ T cells make up the majority of cells and studies have found these cells necessary for the establishment of tumours (Veronese *et al.*, 1992). Tumour regression is often observed following the reduction of immunosuppressive therapy, which allows re-establishment of EBV-specific T-cell immunity, however this also risks rejection of the transplanted organ and PTLD often

recurs (Macsween and Crawford, 2003). More recently, adoptive immunotherapy has been utilised, whereby the use of cultured EBV specific CTLs has been used with some success, and in turn avoids the risk of graft rejection (Haque *et al.*, 2002; Rooney *et al.*, 1998).

1.2.1.4.5 Hodgkin's Disease

Hodgkin's lymphomas (HL) are characterised by Hodgkin and Reed-Sternberg (H-RS) cells and in most cases, derived from germinal-B cells. The precise mechanism of EBV involvement is unclear, but there are several factors that suggest that EBV has a causative role in the pathogenesis of this disease. It was first noticed that antibody titres against EBV were elevated for months or years before the onset of the disease, in addition the incidence of developing HL increases three-fold in individuals with a previous history of IM (Mueller *et al.*, 1989). Furthermore, EBV DNA has been detected in over 50% of Hodgkin's disease tumours.

In HL the expression pattern of EBV-encoded genes is limited to type II latency, and resembles that seen in endemic NPC. It is possible that the expression of the LMPs results in the activation of the NF-κB pathway and consecutive up-regulation of anti-apoptotic genes, thus allowing the pre-apoptotic H-RS cell-progenitors to survive negative selection in the germinal centre. However, as only 50% of cases are EBV-positive, it is highly likely that there are other agents or events that aid in the malignant transformation seen in the EBV-negative cases (Thomas *et al.*, 2004). As seen with current immunotherapy treatment for PTLD, several pilot studies are underway to assess the potential use of CTL therapy for Hodgkin's disease (Chapman *et al.*, 2001; Roskrow *et al.*, 1998; Su *et al.*, 2001).

1.3 Animal Gammaherpesviruses

There are several important reasons for studying animal gammaherpesviruses particularly due to the large degree of homology between the human and animal viruses from this subgroup. Understanding genome arrangement and disease pathogenesis due to animal herpesviruses infection may give an insight into mechanisms that are utilised by some of the human herpesviruses such as EBV and KSHV. As previously mentioned both EBV and KSHV have an extremely restricted host range *in vivo* which has hindered studies of pathogenesis and an even greater reason for the utilisation of animal models.

1.3.1 Herpesvirus Saimiri

Herpesvirus Saimiri (HVS) is the classical prototype of the *Rhadinoviruses* and is ubiquitous in its natural host, the squirrel monkey (*Saimiri sciureus*). HVS infection is asymptomatic and establishes lifelong persistence in this species, whereas experimental infection of other New World primates can result in acute peripheral T-cell lymphomas (Fickenscher and Fleckenstein, 2001). Lymphoblastoid cell lines have been established from tumours from New World primates such as the marmoset and owl monkey. In contrast to EBV and KSHV, HVS replicates productively *in vitro* and is able to immortalise both monkey and human T-cells (Biesinger *et al.*, 1992). Transformed human T cells harbour HVS but do not release infectious virus, the viral genome remains exclusively in an episomal state that does not integrate into the cellular genome (Fickenscher *et al.*, 1996). It is due to these features that HVS has been recently viewed as a potential gene therapy vector and studied by several groups (Smith *et al.*, 2001; Stevenson *et al.*, 2000).

The HVS genome is comprised of a 112.9kb unique region flanked at either end with 1.4kb terminal repeat sequences (Figure 1.6). There are 76 major ORFs and a set of seven U-RNA genes (Albrecht *et al.*, 1992). Like other viruses in the herpesvirus family, HVS contains gene blocks with highly conserved genes but also unique blocks possessing the transforming oncogenes and genes with cellular homology. Many of the cellular homologues are similar to those found in KSHV and include a complement control protein homologue (ORF4), v-FLIP, v-cyc, v-GPCR

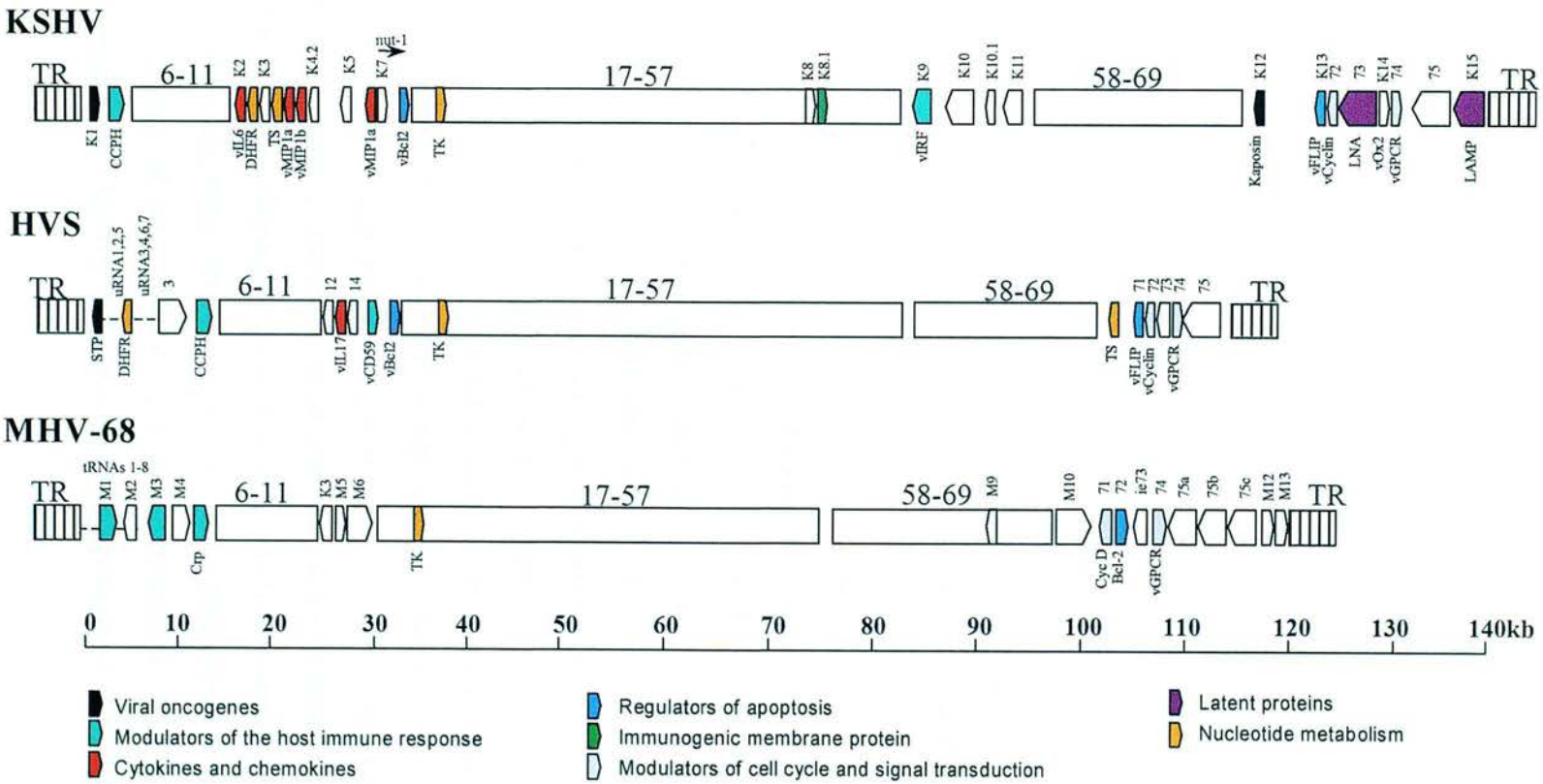

Figure 1.6 Genomic structure of KSHV, HVS and MHV-68

and vbcl-2. Studies have found that although the HVS ORF73 has only limited sequence homology with LANA of KSHV, it may function in a similar manner. It has recently been determined that HVS ORF73 is required for episomal maintenance and is able to regulate viral gene expression to suppress lytic replication in permissive cells (Calderwood *et al.*, 2004; Schafer *et al.*, 2003). Another similarity with KSHV may be the gene expression pattern during latency, as studies using a human lung carcinoma cell line containing episomal HVS DNA showed latent expression of ORFs 71, 72 and 73, which correspond to the v-FLIP, v-cyc and LANA homologues respectively (Hall *et al.*, 2000).

HVS isolates are divided into three subgroups A, B and C, based on sequence divergence at the left end of the unique region of the genome and pathogenic properties (Medveczky *et al.*, 1989, 1984). Subgroups A and C are highly oncogenic and *in vivo* infection can result in the formation of lymphomas, however only subgroup C is able to transform human T cells *in vitro* (Biesinger *et al.*, 1992). All three subgroups possess an ORF encoding a saimiri transformation-associated protein (STP), although only subgroup C also encodes Tip (tyrosine kinase interacting protein); STP and Tip are transcribed from a biscistronic mRNA (Fickenscher *et al.*, 1996). Subgroup B contains a non-transforming STP gene, STP-B (Choi *et al.*, 2000a). It has been reported that STP-C interacts with cellular *ras*, and that in the lesser pathogenic subgroup A, STP-A interacts with cellular *src* kinase (Jung *et al.*, 1991; Jung and Desrosiers, 1995). All STPs and Tip are essential for transformation in cell culture and *in vivo*, however they are dispensable for both *in vitro* and *in vivo* replication (Duboise *et al.*, 1998).

The use of HVS as a model to study herpesvirus pathogenesis has several advantages given the amount of homology with other herpesviruses and that the virus is able to replicate and transform cells *in vitro*. However, studies *in vivo* do pose several limitations, primarily those of cost and the restrictions on primate research. Another animal model allows the utilisation of a natural gammaherpesvirus infection within laboratory mice; this model allows viral pathogenesis *in vivo* to be studied without many of the prohibitive aspects associated with primate research. Furthermore, with the ability to generate transgenic mice, the host immune system

can be manipulated in such a manner to allow studies to be performed that focus on the effects of individual viral genes on pathogenesis.

1.3.2 Murine Gammaherpesviruses

In 1980 during a field study in Slovakia five novel herpesviruses were isolated from murid hosts including MHV-60, -68 and -72 from the bank vole (*Clethrionomys glareolus*) and MHV-76 and -78 from the yellow-necked wood mouse (*Apodemus flavicollis*) (Blaskovic *et al.*, 1980).

1.3.2.1 MHV-68 and MHV-76

In the past a large amount of research has focused on MHV-68 due to its use as a model for gammaherpesvirus infection in a natural host species. Following the isolation of MHV-68 it was shown to be genetically related to other viruses in the *Rhadinovirus* subgroup, such as EBV and HVS (Efstathiou *et al.*, 1990a). The MHV-68 genome consists of 118kbp of unique DNA flanked at each end by variable numbers of 1.23kbp terminal repeat regions. Sequencing of the genome has identified 73 protein-coding ORFs and 8 tRNA-like molecules (Figure 1.6) (Efstathiou *et al.*, 1990b; Virgin *et al.*, 1997). A more recent study on MHV-76 has shown this virus to be a deletion mutant of MHV-68. The genome of MHV-76 is essentially identical to that of MHV-68, except for a 9,538bp deletion at the left-hand end of the genome resulting in the loss of four unique genes of MHV-68 (M1, M2, M3 and M4) and the eight viral tRNA-like genes (vtRNAs) (Macrae *et al.*, 2001). The majority of ORFs in both viruses are co-linear and homologous to regions in other γ-herpesviruses (Figure 1.6). It is therefore not surprising to find that MHV-68 and MHV-76 possess several functional homologues of cellular genes including bcl-2 (M11), G-protein-coupled receptor (GPCR) (ORF 74), cyclin D (ORF 72) and a complement – regulatory protein (ORF 4).

During lytic infection there is a conventional cascade of gene expression, immediate early genes such as ORF 50 (Rta) and ORF 73 (LANA homologue), early genes such as Thymidine kinase (ORF 21) and late genes such as gp150 have been identified (Ebrahimi *et al.*, 2003). The glycoprotein gp150 may play an equivalent role to gp350/220 of EBV, as in addition to sequence homology, antibodies to this

protein neutralise virus infectivity in the absence of complement; thus suggesting a potential role in binding or penetration (Stewart *et al.*, 1996). Gp150 is located on the surface of the virion and in infected cells localises to the nuclear margins, in the cytoplasm and on the cell surface.

The pattern of viral gene expression during infection in the lung differs remarkably to that seen during infection of the spleen, i.e. lytic versus latent infection. As the virus enters the latent phase of infection, gene expression is progressively shut down, however, the expression pattern can vary depending on the cell type. For instance, M2 expression is only detected in B cells in the spleen and not in splenic macrophage or dendritic cells, which also harbour latent virus (Macrae *et al.*, 2003). ORF 73 encodes a protein that shares homology with KSHV LANA and is found to be the most abundant expressed viral transcript in latently infected S11 cells (Martinez-Guzman *et al.*, 2003). Studies have shown that ORF 73 is critical for the establishment of splenic latency (Moorman *et al.*, 2003). Induced mutations in other latency-associated proteins encoded by ORF 74, a GPCR homologue, and M11, a viral bcl-2 homologue, have both displayed a decreased ability to reactivate from latency (Gangappa *et al.*, 2002; Lee *et al.*, 2003; Verzijl *et al.*, 2004). Expression of some of these latent proteins, such as ORF73, ORF 74 and M11 have been detected in the lung 100 days post-infection (Nash *et al.*, 2001; Roy *et al.*, 2000); thus also suggesting the respiratory tract as a site of persistent infection.

1.3.2.2 Pathogenesis

The natural route of infection is still unclear, however by analogy with other animal γ-herpesviruses it seems likely that the respiratory tract is the primary target. Studies have shown that following intranasal infection of four- to six- week old laboratory mice, MHV-68 results in productive infection in alveolar epithelial cells and is accompanied by bronchiolitis (Sunil-Chandra *et al.*, 1992). An inflammatory response initially comprised of macrophage is seen to peak at approximately 3 days post-infection (p.i.), which is then followed by a $CD8^+$ T cell response peaking at day 7 and finally resolves by the second week. The virus is then transported via the mediastinal lymph node (MLN) where dendritic cells, macrophages and B cells become infected. It is believed that these infected dendritic cells are initially

responsible for transporting the virus to the draining lymph node where they seed B cells (Selvarajah, 2001).

Following infection of the lymph node, B cells undergo a rapid expansion that is accompanied by an increase in the number of latently infected B cells, which traffic to the spleen and other lymphoid compartments. Due to the influx and rapid expansion of latently infected B cells in the spleen, splenomegaly (mononucleosis) is commonly observed. Latent viral levels peak at approximately two weeks post infection and then reduce to levels of about 1 infective centre per $5x10^5$ splenocytes to 1 infective centre per 10^6 splenocytes after 3 to 4 weeks, and maintain this established level of latency for life (Usherwood *et al.*, 1996). Studies have suggested that long term latency is preferentially established in CD40(+) memory B cells (Kim *et al.*, 2003). However, in addition to splenic B cells, latent virus has also been found to persist in splenic macrophage and dendritic cells and in lung epithelial cells (Flano *et al.*, 2003; Stewart *et al.*, 1998). Long-term infection of BALB/c mice with MHV-68 can lead to the development of lymphoproliferative diseases (LPD), similar to that observed with EBV infection. Over a period of 3 years 9% of mice develop LPD, with over 50% of these being categorised as high grade; the frequency increases following treatment with immunosuppressive agents (Sunil-Chandra *et al.*, 1994).

Like MHV-68, it is believed that MHV-76 also follows the same course of infection after the intranasal infection of inbred laboratory mice, as depicted in Figure 1.7. Studies by Macrae *et al.* (2001) have observed that MHV-76 has a more attenuated pathology than MHV-68. A more severe and rapid inflammatory response occurs following infection of the lung with MHV-76; viral levels peak at day 4 p.i. and are undetectable by day 10 p.i., whereas MHV-68 infection sees a peak at day 6 p.i. and clearance by day 12 p.i. MHV-76 also establishes latency in the spleen, although at a lower level than MHV-68, but MHV-76 does not induce splenomegaly. These *in vivo* differences observed between the two viruses imply that the absent genes (M1-M4 and 8 vtRNAs) play a role in pathogenicity, but are not required for lytic replication or the establishment of latency.

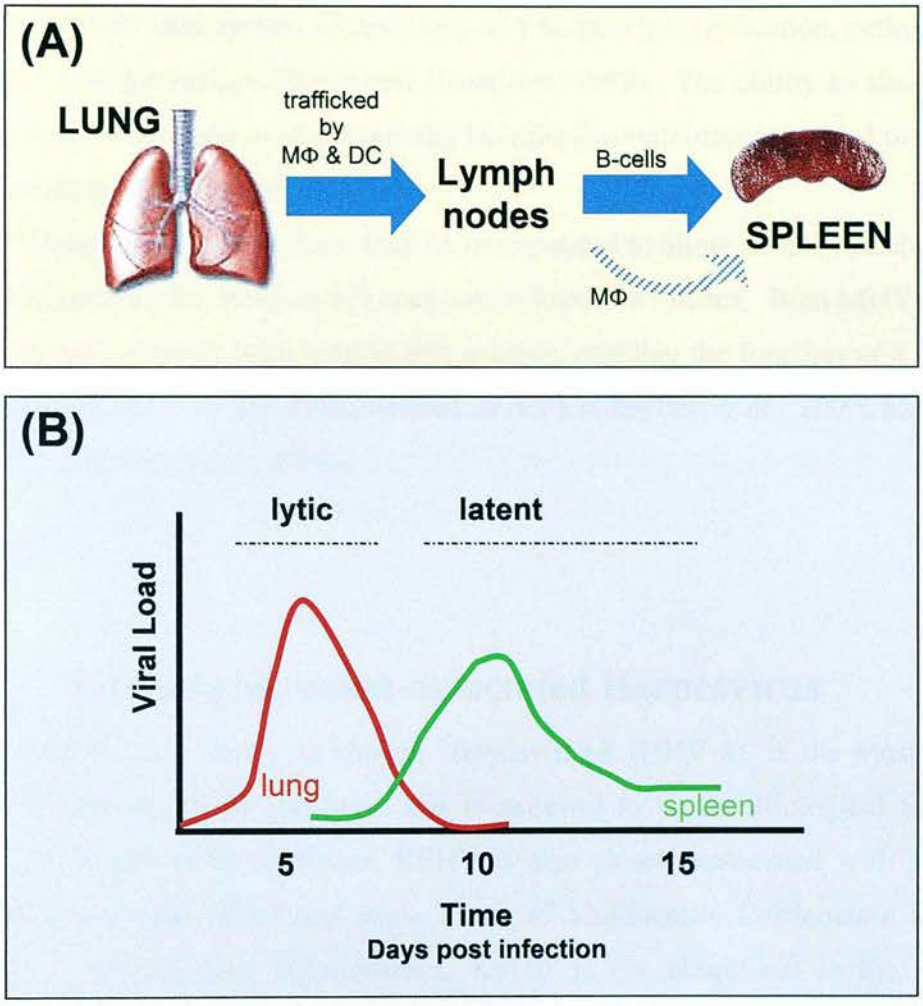

Figure 1.7 Schematic representation of key events during MHV-76 infection *in vivo* following intranasal infection. Image (A) depicts the predominant organs involved during infection and (B) outlines the viral load. Initial lytic replication occurs in the lung and peaks at about 4 days post infection (p.i.)(red line shows viral titers in the lung (B)). Infectious virus is cleared to undetectable levels by 10 days p.i. This is followed by seeding to lymphoid tissue by macrophage (MΦ) and dendritic cells (DC), followed by amplification of latent virus and further dissemination, predominantly by latently infected memory B cells and possibly by MΦ. A peak of latent virus is observed at day 10 and is followed by a gradual decrease to a persistent low level of latent virus in the spleen (indicated by green line).

Both MHV-68 and MHV-76 are able to infect fibroblast and epithelial cell lines from a number of species *in vitro* and establish lytic and latent infection *in vivo* making them an ideal system for the study of γ-herpesvirus replication, pathogenesis and virus-host interaction (Simas and Efstathiou, 1998). The ability to study these viruses both *in vitro* and *in vivo* has many benefits that will ultimately lead to a better understanding of gammaherpesviruses.

These viruses, like others, may be manipulated to allow an individual gene to be investigated by the creation of knock-out or knock-in viruses. Both MHV-68 and MHV-76 have recently been used in this manner, enabling the function of a gene to be studied in cell lines and also infection in mice (Clambey *et al.*, 2000; Macrae *et al.*, 2003; Townsley *et al.*, 2004).

1.4 Kaposi's Sarcoma-associated Herpesvirus

KSHV, also known as Human Herpesvirus-8 (HHV-8), is the most recent human herpesvirus to be identified and is believed to be the etiological agent of Kaposi's Sarcoma (KS). However, KSHV is also closely associated with primary effusion lymphomas (PEL) and some forms of Multicentric Castleman's Disease (MCD). Unlike most herpesviruses, KSHV is not ubiquitous in the general population; only a small number of people are infected with KSHV in developed countries, whereas in some areas of Africa a large proportion of the population display serological evidence of exposure to the virus (Moore and Chang, 2001).

Prior to the AIDS epidemic, cases of KS were rare and strictly associated to geographic clusters within the Mediterranean and Eastern Europe. However, the tumour's unusual epidemiological pattern (increased number and broader geographic spread) in the 1980's spurred researchers belief that an infectious agent was an etiological factor contributing to the onset of KS. This research lead to the identification of a new herpesvirus, KSHV. In 1994 Chang and Moore's group (1994) initially identified herpes-like sequence in an AIDS-associated KS lesion using representational difference analysis.

Although information on the epidemiological transmission of KSHV is limited, there is speculation that there are two main modes of viral transmission, sexual and non-sexual. In developed countries, sexual transmission is thought to be the most common route of infection as KSHV has been detected in semen (Blackbourn and Levy, 1997). Virion particles have also been detected in saliva; this may be a possible route of transmission in endemic African areas where infection can occur in childhood (Pauk *et al.*, 2000; Vieira *et al.*, 1997). Vertical transmission, from mother to child, of KSHV has also been observed in parts of Africa (Mayama *et al.*, 1998; Sitas *et al.*, 1999), however, these non-sexual routes of transmission in endemic areas are still not fully understood. Finally, KSHV can be transmitted iatrogenically via organ transplantation. Transmission from blood products is uncommon (Moore and Chang, 2001).

1.4.1 Disease Associations

1.4.1.1 Kaposi's Sarcoma

Kaposi's Sarcoma (KS) is a mesenchymal tumour, involving blood and lymphatic vessels that often presents as purple-reddish-brown lesions and nodules on the lower extremities. KS was first described in the 1870's by an Austro-Hungarian dermatologist, Moritz Kaposi, where he described an "idiopathic multiple pigment skin sarcoma" seen on the lower extremities in elderly men (Kaposi, 1872). One patient described died of gastrointestinal (G.I.) bleeding 15 months after the initial appearance of the skin lesions and an autopsy showed visceral lesions in the lung and G.I. tract. This form of KS is now known as "classical" KS; since this first description there have been four clinical variants of KS that are histologically identical but are distinguished by epidemiology factors and disease severity (Hengge *et al.*, 2002b).

(i) *Classical KS* – This form of KS is characterised by benign, indolent tumours often limited to the extremities of elderly white males that are of Ashkenazi Jewish or Mediterranean descent. Classic KS rarely metastasises and is not considered to be fatal.

(ii) *Endemic African KS* – This form was first described in the 1960's when it was noted that an unusually high prevalence of KS was occurring in localised areas throughout sub-Saharan Africa. In this population, KS is not only seen in adult men and women, but also children; it is a more aggressive form of KS and can be fatal in children particularly when there is lymph node involvement.

(iii) *Iatrogenic KS* – This form of KS is seen in iatrogenic immunosupressed organ transplant recipients and in patients that are on immunosuppressive drugs. The development of KS is due to either primary infection with KSHV or reactivation of latent virus. Disease onset is often chronic and rapidly progressive but withdrawal of the immunosuppressive drugs usually results in spontaneous remission.

(iv) *AIDS-associated KS* - This is the best-known form of KS and is estimated to be 300 times more common in AIDS patients than other immunosupressed groups and 20,000 times more common than in the general population. AIDS-KS is an aggressive and quick onset form, and the transmission route of HIV seems to influence the risk of KS development; homosexual men are at much greater risk than men with haemophilia (21:1). KS lesions were the first clinical manifestation in about one quarter of AIDS patients prior to the introduction of HAART (highly active anti-retroviral therapy); since then the incidence of AIDS-KS in the western world has become uncommon. However, it is still a major opportunistic infection in AIDS patients from developing countries.

KS growth is stimulated by various proinflammatory cytokines and growth factors such as tumour necrosis factor -α (TNF-α), interleukin-6 (IL-6), basic fibroblast growth factor (bFGF) and vascular endothelial growth factor (VEGF), aiding in the formation of a hyperblastic polyclonal lesion. It has been demonstrated that several KS cells also express some of the corresponding receptors with high affinities for several of these cytokines; both the cytokines and their receptors enhance inflammation and angiogenesis in an autocrine manner (Arvanitakis *et al.*, 1997; Hengge *et al.*, 2002a; Mesri, 1999; Nicholas *et al.*, 1997). These lesions are

complex and comprised of a variety of cell types. Early lesions contain irregular endothelial lined spaces that surround normal dermal blood vessels, which are also accompanied by a variable inflammatory infiltrate. At the later nodular stage, the lesions are predominately made-up of spindle cells and slit-like vascular spaces containing erythrocytes. The spindle cells are believed to be the neoplastic component, however their origin is disputed. KS spindle cells have been found to express markers for smooth muscle cells, macrophages and dendritic cells (Nickoloff and Griffiths, 1989; Sturzl *et al.*, 1992). It has been shown that the vascular endothelial growth factor receptor- 3 (VEGFR-3) is expressed on all KS spindle cells (Dupin *et al.*, 1999; Jussila *et al.*, 1998). As this marker is most commonly associated with expression on lymphatic endothelium and neoangiogenic vessels (but not by mature vascular endothelial cells), it is likely that the KS spindle cells are derived from an endothelial lineage, which can differentiate into lymphatic cells (Boshoff and Weiss, 2001).

Boshoff and Weiss (2001) have outlined the four main observations that, when viewed together provide evidence that KSHV is the etiological agent of KS. These findings include;

(i) KSHV DNA can be detected by PCR in all forms of KS and is rarely found in other mesenchymal tumours.

(ii) Patients positive for HIV and carrying a higher load of KSHV are at greater risk for developing KS.

(iii) Serological studies indicate that incidence of classic and AIDS-KS correlates broadly with the prevalence of virus infection within the population.

(iv) In advanced KS lesions, latent KSHV transcripts can be detected in most spindle cells.

1.4.1.2 Primary Effusion Lymphomas

Primary effusion lymphomas (PEL), or body cavity-based lymphomas, are a non-Hodgkin B-cell lymphoma and present as malignant effusions in the visceral cavities in the absence of a solid tumour mass. KSHV has been identified in PELs but not in other non-Hodgkin lymphomas. PELs are most commonly seen in HIV positive individuals in the advanced stages of AIDS, however are occasionally seen in HIV-sero-negative patients (Nador *et al.*, 1996). As PEL cells seem to lack several adhesion molecules and 'homing markers' that are associated with other diffuse lymphomas, it is thought that this may add to the unusual effusion phenotype of the lymphoma (Boshoff *et al.*, 1998). As expression of B-cell markers seems limited to CD138, a molecule associated with late stage B-cell differentiation, and the frequent detection of a mutation in the 5' non-coding of BCL-6, it is thought that PEL cells are pre-terminally differentiated, post-germinal centre stage B cells (Gaidano *et al.*, 1999).

Compared with KS, PEL cells contain a very high copy number of KSHV (Boshoff and Chang, 2001). In addition to the establishment of cell lines direct from PEL, the BCP-1 cell line was established from peripheral blood taken from a patient with PEL; thus implying that malignant cells may be present and disseminated in the peripheral blood (Arvanitakis *et al.*, 1996; Boshoff *et al.*, 1998). Some of these cell lines are infected with both KSHV and EBV, while some are only positive for KSHV. KSHV is present in a latent state and lytic *in vitro* infection can be induced by phorbol esters or butyrate. It is therefore due to the ability to study both lytic and latent gene expression *in vitro*, that PEL cells are invaluable to the study of KSHV.

1.4.1.3 Multicentric Castleman's Disease

There are two forms of Castleman's disease; those being (i) localised Castleman's disease, a single angiofollicular lymph-node hyperplasia and (ii) multicentric Castleman's disease (MCD), a multisystem involvement with generalised lymphadenopathy (Hengge *et al.*, 2002a). It is highly likely that there is more than one cause of these diseases, as KSHV is not detected in all cases; KSHV has been detected in nearly all MCD cases when the individual is also HIV-positive and in 40-50% of HIV-negative cases (Chadburn *et al.*, 1997; Corbellino *et al.*, 1996;

Soulier *et al.*, 1995). A role for KSHV in MCD pathogenesis is implied as symptoms of the disease are exacerbated proportionally to the viral load of KSHV detected in peripheral blood mononuclear cells (Grandadam *et al.*, 1997).

KSHV is present in plasmablasts of B-cell lineage within MCD; these cells are not present in cases of MCD that are KSHV-negative (Dupin *et al.*, 2000). Viral IL-6 is highly expressed in these MCD plasmablasts, even higher than levels detected in PEL or KS, thus suggesting that over expression of this cytokine may play a role in MCD pathogenesis (Katano and Sata, 2000; Parravicini *et al.*, 2000; Staskus *et al.*, 1999). KSHV predominately expresses lytic transcripts in MCD. Finally, MCD, in HIV-positive patients, does not commonly resolve through treatment with HAART (Dupin *et al.*, 2000; Zietz *et al.*, 1999).

As a point of interest, there have been a few cases in which an individual has developed two or even three independent KSHV-associated tumours, i.e. KS, PEL and MCD, however this is uncommon (Jones *et al.*, 1998).

1.4.2 Genome

KSHV, the only human *Rhadinovirus*, is closely related to HVS and is believed to have separated from the *H.Saimiri* lineage at about the same time as the host Old and New World Monkeys lineage separated, approximately 35 million years ago (McGeoch and Davison, 1999).

The KSHV genome is approximately 165kb in length and contains a long unique region, LUR (145kb), flanked with variable numbers of terminal repeats (801bp each); the LUR encodes at least 87 genes. Due to the high degree of homology with HVS, most of the KSHV genes have been consecutively named after a HVS counterpart (Figure 1.6). However, KSHV also possesses several genes which are not homologous to any in HVS, these genes are given a K prefix e.g. ORF K1 to K15. Many of these are unique to KSHV and share homology with cellular genes (see Table 1.2), a characteristic of KSHV that will be discussed in more depth later in this chapter.

Table 1.2 KSHV- encoded proteins homologous with cellular proteins.

Viral protein	Viral ORF	Cellular Homologue	Possible Function(s)	Expression Pattern
ORF 4	ORF4	Complement binding protein (CBP)	*Inhibits complement-mediated lysis* *Escape from host immune response*	Lytic
vIL-6	K2	IL-6	Activated gp130 independently Autocrine and paracrine growth stimulation Angiogenesis	Lytic
VMIP-I vMIP-II vMIP-III	K6 K4 K4.1	Macrophage inflammatory proteins	Binds both CC and CX receptors → Chemoattraction Angiogenesis	Lytic
VIRF	K9	Interferon regulatory factor	Blocks IFN- and IRF- mediated transcriptional activation. Inhibition of p300 and p53 Oncogenic	Lytic
v-Bcl-2	ORF16	Bcl-2 family protein	Inhibits apoptosis, Bcl-2 and Bax binding	Lytic
v-FLIP	ORF71	FLICE inhibitory protein	Inhibits Fas-mediated apoptosis Oncogenic	Latent
v-Cyclin	ORF72	D-type cyclin	Associates with CDK6 → Inactivation of pRB ⇒ Promotes G1 to S phase transition	Latent
vOX2	K14	CD200 (or OX2)	*Regulatory/transportation control of macrophage* *? Adhesion*	Lytic
vGPCR	ORF74	IL-8 GPCR	Constitutively active GPCR Binds IL-8 Oncogenic and angiogenic	Lytic

Gene names are taken from the literature and function based on experimental evidence referred to in text, except for those in italics that are based only on homology to characterised genes. Gene expression patterns are taken from Jenner *et al.* (2001).

A high degree of conservation is maintained within KSHV with less than 0.4% nucleotide variation between the central genomic region of KSHV isolated from a KS lesion and from a BC-1 PEL cell line (Neipel *et al.*, 1998; Russo *et al.*, 1996). A higher degree of variation is seen within the internal direct repeat region and areas adjacent to the end terminal repeat sequences, particularly in ORF 75 and within the TRs; variants based on variation in these areas have been identified but do not follow phylogenetic clusters (Poole *et al.*, 1999; Zong *et al.*, 1999). However, the genetic variation in ORF K1 has lead to the division of KSHV into four strains, A to D. These strains can be associated with geographic location, as strain A is more often observed in classic Mediterranean KS, B and C in Africa and strain D is most common among Asian isolates (Hayward, 1999; Zong *et al.*, 1999).

1.4.3 Viral Life Cycle and Gene Expression

As previously mentioned, viral transcripts have been identified in several cell types *in vivo*, including B-lymphocytes, macrophages, endothelial cells, and epithelial cells (Blasig *et al.*, 1997; Boshoff *et al.*, 1995; Diamond *et al.*, 1998; Schulz, 1998). KSHV is able to infect several human cells *in vitro*, such as B cells, endothelial cells, epithelial cells and fibroblast cells. In addition, KSHV can infect a variety of animal cells, such as owl monkey kidney cells, baby hamster kidney (BHK) fibroblast cells, Chinese hamster ovary (CHO) cells, and primary embryonic mouse fibroblast cells (Blackbourn *et al.*, 2000; Flore *et al.*, 1998; Moses *et al.*, 1999; Renne *et al.*, 1998). Unless chemically stimulated, only latent KSHV infection is observed during *in vitro* infection of these cells and as yet, there is no suitable cell culture system to support a natural ongoing lytic replication.

This broad cellular host range for KSHV suggests that the virus may be interacting with one or more ubiquitous host cell surface molecules to gain access to the target cells. Research has demonstrated that the KSHV glycoproteins gB (ORF 8) and K8.1A are able to bind with glycosaminoglycans, such as heparan sulfate, on the cell surface (Akula *et al.*, 2001; Birkmann *et al.*, 2001; Wang *et al.*, 2001). K8.1 is a unique gene to KSHV and encodes the spliced products K8.1A and K8.1B. The K8.1 ORF is a positional homologue of EBV gp350/220, which mediates the initial attachment of EBV to B cells. Recent studies have shown that KSHV gB contains an

RGD motif that is able to bind specifically to integrin α3β1 and thus is likely to be a cellular receptor for KSHV entry (Wang *et al.*, 2003). The α3β1 integrin is expressed on a broad range of cell types, including those cell types susceptible to KSHV infection (Wang *et al.*, 2003). Although blocking this integrin binding site was shown to reduce infectivity in human foreskin fibroblast cells, studies using cells derived from human embryonic kidney cells (293T) did not observe any reduction in infectivity. This suggests that there may be other cellular receptors, which at present are still unknown (Akula *et al.*, 2002; Inoue *et al.*, 2003).

In addition to gB, KSHV also encodes counterparts of gH (ORF22) and gL (ORF47), as possessed by other herpesviruses. Observations using a cell-based assay with susceptible cells as targets showed that only gB, gH and gL are required for virally-induced membrane fusion (Pertel, 2002). On the other hand a more recent paper has suggested that KSHV infection of human fibroblast cells occurs through endocytosis and not fusion to the cell membrane (Akula *et al.*, 2003). As viral entry into a cell is a complex and often a multi-step process, cell attachment and internalisation can be distinct steps, which may both need to be focused on when studying viral entry.

KSHV encodes two lytic transcriptional activators, K-bZIP (ORF K8) and RTA (replication and transcription activator) (ORF 50). These genes act as a master control switch that cause a cascade of lytic viral gene expression and are homologues of the EBV Zta and Rta. RTA is the major transactivator and induces expression of Kb-ZIP, an immediate-early gene product (Sun *et al.*, 1999). RTA autostimulates its own expression and acts as a positive feedback mechanism and thus controls the lytic gene transcription cascade (Gradoville *et al.*, 2000). KSHV contains many of the common genes required for replication and virion assembly as encoded by other herpesviruses, however, KSHV also possess several more homologues of cellular proteins. For instance, with particular reference to DNA synthesis enzymes, in addition to DNA pol (ORF 9), TK (ORF 21), and ribonucleotide reductase (ORF 60 and 61) genes, KSHV also encodes genes encoding thymidylate synthase (ORF70), dihydrofolate reductase (ORF2) and FGART (N-formylglycinamide ribotide amidotransferase, ORF75). It is thought that these homologues may either be

supplementing the G1 and S phase regulated cellular genes or extend the S-phase of DNA synthesis during the cell cycle (Cinquina *et al.*, 2000).

In vitro lytic replication of KSHV can be triggered by chemical agents, including butyrate and the phorbol ester, TPA (12-*O*-tetradecanoylphorbol-13-acetate), as seen with EBV (Miller *et al.*, 1997). The natural trigger for reactivating KSHV infection is still unknown, however simultaneous infection with other viruses, such as HIV, may play a role in this switch from latency.

The precise pathway taken for viral assembly and egress is still unclear but it is thought that primary envelopment occurs in the nuclear membrane. This is followed by de-envelopment; the capsid then binds into the trans-golgi network (TGN) and is finally secreted out of the cell. On entry into a new host cell, the linear KSHV genome re-circularises at its terminal repeat region to form a circular episome, which is tethered to the cellular chromosome by the latency-associated nuclear antigen (LANA) encoded by ORF 73. This association allows the equal segregation of latent viral genomes to daughter cells during mitosis. The origin-of-plasmid replication (ori-P), the actual site where LANA binds the viral DNA has been identified to lie within the terminal repeat of KSHV; the C terminus of LANA binds to a 20-bp imperfect palindrome within the terminal repeat (Garber *et al.*, 2001). Viral gene expression is minimal during latency, where the primary roles are involved with evading the host immune responses; the virus relies on cellular nucleic acid replication machinery for survival and the expression of its latent proteins.

Two polycistronic transcripts located at the right end of the genome are constitutively expressed in PEL cells; their levels do not increase following induction. The first transcript (5.3 Kb) encodes LANA (ORF 73), v-cyclin (ORF 72) and v-FLIP (ORF 71), while the second smaller transcript (1.7kb) is a spliced variant of the first; it only encodes v-cyclin and v-FLIP (Sarid *et al.*, 1999; Talbot *et al.*, 1999) (Figure 1.8).

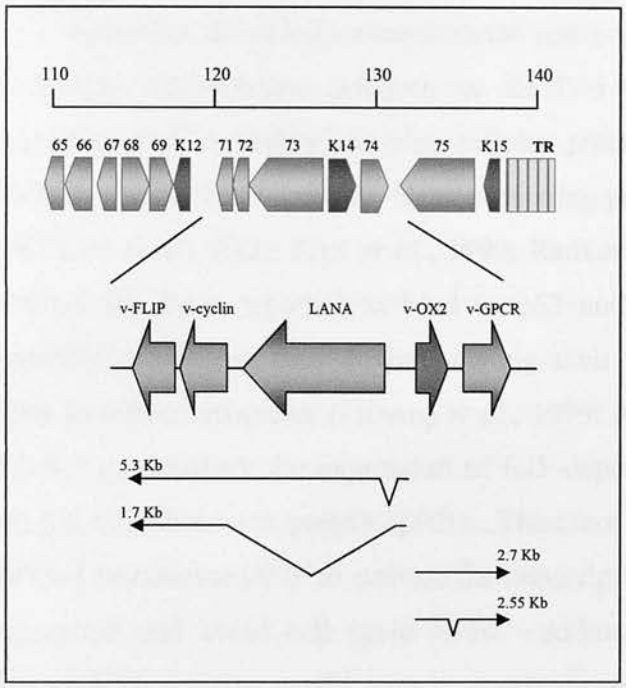

Figure 1.8 Alignment of genes from the right end of the KSHV genome and mRNA transcripts from ORFs 71 to 74 encoding v-FLIP, v-cyclin, LANA, v-OX2 and v-GPCR, respectively. Diagram adapted from Talbot *et al.*, 1999.

1.4.3.1 *Latent nuclear antigen (LANA-1, LNA-1)*

LANA-1 (encoded by ORF 73) is a protein of approximately 200KDa in size. KSHV-infected PEL cells and KS-spindle cells can be verified for the presence of latent virus by staining for LANA-1 (Ballestas *et al.*, 1999); as LANA-1 is one of the few proteins expressed during latency, antibodies to LANA-1 are often used as serological evidence for infection (Dupin *et al.*, 1999).

LANA-1 is an important nuclear protein involved in a variety of roles essential for the establishment of latency. Firstly, LANA-1 is required for the long-term maintenance of viral episomal DNA. By acting as a "molecular bridge", LANA-1 tethers the viral episome to the host chromosome and aids in efficient segregation of episomes to progeny nuclei. The C-terminus of LANA-1 binds preferentially and directly to the terminal repeats (TRs) of KSHV, whereas the N-terminus mediates attachment to nuclear chromatin during interphase and to mitotic chromosomes (Piolot *et al.*, 2001; Viejo-Borbolla *et al.*, 2003). Studies on LANA-1 have demonstrated it is essential, and identified areas of importance within the protein required for DNA binding, replication and episome persistence (Ballestas and Kaye, 2001; Komatsu *et al.*, 2004).

Secondly, it has been demonstrated that LANA-1 has the ability to modulate the cellular transcription program in KSHV-infected cells, through the direct interaction with a variety of host cellular proteins including RING3, mSin3A, CREB-2 (Cyclic AMP response element binding protein), and CBP (Krithivas *et al.*, 2000; Lim *et al.*, 2000; Platt *et al.*, 1999; Radkov *et al.*, 2000). More importantly LANA-1 has been reported to bind to p53 and repress the expression of p53-dependent promoters, thus downregulating their transcriptional activity and their ability to induce apoptosis (Friborg *et al.*, 1999; Katano *et al.*, 2001). In addition, LANA-1 can mediate the expression of E2F-dependent transcription by interacting with the retinoblastoma protein (pRB). Therefore by competing with E2F for pRb, LANA-1 has released E2F to activate the transcription of genes involved in cell cycle progression and avoid cell cycle arrest. Although, under normal circumstances aberrant E2F activity would trigger apoptosis via the p53 pathway, this is also inhibited by LANA-1. Therefore LANA-1 allows KSHV infected cells to promote cell cycle progression whilst inhibiting apoptosis (Radkov *et al.*, 2000). These functions are similar to those seen in other oncogenic proteins such as the large T antigen of SV40 and the E6/E7 protein of HPV.

Although no obvious sequence homology is shared between LANA and the EBV nuclear antigen-1 (EBNA-1), they are partially orthologous (functionally equivalent). EBNA-1 is responsible for episomal maintenance and transcriptional regulation. More recently, the ORF 73 from HVS has been shown to possess a *cis*-acting sequence that enables the efficient persistence of episomes in HVS infected cells (Calderwood *et al.*, 2004; Verma and Robertson, 2003).

1.4.3.2 *v-Cyclin (vCYC)*

ORF 72 encodes a protein, v-cyclin, that shares homology with human D-type cyclins and the v-cyclin of HVS; as KSHV-v-cyclin has only 32% amino acid identity with the HVS v-cyclin, it is surprising that they also share several biochemical features (Li *et al.*, 1997). Cyclins are utilised during the progression through the cell cycle; human cyclin D is primarily generated during the G1 and S phase, and activates the cyclin-dependent kinases (CDK4 and CDK6), which phosphorylate target proteins such as pRB. *In vitro* studies have shown that KSHV

v-cyclin is able to phosphorylate pRB following the formation of a complex with CDK6, in a similar manner to v-cyclin from HVS, and to a lesser extent forms a complex with CDK4 (Godden-Kent *et al.*, 1997; Li *et al.*, 1997). v-Cyclin also possesses another advantage in that unlike the cellular cyclins, it is resistant to the CDK inhibitors p16, p21 and p27 and thus avoids G1 arrest (Swanton *et al.*, 1997). The evasion of p27 arrest is mediated by the direct phosphorylation of p27 by the v-cyclin/CDK6 complex resulting in the degradation of p27 (Ellis *et al.*, 1999; Mann *et al.*, 1999). The v-cyclin/CDK6 complex also has the ability to phosphorylate histone H1, Cdc25a, Id-2, E2F-4, orc1 and cdc6 (Duro *et al.*, 1999; Godden-Kent *et al.*, 1997; Laman *et al.*, 2001; Li *et al.*, 1997; Mann *et al.*, 1999).

In cells with elevated levels of CDK6, v-cyclin not only accelerates entry into S phase, but also results in apoptosis independent of pRB and p53 (Ojala *et al.*, 1999). This is likely to be due to the phosphorylation of the cellular anti-apoptotic factor Bcl-2 by the v-cyclin/CDK6 complex that renders it inactive (Ojala *et al.*, 2000). KSHV also encodes a viral homologue of the cellular Bcl-2, v-Bcl-2, that can inhibit the v-cyclin/CDK6-induced apoptosis, however as v-Bcl-2 is only expressed during lytic infection it is not clear if it plays a relevant role during latency. v-Cyclin is expressed during both latency and lytic viral replication of KSHV (Dittmer *et al.*, 1998; Sarid *et al.*, 1998).

1.4.3.3 *v-FLIP*

Normal cell death can be induced via the engagement of the death receptor e.g. Fas, resulting in the recruitment of intracellular adapter molecules such as the Fas-associated death domain (FADD). These molecules can in turn interact and activate the upstream capsases via the interaction with the death effector domain (DED) or caspase recruitment domain (CARD), thus resulting in the activation of downstream caspases and ultimately death of the cell (Ashkenazi and Dixit, 1998; Djerbi *et al.*, 1999; Thornberry and Lazebnik, 1998). Several γ-herpesviruses and the molluscipox virus encode a protein able to prevent cell death by this route, therefore allowing extended viral replication. Viral FLICE (FADD-like IL-1β-converting enzyme)-inhibitory proteins (vFLIPs) were first identified and knowing that many

viruses possesses cellular homologues, cellular FLIPs were later identified (Irmler *et al.*, 1997).

KSHV v-FLIP contains two DEDs and protects cells from Fas-mediated apoptosis by inhibiting caspase activation and thus permits clonal growth. Studies in which mice were injected with v-FLIP-expressing B cells developed aggressive tumours by preventing death receptor–induced apoptosis triggered by CTLs; thus displaying a role as a tumour progression factor (Djerbi *et al.*, 1999). It is therefore feasible that one role for v-FLIP is to prevent apoptosis triggered by CTLs, which may also explain the close linked expression of its neighbouring ORF encoding v-cyclin. As v-cyclin possesses an IRES (internal ribosome entry site), it is likely that this allows the bi-cistronic transcript to be expressed as required throughout the cell cycle, thus protecting infected cells from CTL-mediated apoptosis; unlike cap dependent expression, an IRES is not susceptible to inhibition of translation in the G_2/M phase (Bieleski and Talbot, 2001; Grundhoff and Ganem, 2001). Furthermore, this protein is believed to be involved in the pathogenesis of KS, due to the detection of v-FLIP transcripts in late stage KS lesions and the reduced levels of apoptosis (Sturzl *et al.*, 1999a).

LANA-1, v-cyclin and v-FLIP are the predominant proteins detected during latency, although expressions of other viral transcripts such as K7, nut-1 (T1.1/PAN RNA) and vOX2 (K14) have been detected. It is believed that detection of these transcripts are due to the small minority (1%) of spontaneously lytic cells, as over a 100-fold increase in expression is observed following lytic induction (Jenner *et al.*, 2001). It should be noted that this expression pattern is the norm in both KS lesions and PEL tumours; however, KSHV infected cells in MCD lymph nodes display a different pattern of gene expression. Only a small proportion of cells in MCD are KSHV positive, and in addition to expressing LANA, many also co-express several other proteins, including vIL-6, K8.1, K10 and K11. It is unknown if there are more cells present undergoing lytic replication or if in MCD there is a expanded pattern of latent KSHV gene expression (Moore and Chang, 2001).

Another transcript detected in PEL cell lines is K15 (Paulose-Murphy *et al.*, 2001), although it is upregulated with TPA induction of the latent virus. ORF K15 encodes a transmembrane protein that is not only located in a similar location to

EBV's LMP-2A, but K15 shares features with both LMP-1 and LMP-2A. In short, K15 has SH2, SH3 and TNFR-associated factor (TRAF) binding domains and is able to activate NK-κB pathways, but can also bind to the HS1 associated protein X-1 (HAX-1), a protein with anti-apoptotic function (Brinkmann *et al.*, 2003; Choi *et al.*, 2000b; Sharp *et al.*, 2002). Additionally, the T0.7 transcript, containing Kaposin (K12) is also present in many spindle cells of advanced tumours (Staskus *et al.*, 1997) and will be discussed further in the following section.

1.4.4 Molecular Mimicry

KSHV possesses numerous genes encoding proteins that share striking homology with cellular proteins (Table 1.4 and Figure 1.9). Several of these ORFs encode proteins that are involved with KSHV pathogenesis by a variety of means such as disrupting cellular signal transduction pathways, including interferon-mediated anti-viral responses, cytokine-regulated cell growth, apoptosis and cell cycle control (Figure 1.9).

1.4.4.1 *Anti-apoptotic viral genes*

Most DNA viruses contain genes that are able to inhibit apoptosis. As mentioned earlier, KSHV encodes two anti-apoptotic genes v-FLIP and v-Bcl-2. v-FLIP has the ability to protect against Fas/APO1 mediated apoptosis by inactivating various caspases, whereas v-Bcl-2, can block both Bax-mediated and virally induced apoptosis (Cheng *et al.*, 1997; Friborg *et al.*, 1998; Sarid *et al.*, 1997).

1.4.4.2 *Viral cytokine homologues*

1.4.4.2.1 *Viral macrophage inflammatory proteins (vMIPs)*

The ability to control inflammatory responses is an advantage; several herpesviruses have captured and modified cellular chemokine and chemokine receptors, thus allowing them to modulate the host immune response (Choi *et al.*, 2001; Parry *et al.*, 2000). KSHV encodes three multifunctional CC chemokines, vMIP-I, vMIP-II, and vMIP-III, which all share between 25-40% homology at the amino acid level with the cellular macrophage inflammatory protein α (MIP-1α) (Moore *et al.*, 1996; Nicholas *et al.*, 1997). vMIP-I and vMIP-III are chemokine

receptor agonists, whereas vMIP-II has a more unusual broad spectrum of receptor binding activities. vMIP-II can block the cheomoattractant signalling of CC chemokine receptor 1 (CCR1), CCR2, CCR3, CCR5 and CXCR4 by acting as a competitive antagonist (Kledal *et al.*, 1997; Murphy, 2001).

1.4.4.2.2 *vIL-6*

A potential role of IL-6 in KS and MCD was suspected long before the discovery of the virus, let alone its viral homologue, vIL-6; proliferation of cultured KS cells was enhanced in the presence of IL-6 and a correlation between elevated IL-6 levels and disease development in MCD was observed (Ishiyama *et al.*, 1996; Miles *et al.*, 1990; Yoshizaki *et al.*, 1989). Initial findings by Molden *et al.* (1997) showed that unlike cellular IL-6 (hIL-6), vIL-6 could activate specific JAK/STAT signalling via interactions with the gp130 signal transducing surface marker, independently of the IL-6Rα subunit (gp80). Although it has been disputed whether vIL-6 is able to associate with the IL-6Rα subunit (Aoki *et al.*, 1999; Li *et al.*, 2001), a recent study by Boulanger *et al.* (2004) supports and verifies that vIL-6 can also form a hexameric complex with gp130 and IL-6Rα, which has enhanced signalling potency.

Additionally, like hIL-6, vIL-6 is able to induce VEGF expression that mediates angiogenicity; vIL-6 is able to affect both B-cell lineage haematopoiesis and angiogenesis (Mesri, 1999; Hoischen *et al.*, 2000). Studies have shown that vIL-6 can stimulate all of the known hIL-6 induced signalling pathways, therefore potentially contributing towards disease progression through the activation of IL-6 stimulated growth and anti-apoptotic pathways (Osborne *et al.*, 1999).

1.4.4.3 *Genes associated with transformation*

1.4.4.3.1 *K1*

KSHV contains several ORFs that share similarities to other genes with transformation properties. K1 is located at a position equivalent to the oncogenes LMP1 of EBV and STP of HVS. The extracellular domain of the K1 protein has homology with the variable region of the lambda chain of the immunoglobulin (Ig) light chain, and is similar to Ig-α and Ig-β. The cytoplasmic tail contains a

functional ITAM (immuno-receptor tyrosine-based activation motif) (Lee *et al.*, 1998a). The ITAM in K1 is able to elicit signals that in turn activate cellular transduction events (Lagunoff *et al.*, 1999). In addition, K1 is also able to down-regulate B-cell receptor (BCR) surface expression, as the amino-terminal of the protein can specifically interact with the μ chains of BCR complexes and inhibit its intracellular transport (Lee *et al.*, 2000). Various studies support a potential pathogenic role for K1. A recombinant HVS, in which STP was replaced with KSHV K1, was able to transform T lymphocytes and induce lymphomas in common marmosets (Lee *et al.*, 1998b). In addition, a recent study also found the development of a salivary gland tumour and increased inflammatory response in mice infected with a recombinant murine gammaherpesvirus (MHV-76) expressing the KSHV K1 gene (Douglas *et al.*, 2004).

1.4.4.3.2 *vGCR/ vGPCR*

Another gene with a potential role in increasing the tumorigenicity of virally infected cells is vGCR, a homologue of the human receptor for the angiogenic chemokine IL-8 (IL-8R); vGCR is a constitutively active seven-transmembrane protein. This protein is expressed during the early phase of lytic infection and can bind to a broad spectrum of chemokines including IL-8, MGSA, NAP-2, and RANTES (Cesarman *et al.*, 2000; Ho *et al.*, 1999). Studies on vGCR have found that the N-terminal extracellular region is not necessary for constitutive signalling, whereas it plays a more crucial role in the binding of chemokine ligands (Ho *et al.*, 1999). It has been demonstrated that the angiogenic response by vGCR is mediated by the up-regulation of VEGF, which can activate the protein kinases JNK/SAPK and p38MAPK and trigger a cascade of signal transduction pathways similar to other inflammatory cytokines (Bais *et al.*, 1998). More recently, Cannon *et al.*, (2003) have shown that expression of vGCR during latency in PEL cells, increased the expression of vIL-6 and VEGF, two cytokines also involved in the pathogenesis of KSHV-associated diseases.

1.4.4.3.3 *vIRF*

Many viruses have evolved various means to overcome cellular IFN defence mechanisms, such as EBNA-2 of EBV which inhibits IFN signalling by interfering

with the induction of IFN-stimulated genes (Kanda *et al.*, 1992). In KSHV the K9 ORF encodes vIRF, a unique viral protein that shares 13% amino acid identity with several IFN regulatory factors (IRFs). vIRF expression reduces transcriptional activation induced by IFN - α/β/γ (Gao *et al.*, 1997; Li *et al.*, 1998), but does not compete with the cellular IRF-1 for DNA binding nor form a complex with IRF-1 (Zimring *et al.*, 1998). Additionally, vIRF displays oncogenic properties as *in vitro* expression induced transformation of rodent fibroblast cells and tumours in nude mice (Li *et al.*, 1998). It is believed that these properties are in part due to the interaction of vIRF with p300 and CREB-binding protein (CBP) (Burysek *et al.*, 1999; Li *et al.*, 2000; Seo *et al.*, 2000). This results in the displacement of PCAF from the p300 complex and in turn inhibits the histone acetyltransferase (HAT) activity of p300, thus leading to the downregulation of transcriptional activation of the early inflammatory gene promoter (Burysek *et al.*, 1999). Jayachandra *et al.* (1999) also demonstrated that induction of the myc protooncogene is required for cell transformation by vIRF and that vIRF increases myc transcription.

More recently studies have shown that vIRF can interact with p53 and inhibit p53-mediated transcriptional regulated apoptosis (Nakamura *et al.*, 2001; Seo *et al.*, 2001). Finally, vIRF has the ability to auto-activate its own promoter, thus enabling the expression of this protein to be regulated to efficiently evade host tumour suppressor pathways (Wang and Gao, 2003).

1.4.4.3.4 *Kaposin*

T0.7 is an abundantly expressed latent transcript containing three small ORFs, derived from ORF K12 (Kaposin) and either of two reading frames within repetitive elements (DR1 and DR2) upstream of K12 (Sadler *et al.*, 1999). This transcript has been detected by *in situ* hybridisation in all KS tumours throughout all stages, i.e. early to late, and in PEL and MCD (Sturzl *et al.*, 1997, 1999b). Expression of these proteins are upregulated following induction of lytic viral replication in both KS and PEL cell lines (Sadler *et al.*, 1999), and therefore may serve functions during both latency and lytic replication. Studies on K12 have shown that this protein has transforming properties (Kliche *et al.*, 2001; Muralidhar *et al.*, 1998, 2000). Muralidhar *et al.*, (1998) observed the transformation of Rat-3 cells due to the expression of K12, this led to the development of high grade, highly

vascular, undifferentiated sarcomas following injection of athymic mice. However, research on K12 is limited and complex; the potential multiple biological functions that this protein may possess are still not fully known.

1.4.4.4 *Modulators of Immune responses*

1.4.4.4.1 *K3 and K5*

The ability to outwit and evade the hosts defence system is a high priority during viral infection. There are two major branches of the immune system: (i) the early non-specific or innate response includes the use of interferons, NK cells and macrophage, whereas (ii) the specific or adaptive response is lead by CTLs, helper-T cells and anti-viral antibodies (Ploegh and Watts, 1998). As CTLs recognise viral antigens presented as peptides bound to class I MHC (MHC I) expressed on the surface of infected cells, it is to no great surprise that many viruses have evolved mechanisms to evade CTL recognition. For example, HSV-1 encodes a protein, ICP47, that binds to TAP and prevents assembly of MHC I in the ER, whereas EBNA-1 of EBV is not efficiently processed and not presented by MHC I (Fruh *et al.*, 1995; Hill *et al.*, 1995; Levitskaya *et al.*, 1995). KSHV encodes two proteins, K3 and K5, which are able to drastically down-regulate surface expression of MHC I. Unlike other viral evasion methods, K3 and K5 do not influence the expression or intracellular transport of MHC I, but employ a unique mechanism whereby they induce rapid endocytosis of MHC I (Coscoy and Ganem, 2000; Ishido *et al.*, 2000).

K3 and K5 exhibit 40% amino acid identity with each other and are expressed during the early lytic cycle of viral replication. Although K3 and K5 share similar sequence and function, they differ in specificity; K3 down-regulates all four HLA allotypes (A-D), whereas K5 only down-regulates HLA-A and –B (Ishido *et al.*, 2000). Even though some protection is given against CTLs, these cells are now more susceptible to NK cell clearance. However, K5 is also able to repress ICAM-1 and B7-2, both of which are ligands for NK-cells; thus K5 expression can also reduce NK-cell mediated cytotoxicity (Ishido *et al.*, 2000). Interestingly, it has recently been suggested that K3 and K5 may aid in evading host immune responses during latent infection, as expression of MHC I is also reduced on cells harbouring latent virus (Tomescu *et al.*, 2003).

1.4.4.4.2 *vOX2*

Another transmembrane protein that may be involved in immune regulation is vOX2, encoded by ORF K14. This protein shares remarkable homology with the human OX2 gene (recently designated CD200) and will be discussed further in section 1.5.

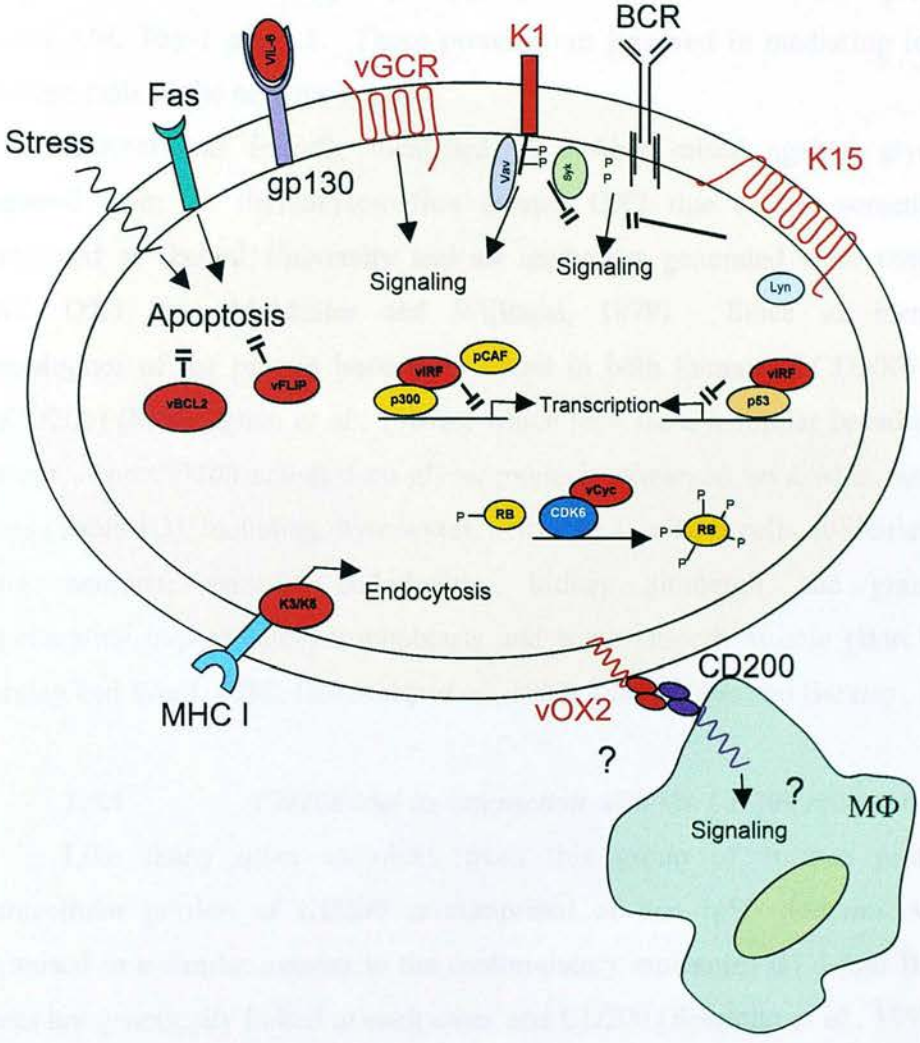

Figure 1.9 KSHV proteins influence on cellular transduction pathways. Proteins expressed by KSHV are indicated in red and more detailed descriptions are given in the text of section 1.4.4. 'Activated' pathways are indicated by → and 'blocked' pathways are indicated by —II (Image adapted and modified from Choi *et al.*, 2001).

1.5 CD200

Many cells express a vast number of surface molecules that are involved in a variety of roles. The immunoglobulin superfamily (IgSF) domains are the most predominant on the surface of leukocytes and approximately a third of all surface proteins fall into this group (Preston *et al.*, 1997). The OX2 protein, recently assigned CD200, is a leukocyte IgSF glycoprotein similar to other glycoproteins such as N-CAM, Thy-1 and L1. These proteins are involved in mediating interactions between cells of the nervous system.

CD200 was initially identified by mAb's raised against glycoproteins prepared from rat thymocytes; first termed OX2 due to the screening being performed at Oxford University and all antibodies generated were termed OX1, OX2, OX3 etc. (McMaster and Williams, 1979). Since its identification, homologues of the protein have been found in both humans (hCD200) and mice (mCD200) (McCaughan *et al.*, 1987a), which also share a similar broad expression pattern. The CD200 cell-surface glycoprotein is expressed on a wide range of cell types (Table 1.3), including thymocytes, activated T cells, B cells, follicular dendritic cells, neurons, vascular endothelium, kidney glomeruli, the granulosa of degenerating copora lutea, trophoblasts and some smooth muscle (Barclay, 1981; Barclay and Ward, 1982; Bukovsky *et al.*, 1983, 1984; Webb and Barclay, 1984).

1.5.1 *CD200 and its interaction with the CD200 receptor*

Like many other members from this group of surface proteins, the extracellular portion of CD200 is comprised of two IgSF domains, which are organised in a similar manner to the costimulatory molecules B7-1 and B7-2; these genes are genetically linked to each other and CD200 (Borriello *et al.*, 1997). Many IgSF proteins are involved in the control of the immune system. However, due to a short cytoplasmic region with no known signalling motifs, CD200 is not thought to be directly involved in signalling. CD200 has recently been shown to interact with another surface glycoprotein termed CD200-receptor (CD200R or OX2R) (Figure 1.10). Like CD200, the receptor consists of two IgSF domains also in the common V/C2 set arrangement, but in contrast CD200R also possesses a longer cytoplasmic region (67 a.a compared with 19 a.a in CD200). The cytoplasmic tail contains three

tyrosine residues that can be phosphorylated, one of which is contained within an NPXY PTB-binding motif, thus suggesting that it can signal (Wright *et al.*, 2000, 2003). Genes sharing homology to the receptor have also been found in both mice and rats, termed mCD200R and rCD200R respectively.

CD200R was initially found to be expressed only on cells of myeloid lineage and a small subset of T cells as detailed on Table 1.3 (Borriello *et al.*, 1997; Preston *et al.*, 1997). More recently, a group from the University of Oxford, have detected CD200R expression in humans and mice to be strongest on macrophage and neutrophils but also on other leukocytes including monocytes, mast cells and some subsets of T lymphocytes (Wright *et al.*, 2003).

Table 1.3 Summary of tissue distribution of human and mouse CD200 and CD200R

CD200[f]	hCD200R*	mCD200R*
Activated T Cells	Dendritic Cells	Macrophage
B Cells	Granulocytes	Monocytes
Follicular Dendritic Cells	Macrophages	Granulocytes
Neurons	Monocytes	Mast Cells
Kidney Glomeruli	γδT Cells	γδT Cells
Vascular Endothelium	Mast Cells	Dendritic Cells
Trophoblasts		
Thymocytes		
Some smooth muscle		
Granulosa of degenerating corpora lutea		

[f]Data summarised from mouse, rat and human due to the similar expression pattern, references from (Barclay, 1981; Barclay and Ward, 1982; Bukovsky *et al.*, 1984; Webb and Barclay, 1984; Wright *et al.*, 2001). *Human and mouse CD200R expression graded with cells expressing larger amounts at the top and smaller amounts towards the bottom of the column, results summarised from (Wright *et al.*, 2003).

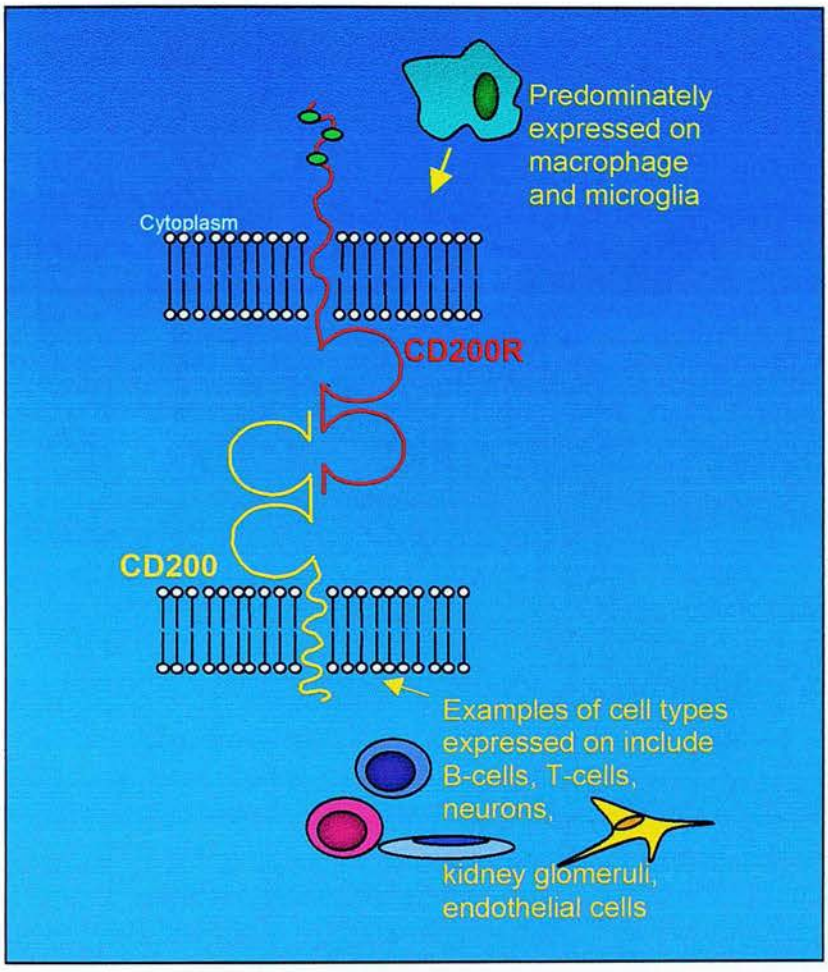

Figure 1.10 Schematic representation of CD200:CD200R ligand:ligand-receptor interaction. Both CD200 and CD200R are IgSF glycoproteins comprised of two extracellular domains (V/C2 arrangement), a single transmembrane region and a cytoplasmic region; CD200 only posses a short sequence with no known signaling motifs, while on the other hand CD200R encodes a longer cytoplasmic region with three tyrosine residues (●) that can be potentially phosphorylated and involved in signal transduction. CD200 is expressed on a wide range of cells, whereas CD200R is restricted to cells of myeloid-lineage and some subset of T cells. The interaction interface involves the N-terminal domain, resulting in a cell-cell interaction spanning four IgSF domains, similar to many interactions found between T cells and antigen presenting cells.

In humans, both the CD200 and CD200R gene are located near to each other on chromosome 3 and are transcribed in the same direction, unlike mCD200 and mCD200R, which are both found on mouse chromosome 16 but transcribed in different directions (McCaughan *et al.*, 1987b; Wright *et al.*, 2003). Further phylogenetic analysis of CD200R and other IgSF proteins indicates that CD200 and its receptor are closely related to each other and likely to have evolved from a common ancestral protein (Figure 1.11) (Wright *et al.*, 2000).

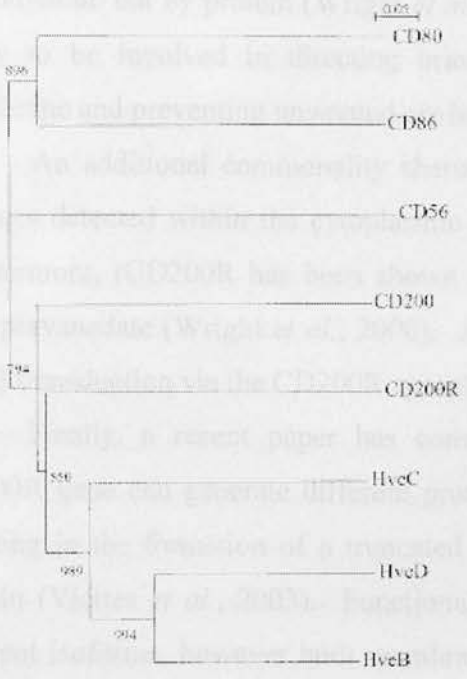

Figure 1.11 Phylogenetic analysis of human CD200, CD200R and some human herpesvirus entry proteins. The N-terminal Ig domains of hCD200; hCD200R; human herpesvirus entry proteins HveB, C and D; and other human Ig-like proteins (CD56, CD80, and CD86) were aligned using ClustalW, manually refined and then construction of a Neighbour-joining tree with 1000 bootstrap trials (In Hve proteins and CD56, only the membrane distal two domains were compared). Redrawn with permission from Wright *et al.*, 2003.

Using soluble fusion proteins and recombinant proteins, Wright *et al.* (2003) were able to confirm that both the mouse and human CD200 bound to their respective receptors and that hCD200:hCD200R interact with an equilibrium – binding affinity (K_D) of ~0.5μM at 37°C and a kinetic off rate (K_{off}) of ~0.15 s^{-1}, similar to those seen in equivalent interactions in mice and rats (Wright *et al.*, 2000, 2003); these values are typical of many leukocyte protein membrane interactions. Cross species binding was also tested, revealing that hCD200 was able to interact with both mouse and rat CD200R, although binding to mCD200R was weaker (Wright *et al.*, 2003).

Another unusual feature possessed by both CD200 and CD200R when compared with other IgSF proteins, is the high amount of potential N-linked glycosylation sites; CD200R has eight sites in the human and rat and ten in mouse sequences (Wright *et al.*, 2000, 2003), whereas the six predicted sites in CD200 are conserved in all three species (Borriello *et al.*, 1997; Clark *et al.*, 1985; McCaughan *et al.*, 1987a). Following analysis of mutagenesis studies (Preston *et al.*, 1997) and comparison with other IgSF interactions (van der Merwe *et al.*, 1993), it has been suggested that the CD200:CD200R immunoglobulin binding is not mediated by carbohydrate but by protein (Wright *et al.*, 2000). The high carbohydrate content is likely to be involved in directing orientation of the protein in relation to the membrane and preventing unwanted *cis*-interactions (Wright *et al.*, 2000).

An additional commonality shared between the CD200Rs is three tyrosine residues detected within the cytoplasmic region that is conserved between species. Furthermore, rCD200R has been shown to be phosphorylated following treatment with pervanadate (Wright *et al.*, 2000). At present the mechanism and pathway for signal transduction via the CD200R cytoplasmic receptor is still unknown.

Finally, a recent paper has commented on the findings that the human CD200R gene can generate different protein isoforms through alternative splicing, resulting in the formation of a truncated soluble protein containing only the V Ig domain (Vieites *et al.*, 2003). Functional studies have not been performed on the different isoforms, however both membrane-bound and soluble versions have been detected in the thymus, liver, spleen and placenta by Northern-blot analysis (Vieites *et al.*, 2003). On a similar note, a gene related to the human receptor, termed CD200 receptor-like ($hCD200RL_a$), and an additional four genes in mice have been detected ($mCD200RL_{a-d}$), which have all presumably evolved from recent gene duplications (Wright *et al.*, 2003). Analysis suggests that the $hCD200RL_a$ is non-functional, whereas $mCD200RL_a$ and $mCD200RL_b$ are able to pair with the activatory adaptor protein, DAP12 (possibly transmitting activating signals), but not with the mCD200 ligand (Wright *et al.*, 2003).

1.5.2 *CD200:CD200R Function Studies*

A variety of roles for CD200 in antigen presentation have been proposed including both stimulatory (Borriello *et al.*, 1997) and tolerogenic (Gorczynski *et al.*, 1999a, 1998, 2000d). In addition, CD200 has also been suggested to generate a down-regulatory signal on myeloid-lineage cell populations (Barclay *et al.*, 2002; Hoek *et al.*, 2000). Although CD200 was identified over 20 years ago, insights into its importance and function are only just coming to realisation, and a full understanding of its role within the immune system is still not clear. Early studies by Borriello *et al.* (1997) indicated that mCD200 has the ability to mediate a costimulatory signal to murine $CD4^+$ T cells leading to proliferation. The expansion of T cells was seen to neither be independent of the B7/CD28 pathway nor result in detectable levels of IL-2, IL-4 or IFN-γ; however, T cell proliferation was inhibited by approximately 80% by anti-mCD200 mAb (Borriello *et al.*, 1997). Additionally, several studies by Gorczynski's group (Clark *et al.*, 2001a, 2001b; Gorczynski *et al.*, 1999a, 1999b, 1999c, 2000a, 2000b, 2000c, 2002a, 2002b, 2002c) have shown that CD200 expression contributes toward not only the survival of allografts and xenografts but also successful pregnancies. Observations by this group have found that mCD200 expression increased following the treatment of mice with portal vein (pv) donor-specific immunisation, which promotes renal allograft survival (Gorczynski *et al.*, 1998). Furthermore, antibodies to CD200 abolished graft prolongation in both the mouse renal allograft and rat small intestinal allograft model (Gorczynski *et al.*, 1998, 1999c), and additionally blocked the polarization of T cells to produce type 2 cytokines (IL-4, IL-10, IL-13) that are normally induced by pv immunisation. Further investigations using a soluble immunoadhesion, CD200:Fc (extracellular domain of CD200 linked to a mutated murine IgG2aFc region) exemplified previous findings, as T cell allostimulation and type I cytokine production (IL-2 and IFN-γ) were blocked by CD200:Fc and both allograft and xenograft survival was prolonged (Gorczynski *et al.*, 1999b, 2002c).

These studies and several others by Gorczynski's group (Gorczynski *et al.*, 1999b, 2000d, 2001a, 2004) present evidence supporting their hypothesis that CD200 is involved in the delivery of a "coregulatory" signal that is able to modify the functional outcome of the TCR:Ag encounter. More specifically, a negative

"tolerizing" signal to the T cells involved in the graft survival experiments. When it later became apparent that CD200 interacts with its receptor, CD200R (expressed on a sub-population of activated T cells, predominately $\gamma\delta TCR^+$ T cells, and macrophages), the CD200:CD200R engagement was consistent with their hypothesis that these proteins were indeed involved in an immunoregulatory role.

With respect to CD200's involvement as an immunoregulatory protein involved in pregnancy, Th1 cytokine-dependent abortions in CBA/JxDBA/2 mouse models have been linked with the down-regulation of CD200 on trophoblast and in decidua preceding the abortion process. This was evident as the addition of soluble CD200:Fc results in a marked decrease in abortion. Whereas in an opposing system, the administration of CD200 mAb was found to boost abortion rates (Clark *et al.*, 2001a, 2001b). Furthermore, it has been demonstrated that CD200 is able to activate production of indole amine 2,3-dioxygenase (IDO) by antigen-presenting macrophage that can in turn suppress antigen-specific T cell responses (Gorczynski *et al.*, 2002b). In a recent study by Clark *et al.* (2003), data supports the findings that CD200 expression on placental trophoblasts from successful human pregnancies displayed the Th1→Th2 shift previously observed in mouse models (Clark *et al.*, 2001a). Thus down-regulation of CD200 may also be a reason for foetus rejection in humans. Further studies on first trimester termination and spontaneous miscarriage tissue samples need to be investigated to verify CD200 expression patterns and the mechanism of suppression. It is still not clear if suppression was due to: co-stimulation of antigen-activated γδT cells releasing cytokines IL-10 and TGF-β that inhibit Th1-type response; activation of IDO; or by some alternative mechanism.

Strong evidence supporting the CD200:CD200R interaction playing a regulatory role is seen in data from Barclay's group at Oxford University. The most striking observations were made using C57BL/6 CD200 knockout (KO) mice. The phenotypic changes of these $CD200^{-/-}$ mice elucidated the importance of CD200 on the regulation of myeloid-lineage cells; these mice were normal in all aspects of appearance, life-span and behavioural patterns, but did possess an increase in the number of macrophage and granulocytes within the spleen, and enlarged mesenteric lymph nodes, also due to an increase population size of macrophages (Hoek *et al.*, 2000). Additionally, the resident CNS macrophage, microglia (MG), also displayed

features of activation, including increased CD11b and CD45 expression, less ramified, shorter glial processes and a disordered arrangement, in contrast to the ordered and ramified appearance seen in wild-type mice (Hoek *et al.*, 2000). The MG in the spinal cord also formed clustered groups, a phenotype normally associated with neurodegeneration. Using the facial transection model allowed localised MG activation to be studied; in $CD200^{-/-}$ mice a fast MG response was detected just 2 days after surgery with a peak at day 4, compared with days 4 and 7, respectively, in wild-type mice (Hoek *et al.*, 2000).

Other experiments were performed on these KO mice to investigate disease progression using two autoimmune models involving myeloid lineage cells. Experimental autoimmune encephalomyelitis (EAE), a model whereby the migration of activated T lymphocytes, macrophage and granulocytes to the CNS results in the activation of MG, tissue damage and neurological deficits including paralysis. These manifestations are induced in wild-type mice after injection with MOG (myelin oligodendrocyte glycoprotein) peptide and the development of the resultant pathogenesis occurs significantly earlier in $CD200^{-/-}$ mice, along with a greater number of activated macrophage and MG (Hoek *et al.*, 2000). EAE was also shown to be exacerbated in rats when MDG peptide was administered with an anti-CD200 mAb (Wright *et al.*, 2000).

The second model, collagen-induced arthritis (CIA), mimics rheumatoid arthritis and also involves an autoimmune response due to the same cell types as seen in EAE. Following an injection of collagen, the incidence of disease in wild-type mice is reasonably low (<10%), due to their relative resistant to CIA, whereas an incidence of over 50% and early onset of disease was observed in the $CD200^{-/-}$ mice. These results were further corroborated by data showing that wild-type mice became more susceptible to CIA when infected with an adenovirus encoding a soluble Ig-fused CD200R (Hoek *et al.*, 2000). Furthermore, administration of CD200:Fc or anti-CD200R to DBA/1 mice, which are susceptible (>50%) to CIA, resulted in the suppression of disease development (Gorczynski *et al.*, 2001b, 2002a). A passing comment should be made at this point with regards to the more recent finding that some mast cells have been shown to express the CD200 receptor (Wright *et al.*, 2003) and that both the EAE and CIA models are dependent on functional mast cells

(Lee *et al.*, 2002; Secor *et al.*, 2000). Therefore, it is possible that some of the results observed may also be due to a contribution from the mast cell population.

Other studies on myeloid activity within the retina of CD200 KO mice found that not only were there greater numbers of activated MG but that MG migration may also be mediated via the ligation of CD200R (Broderick *et al.*, 2002; Dick *et al.*, 2001, 2003).

In summary many of these studies have provided data to support the theory that CD200 interaction with the CD200R results in the down-regulation of myeloid-derived cells. Further evidence elucidating this proposed role is the finding that CD200R associated with SH2-containing inositol phosphatase (SHIP), which is consistent with a role in down-regulation of phagocytic activities (Barclay *et al.*, 2002). However, this does pose several questions (reviewed by Nathan and Muller, 2001); if the CD200:CD200R combination results in the down-regulation of myeloid cells, does this imply that these cells would normally be active all the time and if so, what overrides the CD200 signal, and then finally how is homeostasis restored after an inflammatory response is no longer required? It is more likely that the CD200:CD200R interaction is involved in modulating myeloid cell functions such as proliferation, survival, trafficking and migration.

More recently it has been proposed that CD200 may be a "don't eat me signal" or as coined in a review by Elward and Gasque (2003), a self associated molecular pattern (SAMP). Their hypothesis states that SAMPs are utilised as a mechanism to control the human and cellular innate immune response, in a manner similar to MHC Class I expression by host cells evading killing by natural killer (NK) cells. Therefore it is possible that CD200 and other SAMPs are signals assisting with the control of phagocytosis and associated inflammatory responses.

Indeed, if CD200 is truly involved in distinguishing between "eat me" and "don't eat me" signals or alternative control mechanisms of myeloid-derived cell populations or T cells, it is highly likely that this would be an advantageous target for pathogens. Therefore it is not so surprising to find that several viruses have acquired a viral homologue of CD200.

1.5.3 *Viral Homologues of CD200*

Although it is not unusual to observe molecular piracy occurring during viral evolution, it is uncommon for viruses to encode proteins with IgSF domains compared to vertebrates where they are extremely common. CD200 homologues have been found in both the *Betaherpesviridae* (HHV-6 and HHV7) and the *Gammaherpesviridae* (KSHV and Rhesus Rhadinovirus [RRV]), but also more recently in viruses from the *Poxviridae* (Myxomavirus [MYX], Yaba-like disease virus [YLDV], Yaba monkey tumour virus, shope fibroma virus, and lumpy skin disease virus) (Table 1.4). Information regarding characterization studies on most of the viral homologues has yet to be reported. Illustrated in Figure 1.12 are schematic representations of the CD200-homologues for KSHV, RRV, MYX and YLDV. Like their cellular counterpart, many viral CD200s are also highly glycosylated and share some conserved sites. However, in contrast to the membrane-bound cellular CD200, the viral CD200s encoded by the *Poxviridae* are truncated, only encoding the V-like Ig domain, several of which are not membrane bound (i.e. produce a soluble protein) (Figure 1.12).

As viral homologues of CD200 are present in a range of evolutionary disparate viruses, it suggests that the gene was captured independently several times during viral evolution. This is further supported by the fact that many closely related viruses (to those encoding a viral CD200 homologue), such as HVS or the swinepox virus do not possess a CD200 homologue. Therefore it can be assumed that acquiring host CD200 has its advantages in viral evolution and thus may play an important role in the lifecycle of many viruses.

1.5.4 *KSHV K14*

KSHV encodes a unique ORF known as K14 or vOX2 (Accession number U75698) that generates a membrane bound protein that shares remarkable homology with the human CD200 IgSF protein (Figure 1.12). vOX2 is expressed as a bicistronic message along with vGPCR (Figure 1.8) as an early product during lytic replication (Jenner *et al.*, 2001; Paulose-Murphy *et al.*, 2001; Talbot *et al.*, 1999).

Limited information is available on KSHV vOX2 and its role in viral pathogenesis. Importantly, vOX2 has been reported to bind with the human CD200R

and intriguingly, with near identical kinetics to the hCD200:hCD200R interaction (Barclay *et al.*, 2002; Foster-Cuevas *et al.*, 2004). One intriguing feature additionally possessed by vOX2, but not its cellular counterpart, CD200, is the encoding of a tripeptide sequence Arg-Gly-Asp (RGD) (Figure 1.12). Although it is not known if this motif is functional; the RGD sequence is commonly associated with binding to integrins, which are involved in cell adhesion, cell migration, thrombosis and lymphocyte interactions (Hynes, 1987, 1992, 1999). An RGD motif found in the foot and mouth disease virus (FMDV) P1 protein is believed to be involved in the virus-receptor interaction (Baxt and Becker, 1990; Fox *et al.*, 1989; Grubman and Baxt, 2004).

In 2002, Chung *et al.*, reported data suggesting that vOX2 may act in an opposite manner to cellular CD200; instead of delivering a restrictive signal, their results implied that vOX2 may deliver an activating signal to myeloid-lineage cells. Therefore by promoting the production of inflammatory cytokines, vOX2 may be assisting angiogenic proliferation of KSHV-infected cells. In contrast to this paper, a more recent study by Foster-Cuevas *et al.* (2004) describe findings that not only describe the direct engagement of vOX2 with the host CD200R, but also the ability of this interaction to restrict TNF-α production by activated macrophages. Therefore via the direct cell surface engagement with CD200R, vOX2 may be able to regulate locally activated macrophage and subvert the host immune system, thus allowing increased viral replication. However, all of these findings have only been derived from *in vitro* studies using recombinant proteins; the role of vOX2 *in vivo* is still not know and may reveal a different role.

Table 1.4 Viruses possessing homologous genes to the cellular CD200

Family		*Virus*	*ORF*	*Reference*
Herpesviridae	*Betaherpesvirinae*	HHV-6	U85	(Gompels and Kasolo, 1996)
		HHV-7	U85	(Nicholas, 1996)
	Gammaherpesvirinae	KSHV	K14	(Russo *et al.*, 1996)
		RRV	R14	(Desrosiers *et al.*, 1997) (Searles *et al.*, 1999)
Poxviridae	*Chordopoxvirinae*	Myxomavirus	M141R	(Cameron *et al.*, 1999)
		Shope fibroma virus	S141R	(Willer *et al.*, 1999)
		Yaba-like disease virus	141R	(Lee *et al.*, 2001)
		Yaba monkey tumour virus	Yb-C2R	(Kilpatrick and Rouhandeh, 1985)
	Capripox	Lumpy skin disease virus	LD138	(Tulman *et al.*, 2001) (Kara *et al.*, 2003)

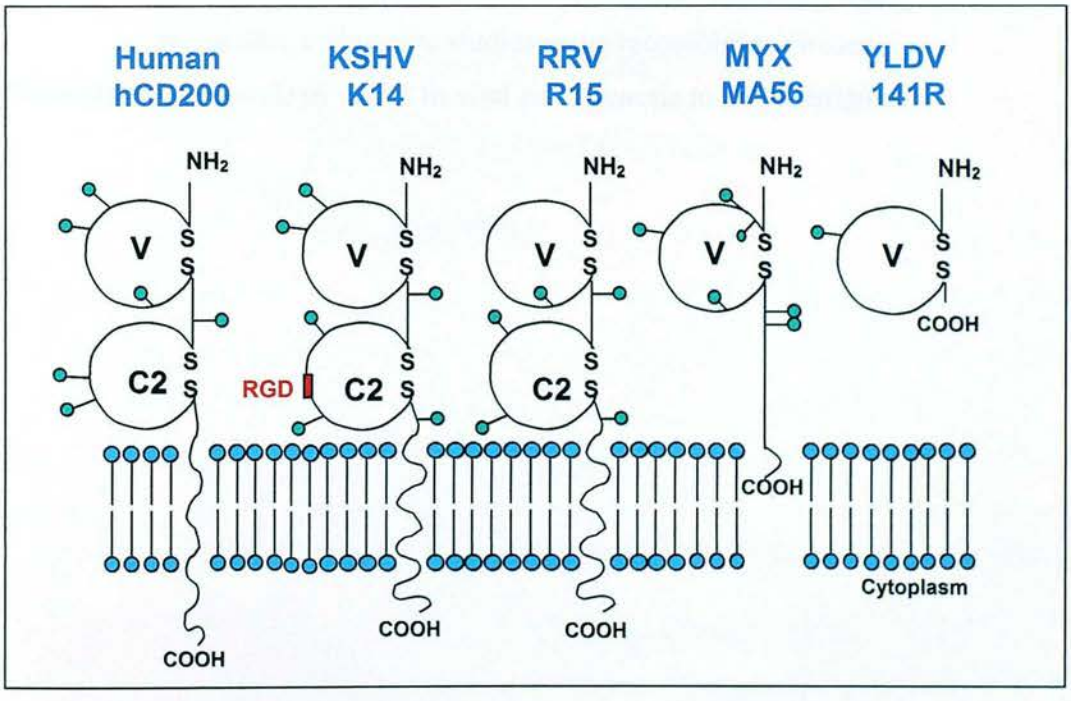

Figure 1.12 Schematic representation of the human CD200 protein and viral homologues from KSHV, RRV, MYX and YLDV. Ig domains of the variable (**V**) or constant 2 (**C2**) type are represented by circles. Positions of cysteines (**S**), forming the intramolecular disulfide bonds, and predicted sites for attachment of N-glycans (●) are indicated. NH_2, amino terminus; COOH, carboxyl terminus; RGD, Arg-Gly-Asp.

1.6 Project Aims

The potentially important role of CD200 within the complexity of the immune system in humans, mice and rats is only just becoming apparent. Recent findings of viral CD200-homologues is intriguing and suggests that this protein may play an important role in viral survival. The investigation of the role of KSHV's CD200-homologue, vOX2, will be important in getting closer to understanding KSHV pathogenesis.

The core objective of this project was to characterise the vOX2 protein and gather a better understanding of the potential contribution of vOX2 to viral pathogenesis *in vivo*. This was achieved by:

- Protein expression studies
- Generation of MHV-76 recombinant viruses with the incorporation of vOX2 and selection markers (GFP-hygromycin resistance)
- Generation of appropriate control recombinant viruses
- *In vitro* and *in vivo* studies using recombinant viruses

Thus allowing the role of vOX2 in viral pathogenesis to be investigated.

Chapter Two: Materials and Methods

2.1 Tissue Culture

2.1.1 Cell Lines

All cells were obtained from in-house stocks (Table 2.1) and were cultured in sterile plasticware (Nunc) and incubated at 37°C in a humidified atmosphere containing 5% CO_2. Growth medium for all adherent and suspension cell lines is indicated in Table 2.1.

2.1.2 Harvesting Adherent Cell Lines

All adherent cell lines (Table 2.1) were harvested by trypsinisation, unless otherwise stated. Following decantation of medium from the flask, cells were briefly rinsed with 0.02% w/v versene, then incubated with 0.05% w/v trypsin for 3-5 minutes until the cells detached from the flask. Fresh medium was added to the cells, and then transferred to a sterile Falcon tube and the cells were pelleted by centrifugation at *500xg* for 7 minutes. Cell pellets were resuspended in 10ml fresh medium and counted. A new T175cm^2 tissue culture flask with fresh medium would be reseeded with between 0.5-5 x10^6 cells, depending on the next requirement of cells.

2.1.3 Harvesting Suspended Cell Lines

Viable cells were separated from dead cells by a ficoll gradient in all suspended cell lines. An equal volume of suspended cells were over-laid onto Ficoll-Hypaque (Pharmacia) and separated by centrifugal force (500x*g* for 20 minutes at 4°C), forming a buffy coat (interface between the medium and ficoll) of live cells and a pellet of dead cells. The buffy coat was collected and transferred to a new sterile universal and pelleted by centrifugation at 500x*g* for 7 minutes. The pellet was resuspended in 10ml of fresh medium and counted. A gradient separation of live and dead cells was only performed approximately once every four weeks, fresh medium was added to the flask twice a week. If cells were required at times other than at the time of a gradient separation, an aliquot of suspended cells were taken and pelleted by centrifugation at 500x*g* for 7 minutes, resuspended in fresh medium and then counted.

Table 2.1 Cell lines used in tissue culture.

Cell Line	Cell Type	Adherent/ Suspension	Growth Medium
BHK-21	Baby hamster kidney cells	Adherent	Glasgow's modified Eagle's medium* (GMEM), 10% v/v new born calf serum* (NBCS), 10% w/v tryptose phosphate broth (TPB)*, 70µg/ml penicillin§, 10µg/ml streptomycin and 2mM L-glutamine
HEK-293	Human embryo kidney epithelial cells	Adherent	Dulbecco's modified Eagle's medium* (DMEM), 10%v/v foetal calf serum† (FCS), 70µg/ml penicillin§, 10µg/ml streptomycin, and 2mM L-glutamine
BC3 BCBL-1	Human, Primary effusion lymphoma B-cell line; KSHV(+ve)	Suspension	Roswell Park Memorial Institute 1640 (RPMI), 20% v/v FCS†, 70µg/ml penicillin§, 10µg/ml streptomycin, 50µM β-mercaptoethanol, and 2mM L-glutamine
BJAB	Human, Primary effusion lymphoma B-cell line; KSHV(-ve)	Suspension	

*denotes product is from Invitrogen Life Sciences, § denotes product is from Merck and †denotes product is from Sigma

2.1.4 Counting Cells

Cells were counted by mixing a 1:1 mix of cell suspension with 0.4% Trypan Blue (Sigma), then loaded on to a haemocytometer. The unstained viable cells were counted per 1mm square.

2.1.5 Transfection of Adherent Mammalian Cells

2.1.5.1 Electroporation

BHK-21 were harvested, counted and resuspended to 2.5 x 10^6 cells/ml. An 800µl aliquot of the cell suspension (2x10^6 cells) was loaded into a chilled 4mm electroporation cuvette (EquiBio) followed by 5 -20µg of DNA. The mixture was thoroughly mixed and then electroporated using an Easyject electroporator (EquiBio) using the double pulse program (pulse 1:600V, 25µF, 99mΩ, then following a 0.1s delay pulse 2: 250V, 1050µF, 99mΩ). Immediately after electroporation, the mixture was transferred to 10ml of fresh medium, and then sub-cultured into 2 wells of a 6 well plate and incubated at 37°C.

2.1.5.2 Lipid-based using Effectene® Transfection Reagent (QIAGEN)

Adherent cells were seeded in a 6 well plate 24 hours prior transfection, so that the cells were between 40-80% confluent on the day of the transfection. A mixture containing 0.4µg DNA and DNA-condensation buffer (Buffer EC) to a total volume of 100µl was added to 3.2µl Enhancer and incubated at RT for 2-5 minutes. After the addition of 10µl Effectene Transfection Reagent to the DNA/Enhancer mixture, the sample was incubated for 5-10 minutes at RT. The adherent cells were rinsed with PBS and then replaced with 1.6ml fresh medium. Fresh medium (600µl) was added to the DNA mixture, mixed and immediately added drop-wise to the adherent cells, then incubated at 37°C. Transiently transfected cells were harvested 24 to 48 hours post-transfection. For the generation of secreted protein, growth medium was removed 24 hours post-transfection and replaced with the same amount of Optimem for a period of no less than 30 hours.

2.1.6 Lytic Induction of KSHV Infected Cell Lines

KSHV infected cell lines contain the virus in a state of latency. Lytic infection was induced following an overnight incubation with 3mM Butyrate (SIGMA).

2.1.7 Inhibition of Glycosylation

Glycosylation of proteins was inhibited by an overnight incubation of cells with 0.1μg/ml Tunicamycin (SIGMA)

2.1.8 Cell Lysis

Cells were pelleted by centrifugation (500x*g* for 5 minutes), medium removed and then resuspended in an appropriate amount of cell lysis buffer (1xPBS, 1%$NaPO_4$, 2mM EDTA). Samples were mixed vigorously for 15 minutes. Cellular debris was pelleted by centrifugation (500x*g* for 1minute).

2.2 Molecular and Cloning Techniques

2.2.1 Polymerase Chain Reaction (PCR)

Most polymerase chain reactions (PCR) contained a reaction mixture comprised of 20mM Tris[pH8.4], 1.5mM $MgCl_2$, 0.25mM each of dATP, dGTP, dCTP and dTTP (Promega), 10pmol of each primer, 100-500ng DNA template and 1U *Taq* DNA polymerase (Promega) in a final volume of 50μl. All sets of reactions included a negative control, where template DNA was substituted with nuclease free H_20. PCR primers were obtained from Sigma-Genosys or Invitrogen Life Technologies unless otherwise stated. A detailed list of sequence and cycling settings are described in Appendix 2.

All reactions were set up in a contamination-free environment using barrier tips to minimize the risk of false positive reactions. PCR was performed in either thin-walled 0.5ml tubes or 0.2ml tubes on either a Biometra T3 Thermalcycler or Techne - Progene thermal cycler (both with heated lids). 30-40 cycles of PCR amplification was performed, consisting of an annealing (at primer specific temperatures), extension at 72°C and denaturing stage at 95°C, each stage was held

for 45 seconds unless otherwise stated (see Appendix 2 for primer specific annealing length and temperature).

2.2.2 Purification of PCR Products

Amplified DNA was purified using the QIAGEN PCR Purification System. Samples were mixed with a 5x volume of PB Buffer and then loaded into the spin cartridge. DNA bound to the membrane when the columns were centrifuged at 12,000x*g* for 1 minute, the column was then washed with 700µl Wash Buffer (PE) and the membrane dried by centrifugation twice at 12,000x*g* for 1 minute. The DNA was recovered by the addition of 30 - 50µl Elution Buffer, incubated for 1 minute and then centrifuged for 2 minutes at 12,000x*g*. This same method was also used to 'clean-up' a restriction digest reaction.

2.2.3 Agarose Gel Electrophoresis

DNA was analysed by electrophoresis on an agarose gel containing 0.5-2% (w/v) agarose (Sigma) and 0.5µg/ml ethidium bromide (Sigma) in TBE buffer. DNA samples were mixed 10:1 with gel loading buffer (15% w/v Ficoll type 400, 0.25% w/v bromophenol blue and 0.25% w/v xylene cyanol) and loaded into the gel. In conjunction with the samples, a DNA molecular weight marker (1µg of 1Kb DNA ladder or 1Kb Plus DNA ladder, Invitrogen) was also run. Electrophoresis was performed at 70-130V in a horizontal tank (BIO-RAD) filled with 0.5x TBE buffer. DNA bands were visualized under ultraviolet light using an ultraviolet transilluminator (UVP).

2.2.4 Gel Extraction of DNA

DNA was extracted from an agarose gel using the Qiaquick Gel Extraction system (QIAGEN). The desired band of DNA (viewed by UVP) was cut out and transferred to a sterile 0.5ml eppendorf and weighed. Three times the volume buffer QG was added to one volume of gel (100mg≈100µl) and heated at 50°C until completely dissolved. One gel volume of isopropanol was added to the dissolved DNA mixture and samples were loaded into the spin cartridge. DNA was bound to the membrane by centrifugation of the cartridge at 10,000x*g* for 1 minute. The

cartridge was then washed with 750µl buffer PE and the membrane dried by centrifugation twice at 10,000x*g* for 1minute. The DNA was eluted in 30-50µl of Elution Buffer, which was incubated for 1 minute and then centrifuged for 2 minutes at maximum speed.

2.2.5 Ethanol Precipitation

DNA was precipitated by the addition of 0.3 volume 7.5M ammonium acetate or 0.1 volume 3M sodium acetate [pH5.2], and then 3 volumes of 96% (v/v) ethanol (-20°C). The mixture was mixed thoroughly and incubated at -20°C for 10 – 30 minutes. The precipitated DNA was pelleted by centrifugation at 12,000x*g* for 5 minutes, washed with 70% (v/v) ethanol, air-dried for 5 minutes and then resuspended in an appropriate volume of TE buffer.

2.2.6 Quantification of DNA and RNA

DNA and RNA samples were quantified using a Gene Quant II from Pharmacia Biotech. A 4µl aliquot of the sample was loaded into a fine glass capillary and measured with a pathlength of 0.5mm at a 260nm absorbance. The Gene Quant II automatically calculated the concentration of DNA and RNA. Alternatively, approximate concentrations of DNA were made by visually comparing the intensity of DNA electrophoresed on an agarose gel with a known DNA concentration (1Kb DNA ladder, Invitrogen Life Technologies).

2.2.7 Restriction Enzyme Digestion

DNA restriction enzymes were obtained from either New England Biolabs or Roche and used according to the manufacturer's instructions. Buffers (x10) and BSA (x100) were supplied with the enzymes. Digest reactions were typically performed for 2 hours at 37°C in a suitable volume containing 5-10 units of enzyme per 1-10µg DNA.

2.2.8 Blunt-ending DNA

To blunt-end DNA following restriction enzyme digestion or PCR, 1U of T4 DNA polymerase (Roche) and dNTP's (0.25mM of each dATP, dGTP, dCTP, dTTP)

was added and incubated at 12°C for 15 minutes, then inactivated by incubation at 75°C for 10 minutes.

2.2.9 De-phosphorylation of Linearised Plasmid DNA

To inhibit self re-ligation of plasmid vectors, particularly a blunt-end ligation, the 5'-phosphate group on each end of the linear plasmid DNA was removed using shrimp alkaline phosphatase [SAP] (Roche). In a 10µl reaction, 1U of SAP was added to up to 1pmol of DNA and 1µl 10x buffer (0.5M Tris-HCl, 50mM $MgCl_2$ [pH8.5]), then incubated at 37°C for 1 hour and inactivated by heating to 65°C for 15 minutes.

2.2.10 Ligation of DNA Fragments

Ligation of DNA fragments were set up using a 1:1-5 ratio of plasmid:insert fragment. Reaction mixture included 1U T4 DNA ligase (Roche) and 1x T4 DNA ligase buffer (30mM Tris-HCl[pH 7.8], 10mM DTT and 1mM ATP) (Roche) in a final volume of 10µl, followed by overnight incubation at 4°C for "sticky-ended" ligations and at room temperature for "blunt-ended" ligations. For rapid-ligation reactions, the mixture included 1U T4DNA ligase (Roche) and 2x rapid-ligation buffer (60mM Tris-HCl [pH7.8], 20mM $MgCl_2$, 20mM DTT, 2mM ATP and 10% (w/v) PEG) (Promega) in a final volume of 10µl and was incubated at room temperature for 5 -10 minutes. All ligation reactions included a negative control, in which dH_20 replaced the DNA insert fragment, allowing the detection of self-ligation of the plasmid.

2.2.11 Addition of *Bgl*II Linker

Following linerisation of the plasmid at the desired site, the DNA fragment was ethanol precipitated (see 2.2.5) and resuspended in 10µl TE. A 50-100-fold molar excess of linker (3µl) to DNA was added with 2µl 10x ligase buffer (500mM Tris-HCl [pH7.5], 100mM $MgCl_2$, 100mM DTT, 10mM ATP), 1U T4 DNA ligase and made up to a final volume of 20µl with dH_20. The reaction was incubated over night at RT and then digested with *Bgl*II to digest excess linkers.

2.2.12 Site-Directed Mutagenesis

Site-directed mutagenesis was performed on a fragment of KSHV DNA using the QuickChange® XL Site-Directed Mutagenesis Kit (Stratagene). HPLC-purified mutagenic primers were designed that possessed the required mutagenic site with approximately 10-15 bases of correct sequence at either side. Reactions were set up as stated in the manufacturers protocol using; 10ng of dsDNA template, 125ng of each primer, 1x reaction buffer (100mM KCl, 100mM $(NH_4)_2SO_4$, 200mM Tris-HCl [pH 8.8], 20mM $MgSO_4$, 1% (v/v) Triton X-100, 1mg/ml nuclease-free BSA, Stratagene), 1µl of dNTP-XL mix, 3µl QuickSolution and 2.5U *Pfu Turbo* DNA polymerase, in a total volume of 51µl. Reactions were heated to 95°C for 1 minute, then 18 cycles of 50 seconds denaturing at 95°C, 50 seconds annealing at 60°C, and extension at 68°C for 2 minutes/kb of plasmid length (10 minutes for vOX2-TOPO and 12 minutes for pSecTag2-A). Following thermal cycling, 10U *Dpn*I restriction enzyme was added to the reaction and incubated at 37°C for 1 hour to digest the parental (non-mutated) supercoiled dsDNA. A 2µl aliquot of the mutated dsDNA mixture was then transformed into XL10-Gold Ultracompetent cells (Stratagene). Once the competent cells (45µl) had thawed gently on ice, 2µl β-ME mix was added and incubated on ice for a further 10 minutes, gently swirled every 2 minutes. Then 2µl of the *Dpn*I-treated DNA was added to the ultracompetent cells and incubated on ice for 30 minutes. Reactions were heat-pulsed at 42°C for 30 seconds and then incubated on ice for 2 minutes. Following the addition of 0.5ml of SOC medium, the transformation reactions were incubated at 37°C for 1 hour with shaking 225-250 rpm. An appropriate volume of each transformation reaction was plated on LB-ampicillin agar plates and incubated overnight at 37°C.

2.2.13 Transformation of Competent Bacteria by Heat Pulse

Escherichia coli bacteria were either One Shot® TOP10 Competent Cells (Invitrogen Life Technologies) or Select96™ Competent Cells (Promega), unless otherwise stated, and were transformed according to the manufacturer's protocol. In brief, competent cells were thawed on ice and a 25µl aliquot transferred to a pre-chilled eppendorf. A 1 - 5µl aliquot of the ligation reaction was added to the

competent cells and incubated on ice for 30 minutes. Reactions were heat-shocked for 30 seconds at 42°C, and then incubated on ice for 2 minutes and 250µl of pre-warmed SOC medium was added to each reaction. Following a 1 hour incubation at 37°C with shaking (225-250rpm), 100µl-200µl of each transformation reaction was plated onto LB agar plates containing the appropriate selection antibiotic (100µg/ml ampicillin or 50µg/ml kanamycin, Sigma), and incubated at 37°C overnight. For blue/white selection of positive colonies in TOPO TA cloning and pGEM-T Easy cloning, additional aliquots of 20µl 200mM isopropyl β-D thioglalactoside (IPTG) and 40µl 2% (w/v) 5-bromo-4chloro-3-indoyl-β-D-galactoside (X-Gal) were added to the LB-Amp plate before the addition of the transformation reaction.

2.2.14 Cloning PCR Products using TOPO TA Cloning Kit

PCR products were directly cloned into pCR2.1-TOPO (Invitrogen) (Appendix 3), as described in the manufacturer's protocol. The kit provided a linearised plasmid with single 3'-thymidine (T) overhangs and Topoisomerase I covalently bound to the vector. The TOPO cloning reaction contained a final concentration of 200mM NaCl, 10mM $MgCl_2$, 1-4µl fresh PCR product and 10ng of plasmid. The reaction was mixed gently and incubated for 5 minutes at room temperature, before transformation into One Shot Top 10 chemically competent cells (see 2.2.12).

2.2.15 Cloning PCR Products using pGEM-T Easy Vector

PCR products were cloned using pGEM-T Easy vector (Promega) (Appendix 3) according to the manufacturer's instructions. A 10µl ligation reaction was prepared which included 2 x Rapid Ligation Buffer, 50ng pGEM-T Easy Vector, 1-3µl PCR product and 3 Units T4 DNA ligase. The ligation reaction was incubated for 1 hour at room temperature and a 2µl aliquot used to transform One Shot Top 10 chemically competent cells (see 2.2.12).

2.2.16 Small Scale Preparation of Plasmid DNA (Mini-Preps)

Mini-preps were usually performed using the alkaline lysis method via the CONCERT mini prep system (Gibco) and performed as described by the

manufactures protocol. An isolated bacterial colony was picked from an agar plate and grown up in 3 - 6 ml LB medium, with the appropriate antibiotic, overnight at 37°C on an orbital shaker. The bacterial solution was pelleted by centrifugation at 10,000x*g* for 5 minutes in an eppendorf, and the bacterial pellet resuspended in 250µl lysis buffer, Buffer G1. A neutralisation buffer, Buffer G2 (250µl), was then added gently mixed by inverting the tube six times and incubated for 5 minutes at RT. Buffer M3 (350µl) was added and the solutions were mixed gently by inversion of the tube and the insoluble fraction was pelleted by centrifugation for 10 minutes at 12,000x*g*. The supernatant was removed and loaded on to a spin column and the DNA bound to the membrane by centrifugation at 12,000x*g* for 1 minute. The spin column was then washed once with Buffer PE (750µl) and dried by two centrifugation steps (12,000x*g*, 1 minute). DNA was eluted from the column by the addition of 50 - 75µl TE [pH 8.0], preheated to 70°C, incubated for 1 minute before centrifuged for 2 minutes at 12,000x*g*. Samples were stored at 4°C or -20°C for long-term storage.

2.2.17 Large Scale Preparations of DNA (Maxi-prep)

Large Scale preparations of plasmid DNA were performed using anion exchange columns in the Endofree Plasmid Maxi Kit (QIAGEN) according to the manufacturer's instructions. Overnight bacterial cultures (250ml for high yielding and 500ml for low yielding) were centrifuged at 6,000x*g* for 15 minutes at 4°C. The pellet was resuspended in 10ml of Buffer P1 (50mM Tris [pH8.0], 10mM EDTA, 100µg/ml RNase A), and then 10ml of Buffer P2 (200mM NaOH, 1% (w/v) SDS) was added and gently mixed by inversion, followed by 5 minutes incubation at RT. A 10ml volume of ice-cold Buffer P3 (3M potassium acetate [pH8.5]) was then added, mixed by gentle inversion and after 10 minutes incubation on ice, the mixture was filtered using a QIAfilter cartridge. Endotoxins were removed by the addition of 2.5ml of Buffer ER and 30 minutes incubation on ice. A QIAGEN-tip 500 anion exchange column was equilibrated using 10ml Buffer QBT (750mM NaCl, 50mM MOPS [pH7.0], 15% (v/v) isopropanol, 0.15% (v/v) Triton X-100), and the filtered lysate added to the equilibrated column and pulled through by gravitational force. The column was washed twice by the same method using 30ml Buffer QC (1M

NaCl, 50mM MOPS [pH 7.0], 15% (v/v) isopropanol) and DNA eluted in 15ml Buffer QN (1.6M NaCl, 50mM MOPS [pH7.0], 15% (v/v) isopropanol). The DNA was precipitated by the addition of 0.7 volumes isopropanol and pelleted by centrifugation at 15,000x*g* for 30 minutes at 4°C. The DNA pellet was washed with 70% (v/v) ethanol before it was air-dried and resuspended in 200µl TE.

2.2.18 DNA Sequencing

DNA sequencing was performed in one of two ways. The first method was performed using the di-deoxy chain termination sequencing method by Mr Ian Bennet (Department of Veterinary Pathology, University of Edinburgh). Reactions were performed using a SequiTherm EXCEL II DNA Sequencing kit (cycle sequencing protocol) on a 4000L automated sequencing machine (MWG-Biotech). Alternatively, DNA sequencing was performed using the BigDye Terminator Cycle Sequencing reaction kit by Ms Jill Lovell (ICAPB ABI Sequencer, University of Edinburgh). BigDye reactions were prepared in 10µl volumes containing 4µl BigDye, 1.6 pmole primer, 2-4µl DNA (200-500ng). Reactions were placed in a thermal cycler for 25 cycles of 95°C for 30 seconds, 50°C for 20 seconds, and 60°C for 4 minutes. The DNA product was then ethanol precipitated (see 2.2.5), and the pellet sent to ICAPB for sequencing.

2.2.19 Sequence Analysis

Sequenced DNA was compared with database sequenced using the basic alignment search tool (BLAST) programs on the NCBI web site http://www.ncbi.nlm.nih.gov/BLAST/ (Altschul *et al.*, 1990).

2.3 Virological Methods

2.3.1 Generation of Recombinant Viruses

Recombinant viruses were generated by co-transfection (electroporation) of BHK-21 cells with purified viral DNA (see 2.1.5.1) and an insert cassette fused to a portion of the viral genome, thus allowing homologous recombination to occur.

In order to do this an extensive cloning procedure was undertaken to generate the insert cassette and it's fusion to a fragment of the viral genome. A schematic

diagram of the cloning strategy used to generate the plasmids used for the construction of the recombinant viruses is outlined in Figure 4.1. Using primers *vOX-1* and *vOX-2* the vOX2 ORF (128113-128930 from KSHV) was amplified from BCP-1 DNA and cloned into the plasmid pCR2.1-TOPO. The vOX2 ORF was then digested out using *BspH*I and *Nco*I, and inserted into pBVIRES.GFP, which was linearised with *Nco*I and then dephosphorylated. The IRES-vOX2 fragment (~1.4Kbp) was cut from the plasmid first with *Nco*I and then *Xho*I, and cloned into the *Sma*I/*Sal*I site in pHygEGFP1 to incorporate the CMV promoter and hygromycin resistant-EGFP (Hyg^R-EGFP) fusion protein. The CMV → vOX2 fragment (~5.4Kbp) was then cut out at the *BsaB*I site, however as this site was inhibited due to being blocked by *dam* methylation the plasmid was first transformed into *dam* negative competent cells, Epicurian Coli® SCSIIO Competent cells (Stratagene). The CMV → vOX2 fragment was digested with *BsaB*I, then a *Bgl*II site was added using a *Bgl*II linker (see 2.2.11). Excess *Bgl*II sites were cut off following digestion with *Bgl*II.

Due to difficulties separating the large CMV → vOX2 from the small backbone (~2.7Kbp), the insert was cloned into the *Bgl*II site in pEGFP-N1, a kanamycin resistant vector (Appendix 3). The CMV → vOX2 insert was then cut out using the same *Bgl*II sites and ligated into the *BamH*I site of pBSIIKS-76LHE (plasmid generated by Macrae, 2002), which incorporates homologous DNA from the left hand end of the genome corresponding to 9539-12569 of MHV-68. Two plasmids were generated: pBSIIKS-76LHE-vOX2F and pBSIIKS-76LHE-vOX2R. The plasmids were digested with *Pvu*II and *EcoR*V to isolate the fused CMV→ vOX2 and 3Kb MHV-76 insert cassette and used in homologous recombination reactions to generate the recombinant viruses.

BHK-21 cells were transfected by electroporation (see 2.1.5.1) with 5µg viral DNA (MHV-76) and 10µg of the linear homologous plasmid. Following transfection, the cells were placed into 6-well plates and incubated at 37°C overnight. The following day fresh medium containing 100µg/ml hygromycin was added to the wells, incubated at 37°C and examined daily for the presence of viral plaques and expression of *gfp*.

2.3.2 Purification of Recombinant Viruses

Following the generation of the recombinant viruses in 6-well plates (see 2.3.1), 4-6 days later the infected cell monolayer was harvested in 1 ml of medium and viral particles released from the cells by freeze-thawing at -70°C three times. Cellular debris was pelleted by centrifugation at 2,000x*g* for 5 minutes and the supernatant containing the virus, used in subsequent purification steps.

All recombinant viruses were purified using a limiting dilution assay. BHK-21 cells were seeded and grown until approximately 60% confluent in a 96 well plate. These cells were then infected with serial dilutions (10^{-1} to 10^{-4}) of virus, with the aim of infecting cells at a concentration of 0.4 PFU/well, therefore a single plaque in 40% of the wells. The assay was incubated at 37°C for 6 days and the lowest dilution well containing *gfp* expression was harvested by scraping the cells into the 200µl of medium. A 100µl aliquot of the sample was freeze-thawed at -70°C three times to release virus particles and kept for further rounds of purifications.

The remaining 100µl sample was pelleted by centrifugation at 500x*g* for 5 minutes, resuspended in 50µl TE buffer and freeze-thawed once. PCR grade Proteinase K (Roche) was added to a final concentration of 400µg/ml to each sample and incubated overnight at 55°C. The Proteinase K was heat inactivated by a 10-minute incubation at 95°C and then 10µl of each sample was used as a template for PCR analysis (see 2.2.1). Plaques positive by PCR for the desired insert (vOX2 or IRES only) and correct orientation were subsequently used to infect the next round of limiting dilution assays. PCR for MHV-68 ORF 74 (vGCR) was used as a control to check for the presence of viral DNA.

Viruses were purified until homogenous by PCR screening and after at least 3 rounds of limiting dilution checked for the presence of wild-type virus (MHV-76) by PCR (primers Trepeat and M4-B, see Appendix 2). If wild-type virus was still present at this stage a 6 well plate was infected with virus at a 10^{-3} dilution from a 96 well plate. After 24 hours incubation at 37°C, the cells were washed with medium and overlaid with medium containing 1% (w/v) LGT agar (Seaplaque® Agarose, Flowgen) and incubated at 37°C for 5 days. The position of viral plaques expressing *gfp* were marked on the underside of the plate, and a Pasteur pipette was used to

remove an agarose plug containing virus-infected cells. The agarose plug was transferred to a sterile tube containing 200µl of medium and freeze-thawed three times. The cellular debris was pelleted by centrifugation at 500x*g* for 5 minutes and the supernatant used in subsequent rounds of purification. Once PCR screening of plaques were positive for the desired insert and negative for wild-type virus, MHV-76, master stocks were made.

Master stocks were made by infecting BHK-21 cells ($3x10^6$) with an MOI of approximately 0.01 and incubating on a shaker at 37°C for one hour, then seeded in a T175cm^2 tissue culture flask and incubated for 4-6 days until 100% cytopathic effect (CPE) was observed. Cells that were still adherent were scraped into the medium and pelleted by centrifugation at 2,000x*g* for 20 minutes. The pellet was resuspended in 1ml of medium and freeze-thawed at -70°C three times to release virus particles. Samples were then clarified by centrifugation at 2,000x*g* for 7 minutes and the supernatant split into five CryoTube™ vials and stored at -70°C.

2.3.3 Preparation of Viral Stocks

(see 2.3.2 for generation of master stock)

MHV-76 and the other recombinant viruses' working stocks were produced from sub-master stocks. Viral stocks were generated by infection of BHK-21 cells. Ten T175cm^2 tissue culture flasks were seeded with a BHK-21 suspension ($3x10^6$ cells per flask) of virally infected cells. Cells were infected with a MOI of 0.01 for 1 hour at 37°C on a shaker, and then incubated in flasks for 5-7 days until 100% CPE was observed.

All cells were scraped off into the medium and pelleted by centrifugation at 2,000x*g* for 20 minutes at 4°C. The cell pellet was resuspended in 3-5 ml sterile PBS and disrupted by dounce homogenization for 30 strokes in a chilled tight-fitting Wheaton-Dounce homogeniser. The cell suspension was transferred to a glass universal and sonicated for 15 minutes, using a sonicating ice bath. After sonication, the suspension was clarified by centrifugation at 2,000x*g* for 20 minutes at 4°C after which the supernatant was carefully removed and kept at 4°C. The cell pellet was again resuspended in sterile PBS (1ml), dounce homogenized 30 times and clarified by centrifugation (2,000x*g*, 20 minutes, 4°C), and the supernatant was removed and

added to the previous aliquot. Aliquots (50µl, 100µl and 200µl) of the supernatant were stored in sterile CryoTube™ vials at -80°C.

2.3.4 Titration of Infectious Virus

Titration of infectious virus was performed by plaque assay on BHK-21 cells as previously described by Sunil-Chandra *et al.* (1992). Samples were thawed at 37°C and serially diluted 10-fold in Glasgow's medium (4ml) in sterile plastic bijoux. A cell suspension of BHK-21 cells ($2x10^6$ cells per bijoux) was added to each dilution, incubated on a shaker for 1 hour at 37°C, and plated into two 60mm Petri dishes to give duplicates. Growth medium was added to the petri dishes to give a final volume of 5ml. Negative controls containing uninfected BHK-21 cells were also included. All plates were incubated for 4 days in a humidified environment with 5% CO_2 and at 37°C. Cells were fixed with 4% (v/v) neutral-buffered formaldehyde (Surgipath) for at least 30 minutes and then stained with 0.1% (w/v) toluidine blue for 15-45 minutes. The number of plaques per dilution was counted using an inverted light microscope, and the number of plaque-forming units (PFU) was calculated per ml or per organ.

2.3.5 Preparation of Purified Viral DNA

Ten T175cm^2 tissue culture flasks of BHK-21 cells were infected with virus in suspension at a MOI of 0.1. When 100% CPE was observed 4-6 days later, the cells were scraped off into the medium and pelleted by centrifugation at 500x*g* for 20 minutes at 4°C. The cell pellet was resuspended in 3ml sterile PBS, and cells disrupted by dounce homogenisation (30 times) in a chilled Wheaton-Dounce homogeniser. The suspension was clarified by centrifugation at 2000x*g* for 20 minutes at 4°C and the supernatant was removed and stored at 4°C. The remaining cell pellet was resuspended in 1ml sterile PBS, dounce homogenised again for 30 strokes and clarified by centrifugation at 2000x*g* for 20 minutes at 4°C. The supernatant was removed and pooled with the previous aliquot of supernatant.

Viral DNA was separated from the supernatant by ultra-centrifugation. The supernatant was overlaid on a sorbitol gradient (20% (w/v) D-sorbitol in PBS, Sigma), and pelleted by centrifugation at 22,100x*g* for 80 minutes at 4°C. The viral

pellet was resuspended in 500µl of 50mM Tris [pH8.0], and 5ml High Molecular Weight Extraction Buffer (0.2M Tris [pH8.0], 0.1M EDTA, 0.5% SDS (w/v)) was added. Proteinase K (Roche) was added to a final concentration of 100µg/ml and the mixture was incubated overnight at 56°C. Viral DNA was then gently extracted four times with phenol chloroform iso-amyl alcohol. The extraction was performed on a rotating tilting platform for 30 minutes each time, followed by a phase separation by centrifugation at 500x*g* for 5 minutes. The DNA solution was then extracted twice with chloroform iso-amyl alcohol. The DNA was precipitated with 0.3 volumes 7.5M ammonium acetate and 3 volumes of cold 96% (v/v) ethanol, and then pelleted by centrifugation at 8,000x*g* for 30 minutes at 4°C. The pellet was washed twice with 70% (v/v) ethanol, air-dried and resuspended in an appropriate amount of TE.

2.3.6 *In vitro* Growth Curves

A single-step growth curve and multi-step growth curve were performed on MHV-76 and the recombinant viruses in BHK-21 cells. A suspension of $4.8x10^6$ BHK-21 cells were infected with an MOI of 5 for the single-step growth curve and $2.4x10^6$ BHK-21 cells were infected with an MOI of 0.05 for the multi-step growth curve. Infection was performed in a sterile plastic universal and incubated for 1 hour at 37°C while shaking. Cells were then pelleted by centrifugation at 12,000x*g* for 7 minutes at 4°C, washed twice with 10ml of fresh medium, and then resuspended in 24ml of fresh medium. A 1ml aliquot was added to each well in a 24 well plate and incubated at 37°C. Samples were taken in duplicate at appropriate time-points by scraping all the cells into the medium and stored in CryoTube™ vials at -80°C. Time-points for the single-step growth curve included: 0, 6, 12, 18, 24, 30, 36, 48, 60 and 72 hours post infection, and for the multi-step growth curve included: 0, 12, 24, 36, 48, 60, 72, 96, 120, and 144 hours post infection. All samples were freeze-thawed three times to release virus and infectious virus was measured by plaque assay (see 2.3.4). All titration reactions were performed in duplicate and on the same day using the same BHK-21 cells to ensure accurate comparison between values.

2.4 Southern Analysis of DNA (Southern Blotting)

The DIG Luminescent Detection Kit (Roche) was used for Southern analysis of DNA.

2.4.1 Digoxigenin (DIG) labelling DNA probes

DNA fragments, between 400bp and 5Kbp, were isolated by agarose gel electrophoresis and quantified. An aliquot of 1 - 3µg of template DNA was added to ddH_20 to a final volume of 16µl, denatured by a 10-minute incubation in a boiling bath, and then quickly chilled in an ice/water bath. A 4µl aliquot of DIG-High Prime (Roche) was added to the denatured DNA, mixed and incubated at 37°C overnight. The reaction was stopped by the addition of 2µl 0.2M EDTA [pH8.0] and heated to 65°C for 10 minutes. Probes were stored at -20°C until used. Prior to immediate use for hybridisation, probes were denatured by heating to 100°C for 5 minutes.

2.4.2 Electrophoresis and Southern Transfer of DNA

Viral DNA samples (2µg per agarose gel lane) were digested with 10 – 20 units of restriction digest enzyme overnight (see 2.2.7), and then loaded onto a 1% (w/v) agarose gel. Whereas, DNA samples extracted from tissue samples (see 2.8.6) were serially diluted and amplified by PCR (see 2.2.1), and then a 10 - 20µl aliquot loaded onto a 1% (w/v) agarose gel. A 5µl aliquot of DNA Molecular Weight Marker III – digoxigenin-labeled (Boehringer Mannheim) was also loaded in one lane of the agarose gel. Once the gel was loaded, DNA samples were electrophoresed at 50-80 volts for 4-7 hours, visualized under ultraviolet light and photographed. The gel was rinsed in distilled water, then denatured by soaking in denaturing buffer (1.5M NaCl, 0.5M NaOH) for 20-30 minutes with gentle agitation, and then rinsed again in distilled water. Neutralising of gel entailed soaking the gel in neutralising buffer (1.5M NaCl, 0.5M Tris-HCl [pH7.2], 0.001M EDTA) for 30 minutes with gentle agitation.

The DNA was then transferred overnight to a nylon membrane (Roche) by capillary transfer using 10x SSC. The blotting rig was assembled by covering a platform (above a tray of 10x SSC) with a 3MM filter paper (Whatman) wick, both

ends soaking in the 10x SSC. The gel was placed on top of the paper wick and the nylon membrane on top of the gel and flattened to ensure no air bubbles were present. The remaining exposed paper wick was covered with saran wrap. Three pieces (one pre-wetted) of 3MM filter paper were stacked on top of the membrane, followed by a stack of dry paper towels and a 500g weight to ensure capillary transfer during the night.

The following morning the blotting apparatus was disassembled, membrane removed and rinsed briefly in 2x SSC. The DNA was UV cross-linked to the membrane using the "auto crosslink" setting on the Stratalinker 2400 (Stratagene) and either stored at 4°C or pre-hybridised (see 2.4.3).

2.4.3 Southern Blot Hybridisation using Digoxigenin-11-dUTP

The membrane was pre-hybridised by incubation in DIG Easy Hyb (Roche) at 50°C for a minimum of 30 minutes in a rotating hybridisation oven (Techne Hybridiser HB-1). The pre-hybridisation buffer was discarded and replaced with the pre-warmed hybridisation solution (2µl DIG-labelled probe in 3.5ml DIG Easy Hyb) and incubated overnight at 50°C in the hybridisation oven. The membrane was washed twice with 2x SSC, 0.1% (w/v) SDS for 5 minutes at RT, then washed twice with 0.1x SSC, 0.1% (w/v) SDS for 15 minutes at 65°C, rinsed briefly in washing buffer (0.1M Maleic acid, 0.15M NaCl; [pH7.5]; 0.3% (v/v) Tween 20), and then incubated for 30 minutes in 1x blocking solution (blocking reagent dissolved in 0.1M Maleic acid, 0.15M NaCl), at RT. Incubation for 30 minutes with the anti-digoxigenin-alkaline phosphatase (Roche), diluted $1:10^4$ with 1x blocking solution, was performed in a 20ml volume at RT. Following this, the membrane was washed for two 15 minute incubations with washing buffer, transferred to a tray and soaked for 2 – 5 minutes in detection buffer (0.1M Tris-HCl, 0.1M NaCl [pH9.5]), before a 5 minute incubation with the chemiluminescent substrate CSPD (Roche) (diluted 1:100 in detection buffer). The membrane was then briefly rinsed in detection buffer, placed on a piece of 3MM filter paper (DNA side up), sealed into a hybridisation bag and incubated for 10 minutes at 37°C to enhance the luminescent reaction. The membrane was then exposed to autoradiographic hyper ECL film (Lumi-film chemiluminescent detection film, Roche) for 3 minutes to 3 hours at RT.

2.4.4 Stripping and Reprobing DNA Blots

The alkali-labile form of DIG-11dUTP enables an easy and efficient means of stripping the membrane. The membrane was rinsed thoroughly with ddH_20, followed by two 15 minute incubations in 0.2M NaOH, 0.1% SDS (w/v), at 37°C, and then a 5 minute incubation in 2x SSC. The membrane was then prehybridised and hybridised with a second probe (see 2.4.3).

2.5 RNA Analysis

2.5.1 Direct Isolation of RNA from tissue or cells

2.5.1.1 Isolation of total RNA using QIAGEN Rneasy Mini Kit

Extraction of tRNA was performed using the QIAGEN RNeasy Kit, which required the disruption of up to 40mg tissue (amounts varied depending on tissue type) or up to $1x10^7$ cells in Buffer RTL and then homogenisation by means of a QIAshredder. Following this, a one volume aliquot of 70% (v/v) ethanol was added and all samples passed through a RNeasy mini column by centrifugation at 8,000x*g* for 15 seconds. The columns were washed twice with 500µl Buffer RPE (8,000x*g* for 15 seconds) and tRNA eluted in two aliquots of 50µl RNase-free water (8,000x*g* for 1 minute).

2.5.1.2 Isolation of mRNA using SIGMA-Messenger RNA Micro Isolation Kit

Messenger RNA was isolated directly from 10^2 to 10^6 cultured cells (or 10 – 250mg tissue) using the Messenger RNA Micro Isolation Kit from Sigma. Cells were rinsed in sterile PBS and then incubated for 15 – 20 minutes in 1ml of pre-heated (45°C) lysis buffer (Stock Buffer with RNase/Protein Degrader). The NaCl concentration was adjusted by the addition of 63µl of sodium chloride (5M solution) to the 1ml lysate solution, and then mixed and passed through a 21 gauge syringe four times to shear the DNA. A vial of oligo (dT) was then added to the lysate, gently rotated for 15-20 minutes at room temperature, and followed by centrifugation of the suspension at 4,000x*g* for 8 minutes. The supernatant was discarded and oligo(dT) cellulose resuspended in 1.3ml binding buffer, mixed and supernatant discarded following centrifugation at 4,000x*g* for 4 minutes. This washing step with binding buffer was repeated another 3 times until the buffer was no longer cloudy.

After the final wash, the oligo(dT) cellulose was resuspended in 0.3ml of binding buffer and transferred to a spin column and centrifuged at 5,000x*g* for 10 seconds. The eluate was discarded and the spin column filled with binding buffer that was used to resuspend the oligo(dT) cellulose followed by centrifugation (5,000x*g*, 10 seconds), and repeated 3 times. The addition of 200µl of low salt wash buffer was added, mixed and centrifuged (5,000x*g*, 10 seconds) to wash the rRNA from the cellulose. This was repeated a second time prior to the elution of the mRNA by the addition of 100µl of elution buffer, mixing, and centrifugation (5,000x*g*, 10 seconds), in a fresh RNase-free tube. This was also repeated, giving a final volume of 200µl.

The 200µl eluate was then mixed with 10µl glycogen carrier, 30µl sodium acetate (2M solution) and 600µl ice-cold absolute ethanol, and frozen on dry ice. The mRNA was recovered by centrifugation of the sample at 4°C for 15 minutes at 16,000x*g*, removal of the supernatant and resuspension of the mRNA pellet in 1 - 10µl of elution buffer and stored at -70°C.

2.5.2 Removal of DNA from RNA Preparations

The RQ1 RNase-Free DNase system from Promega was used to remove DNA from RNA samples prior to RT-PCR. DNase digestion involved the use of 1 unit of RQ1 RNase-Free DNase to a maximum of 1 µg of RNA. A 1-8µl aliquot of RNA, was mixed with 1µl of 10x reaction buffer (400mM Tris-HCl [pH8.0], 100mM $MgSO_4$, 10mM $CaCl_2$), the appropriate amount of RQ1 RNase-Free DNase (1U/µl), and nuclease-free H_20 to a final volume of 10µl. The mixture was incubated for 30 minutes at 37°C and then stopped with the addition of 1µl RQ1 DNase Stop Solution (20mM EDTA [pH8.0]), and incubated at 65°C for 10 minutes. The DNA free RNA was stored at -20°C or immediately used in a RT-PCR reaction.

2.5.3 Reverse-Transcription Polymerase Chain Reaction (RT-PCR)

The ThermoScript™ RT-PCR System (Invitrogen Life Technologies) was used for the generation of cDNA. In a 0.2ml tube 10pg - 5µg RNA was mixed with 10µM gene-specific primer or 50µM Oligo$(dT)_{20}$ primer, and up to a final volume of 10µl with DEPC-treated water. The RNA and primers were denatured by an

incubation of 5 minutes at 65°C and then placed on ice. A master reaction mix was made up of 4µl 5x cDNA Synthesis Buffer (250mM Tris acetate [pH 8.4], 375mM potassium acetate, 40mM magnesium acetate), 1µl 0.1M DTT, 40U RNaseOUT, 1µl DEPC-treated H_20, 2µl 10mM dNTP Mix and 15U ThermoScript RT. A 10µl aliquot of master reaction mix was added to each reaction tube on ice and transferred to a thermal cycler, incubated at 50°C for 1 hour, followed by 5 minutes at 85°C to terminate the reaction. Removal of the RNA template was carried out by the addition of 2 units of *E.coli* RNase H (2U/µl) to each reaction and incubated at 37°C for 20 minutes. Samples of cDNA were stored at -20°C or used immediately in a PCR (see 2.2.1).

2.5.4 Labelling Northern Probes

For the creation of dsDNA probes, DNA was radiolabelled using the Multiprime DNA labelling system kit (Amersham Biosciences). In brief, approximately 25ng of purified denatured DNA (100°C for 2 minutes) and 50µCi of ^{32}P-dCTP were mixed with buffer (solution 1; dATP, dGTP, and dTTP in Tris-HCl, $MgCl_2$, 2-mercaptoethanol), a primer solution (solution 2; Random hexanucleotides) and enzyme solution (solution 3; Klenow). The labelling reaction was mixed and then allowed to proceed for 1 hour at 37°C. Unincorporated radionucleotides were separated from the labelled probe with a Sephadex G50 Nick Column (Amersham Biosciences). The column was rinsed with 2ml of TE buffer [pH8.0], before the addition of 3ml of TE buffer to equilibrate the column. Subsequently, the labelled probe was added to the column, immediately followed by 400µl of TE buffer. The flow-through was discarded and a further 400µl of TE buffer added. The flow-through from this elution contained the radiolabelled DNA probe and was retained. Prior to use for hybridisation, radiolabelled probes were denatured by incubation at 100°C for 5 minutes and then chilled on ice.

2.5.5 Northern Blotting

Ten micrograms of total RNA was used per lane, and was initially diluted to a final volume of 6µl with RNAse-free dH_20, and then mixed with 12µl of RNA

sample loading buffer (62.5% (v/v) deionized formamide, 1.14M formaldehyde, 200µg/ml bromophenolblue, 200µg/ml xylene cyanole, 1.25x MOPS-EDTA-sodium acetate, 50µg/ml ethidium bromide, SIGMA). Samples were incubated at 65°C for 15 minutes and then immediately chilled on ice. Molten agarose (144ml, 1.4%) was cooled to 65°C before the addition of 20ml MOPS (0.2M) and 36ml of formaldehyde (36-38%). The gel was subsequently set, loaded with RNA samples and 2µg Transcript RNA marker (0.2-10kb, SIGMA), and electrophoresed at 85V for 5 hours in running buffer (1x MOPS buffer). Following electrophoresis, the gel was rinsed four times in RNAse-free dH_2O for a period of 10 minutes and then soaked in 10x SSC for a period of 15 minutes with gentle agitation. The membrane (Gene Screen Plus, NEN Lifescience Products) was also soaked for 15 minutes in 10 x SSC. The blot was assembled in the same manner as described for Southern blotting and left overnight (see 2.4.3). The following morning, the membrane was soaked in 2x SSC for 5 minutes with gentle agitation. The RNA was cross-linked to the membrane with a Stratalinker 2400 (Stratagene) and stored at 4°C until hybridisation. The section of the membrane containing the ladder was cut off and soaked for 10 minutes in 1M acetic acid and then stained (0.2% (w/v) methylene blue, 0.4M acetic acid, 0.4M sodium acetate) for approximately 10 minutes. Excess dye was gently rinsed off the ladder with dH_2O and the membrane was allowed to air-dry.

Northern blots were hybridised with dsDNA probes, generated as described in section 2.5.4. Pre-hybridisation (1-2 hours) and hybridisation (4-12 hours using ½ of the radiolabelled probe) were performed at 42°C with Ultrahyb (Ambion). Membranes were washed in 2x SSC, 0.1% (w/v) SDS for 10 minutes at room temperature and then again in pre-warmed 2x SSC, 0.1% (w/v) SDS for 40 minutes at 65°C with gentle agitation. The membrane was then dried on blotting paper and exposed to X-ray film (Kodak Biomax MS film, Amersham Life Sciences) either at RT or at -70°C for 1-20 hours.

2.5.6 Stripping Northern Blots

Double-stranded DNA probes were removed from northern blots by incubation of the nylon membrane with boiling dH_2O containing 0.1% (w/v) SDS for 15 minutes with gentle agitation. The process was repeated before incubation of the

membrane in 2x SSC for 15 minutes with agitation. The membrane was then exposed to autoradiographic film to verify complete removal of the labelled probe.

2.6 Protein Studies

2.6.1 Production of secreted protein

The extracellular portion of the vOX2 protein (nt 128113-128927) was amplified by PCR (see 2.2.1) using primers Sec1 and Sec2 (Appendix 2), and then excised at the restriction enzyme sites *Xho*I and *Hind*III (incorporated with the primers). This fragment of vOX2 was cloned into the *Xho*I/*Hind*III site of pCDNA3.1/*myc*-His(-)A. Following verification of the correct clones by restriction enzyme digestion patterns, samples were transfected using the Effectene transfection reagent (QIAGEN) (see 2.1.5.2) into HEK293 cells and incubated for 24hours at 37°C. Transfection reactions were scaled up to use T175cm^2 flasks.

After the initial 24hour incubation, growth medium was removed and replaced with 10ml Optimem (Gibco) and incubated for a further 24-36 hours at 37°C. All the Optimem (containing secreted protein) was removed and purified for the *myc*-His_6 tagged proteins using the SIGMA His-Select™ HC nickel affinity gel. A 1ml aliquot of the His-Select™ HC nickel affinity gel was pelleted by centrifugation at 5,000x*g* for 30 seconds, then rinsed twice with dH_20 and twice with equilibrium buffer (50mM sodium phosphate [pH 8.0], 0.3M sodium chloride). The affinity gel was pelleted between each washing stage. The Optimem solution was then added to the affinity gel and gently mixed for 30 minutes at RT. The sample was pelleted again and remaining Optimem solution removed. The affinity gel was washed two times with 10 gel volumes of wash buffer (same as equilibrium buffer) for 4 minutes and then pelleted between washes. The pelleted affinity gel was mixed with 2 gel volumes of elution buffer (50mM sodium phosphate [pH8.0], 0.3M sodium chloride, 250mM imidazole) for 10 minutes, then pelleted by centrigfugation at 5,000x*g* for 5 minutes. The supernatant was removed and saved. Another 2 gel volumes of elution buffer was added and elution of the histidine proteins repeated.

Aliquots of eluted protein were then concentrated using Viaspin4 columns from Vivascience. A 4ml volume of protein was loaded into a Vivaspin4 column and concentrated to a 100-300µl volume by centrifugation of the column at 5000x*g*

for 5-7 minutes. Concentrated proteins were analysed by SDS-PAGE and Western blotting (see 2.6.2 and 2.6.3). In addition, approximately $1x10^6$ transfected cells were pelleted and lysed in ~100µl lysis buffer (see 2.1.8). An aliquot of the lysed cells was also analysed by SDS-PAGE and Western blotting.

2.6.2 Sodium Dodecyl Sulphate – Polyacrylamide Gel Electrophoresis (SDS-PAGE)

SDS-PAGE analysis of proteins was performed using a BIO-RAD electrophoration and blotting system (by the method of Laemmli, 1970). The apparatus was assembled as stated in the manufacturer's instructions, ensuring the glass plates were clean and dry before use. Depending on the resolution required, resolving gels contained 10%, 12% or 15% (w/v) acrylamide (BIO-RAD [40% (w/v) acrylamide: 2% (w/v) bis-acrylamide]), 375mM Tris [pH8.8], 0.1% (w/v) SDS, 0.06% (w/v) ammonium persulphate and 0.08% (v/v) TEMED (Sigma). The resolving gel was poured and allowed to set before the stacking gel (5% (w/v) acrylamide, 125mM Tris [pH6.8], 0.1% (w/v) SDS, 0.08% (w/v) ammonium persulphate and 0.2% (v/v) TEMED) was poured on top and a plastic comb inserted to form the sample wells. Once set, the gels were assembled in the tank and 500ml SDS-PAGE running buffer (25mM Tris, 250mM glycine, 0.1% (w/v) SDS) was added to the reservoirs. Samples for analysis were all diluted 1:2 with 2xLaemmli Loading Buffer (BIO-RAD) (50µl of β-mercaptoethanol was added to every 950µl of buffer) and heated for 10 minutes at 95°C. Samples were pelleted by centrifugation at 8,000x*g* for 2 minutes and then loaded onto the gel. In addition to the samples, a 10µl aliquot of Rainbow ladder (Amersham Bioscience) was loaded and run on the gel. Electrophoresis was performed at 30mA per gel, until the dye front had reached the bottom of the gel.

2.6.3 Western blotting

After analysis of protein samples by SDS-PAGE gel as previously described, the proteins were transferred to a nitrocellulose membrane hybond-ECL (Amersham Biosciences) by the tank transfer system using a Mini-Trans Blot Cell (BIO-RAD). The transfer apparatus was assembled according to the manufacturer's instructions,

the tank filled with transfer buffer (25mM Tris, 250mM glycine, 20% (v/v) methanol) and the transfer was performed at 400mA for 1 hour.

2.6.4 Immunoblotting

Membranes were incubated in western blocking buffer (1% (w/v) BSA, 0.05% (v/v) Tween-20 and 0.05% (w/v) Sodium Azide in PBS) containing 2% (v/v) normal rabbit or goat serum (depending on which species the secondary antibody was raised in), for approximately 1 hour at RT on a rotation bed. The membrane was then washed three times with PBS and then incubated with the primary antibody for 1 hour to overnight. Antibodies, working dilutions and their source are outlined in Table 2.2. All antibodies were diluted in the western blocking buffer. After incubation with the primary antibody, the membrane was washed three times with PBS and then incubated with the secondary antibody for 1 hour to overnight. If required, the membrane was then incubated with a tertiary streptavidin conjugate for 1-3 hours. The membrane was then washed another three times and alkaline phosphatase (AP) activity detected. A BCIP/NBT tablet (Roche) was dissolved in 10ml of dH_20 and the membrane immersed in the solution for 5 – 45 minutes, then thoroughly rinsed in water and air-dried.

Table 2.2 Antibodies used in immunoblotting analysis.

Antigen Detection	Primary Antibody	Secondary Antibody	Tertiary Conjugate
GST	Rabbit anti-GST Polyclonal 1:500 (SIGMA)	Goat anti-rabbit Ig linked to AP 1:2000 (SIGMA)	N/A
vOX2	Rabbit anti-vOX2/GST 1:50		
myc	Mouse anti-*myc* 1:2500 (SIGMA)	Goat anti-mouse linked to biotin 1:500 (SIGMA)	Streptavidin – AP 1:500 (SIGMA)

Suppliers are indicated in green, and working dilutions in blue.

2.7 Antibody Production

2.7.1 Production of a GST Fusion Protein

The vOX2 ORF was amplified by PCR using primers GEX1 and GEX2 (see Appendix 2 and 3) from DNA extracted from a BCP-1 cell line. The PCR product was then cloned into the pGEMT-Easy Vector (Progema), excised using *Apa*I and *Sac*II and purified. The vOX2 insert was then ligated into the bacterial expression vector pGEX-4T-1 (Amersham Pharmacia) in frame with the *Schistosoma japonicum* glutathione-S-transferase gene (GST), using the *Sma*I site. Ligation and transformation of bacteria by heat pulse were performed (see 2.2.10 and 2.2.13). Clones positive after mini-prep and restriction enzyme digestion for the inserted DNA with *Nde*I and *Xho*I, were tested for expression of the fusion protein by loading a sample of an overnight culture on a SDS-PAGE gel for Western analysis (see 2.6.2 and 2.6.3).

2.7.2 Preparation of Glutathione Sepharose 4B

The Glutathione Sepharose 4B (Amersham Pharmacia) matrix mixture was thoroughly mixed before a 1.33ml aliquot is removed. The matrix was sedimented by centrifugation at 500x*g* for 5 minutes before removal of the supernatant. The matrix was then washed in 10ml of cold PBS, to remove the ethanol storage solution, and then pelleted as before. After the supernatant was decanted, the matrix was resuspended in 1ml PBS, resulting in a 50% slurry mix that was kept at 4°C for up to 1 month.

2.7.3 Purification of GST-vOX2 Fusion Protein

For the preparation of large-scale bacterial sonicates, overnight cultures were grown in LB containing 100µg/ml ampicillin, of the clone of interest. The following day, cultures were diluted 1:10 fold into 200ml fresh LB and ampicillin. Cultures were incubated at 37°C in an orbital shaker and grown to log phase (2-4 hours). Protein expression was then induced by the addition of IPTG (Invitrogen Life Technologies) to a final concentration of 0.1mM, and incubated for a further 3 hours. The bacterial culture was pelleted by centrifugation at 7,700x*g* for 10 minutes at 4°C, and supernatant discarded (the pellet can be kept at -20°C until used). The pellet was

resuspended in 10ml ice-cold PBS with 100µl Proteinase Inhibitor (100x) (SIGMA), and cells disrupted by probe sonication for 30-45 seconds. An aliquot of 20% (v/v) Triton X-100 was added to a final concentration of 1% (v/v) and mixed gently for 30 minutes at RT. Cellular debris was pelleted out of the mixture by centrifugation at 12,000x*g* (4°C) for 10 minutes and set aside. To the supernatant, a 200µl aliquot of the 50% Glutathione Sepharose 4B slurry mix was added and mixed gently for 30 minutes at RT. The absorbed fusion protein was concentrated by centrifugation of the suspension at 500x*g* for 5 minutes. The supernatant was discarded, the Glutathione Sepharose 4B pellet washed with 100µl of PBS and then pelleted by centrifugation at 500x*g* for 5 minutes. This was repeated twice more for a total of three washes.

To elute the vOX2-GST fusion protein, 100µl of glutathione elution buffer (10mM reduced glutathione in 50mM Tris-HCl [pH 8.0]) was added to the pellet and incubated at RT for 10 minutes with gentle rotation. After centrifugation at 500x*g* for 5 minutes the supernatant containing the eluted protein was removed, and an additional 100µl elution buffer added to the pellet. This procedure was repeated twice to give three aliquots of eluted protein that were pooled and stored at -20°C.

To cleave the vOX2 protein from the GST the Glutathione Sepharose 4B pellet (with the fused protein) was resuspended in 100µl thrombin solution (500 cleavage units in 0.5ml pre-chilled PBS, stored in aliquots at -80°C), and mixed gently at room temperature for 4-16 hours. The GST bound to the matrix is pellet by centrifugation at 500x*g* for 5 minutes and the supernatant containing the vOX2 protein stored at -20°C.

The desired eluted protein and various samples along the procedure were analysed by Western Blot (see 2.6.4) for the presence of the vOX2 protein.

2.7.4 Immunisation of a Rabbit for Antibody Production

A 400µg sample of vOX2-GST fusion protein was sent to Diagnostic Scotland for the immunisation of a rabbit. The rabbit was immunized and boosted three times over a three-month period. Blood samples were taken periodically after and before the immunisation process and the serum sample returned for analysis.

2.7.5 Purification of Antibody from Rabbit Serum (using MAb Trap and HiTrap Desalting Kit)

MAbTrap™ Kit (Amersham Pharmacia), an affinity chromatography kit, was used for the purification of the vOX2-GST antibody, followed by the removal of low molecular weight contaminants using the HiTrap Desalting Kit (Amersham Pharmacia). The pre-packed column is filled with 1ml Protein G Sepharose High Performance and was initially prepared by passing through 5ml of distilled H_20 at a rate of 1 drop per second. The column was then equilibrated with 3ml of 1x binding buffer. The serum sample was prepared by extracting any particles that may be present by filtering the sample through a 0.45μm filter and then diluting 1:1 with 1x binding buffer. The prepared serum sample (5ml) was then applied to the column and washed with 5-10ml of binding buffer until no material appears in the effluent. The antibody was eluted with 3-5ml 1x elution buffer and collected in 1ml aliquots. The absorbance (A_{280}) was measured and the first two 1ml aliquots were pooled together. The purified IgG fractions were then desalted using the HiTrap Desalting column, packed with a size exclusion matrix Sephadex G-25 Superfine. The column was first equilibrated with 25ml of sterile PBS and then loaded with 1.5ml of the purified IgG fraction. The high molecular weight components were eluted with the addition of 1.5ml of sterile PBS and collected in a tube and stored at -20°C. Both columns were equilibrated with 1- 25ml 20% (v/v) ethanol for storage and future use. The antibody was tested by Western Blot analysis (see 2.6.4)

2.8 Animal Experiments

2.8.1 Infection of Mice

All animal experiments were performed under a Home Office Personal and Project License issued under the Animal (Scientific Procedures) Act 1986. BALB/c and C57/Blacks mice (3-4 weeks old) were supplied from Harlan and kept in-house for one-week prior to use. Mice were anaesthetised with halothane (Merial) in an anaesthetic chamber and inoculated intranasally with $2x10^5$ PFU virus, in 40μl sterile PBS. At various time points post-infection, mice were euthanased by CO_2 asphyxiation and tissues harvested for analysis. Spleen and MLN samples were either kept in complete RPMI medium on ice, snap frozen at -80°C or in 10% (v/v)

neutral buffered formaldehyde (Surgipath). Lung samples were either snap frozen at -80°C, inflated and stored in 10% (v/v) neutral buffered saline, or inflated with 50% OCT (in sterile PBS) (Surgipath) then frozen on dry ice and isopentane (methyl-2-butane) and stored at -80°C.

2.8.2 Determination of Spleen Weight

Spleen weights were determined using a Mettler AE 163 balance (to the nearest mg).

2.8.3 Infective Centre Assay for the Detection of Latent Virus

Freshly harvested spleen samples (kept in complete RPMI medium) were teased to a single cell suspension using a scalpel blade in a 60mm Petri dish containing 3ml of complete RPMI medium (RPMI 1640 supplemented with 10% (v/v) FCS, 70μg/ml penicillin, 10μg/ml streptomycin, 50μM β-mercaptoethanol, 2mM L-glutamine and 25mM HEPES) (Invitrogen Life Technologies). The cell suspension was then transferred to a sterile universal and pelleted by centrifugation at 600x*g* for 5 minutes at 4°C. The supernatant was discarded and remaining red blood cells lysed by osmosis due to the addition of 1ml of sterile dH_20 and mixed, followed by the immediate addition of 9ml of sterile PBS to establish equilibrium. The cellular debris was allowed to settle to the bottom of the universal and the top 8ml, containing the cell suspension was carefully removed and pelleted in a fresh universal by centrifugation at 600x*g* for 5 minutes at 4°C. The pellet was resuspended in 5ml complete RPMI medium and counted.

Petri dishes were filled with 5ml complete RPMI medium, $2x10^6$ BHK-21 cells and a 10^{-1}, 10^{-2} or 10^{-3} dilution of splenocytes. The mixture was gently agitated and incubation at 37°C for 5 days. Monolayers were fixed with 4% (v/v) neutral buffered formaldehyde (Surgipath) for at least 30 minutes and then fixed with 0.1 % (w/v) toluidine blue for 15- 45 minutes. All assays were performed in duplicate. The number of plaques per spleen were counted using a light microscope. A 1.8ml aliquot of the excess splenocytes was kept in a CryoTube™ and stored at -80°C for other DNA analysis.

This method was also used for the detection of latent virus in MLNs.

2.8.4 Titration of Infectious Virus in Lung Samples

Lung samples stored at -80°C were thawed and homogenized twice in a glass tissue homogeniser, in a total volume of 1.8ml Glasgow's complete medium. Samples were freeze-thawed to disrupt cell membranes and clarified by centrifugation at 2,000x*g* for 5 minutes at 4°C. Titration of infectious virus was performed by plaque assay on BHK-21 cells (see 2.3.4).

2.8.5 Analysis of Data

Data was analysed using GraphPad Prism software (San Diego, California), version 3.0 for Windows. In all cases, a two-way analysis of variance with Bobferroni's post-test was used and p values are indicated in the text.

2.8.6 Isolation of DNA from Mouse Tissue

A QIAamp® DNA Mini Kit was used for the isolation and purification of DNA from mouse tissue samples. Approximately 25mg of lung tissue or 10mg of spleen tissue or 10^6-10^7 splenocytes were resuspended in 180µl Buffer ATL. After the addition of 20µl of 19mg/ml Proteinase K (Qiagen), samples were vortexed and incubated for 4-16 hours at 56°C with gently agitation. A 200µl aliquot of Buffer AL was added to all samples, mixed and incubated at 70°C for 10 minutes before the addition of 200µl of ethanol (96%) and final mix. The samples were then transferred to a QIAamp Spin column and passed through the column by centrifugation at 6,000x*g* for 1 minute. The filtrate was discarded and column first washed with Buffer AW1 (500µl) and then Buffer AW2 (500µl), with centrifugation at 6,000x*g* for 1 minute after each wash, and twice after the last wash to ensure all residual buffer was discarded. The QIAamp Spin Column was then transferred to a sterile collection tube to elute the DNA. Between 30µl to 40µl of Buffer AE was added to the column, incubated at room temperature for 5 minutes and then the DNA was eluted by centrifugation of the column at 6,000x*g* for 1 minute. This step was repeated to give a final volume of 60µl-80µl of DNA, samples were stored at -20°C.

2.8.7 Simultaneous Isolation of RNA and DNA from Animal Tissue

For the simultaneous isolation of RNA and DNA from animal tissue a QIAGEN RNA/DNA kit was used. This initially involved the homogenisation of the tissue samples with a mortar and pestle set in a liquid nitrogen bath, in order to keep the samples frozen. Once ground to a powder, with most of the liquid nitrogen evaporated off, the frozen samples were added to a cooled tube of lysis buffer (1.5ml) and then mixed. The homogenised samples were then passed through a QIAshredder column (Qiagen) by centrifugation at 10,000x*g* for 2 minutes. The elute was collected and 500µl of Buffer QRV1 was added, mixed and centrifuged at 15,000x*g* (4°C) for 20 minutes. The supernatant was transferred to a RNase-free collection tube and 0.8 volumes of ice-cold isopropanol added, mixed and incubated on ice for 5 minutes. Samples were then centrifuged at 15,000x*g* for 30 minutes at 4°C, supernatant discarded and 150µl Buffer QRL1 added to the nucleic-acid pellet.

The tubes were heated at 60°C for 3 minutes and mixed to dissolve the pellet. An 1.35ml aliquot of Buffer QRV2 was added, mixed and centrifuged at 5,000x*g* (4°C) for 5 minutes, during which the QIAGEN-tips were equilibrated by the addition of 1ml of Buffer QRE. The supernatant was then applied to the QIAGEN-tip and allowed to enter the resin by gravity flow. The flow-through was set aside and kept at room temperature, for isolation of the DNA later.

The QIAGEN-tips were then washed by the addition of 2ml (2x 1ml) of Buffer QRW, and the RNA eluted by the addition of 1ml of pre-heated (45°C) Buffer QRU. A 1 volume of ice-cold isopropanol was added to the RNA elute and kept on ice while the final extraction of DNA was made.

The DNA elute from earlier was placed into the same QIAGEN-tip and allowed to enter the resin by gravity flow, this was then repeated with the eluted flow-through and finally the QIAGEN-tip was washed with 3ml (3x 1ml) of Buffer QC. The genomic DNA was eluted into 1ml of pre-heated (45°C) Buffer QF. Room-temperature isopropanol (0.7 volumes) was added to the eluted DNA solution, mixed thoroughly, and incubated at room temperature for 10 minutes. The RNA (on ice) and the DNA were then centrifuged at 15,000x*g* for 30 minutes at 4°C. The supernatant was carefully removed and the pellet was washed with ice-cold 70% (v/v) ethanol and then again pelleted by centrifugation at 15,000x*g* (4°) for 20

minutes. The pellets were air dried for approximately 10 minutes and the DNA dissolved in TE and RNA dissolved in RNase-free water. DNA and RNA samples were stored at -20°C.

2.8.8 Histopathology

Lung, spleen and MLN samples taken from the animal experiments were stored in various methods. Mice were euthanased by CO_2 asphyxiation and the lungs were inflated via the trachea. Samples fixed in 10% (v/v) neutral buffered formaldehyde were processed routinely into paraffin wax-embedded sections at the Pathology Department, Easter Bush. Lung, spleen and MLN samples were snap frozen in liquid nitrogen and sectioned at Easter Bush. In addition, some lungs samples were inflated with 50% (v/v) OCT then slowly frozen on a mix of isopentane and dry-ice, and then also sent to Easter Bush to be sectioned. One section from all samples was stained with haematoxylin and eosin, and examined by light microscopy.

2.9 Microscopy

2.9.1 Fixation of Cells to Slides

Cells were resuspended to 0.5 - $1x10^6$ cells/ml in sPBS and either air-dried or attached by centrifugation using a Cytospin 2 (ThermoShandon) onto a glass slide (BDH). Most cells were fixed by immersion of the slides into ice-cold methanol/acetone (1:1) for 2 minutes and then air-dried. Other cells and tissue samples (frozen) were fixed by incubating the slide in 4% (w/v) paraformaldehyde in PBS for 10 minutes to 2 hours at RT. The slides were then washed in PBS and used immediately, or air-dried and stored at -20°C.

2.9.2 Immunostaining

Slides were incubated for a minimum of 30 minutes at RT in immuno-blocking solution (1% (w/v) BSA, 1% (v/v) TritonX-100 and 0.1% (w/v) Sodium azide, in PBS) with 2% (v/v) normal goat or rabbit serum (depending on which species the secondary antibody was raised in), to prevent non-specific antibody binding. The slides were then washed three times for three minutes (with gentle

agitation) in PBS and incubated with an appropriate amount of diluted primary antibody for 1 hour at RT. After three washes with PBS, the slides were incubated for 1 hour at RT with the diluted secondary antibody. After the final three washes, with PBS, slides were allowed to dry and were mounted in fluorescent mounting medium (DAKO). Fluorescence was examined using a Nikon Diaphot 200 Ultraviolet Microscope.

Antibodies, working dilutions and their source are outlined in Table 2.3. All antibodies were diluted in the immuno-blocking buffer.

Table 2.3 Antibodies used in immunostaining.

Antigen Detection	Primary Antibody	Secondary Antibody	Method of fixation
MHV-76	Rabbit anti-MHV-68 polyclonal 1:250	Goat anti-rabbit alexa fluor 546 (red) 1:200 Molecular Probes	(Frozen samples) 4% PFA
vOX2	Rabbit anti-vOX2-GST polyclonal 1:50	Goat anti-rabbit FITC (green) 1:100-1:200 SIGMA	4% PFA
FLAG	Mouse anti-FLAG 1:200 SIGMA	Rabbit anti-mouse alexa fluor 594 (red) 1:800 Molecular Probes	methanol/acetone (1:1)
mCD200	Rat anti-mCD200 1:200-2000 Serotec	Goat anti-rat alexa fluor 350 (blue) 1:400-1000 Molecular Probes	(Frozen samples) 4% PFA or methanol/acetone (1:1)

Working dilutions are indicated in blue and commercial suppliers in green. Abbreviations: PFA; paraformaldehyde.

Appendix 1: General Solutions

Unless otherwise stated, all chemicals were obtained from Sigma or Merck BDH

Hank's buffered salt solution (HBSS)	150mM NaCl, 25mM HEPES, 5mM KCl, 5mM glucose, 1mM $CaCl_2$, 1mM KH_2PO_4, 1mM $MgCl_2$, 1mM Na_2HPO_4, 1mM $MgSO_4$, 0.001% (w/v) phenol red [pH 7.0]
Luria-Bertani (LB) medium	1% (w/v) tryptone, 1% (w/v) NaCl 0.5% (w/v)yeast extract
LB Agar	1x LB broth, 1.5% (w/v) Bacto-Agar
Phosphate-buffered saline (PBS)	150mM NaCl, 2.5mM KCl, 10mM Na_2HPO_4, 1mM KH_2PO_4 [pH 7.4]
Rnase-free H_2O	dH_2O, 0.1% (v/v) Diethylpyrocarbonate, Autoclave
SOC medium	1x LB broth, 20mM glucose, 20mM $MgCl_2$
20 x SSC	3M NaCl, 300mM Na citrate [pH7.0]
TE buffer	10mM Tris-HCl [pH8.0], 1mM EDTA
TBE buffer	45mM Tris-borate, 1mM EDTA
Tris-buffered saline (TBS)	50mM Tris-HCl, 150mM NaCl [pH 7.6]

Appendix 2: Oligonucleoties utilized in this study

All primers were synthesized by SIGMA Genosysis, Invitrogen or Gibco BRL Life Technologies

Primer	Primer sequence	Anneal Temp	Amplified Region
OXF1 **OXR-Flag**	*Kpn*I 5'-GGGGTACCATGGTACACACATTTTTTGATTGTCCC-3' *Xba*I 5'-GCGCTCTAGATTACTTGTCGTCGTCGTCCTGTAGTC CTGGGTGGATAGGGGGTCC-3'	57°C (30s)	KSHV K14 nt 127884-128927 1079bp product
OXF2 **OXR-Flag**	*Kpn*I 5'-GGGGTACCATGGCTAGCCTCTTCATTTCATTACC-3' see sequence above	57°C (30s)	KSHV K14 nt 128113-128927 1308bp product
GEX1 **GEX2**	5'-GGGGTA CCATGGCTAGCCTCTTCATTTCATTACC-3' 5'-CCCAAGCTTGC CTGGGTGGATAGGGGGTC-3'	57°C (30s)	KSHV K14 nt 128113-128917 821bp product
Sec1 **Sec2**	*Xho*I 5'-GACTCTCGAGCCATGTCTAGCCTCTTCATTTC-3' *Hind*III 5'-GACTAAGCTTTCCCTGGGCCGCGGAAGGTC-3'	57°C (30s)	KSHV K14 nt 128113-128805 710bp product
vOX-1 **vOX-2**	*BspH*I *Asc*I 5'-GCTCATGAGGCGCGCCATGTCTAGCCTCTTCATTTC-3' *Nco*I *Fse*I 5'-GCCCATGGCCGGCCTCACTGGGTGGGTGGATAGGGG GT-3'	57°C (30s)	KSHV K14 nt 128113-128930 847bp product
RGD3 **RGD4**	*Sma*I/*Xma*I 5'-GAGGACCGTGAGGCTGCCCCGGGCCGATAATACCAC CCCAG-3' *Sma*I/*Xma*I 5'-CTTGGGGTGGTATTATCGGCCCGGGGCAGCCTCACGG TCCTC-3'	60°C*	KSHV K14 nt 128666*
ORF74-5' **ORF74-3'**	5'-GCCACGATGCTTGTCCTGCG-3' 5'-TTAGGAGCTTAGTCTACAAACRG-3'	55°C (1min)	MHV-68 ORF74 nt 105057-106067 1010bp product
PolyA-rev **M4-B**	5'-CCACAACTAGAATGCAGTC-3' 5'-CGCGGAATTCGGTTCTAGAAAGTCATAAATCTCAATA CC-3'	55°C (45s)	pHygEGFP polyA nt 2932-3127 and MHV-68 M4 frag. nt 9539-9785 442bp product
CMV-A **M4-B**	5'GGGCAGTTTACCGTAAATACTCC-3' see above sequence	55°C (45s)	pHygEGFP CMV nt 1-364 and MHV-68 M4 frag. nt 9539-9785 611bp product

Trepeat **M4-B**	5'-GCGCCAGGAGGAGCTAGGCCACG-3' see above sequence	55°C (45s)	MHV-76 left-end frag. nt 119382-9786 317bp product
ORF50-F **ORF50-R**	5'-GACGGATCCGGCACATTTGCTGCAGAACCC-3' 5'-TGCCTTAAGGAACGGCGCCTGTGTACTC-3'	55°C (45s)	MHV-68 ORF50 nt 68483-68838 355bp product
GAPDH-1 **GAPDH-2**	5'-TGGATATTGTTGCCATCAATGACC-3' 5'-GATGGCATGGACTGTGGTCATG-3'	58°C (30s)	~360bp product
mCD200-5' **mCD200-3'**	5'-AGTGGTGACCCAGGATGAA-3' 5'-GTACTATGGGCTGTACATAG-3'	53°C (45s)	Murine CD200 338bp product
mCD200R-5' **mCD200R-3'**	5'-GCCCTAGCAGTGCTCTTAAT-3' 5'-GAGCCATTGCTGTGTGATTCA-3'	54°C (45s)	Murine CD200R 556bp product

* This set of primers was used for the site directed mutagenesis of the RGD sequence within vOX2 (in pCR2.1-TOPO/vOX2), with the following cycling conditions: 1x 95°C for 1min, 18x (95°C for 50s, 60°C for 50s, 68°C for 10min [2min/plasmid kb]), 1x 68°C for 7min.

Appendix 3: Cloning vectors utilised in this study

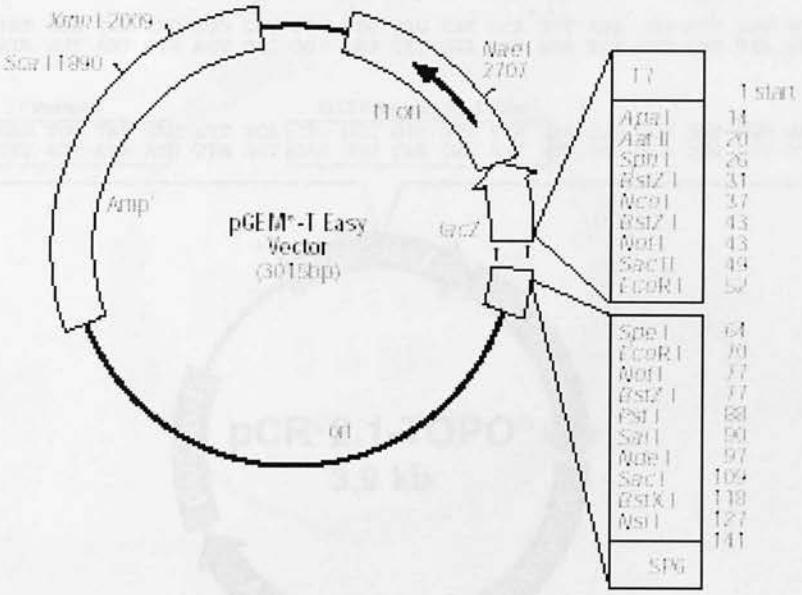

Vector pGEM-T Easy.

This vector was obtained from Promega.

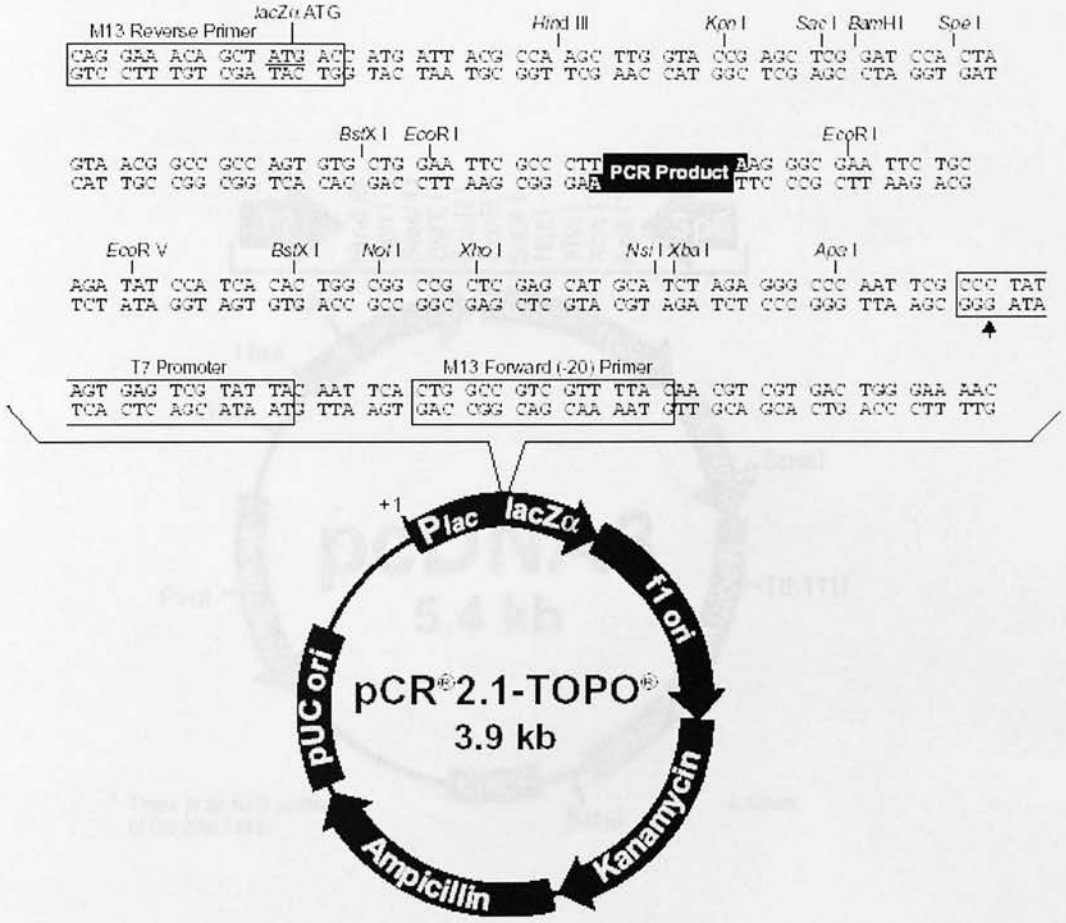

Vector pCR®2.1-TOPO.

The vector pCR®2.1-TOPO was obtained from Invitrogen.

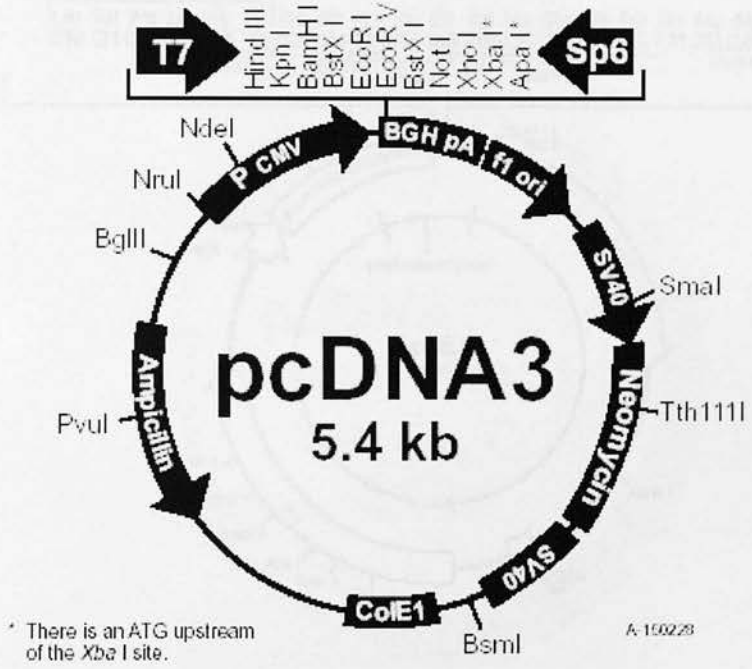

Vector pcDNA3.
The vector pcDNA3 was obtained from Invitrogen.

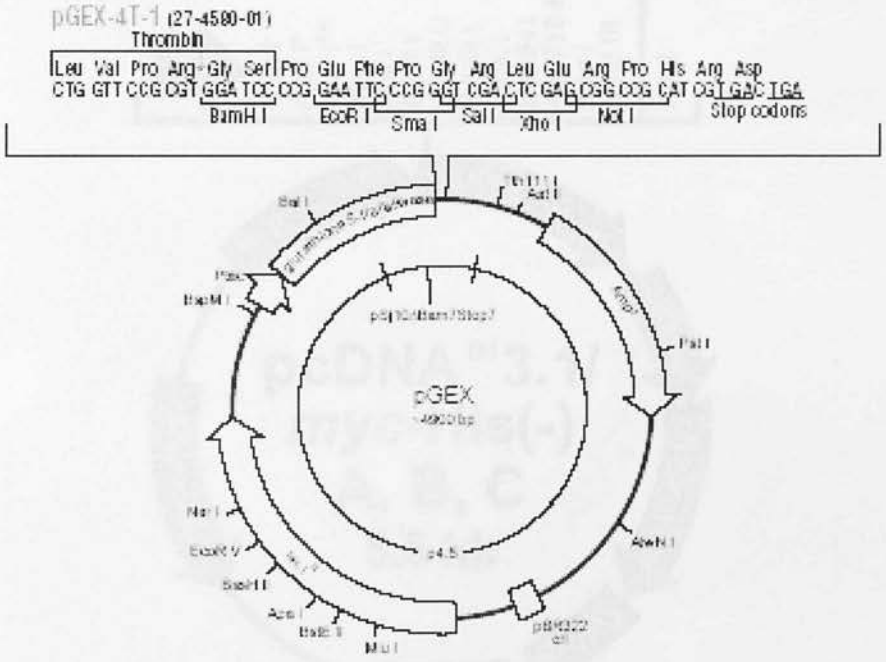

Vector pGEX-4T-1.

The vector pGEX-4T-1 was obtained from Pharmacia Biotech.

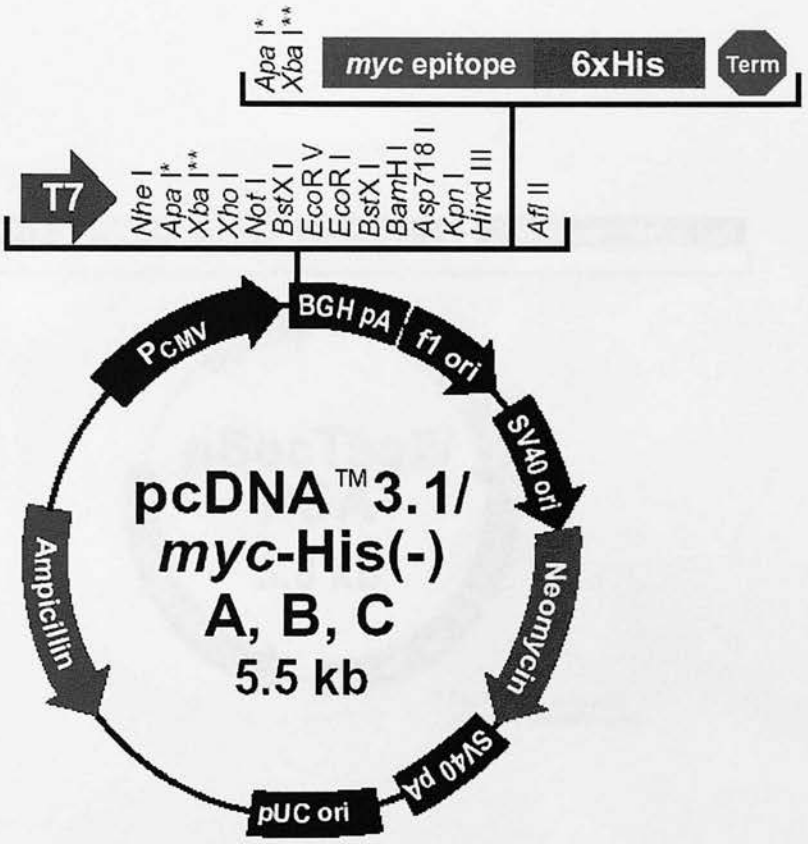

Vector pcDNA™3.1/*myc*-HIS(-).
The vector pcDNA3.1/*myc*-His(-) was obtained from Invitrogen.

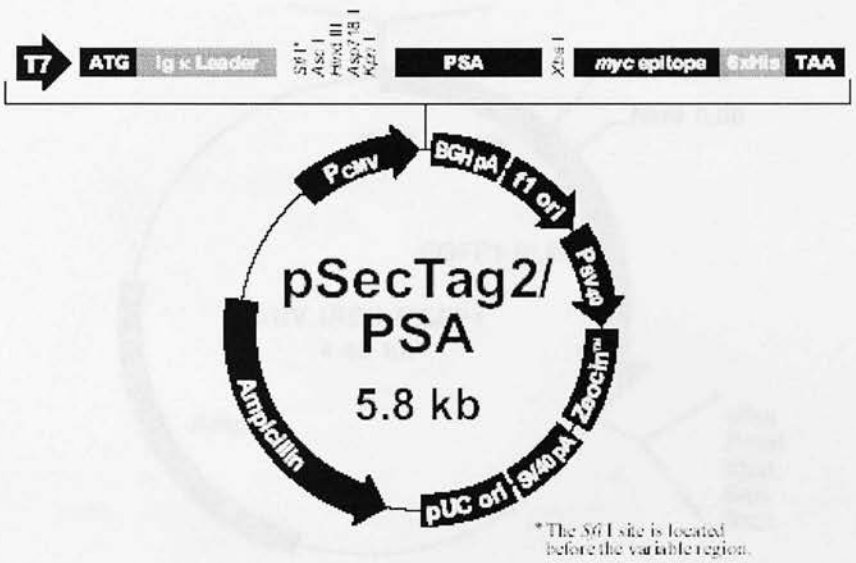

Vector pSecTag2/PSA.

The vector pSecTag2/PSA was obtained from Invitrogen.

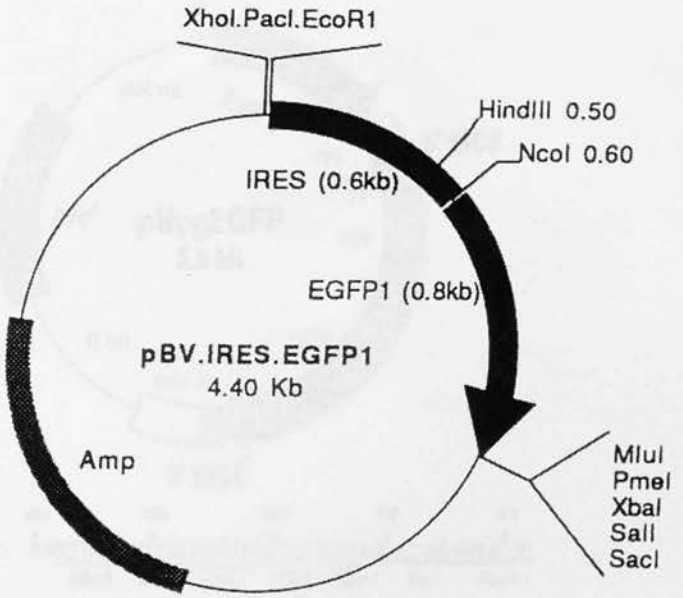

Vector pBV.IRES.EGFP1

The vector pBV.IRES.EGFP1 was kindly supplied by Dr James Stewart, at the University of Edinburgh.

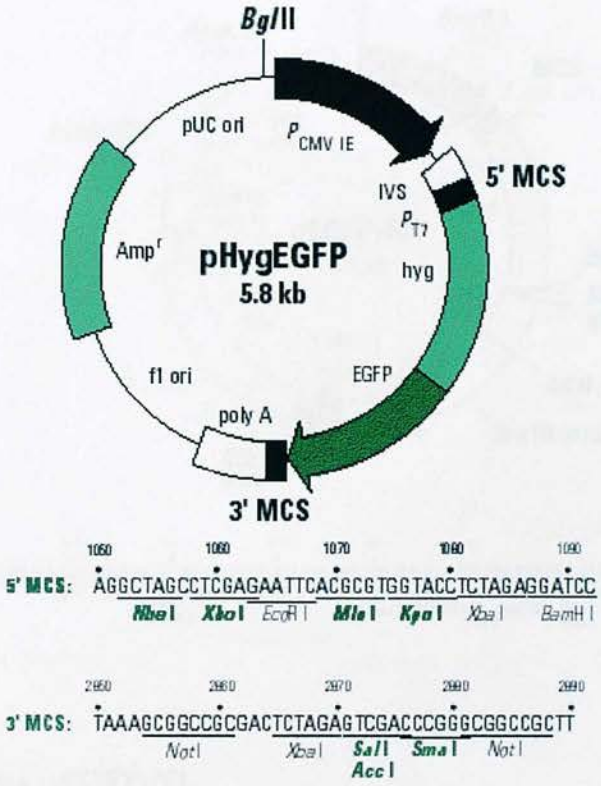

Vector pHygEGFP.
The vector pHygEGFP was obtained from BD Biosciences Clontech.

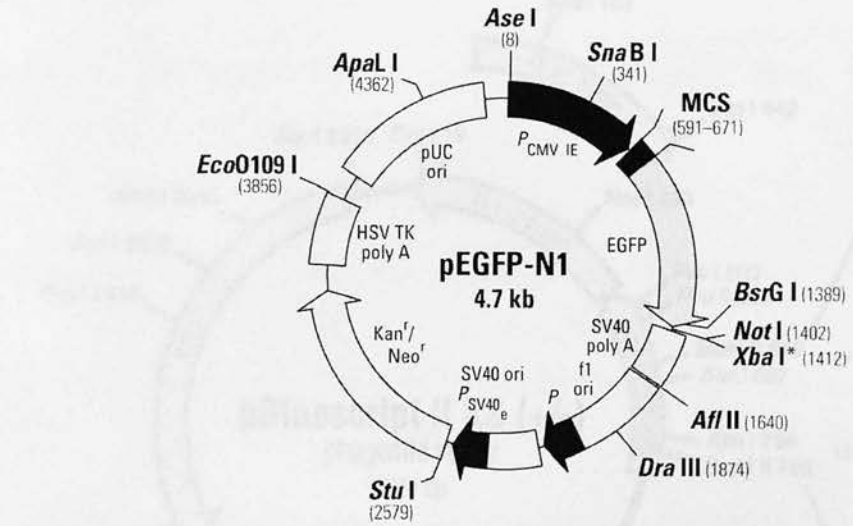

Vector pEGFP-N1.

The vector pEGFP-N1 was obtained from BD Biosciences Clontech.

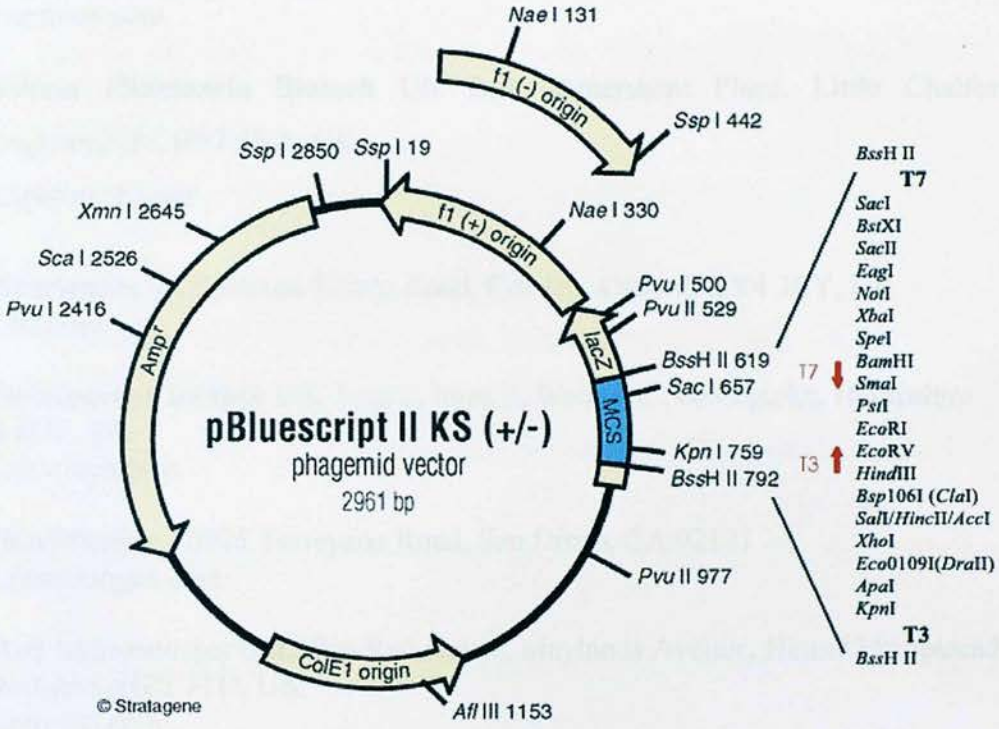

Vector pBluescript II KS(-)

The vector pBluescript II KS (-) was obtained from Stratagene. The clone pBSIIKS-76LHE, was generated by Alastair Macrae by inserting a 3Kb fragment of MHV-76 (corresponding to 9539-12569 of MHV-68 accession number U97553) into the *BamH*I and *Eco*RI site in the multiple cloning site.

Appendix 4: Commercial suppliers of reagents and equipment used in this study

Ambion Inc., Ambion (Europe) Ltd., Ermine Buisness Park, Spitfire Close, Huntingdon, Cambridgeshire, PE29 6XY, UK
www.ambion.com

Amersham Pharmacia Biotech UK Ltd., Amersham Place, Little Chalfont Buckinghamshire, HP7 9NA, UK

www.apbiotech.com

BD Biosciences, 21 Between Towns Road, Cowley, Oxford, OX4 3LY, UK
www.bd.com

BD Biosciences Clontech UK, Unit 2, Intec 2, Wade Rd., Basingtoke, Hampshire RG24 8NE, UK
www.clontech.com

BD PharMingen, 10975 Torreyana Road, San Diego, CA 92121
www.pharmingen.com

Bio-Rad Laboratories Ltd., Bio-Rad House, Maylands Avenue, Hemel Hempstead Hertfordshire, HP2 7TD, UK
www.bio-rad.com

DAKO Ltd., Denmark House, Angel Drove, Ely, Cambridgeshire, CB7 4ET, UK
www.dako.com

EquiBio, Action Court, Ashford Road, Ashford, Middlesex, TW15 1XB, UK
www.equibio.com

Flowgen, Novara House, Excelsior Road, Ashby Park, Ashby de-la Zouch, Leicestershire, LE65 1NG, UK
www.flowgen.co.uk

Invitrogen Life Technologies, Invitrogen Ltd, 3 Fountain Drive , Inchinnan Business Park, Paisley, PA4 9RF, UK
www.invitrogen.com

Merck Ltd., Hunter Boulevard, Magna Park, Lutterworth, Leics, LE17 4XN
www.merckeurolab.ltd.uk

Millipore (U.K.) Limited, Units 3&5 The Courtyards, Hatters Lane, Watford, WD18 8YH
www.millipore.com

Miltenyi Biotec Ltd., Almac House, Church Lane, Bisley, Surrey, GU24 9DR
www.miltenyibiotec.com

Molecular Probes Europe, Poort Gebouw ,Rijnsburgerweg 10 ,2333 AA Leiden
The Netherlands
www.probes.com

MWG-Biotech AG, Mill Court, Featherstone Road, Wolverton Mill South, Milton Keynes, MK12 5RD, UK
www.mwg-biotech.com

New England Biolabs (UK) Ltd., 73 Knowl Piece, Wilbury Way, Hitchin, Hertfordshire, SG4 0TY, UK
www.neb.com

Roche Diagnostics Ltd., Bell Lane, Lewes, East Sussex, BN7 1LG, UK
http://biochem.roche.com

QIAGEN Ltd., Boundary Court, Gatwick Road, Crawley, West Sussex, RH10 2AX
www.qiagen.com

Santa Cruz Biotechnology, 2161 Delaware Avenue, Santa Cruz, CA 95060 USA
www.scbt.com

Serotec Ltd., 22 Bankside, Station Approach, Kidlington, Oxford, OX5 1JE, UK
www.serotec.com

Sigma-Aldrich Company Ltd., The Old Brickyard, New Road, Gillingham, Dorset, SP8 4XT, UK
www.sigma-aldrich.com

Stratagene Europe, Gebouw California, Hogehilweg 15 ,1101 CB Amsterdam Zuidoost,The Netherlands

www.stratagene.com

Surgipath Europe Ltd., Venture Park, Stirling Way, Bretton, Peterborough PE3 8YD, UK
www.surgipath.com

ThermoHybaid, Action Court, Ashford Road, Ashford, Middlesex, TW15 1XB, UK
www.thermohybaid.com

Vivascience AG, Feodor-Lynen-Strasse 21, 3065 Hanover, Germany
www.vivascience.com

Chapter Three: Characterisation of the vOX2 protein

Chapter Three: Protein Expression Studies

At the time of commencing these studies, information on the KSHV vOX2 protein was very limited. The aim of the following work was to characterise the vOX2 protein, including the generation of an antibody against vOX2, determination of the cellular localisation and interaction with cellular receptors. This was hoped to aid in further understanding the function of vOX2 and its potential role in KSHV pathogenesis.

3.1 Analysis of vOX2 protein sequence

The vOX2 ORF is predicted to encode either a 348 or 271 amino acid protein; there are two potential initiating codon sequences that could be used (Figure 3.1). However, a common signal peptide sequence is encoded directly after the second methionine initiating coding site suggesting that the second site is utilised. Neither initiating coding site contain a Kozak sequence. There are 5 or 6 potential N-linked protein glycosylation sites in vOX2. Several conserved cysteine (C) residues and blocks of homologous sequence with the human, mouse and rat CD200 protein, suggest that the vOX2 protein is also made up of IgG domains as illustrated in Figure 1.12 (Figure 3.3 shows homology with 271aa vOX2 protein). A hydropathicity plot of the vOX2 protein and hCD200 amino acid sequence was performed (Figure 3.2); this also confirmed a similar pattern between both proteins. Areas containing any transmembrane or membrane-anchoring regions typically contain a 20 amino acid hydrophobic region (Kyte and Doolittle, 1982). Both vOX2 and hCD200 contain a single transmembrane region.

A database search was performed using the program "BLAST' against all protein entries and found sequence homology with other viral CD200 homologues listed in Table 1.4 including HHV-6, HHV-7, RRV, and Myxomavirus.

```
  1    MIHTFFDCPG RRVVEGGVIS SYFLIGAPGR TAIKTEEGVS
 41    ALQNLPPTVL PVAGTGSVVR PVVCAPPWTT PSASRGSMSS
 81    LFISLPWVAF IWLALLGAVG GARVQGPMRG SAALTCAITP
121    RADIVSVTWQ KRQLPGPVNV ATYSHSYGVV VQTQYRHKAN
161    ITCPGLWNST LVIHNLAVDD EGCYLCIFNS FGGRQVSCTA
201    CLEVTSPPTG HVQVNSTEDA DTVTCLATGR PPPNVTWAAP
241    WNNASSTQEQ FTDSDGLTVA WRTVRLPRGD NTTPSEGICL
281    ITWGNESISI PASIQGPLAH DLPAAQGTLA GVAITLVGLF
321    GIFALHHCRR KQGGASPTSD DMDPLSTQ
```

Figure 3.1 Diagrammatic representation of the potential post-translational modifications present in the vOX2 protein. The KSHV vOX2 DNA sequence (nt 127884 to 128940) is translated into 348 or 271 amino acids, depending on which initiating codon sequence is utilised. There are two possible in-frame methionine initiating coding sequences, underlined in purple, and a common signal peptide sequence, indicated in pink. The predicted N-linked glycosylation sites are shown in red. The RGD motif is indicated in green.

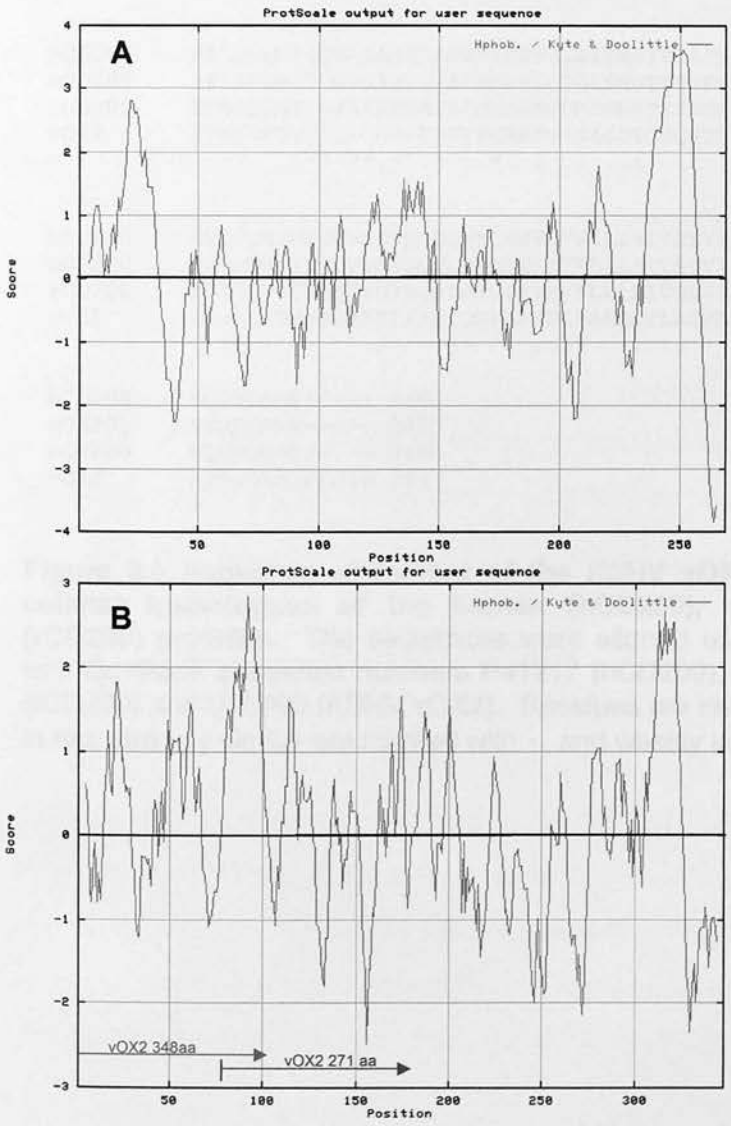

Figure 3.2 Hydropathicity plot of the human CD200 and KSHV vOX2 protein. Hydrophobicity plots using the method of Kyte and Doolittle (1982) display hydrophobic regions of the protein as positive values and hydrophilic regions are assigned negative values for proteins (A) human CD200 and (B) KSHV vOX2 (vOX2 protein of 348 aa and 271 aa are indicated at the bottom of the plot). The first large hydrophobic peak in both plots (position ~25 in plot A and ~90 in plot B) is the signal sequence, whereas the second peak (position ~250 in plot A and ~310 in plot B) is representative of a single transmembrane region.

```
                V domain →
hCD200      QVQVVTQDEREQLYTPASLKCSLQNAQEALIVTWQKKKAVSPENMVTFSENHGVVIQPAY 60
mCD200      QVEVVTQDERKALHTTASLRCSLKTSQEPLIVTWQKKKAVSPENMVTYSKTHGVVIQPAY 60
rCD200      QVEVVTQDERKLLHTTASLRCSLKTTQEPLIVTWQKKKAVGPENMVTYSKAHGVVIQPTY 60
vOX2        --AVGGARVQGPMRGSAALTCAITPRADIVSVTWQKRQLPGPVNVATYSHSYGVVVQTQY 58
              *     :  :  .*:* *::    : : *****::  .* *:.*:*. :***:*. *

                                                  V domain  ←|→ C2 domain
hCD200      KDKINITQLGLQNSTITFWNITLEDEGCYMCLFNTFGFGKISGTACLTVYVQPIVSLHYK 120
mCD200      KDRINVTELGLWNSSITFWNTTLEDEGCYMCLFNTFGSQKVSGTACLTLYVQPIVHLHYN 120
rCD200      KDRINITELGLLNTSITFWNTTLDDEGCYMCLFNMFGSGKVSGTACLTLYVQPIVHLHYN 120
vOX2        RHKANITCPGLWNSTLVIHNLAVDDEGCYLCIFNSFGGRQVSCTACLEVTSPPTGHVQVN 118
            :.: *:*  ** *::::.: * :::*****:*:** **  ::* **** :   *   :: :

hCD200      FSEDHLNITCSATARPAPMVFWKVPRSGIENSTVTLSHPNGTTSVTSILHIKDPKNQVGK 180
mCD200      YFEDHLNITCSATARPAPAISWKGTGTGIENSTESHFHSNGTTSVTSILRVKDPKTQVGK 180
rCD200      YFEDHLNITCSATARPAPAISWKGTGSGIENSTESHSHSNGTTSVTSILRVKDPKTQVGK 180
vOX2        STEDADTVTCLATGRPPPNVTWAAPWNNASSTQEQFTDSDGLTVAWRTVRLPRGDNTTPS 178
              **  .:** **.**.* : *  . .. ..:     ..:* * .   :::   .. . .

                                                C2 domain  ←|→ Transmembrane
hCD200      EVICQVLHLGTVTDFKQTVNKGYWFSVPLLLSIVSLVILLVLISILLYWKRHRNQDRGEL 240
mCD200      EVICQVLYLGNVIDYKQSLDKGFWFSVPLLLSIVSLVILLVLISILLYWKRHRNQERGES 240
rCD200      EVICQVLYLGNVIDYKQSLDKGFWFSVPLLLSIVSLVILLVLISILLYWKRHRNQERGES 240
vOX2        EGICLITWGNESISIPASIQGPLAHDLPAAQGTLAGVAITLVGLFGIFALHHCRRKQGGA 238
            * ** :   .   .   :::    ..:*   . :: * : ::  : ::  :* .:.:*

hCD200      SQGVQKMT----- 248
mCD200      SQGMQRMK----- 248
rCD200      SQGMQRMK----- 248
vOX2        SPTSDDMDPLSTQ 251
            *   : *
```

Figure 3.3 Sequence alignment of the KSHV vOX2 protein with the CD200 cellular homologues of the human (hCD200), mouse (mCD200) and rat (rCD200) proteins. The sequences were aligned using the "ClustralW" program with GenBank accession numbers P41217 (hCD200), O54901 (mCD200), P04218 (rCD200) and U75698 (KSHV vOX2). Residues are identical are marked with * and in red, strongly similar are marked with :, and weakly similar with ..

3.2 Cellular localisation of vOX2

In order to determine the true methionine initiation codon site and to confirm vOX2 is expressed on the cell surface, the vOX2 ORF was tagged with a FLAG tag and expressed *in vitro*. The vOX2 ORF was amplified with either OXF1 or OXF2 as the forward primer and used the OXR-Flag as the reverse primer (see 2.2.1 and Appendix 2), respectively generating amplified products of ~1080bp and ~1310bp in size. The OXR-Flag primer incorporates a FLAG tag sequence (and *Xba*I restriction enzyme site) directly after the vOX2 sequence and is expressed on the intracellular C-terminus of the protein. After being cloned into the PCR cloning vector, pGEMT-easy (see 2.2.15 and Appendix 3), the vOX2 ORF was cut out at *Kpn*I and *Xba*I sites and cloned into pcDNA3 (Appendix 3) generating pcDNA3/vOX_{348} and pcDNA3/vOX_{271}. Following the verification of the clones, vectors were transfected into HEK293 cells using the effectene transfection reagent (QIAGEN) (see 2.1.5.2). The cells were harvested 48 hours after transfection, and air-dried onto glass slides. Samples were fixed in ice-cold methanol/acetone (1:1) (see 2.9.1).

Samples were stained by indirect immunofluorescence targeting the fused FLAG epitope, using mouse anti-FLAG, followed by anti-mouse Ig alexa-fluro 594 (red). Red fluorescence was visualised on the surface of cells in both sets of transfected cells (Figure 3.4 A and B). This indicates that the second methionine of vOX2 at amino acid 78 can be used as an initiation codon. Control cells that were incubated with no primary antibody followed by anti-mouse Ig alexa fluro 594 conjugate showed no red fluorescence (Figure 3.4-C).

3.3 Generation of anti-vOX2 antibody

In order to further investigate vOX2 interaction and function both *in vitro* and *in vivo*, it was decided to generate an antibody against the vOX2 protein. Initial attempts were undertaken to generate a vOX2-GST fusion proteins using the pGEX expression system (see 2.7), as this system provides a convenient method to express and purify proteins. The vOX2 ORF was amplified by PCR using primer pair GEX1 and GEX2 (see 2.2.1 and Appendix 2). The amplified product (~820bp) was first cloned into the PCR cloning vector pGEMT-Easy and then excised with *Apa*I and

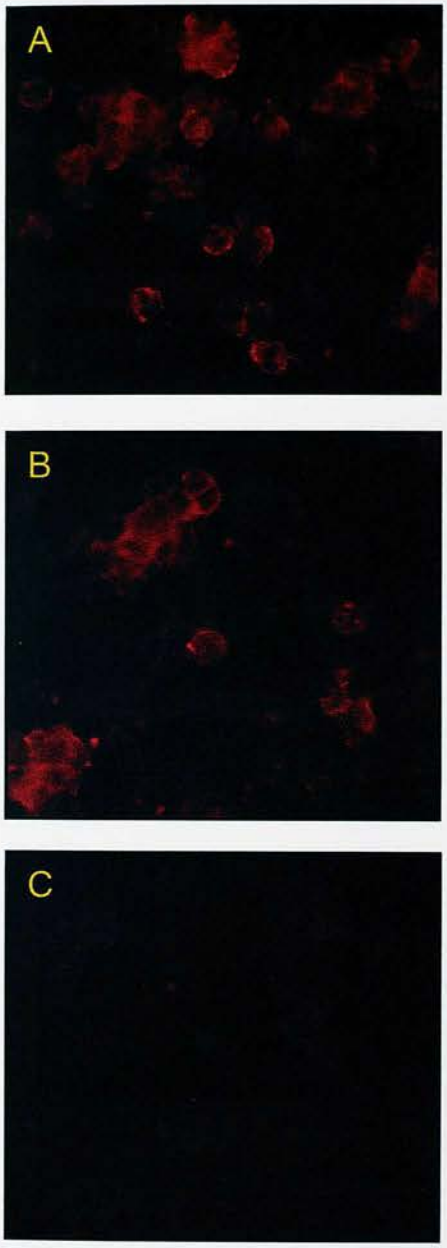

Figure 3.4 Expression of vOX2-FLAG -epitope tagged protein in HEK293 cells. HEK293 cells were transfected with (A) pcDNA3/vOX_{348}, (B) pcDNA3/vOX_{271} or (C) no plasmid-HEK293 cells only. Cells were air dried on to slides and fixed with ice-cold methanol/ acetone, then stained with mouse anti-FLAG (1:200), and finally with anti-mouse conjugated with alexa fluro 594 (red) (1:800). (All images at x400 magnification)

*Sac*II; these restriction enzyme sites are located within the vOX2 ORF, *Apa*I is directly after the signal sequence and *Sac*II is located before the transmembrane and cytoplasmic region. The extracellular portion of the vOX2 ORF was then blunt-ended and cloned into the *Sma*I site of pGEX-4T1 (Appendix 3), to form the vector pGEX/vOX2, a control plasmid pGEX/GST was also generated. The vOX2 gene was inserted in frame with the glutathione S-transferase gene of *Schistosoma japonisum*, and would be expressed as a GST fusion protein. XL-1 blue bacterial clones positive for the vOX2 insert in pGEX-4T1 by mini-prep were tested for their ability to express the vOX2-GST fusion protein. Expression of the fusion protein was induced by the addition of 0.5mM IPTG during the exponential growth phase of the culture (see 2.7.3). Following induction with IPTG, the repression of the P_{tac} promoter by the *lac* repressor is stopped leading to expression of the fusion protein via the P_{tac} promoter. The bacterial culture was harvested approximately 3 hours after induction, and the bacterial pellet sonicated and the cell lysate analysed on a 12% gel. As shown in Figure 3.5, a band with an apparent molecular mass of ~50kDa indicates the vOX2-GST fused protein, whereas GST alone is visualised as a band ~ 27kDa; the predicted size of the extracellular portion of vOX2 is ~22kDa.

Following the identification of the vOX2-GST protein and batch purification, a 400μg sample was sent to Diagnostic Scotland for the immunisation of a rabbit. Following the initial immunisation, the rabbit received three booster injections over a period of three months. A blood sample was taken prior to immunisation (pre-bleed) and periodically after and before each booster injection. The serum was separated from the blood sample and returned for analysis of anti-vOX2 reactivity. The serum was first purified using the MAbTrap™ Kit (Amersham Pharmacia), an affinity chromatography kit, followed by the removal of low molecular weight contaminants using the HiTrap Desalting Kit (Amersham Pharmacia) (see 2.7.5). These two procedures assisted in producing a moderately pure IgG antibody sample.

The anti-vOX2 reactivity of the purified rabbit serum was assessed by immunoblot. Identical 12% SDS-PAGE gels were prepared and loaded with purified vOX2-GST fusion protein and GST only. Following Western blotting, membranes were either incubated with the purified pre-bleed or third (final) bleed rabbit antibody and then anti-rabbit conjugated to AP. Figure 3.6 shows that the third bleed

antibody sample recognises the vOX2-GST fusion protein (panel B), whereas the pre-bleed sample does not (panel A). The band (~50kDa) was in the predicted region of the ~49kDa vOX2-GST fusion protein. There were a few extra bands present in both lanes on panel B (third bleed), suggesting that the rabbit also produced antibodies against other proteins present in the vOX2-GST preparation.

The reactivity of the rabbit antibodies to the vOX2 protein was also assessed against a KSHV infected cell line, BC3. A combination of latently infected and lytically induced cells (overnight incubation with 3mM Butyrate, see 2.1.6) were tested. Glycosylation was also inhibited in some samples by an overnight incubation with Tunicamycin (0.1μg/ml) (see 2.1.7). A KSHV negative cell line, BJAB, was also used. Samples were loaded on to an SDS-PAGE gel, transferred by Western Blot and incubated with the third bleed purified rabbit antibodies. This was followed by incubation with anti-rabbit conjugated to AP. Figure 3.7 shows no detection of vOX2 in any of the latent or lytically induced KSHV infected cell lines, nor the KSHV negative cell line. An aliquot of vOX2 (cleaved from the vOX2-GST fusion protein) was loaded into the last lane as a positive control.

Other techniques such as immunofluorescence were also used to assess the reactivity of the rabbit antibody. BHK-21 cells infected with recombinant viruses encoding the vOX2 ORF and GFP (see Chapter 4 and 5) were fixed to slides and stained using the purified final bleed rabbit antibody, followed by anti-rabbit alexa fluor 546 (red). A combination of varying dilutions and fixation methods was performed, but all with no success (Figure 3.8). It is possible that the antibody generated was recognising an incorrectly folded protein since the vOX2-GST fusion protein was not glycosylated.

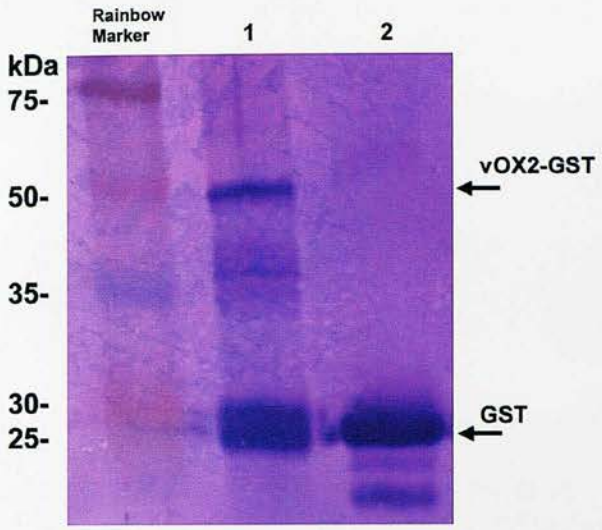

Figure 3.5 Expression of the vOX2 protein as a GST-fusion protein. Bacterial colonies transfected with pGEX/vOX2 or pGEX/GST were tested for the expression of the GST fused proteins after induction with IPTG. Purified protein (lane 1 = vOX2-GST; lane 2 = GST) were analysed on a 12% SDS-PAGE gel. The immunoblot was probed with anti-GST, followed by anti-rabbit Ig-AP and visualized using Roche NBT/BCIP solution. Molecular weights are given in kilodaltons (kDa) relative to the rainbow maker in the left lane.

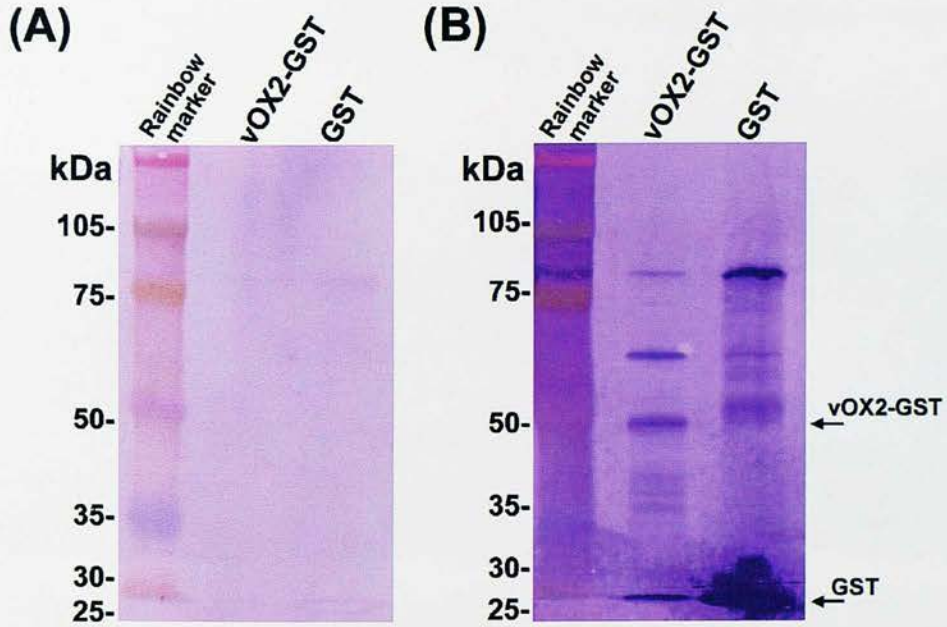

Figure 3.6 Reactivity of purified rabbit anti-vOX2 antibody. The ability of rabbit antibodies to detect the vOX2 protein was assessed by immunoblot. Samples of purified protein vOX2-GST (lane 2) and GST (lane 3) were separated on a 12% SDS-PAGE gel, and transferred onto a membrane by Western blot. The blots were probed with pre-bleed (A) and third bleed (B) purified rabbit serum. The rabbit antibodies were detected using anti-rabbit Ig conjugated to AP and visualized using Roche NBT/BCIP solution. Rainbow protein molecular weight markers were run in the left lane and given in kilodaltons.

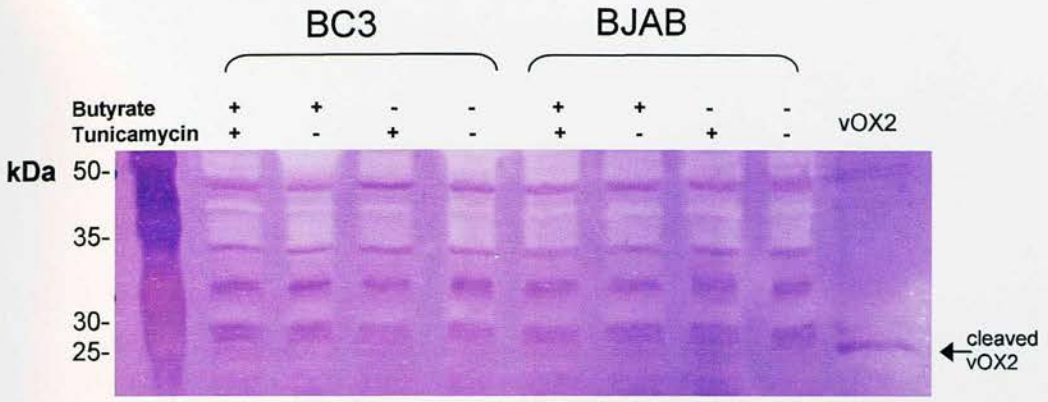

Figure 3.7 Detection of vOX2 expression in KSHV infected cells. A KSHV infected cell line (BC3) and a cell line negative for KSHV infection (BJAB) were grown overnight with either Butyrate (3mM) or Tunicamycin (0.1μg/ml) or a combination of both. The addition of Butyrate results in the induction of lytic replication of KSHV and Tunicamycin inhibits glycosylation of proteins. Aliquots of lysed cell samples were loaded on to a 12% SDS-PAGE gel and then transferred to a membrane by Western Blot. Membranes were incubated in blocking solution (with 2% normal goat serum), then purified final bleed rabbit anti-vOX2 serum (1:50), and finally with goat anti-rabbit Ig conjugated to AP (1:2000). Proteins were visualized using Roche NBT/BCIP solution. An aliquot of vOX2 (cleaved from the purified vOX2-GST protein) was loaded into the last lane as a positive control. Rainbow protein molecular weight markers were run in the left lane and given in kilodaltons.

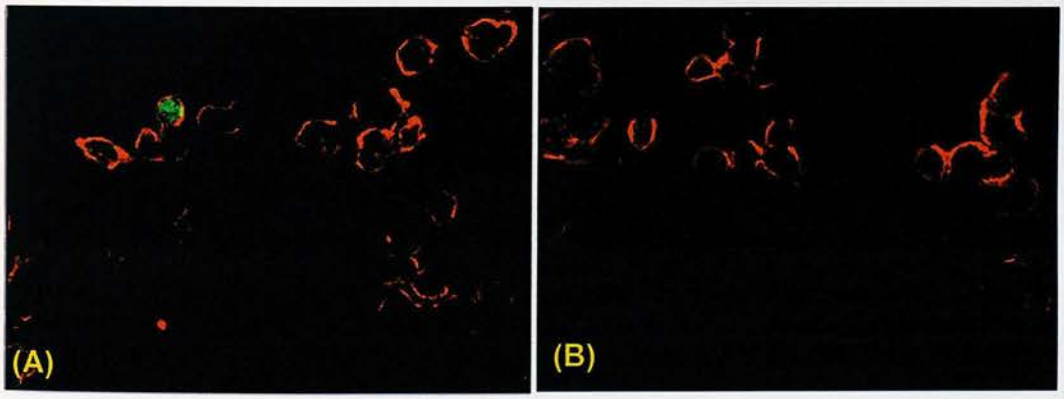

Figure 3.8 Detection of vOX2 expression in BHK-21 cells infected with a MHV-76 recombinant virus encoding the vOX2 ORF and EGFP*. BHK cells were infected with a MOI of 0.5 with either (A) a MHV-76 recombinant virus encoding the vOX2 ORF and EGFP or (B) MHV-76. After a 24hour period, cells were harvested and air-dried onto slides. Samples were fixed with 4% w/v paraformaldehyde and then incubated with the purified final bleed rabbit anti-vOX2 serum, and then anti-rabbit alexa fluor 546 (red). Cells infected with the recombinant virus can be visualised by the expression of *gfp*. Control slides in which no primary antibody was used, were stained simultaneously and no background/non-specific fluorescence was detected (image not shown) (Magnification at x400). *see chapter 4 for detailed information regarding the creation of this recombinant virus.

3.4 Expression of secreted vOX2 protein

Partly due to the inability to generate an antibody against vOX2 using a bacterial system, it was decided to generate vOX2 as soluble protein with an epitope tag. Upon successful production of the soluble protein, it would provide the opportunity to generate an antibody targeting the soluble protein. However, even without the antibody, this soluble protein could also be used to study protein interactions, in particular engagement with its predicted receptor, CD200R. The epitope tag could be used to detect the protein by the use of commercially available antibodies. It was decided to clone the vOX2 ORF into pcDNA3.1/*myc*-His-A (see 2.6.1 and Appendix 3) (this plasmid will be referred to as pcDNA3.1 throughout this chapter); this plasmid allows the production of a secreted protein tagged with *myc* and six histidine residues (His_6) fused to the carboxy terminus. This method of epitope tagging proteins has been used successfully to characterise a wide variety of proteins (Kao *et al.*, 1994; Lackner and Condit, 2000). In addition the His_6 epitope can be used to concentrate and/or purify proteins via affinity chromatography (Bornhorst and Falke, 2000; Hochuli *et al.*, 1988).

The vOX2 ORF was amplified from BCP1 DNA using primer pair Sec1 and Sec2 generating a product approximately 710bp, comprised of the signal sequence and the extracellular domains (the transmembrane and cytoplasmic portions were not included). This product was digested with *Xho*I and *Hind*III and cloned into pCDNA3.1 (linearised with *Xho*I and *Hind*III) to generate pcDNA3.1/vOX2.

In addition, to study the RGD motif in the vOX2 ORF, site directed mutagenesis was used to mutate this sequence to generate a non-functional RAD (see 2.2.12 and 4.1); the vector pCR2.1-TOPO/vOX2 was mutated to generate pCR2.1-TOPO/vOX2-RAD. The vOX2-RAD ORF was also excised at the *Xho*I/*Hind*III restriction enzyme sites and cloned into the *Xho*I/*Hind*III site of pcDNA3.1 to generate pcDNA3.1/vOX2-RAD.

Both pcDNA3.1/vOX2 and pcDNA3.1/vOX2-RAD were transfected with Effectene (QIAGEN) into HEK293 cells (see 2.1.5.2) in a T175cm^2 flask. After 24hours, the medium was replaced with Optimem (Gibco) and incubated for a further 24hours. At this point all medium was taken off and passed through a His-Select™ HC Nickel Affinity Gel (SIGMA) to purify the sample. The eluted protein (~4ml)

was then concentrated to a volume of approximately 100-300µl, using a Vivaspin4 column (Vivascience) (see 2.6.1).

The same transfection and protein concentration procedure was performed using plasmid pSecTag-PSA (Appendix3) as a positive control for the transfection procedure; this plasmid was provided with an alternative secretion protein plasmid kit that was also tested for use with vOX2 but was not successful. When transfected into cell lines, the ~33kDa prostate-specific antigen (PSA) fused to the *c-myc* epitope and the polyhistidine tag is generated.

Aliquots of all secreted proteins (vOX2, vOX2-RAD and PSA), and of lysed cell pellets (see 2.6.1) were separated on a 12% SDS-PAGE gel and transferred to a membrane by Western Blot. An aliquot of non-transfected HEK293 cells was also subjected to the same experimental procedures was included to eliminate any non-specific hybridisation. Samples were analysed by targeting the fused *myc* epitope; incubation first with mouse anti-*myc* (1:2500), followed by goat anti-mouse conjugated to biotin (1:500) and then a final incubation with streptavadin conjugated to AP (1:500).

Illustrated in Figure 3.8 is the membrane in which a faint band (~45 kDa; indicated by the red arrows) is present in lanes loaded with vOX2 and vOX2-RAD secreted protein. The predicted size of the glycosylated secreted vOX2 fused to the *myc* epitope and the polyhistidine tag is ~44kDa[f]. Additional faint bands (~35kDa) and a smearing effect (~35-45kDa) are visible in the lysed cell samples from vOX2 and vOX2-RAD presumably representing partially and non-glycosylated forms of the protein.

A band of ~33kDa (indicated by the black arrows) is present in the positive control transfection reactions (pSecTag-PSA) and in the last lane an aliquot of PSA from a previous experiment was loaded as an additional positive control for the Western blotting and immunoblotting procedures.

[f] The predicted size for the extracellular domains of vOX2 (and vOX2-RAD) is approximately 25.5kDa, added to this is ~3kDa for the *c-myc* epitope and polyhistidine tag, and a further 3kDa for each N-glycosylation; there are five predicted N-linked glycosylation sites in the vOX2 protein.

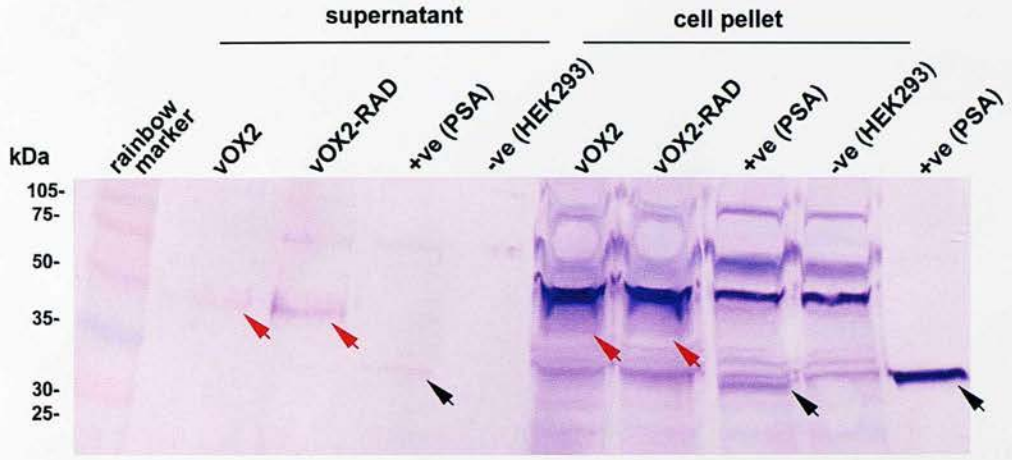

Figure 3.9 Detection of secreted vOX2 and vOX2-RAD proteins. HEK293 cells were transfected with pcDNA3.1/*myc*-His/vOX2, pcDNA3.1/*myc*-His/*vOX2*-RAD or pSecTag-PSA. After the collection and concentration of secreted proteins, samples of protein and lysed cell pellet were separated on a 12% SDS-PAGE gel and transferred by Western Blot. The membrane was incubated with mouse anti-*myc*, followed by goat anti-mouse conjugated to biotin, and then finally streptavidin AP. Proteins were visualized using Roche NBT/BCIP solution. An aliquot of secreted PSA protein from a previous experiment was loaded into the last lane as an additional positive control. Red arrows indicate vOX2 protein and black arrows indicate PSA protein. Rainbow protein molecular weight markers were run in the left lane and given in kilodaltons.

3.5 Discussion

Although not all successful, these studies have shown that the glycosylated extracellular region of the vOX2 protein has a molecular mass of approximately 40kDa and is expressed on the cell surface. Based on hydropathicity plots of vOX2 and its cellular homologue (hCD200) and sequence analysis, it is highly like that the vOX2 protein also assumes the IgSF formation and is comprised of a V and C2 Ig domain, a single transmembrane region and a short cytoplasmic tail. The KSHV vOX2 protein has approximately 27% sequence identity (~60% sequence similarity) with the cellular hCD200, and also mCD200 and rCD200.

Cellular localisation studies whereby the vOX2 ORF was tagged with a FLAG- epitope, confirmed the second methionine at amino acid 78 can be utilised as an initiation codon. Furthermore, a combination of this finding along with the detection of a common signal peptide sequence directly after the second methionine, strongly imply the second methionine to be the true initiation codon. This would therefore result in the generation of a protein that is 271 amino acids in length, a size comparable with its cellular homologue CD200 (hCD200 and mCD200 are both 278 aa) and the RRV protein R14 (253 aa).

Initial attempts were undertaken to generate an antibody against the vOX2 protein using a GST fusion system. An antibody was made, but only one that would recognise the vOX2-GST fused protein, not vOX2 expressed in its natural state, i.e. KSHV infected cells. The antibody was also not able to detect vOX2 when expressed in a variety of other cell types. This was most likely the direct result of generating an antibody targeting a non-glycosylated form of the protein, and as vOX2 has 5 or 6 potential N-linked glycosylation sites, the antibody would probably not have the correct conformation.

In hindsight generating an antibody against an extracellular protein should not have been performed using a bacterial system. However, it has been suggested by Wright *et al.* (2000) that based on mutagenesis studies on the human CD200:CD200R interaction (Preston *et al.*, 1997) (both also possessing high N-linked carbohydrates) and other similar IgSF interactions, engagement is mediated by protein and not carbohydrate. It is further suggested that the role of the carbohydrate

is to aid in preventing unwanted *cis*-interactions and retain the orientation of the protein with respect to the membrane.

As it was desirable to have an antibody recognising the vOX2 protein to study protein interaction, an alternative approach was attempted. Expressing vOX2 as a secreted protein tagged with a *myc*-His_6 epitope would not only allow protein interaction to be investigated through the use of commercial antibodies (targeting the tagged epitope) but also provide another opportunity to generate an antibody against the protein. In addition, a mutated form of the vOX2 protein was to be studied. It is not known if the RGD motif within the vOX2 ORF is functional, therefore by mutating the sequence to generate a non-functional RAD sequence, studies on the mutated vOX2-RAD could also be performed.

Unfortunately this was not fully achieved. The generation of the secreted protein was difficult to optimise and did not yield high amounts of protein. This was mostly associated with the low transfection efficiency (<1%). Eventually after purifying the proteins via affinity chromatography and concentrating the elutant, secreted vOX2 and vOX2-RAD was detected by immunoblot analysis. Not enough protein was generated at this point to perform any protein interaction studies. Unfortunately due to time constraints this experiment could not be continued. Ideally, the system would be optimised further to produce a larger amount of soluble protein which would then be used to (i) generate an antibody targeting the vOX2 protein and (ii) study vOX2 protein interaction with other cell types, in particular its potential receptor, CD200R.

Chapter Four: Generation of Recombinant Viruses

Chapter 4: Generation of recombinant viruses

The study of recombinant viruses into which specific genes have been inserted, deleted and or mutated has become a fundamental tool in elucidating the function of viral genes. This method is used by many groups, for example, in 1968, Ejercito *et al.*, were able to identify mutated genes within a new strain of herpes simplex virus due to an altered plaque phenotype.

Due to the stringent host range and inability to grow permissively in cell cultures, studies of many gammaherpesviruses have been difficult. However, the closely related murid gammaherpesvirus, MHV-68, does not encounter this problem, as it replicates efficiently in cell culture and is often used as a model to study human gammaherpesviruses. With the use of recombinant virus technology the generation and characterisation of MHV-68 mutants has been valuable for studying and predicting the role(s) of several unique genes within the left hand end of its genome (Clambey *et al.*, 2000; Jacoby *et al.*, 2002; Macrae *et al.*, 2003; Townsley *et al.*, 2004). Moreover, MHV-76, a natural deletion mutant of MHV-68, has provided an opportunity to use this virus as a vector to study other unique gammaherpesvirus genes.

The substantial deletion at the left-terminus of the MHV-76 genome, compared to MHV-68, has provided a novel opportunity to insert a unique gene from KSHV along with selection markers, resulting in the generation of recombinant viruses. In addition to *in vitro* studies, these recombinant viruses can be further studied *in vivo*, ultimately allowing observations to be made on the potential role of the gene of interest in an animal model.

4.1 Cloning strategy

A variety of murine recombinant viruses incorporating the KSHV vOX2 ORF were generated. The initial strategy was to construct an MHV-76-based recombinant virus that integrated the KSHV vOX2 ORF, a human CMV promoter and a hygromycin resistant (Hyg^R) - enhanced green fluorescent protein (EGFP) gene by homologous recombination. In addition, a control recombinant virus was generated; this virus contained an identical insert cassette minus the vOX2 gene.

A schematic diagram of the cloning strategy used to generate the plasmids used for the construction of the recombinant viruses is outlined in Figures 4.1-A, -B and -C. The first plasmids generated comprised the insert cassette (CMV, Hyg^R-EGFP, IRES, vOX2, and a polyadenylated tail (AAA)), adjoining 3Kb of MHV-76 DNA within the pBSIIKS-76LHE plasmid; this plasmid was generated by A.MacRae (2002) and incorporates homologous DNA from the left hand end of the genome corresponding to nt 9539-12569 from MHV-68. The cloned insert was incorporated into the pBSIIKS-76LHE plasmid in two orientations resulting in the generation of the clones pBSIIKS-76LHE-vOX2F and pBSIIKS-76LHE-vOX2R. A detailed step-by-step procedure is outlined in Figure 4.1A and sections 2.3.1.

In addition to these clones possessing the vOX2 ORF, control plasmids were also created as outlined in Figure 4.1B. The vOX2 insert was cut out of the plasmids pBSIIKS-76LHE-vOX2F and pBSIIKS-76LHE-vOX2R to generate two control plasmids, pBSIIKS-76LHE-IRES.F and pBSIIKS-76LHE-IRES.R.

In order to investigate whether the RGD motif within vOX2 was functional, a mutated recombinant virus was also generated. The RGD motif within the vOX2 sequence in pCR-TOPO-vOX2 plasmid was changed to a non-functional RAD sequence by site directed mutagenesis (see 2.2.12). The RAD-vOX2 gene was then cloned into the control plasmid pBSIIKS-76LHE-IRES.F and is schematically outlined in Figure 4.1C. All of the final plasmids mentioned above were used in the following experiments, to generate recombinant viruses.

4.2 Generation and Purification of Recombinant Viruses

A homologous recombination strategy was utilised for the generation of recombinant viruses in which the insert cassette was incorporated into the left terminus of the MHV-76 genome, schematically illustrated in Figure 4.2A. All plasmids were digested with *Pvu*II and *Eco*RV to release the insert cassette that contains a 3Kb fragment of MHV-76 (corresponding to the left hand end of the genome, directly after the terminal repeat region). However, in order to find a unique restriction enzyme site outside the insert cassette, the *Pvu*II site in pBlueScriptIIKS was utilised; resulting in the incorporation of ~90bp of the

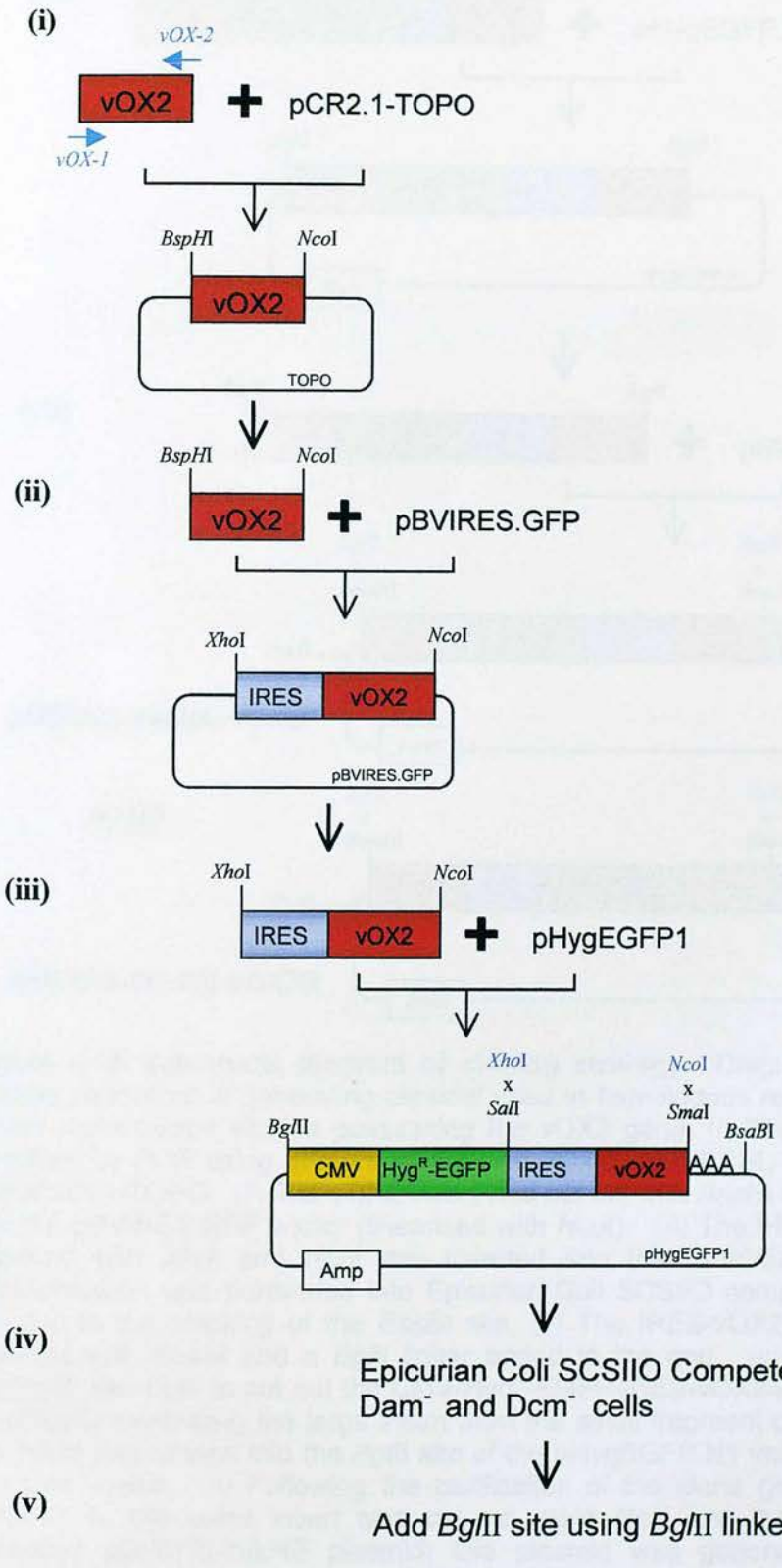
(i)
vOX-2
vOX2
pCR2.1-TOPO
vOX-1
BspHI
NcoI
vOX2
TOPO
(ii)
BspHI
NcoI
vOX2
pBVIRES.GFP
XhoI
NcoI
IRES
vOX2
pBVIRES.GFP
(iii)
XhoI
NcoI
IRES
vOX2
pHygEGFP1
XhoI x SalI
NcoI x SmaI
BglII
BsaBI
CMV
Hyg^R-EGFP
IRES
vOX2
AAA
Amp
pHygEGFP1
(iv)
Epicurian Coli SCSIIO Competent Cells
Dam- and Dcm- cells
(v)
Add BglII site using BglII linker

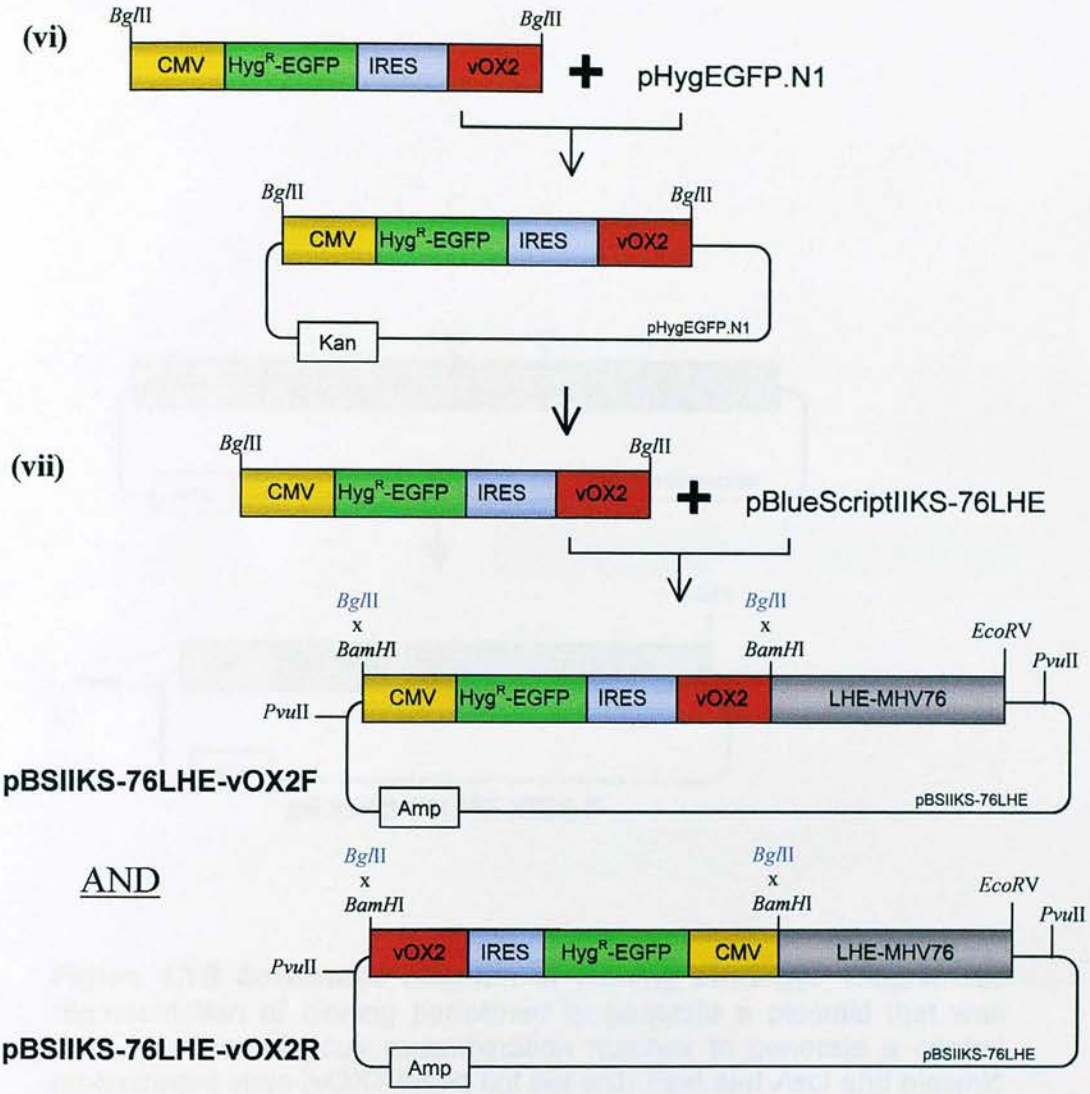

Figure 4.1A Schematic diagram of cloning strategy. Diagramatic representation of cloning performed in generating plasmid used in homologous recombination reactions to create recombinant viruses possessing the vOX2 gene. (i) The entire vOX2 ORF was amplified by PCR using primers *vOX-1* and *vOX-2* from BCBL-1 DNA, and then cloned into pCR2.1-TOPO. (ii) The vOX2 insert was cut out with *BspH*I and *Nco*I, and subcloned into the pBVIRES.GFP vector (linearised with *Nco*I). (iii) The IRES-vOX2 sequence was digested with *Xho*I and *Nco*I and inserted into the *SmaI/SalI* site of pHygEGFP1, transformation was performed into Epicurian Coli SCSIIO competent cells (*Dam*$^-$*/Dcm*$^-$) (iv) due to the blocking of the *BsaB*I site. (v) The IRES-vOX2/pHygEGFP1 clone was digested with *BsaB*I and a *Bgl*II linker added to the end. (vi) The plasmid was then digested with *Bgl*II to cut out the CMV-Hyg^R-EGFP-IRES-vOX2-AAA insert, however due to difficulty separating the large insert from the small fragment of the plasmid backbone, the insert was cloned into the *Bgl*II site of the pHygEGFP.N1 vector; this is a Kanamycin resistant vector. (vii) Following the purification of the clone grown in the presence of Kanamycin, the same insert was cut out using *Bgl*II and then cloned into the B*gl*II linearised pBSIIKS-76LHE plasmid; this plasmid was generated by A.MacRae and incorporates approximately 3Kb of MHV-76 DNA from the left hand end (corresponding to nt 9539-12569 of MHV-68). The insert cassette incorporated into the clone in two orientations, generating pBSIIKS-76LHE-vOX2F (forward) and pBSIIKS-76LHE-vOX2R (reverse). [Note: RE sites in blue indicate insert digestion sites complementary to those in a plasmid]

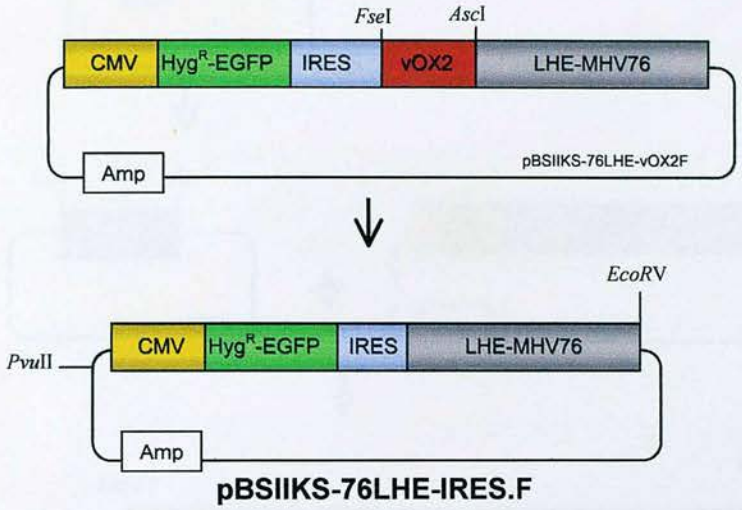

Figure 4.1B Schematic diagram of cloning strategy. Diagramatic representation of cloning performed to generate a plasmid that was used in a homologous recombination reaction to generate a control recombinant virus (vOX2 insert cut out with *Fse*I and *Asc*I and plasmid re-ligated, the same procedure was performed on the reverse plasmid to generate pBSIIKS-76LHE-IRES.R).

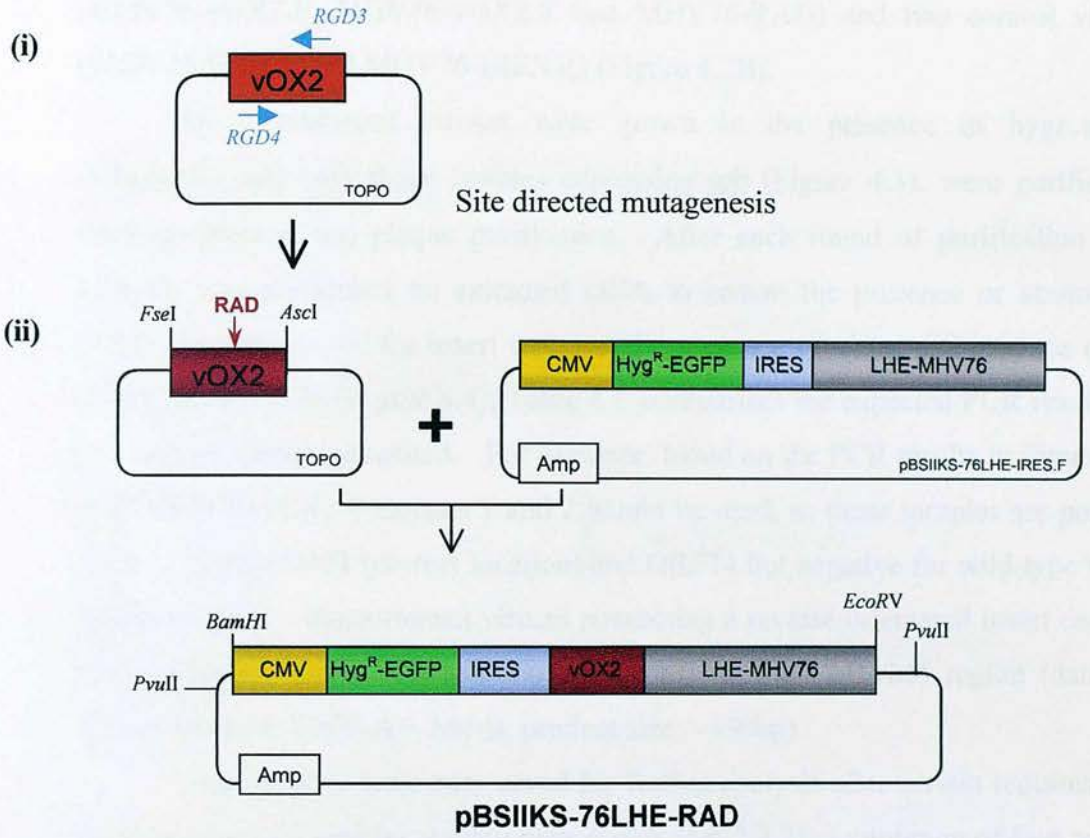

Figure 4.1C Schematic diagram of cloning strategy. Diagramatic representation of cloning performed to generate a plasmid that is to be used in a homologous recombination reaction to generate a recombinant virus possessing a mutated vOX2 gene. (i) The RGD motif is changed to a non-functional RAD site by site directed mutagenesis and then (ii) the mutated vOX2 gene was inserted into the final plasmid to be used for the generation of a recombinant virus.

plasmid. This fragment of DNA was situated either before the CMV promoter or after the polyadenylation.

The recombinant viruses generated included those possessing the vOX2 gene (MHV76-vOX2.F, MHV76-vOX2.R and MHV76-RAD) and two control viruses (MHV76-IRES.F and MHV76-IRES.R) (Figure 4.2B).

All recombinant viruses were grown in the presence of hygromycin (100μg/ml) and only those isolates expressing *gfp* (Figure 4.3), were purified by limiting dilution and plaque purification. After each round of purification PCR analysis was performed on extracted DNA to ensure the presence or absence of vOX2, the position of the insert cassette, the presence of virus, and absence of the wild-type MHV-76 (Figure 4.4); Table 4.1 summarises the expected PCR results for the various viruses generated. For example, based on the PCR results in Figure 4.4, only MHV76-vOX2.F isolates 1 and 2 would be used, as these samples are positive for vOX2, polyA/M4 (correct location) and ORF74 but negative for wild-type virus, unlike isolate 3. Recombinant viruses possessing a reverse orientated insert cassette where checked for correct location by amplifying the CMV/M4 region (data not shown, primers; CMV-A + M4-B, product size; ~450bp)

Viral samples were only saved for further analysis after certain requirements were satisfied: an agarose overlay plaque pick (see 2.3.2); a minimum of four rounds of limiting dilution plaque purification (some viruses required more than four rounds of purification); when an isolate was identified to satisfy all the PCR requirements and to be free of wild-type virus (MHV-76).

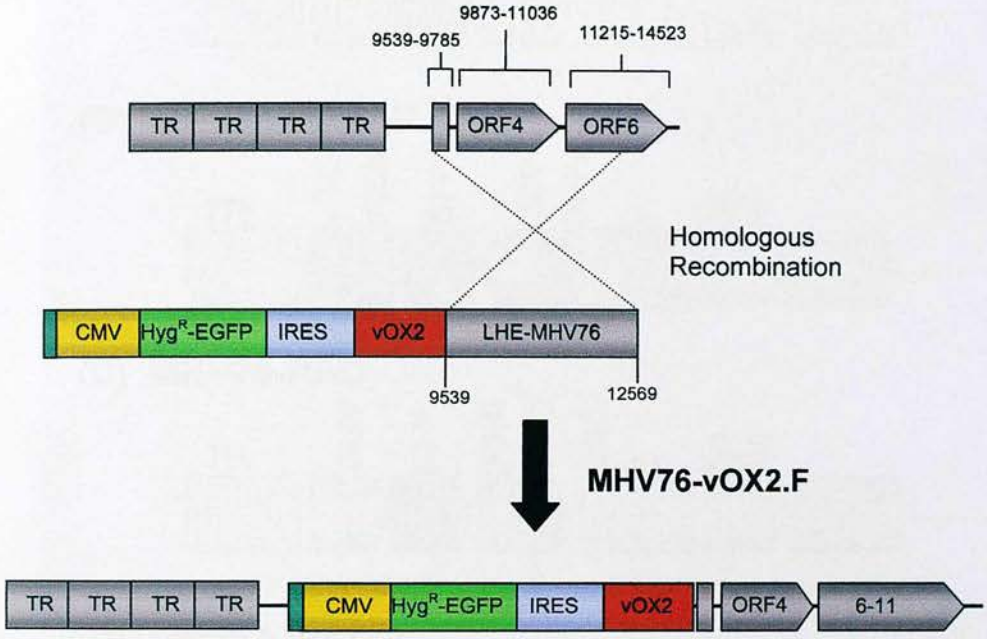

Figure 4.2A Schematic diagram of homologous recombination to generate a recombinant virus. Plasmid pBSKSII-76LHE-vOX2.F was lineraised with *EcoR*V and *Pvu*II, mixed with viral MHV-76 DNA and electroporated. Following a crossover homologous recombination event the CMV→vOX2 insert cassette was incorporated into the left-terminus of the MHV-76 genome to generate the recombinant virus MHV76-vOX2.F (See Figure 4.2B for the schematic diagrams of all the recombinant viruses generated).

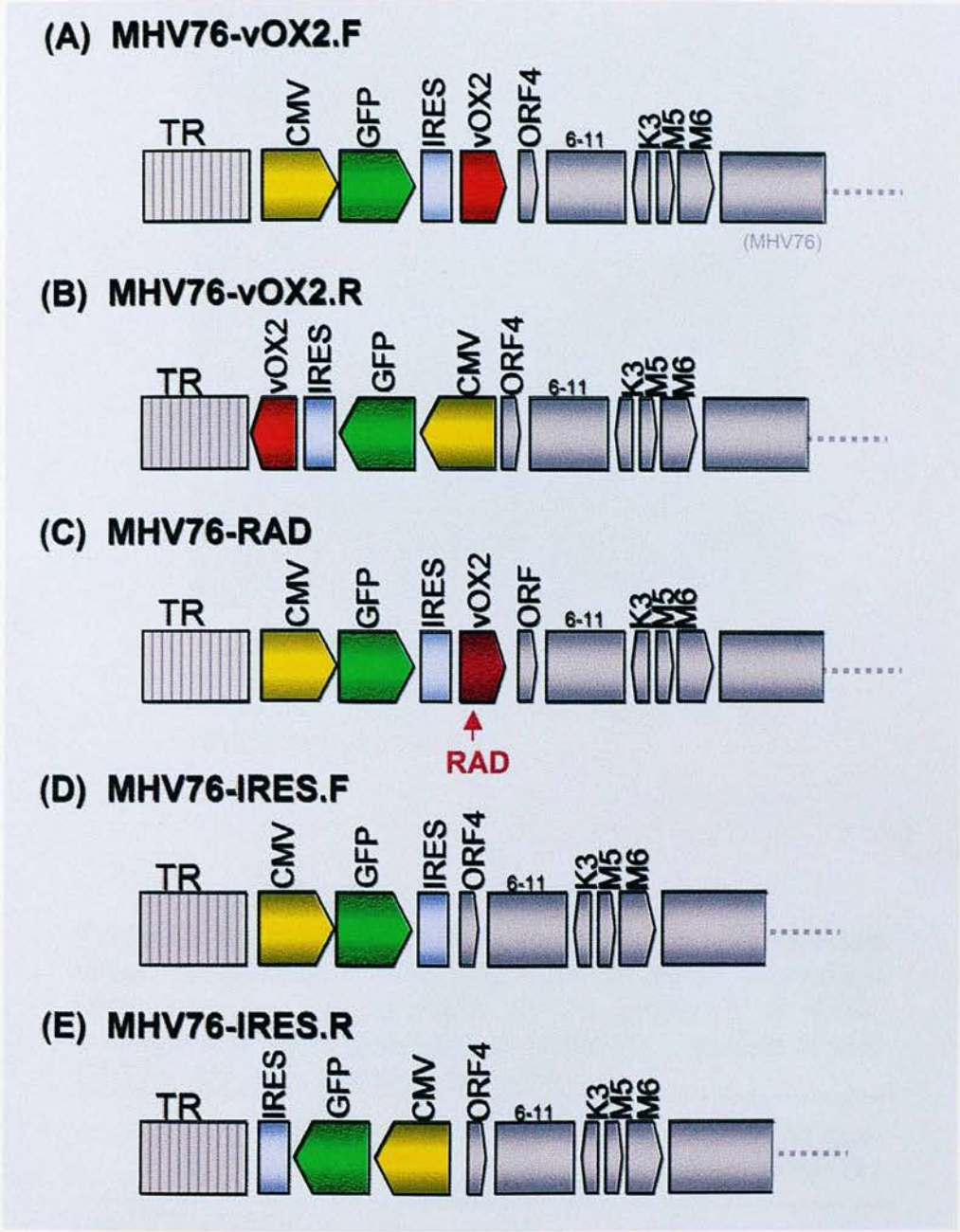

Figure 4.2B Schematic diagram of recombinant viruses generated.
Viruses include; (A) MHV76-vOX2.F, (B) MHV76-vOX2.R, (C) MHV76-RAD, (D) MHV76-IRES.F and (E) MHV76-IRES.R.

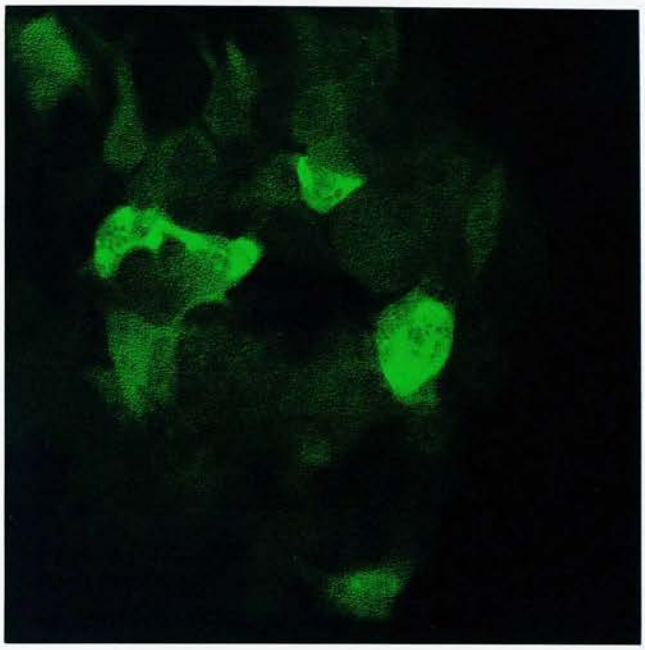

Figure 4.3 Viral plaque expressing *gfp*. BHK-21 cells infected with MHV76-vOX2.F is visualised through the expression of *gfp* (Magnification x1000).

Table 4.1 Summary of PCR analysis during recombinant virus purification. Following each round of purification DNA extracted was amplified for the presence of vOX2, orientation of insert (polyA/M4 or CMV/M4), presence of viral ORF74 and wild-type virus, MHV-76.

	vOX2	*PolyA/M4 or CMV/M4*	*ORF74*	*Wild Type MHV-76*
MHV76-vOX2.F	✓	✓	✓	✗
MHV76-RAD	✓	✓	✓	✗
MHV76-vOX2.R	✓	✓	✓	✗
MHV76-IRES.F	✗	✓	✓	✗
MHV76-IRES.R	✗	✓	✓	✗
MHV-76	✗	✗	✗	✓

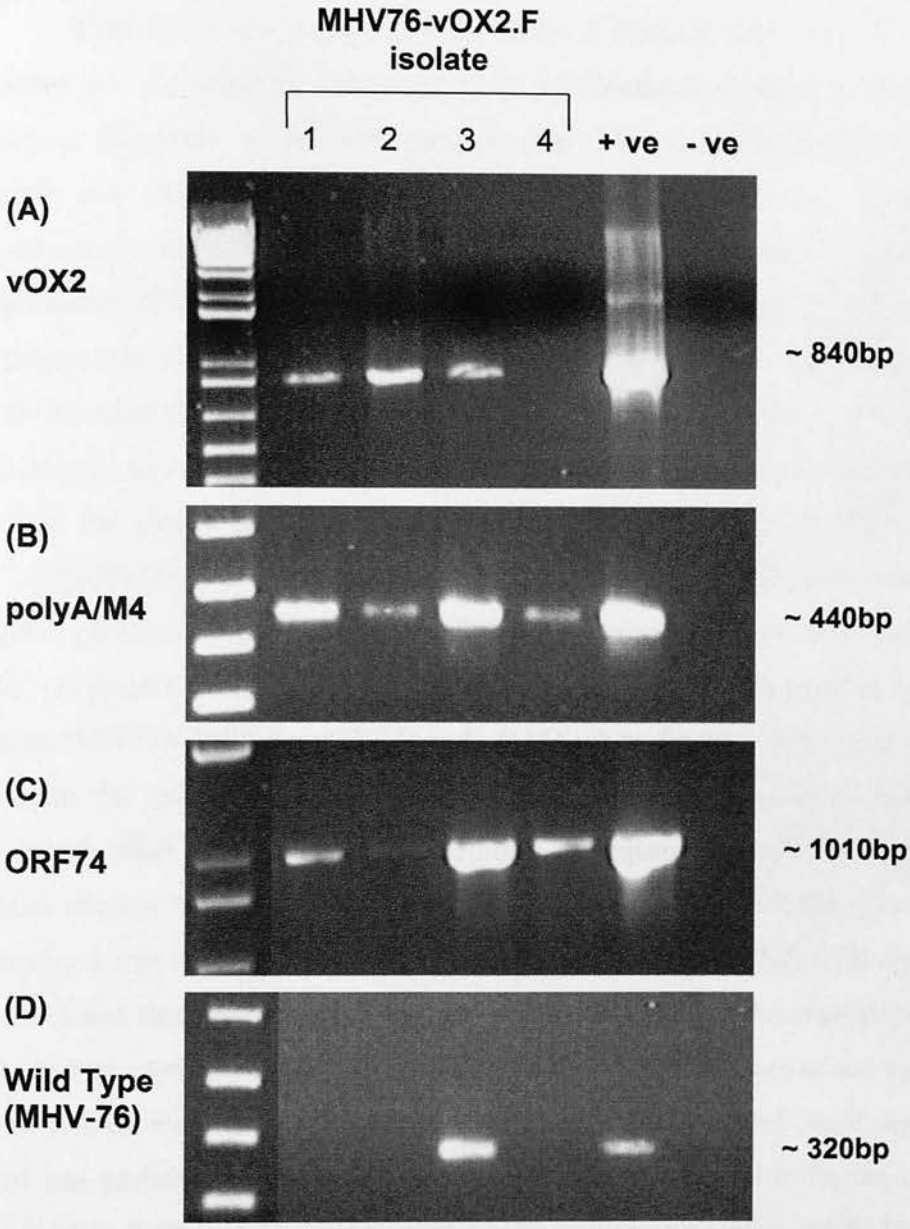

Figure 4.4 PCR analysis during purification of recombinant viruses. Examples of PCR analysis performed during the purification of MHV76-vOX2.F. DNA samples were isolated from limiting dilution samples (e.g isolates 1 to 4), grown in 96 well plates, and amplified for (A) vOX2, (B) polyA-M4, (C) ORF74 and (D) the presence of wild-type virus, MHV-76 (Primers used include; (A) vOX2F + vOX2R; (B) polyA-R + M4-B; (C) ORF74-5'+ ORF74-3'; (D) Trepeat + M4-B). PCR products were analysed on a 1.2% agarose gel concurrently with a 1Kb+ DNA molecular weight marker (on left hand end). All reactions included the use of a positive control (+ve) (DNA from pBSIIKS-76LHE-vOX2F for (A) and (B); DNA from MHV-76 for (C) and (D)) and a negative control (-ve), dH_20 for all sets.

4.3 Southern Analysis

Viral DNA was extracted from infected BHK-21 cells (see 2.3.5) for two isolates per recombinant virus, and used for Southern analysis to determine the genomic alignment at the left-terminus (see 2.4) (southern images shown only include the final virus isolate used in all further experiments). Following the digestion of viral DNA with either *Mfe*I or *Nhe*I, samples were analysed using a digoxigenin (DIG)- hybridisation probe. Isolates were firstly hybridised with a sequence specific probe against the left-terminus of MHV-76 adjoining the cloned insert cassette; this probe is referred to as the '76' probe (nt 9539-10461 from MHV-68) (Figure 4.6A). Following this the membrane was stripped and re-probed directly against the cloned selection markers using a 'GFP' probe (nt 1821-2878 from pHygEGFP) (Figure 4.6B). Southern analysis showed that the recombinant viruses yielded profiles similar to those predicted following digestion with either *Mfe*I or *Nhe*I (Figures 4.5B-E). For example, a 1.1kb fragment is observed in recombinant viruses MHV76-IRES.F, -vOX2.F and –RAD when digested with *Mfe*I and probed with the '76' probe (Figure 4.6A). In contrast, when probed with the 'GFP' probe a laddering effect is seen due to the addition of sequences from the terminal repeat region (Figure 4.6B). As the laddering effect from MHV76-RAD was not clearly visualised, this sample was also checked by digesting viral DNA with either *BamH*I or *Xba*I and then probed using the '76' probe; this yielded the correct profile (data not shown). Another initial discrepancy was detected in the size of the hybridisation band yielded by MHV76-IRES.R (generated by Dr J Douglas) when digested with *Nhe*I and probed with the 'GFP' probe. This was confirmed to be the correct size (~4.0kb) as further southern blot analysis and sequencing performed by Dr J Douglas (data not shown) identified an inclusion of approximately 1kb of a cloning plasmid (pBlueScriptKSII) after the terminal repeat region but before the polyadenylated tail. This fragment of plasmid contained an *Nhe*I digestion site, thus yielding the profile seen in Figure 4.6B.

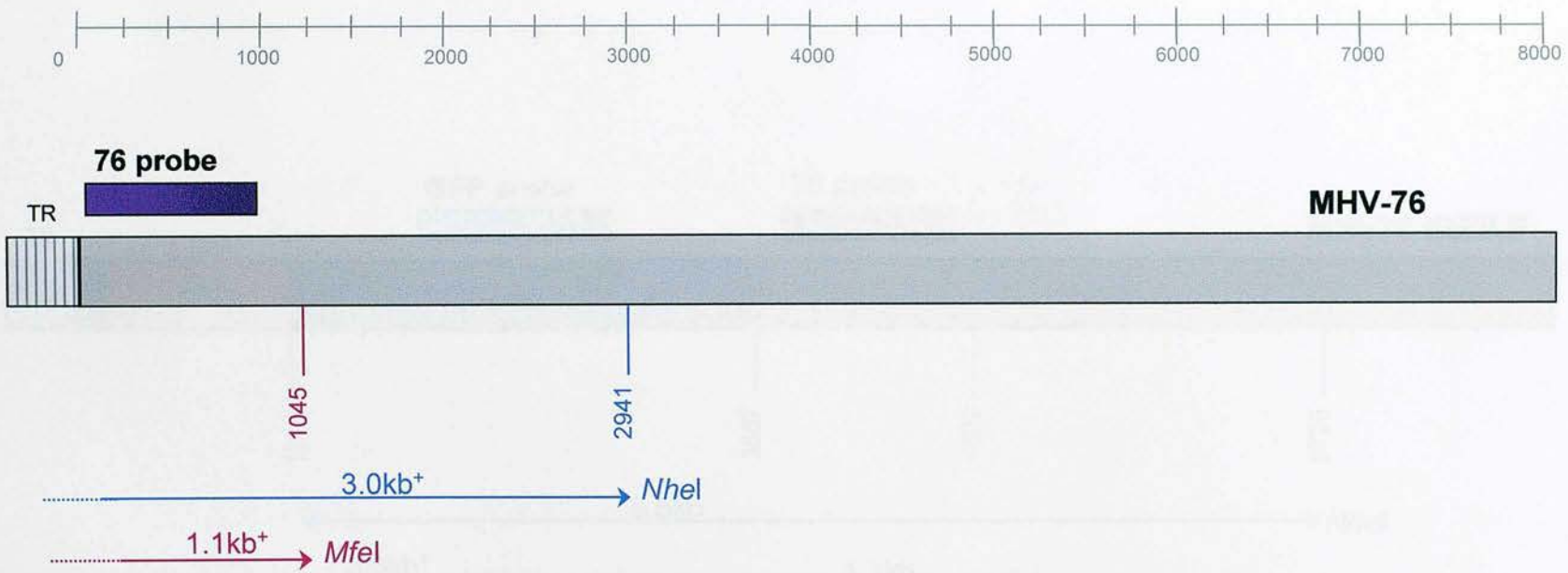

Figure 4.5A Interpretation of the restriction endonuclease map of the left-terminus for MHV-76 for the restriction enzymes *Nhe*I and *Mef*I. A 8kb portion of the left-terminus of the virus and its terminal repeat region is schematically shown in grey. Restriction endonuclease digestions sites for *Nhe*I (blue) and *Mfe*I (pink) and predicted fragment sizes are illustrated. + denotes fragments that are bound to the TR and thus appear as a ladder of larger bands on Southern blot. The location of the 76 probe (nt 9539-10461 from MHV-68), in purple, used in Southern analysis is shown above; the GFP probe (nt 1821-2878 from pHygEGFP) is omitted as no complementary sequence is expected to be present within MHV-76.

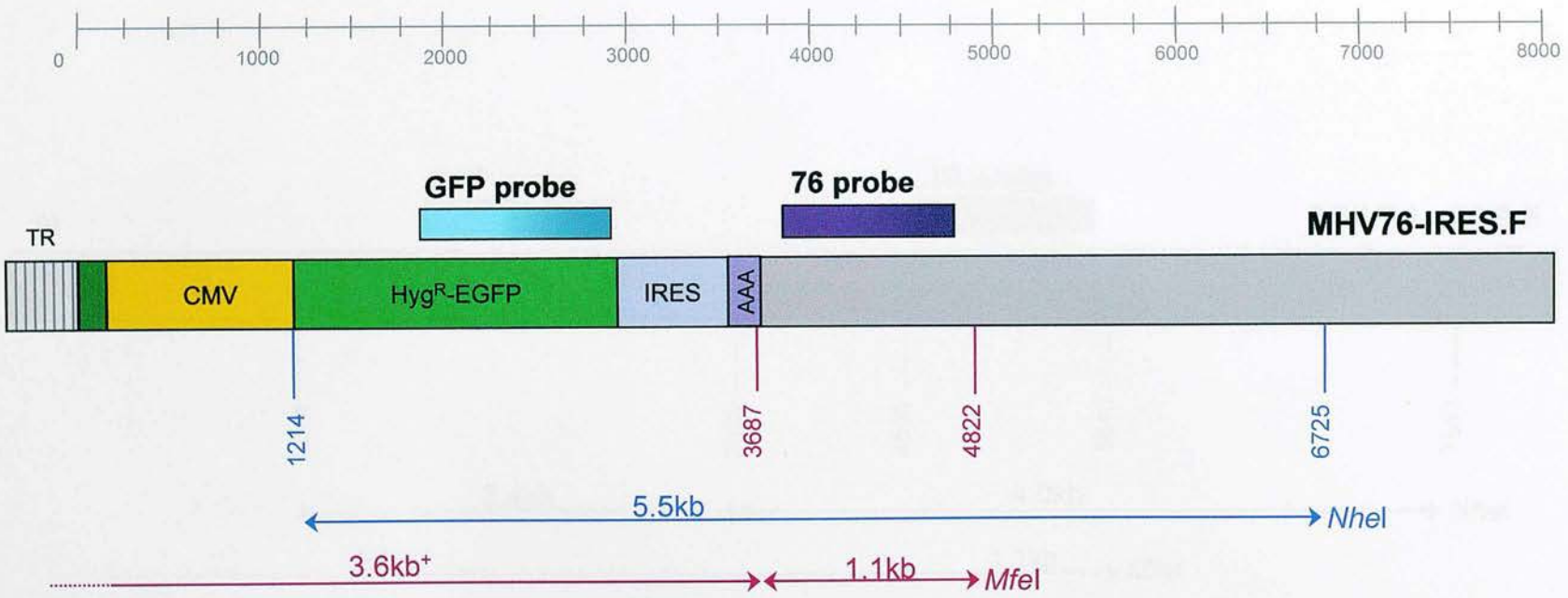

Figure 4.5B Interpretation of the restriction endonuclease map of the left-terminus for the recombinant virus MHV76-IRES.F for the restriction enzymes *Nhe*I and *Mef*I. A 8kb portion of the left-terminus of the recombinant virus is schematically shown: MHV-76 (grey), CMV (yellow), Hyg^R-EGFP (light green), IRES (light blue), polyadenylation (mauve), small portion of pBlueScriptKSII (dark green) and MHV-76 terminal repeats (TR)(grey). Restriction endonuclease digestions sites for *Nhe*I (blue) and *Mfe*I (pink) and predicted fragment sizes are illustrated. $^+$ denotes fragments that are bound to the TR and thus appear as a ladder of larger bands on Southern blot. The location of the GFP probe (nt 1821-2878 from pHygEGFP), in blue, and 76 probe (nt 9539-10461 from MHV-68), in purple, used in Southern analysis are shown above.

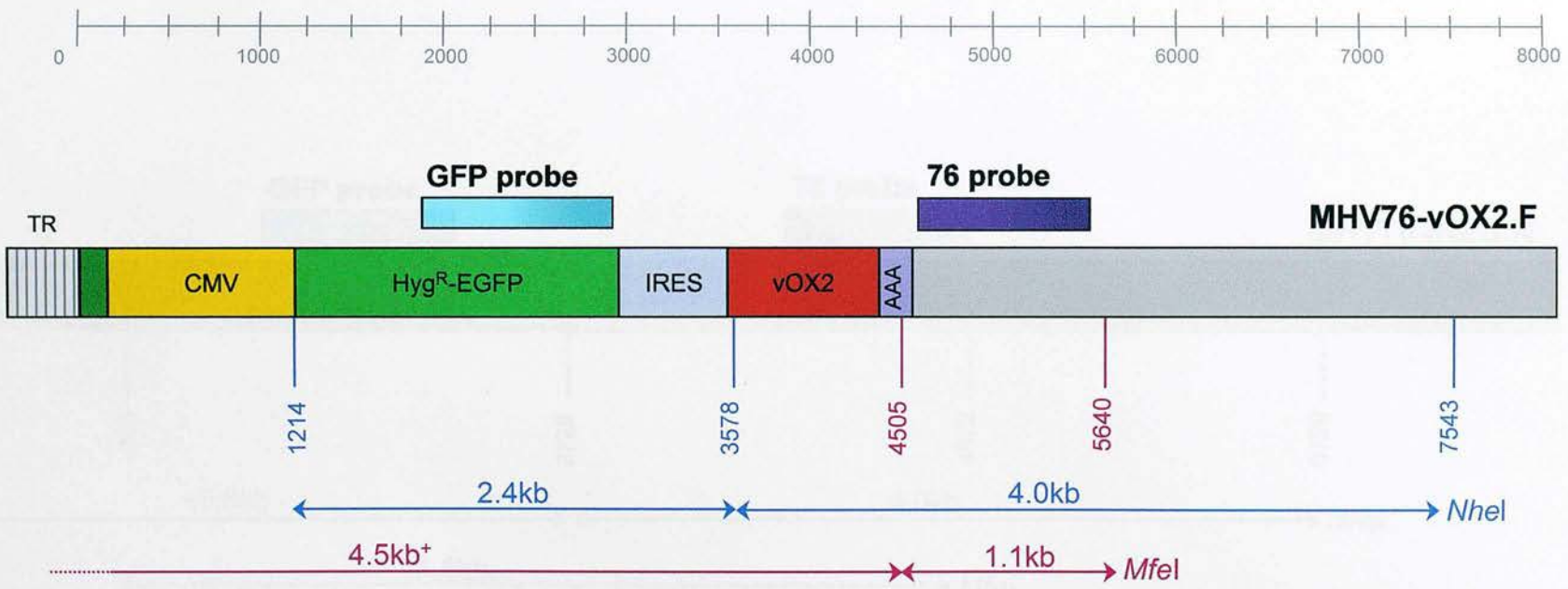

Figure 4.5C Interpretation of the restriction endonuclease map of the left-terminus for the recombinant virus MHV76-vOX2.F and MHV76-RAD for the restriction enzymes *Nhe*I and *Mef*I. A 8kb portion of the left-terminus of the recombinant virus is schematically shown: MHV-76 (grey), CMV (yellow), Hyg^R-EGFP (light green), IRES (light blue), vOX2 (red), polyadenylation (mauve), small portion of pBlueScriptKSII (dark green) and MHV-76 terminal repeats (TR)(grey). Restriction endonuclease digestions sites for *Nhe*I (blue) and *Mfe*I (pink) and predicted fragment sizes are illustrated. $^+$ denotes fragments that are bound to the TR and thus appear as a ladder of larger bands on Southern blot. The location of the GFP probe (nt 1821-2878 from pHygEGFP), in blue, and 76 probe (nt 9539-10461 from MHV-68), in purple, used in Southern analysis are shown above. The same sites are applicable for the MHV76-RAD recombinant virus.

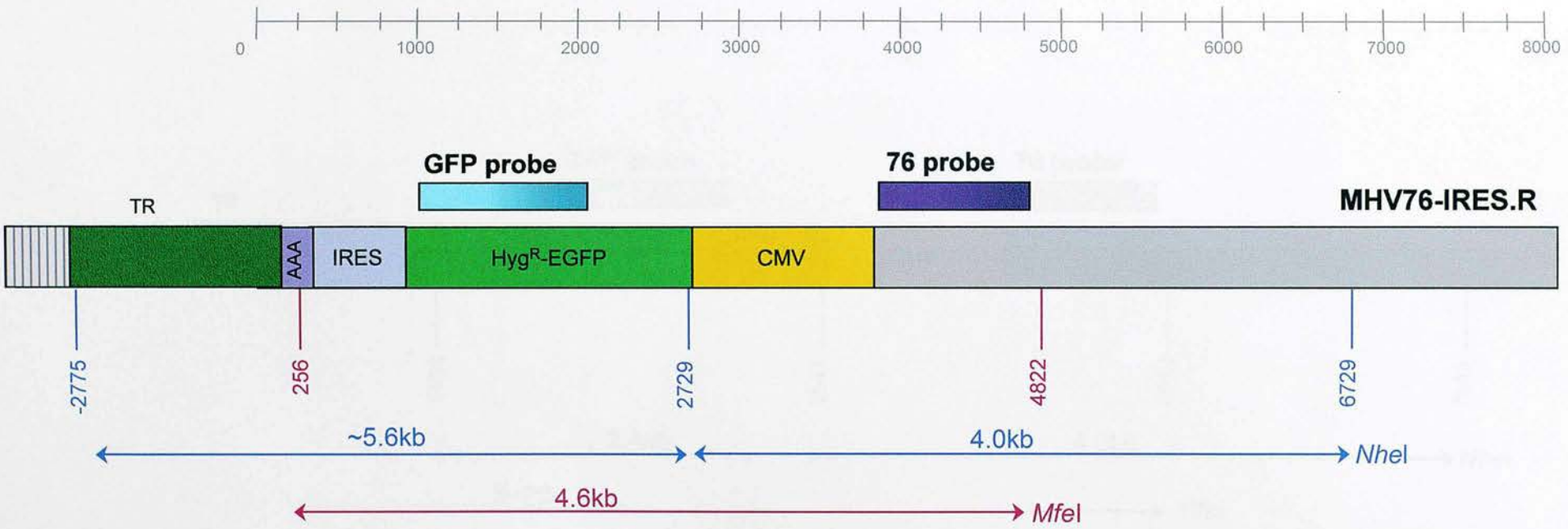

Figure 4.5D Interpretation of the restriction endonuclease map of the left-terminus for the recombinant virus MHV76-IRES.R for the restriction enzymes *Nhe*I and *Mef*I. A 8kb portion of the left-terminus of the recombinant virus is schematically shown: MHV-76 (grey), CMV (yellow), Hyg^R-EGFP (light green), IRES (light blue), polyadenylation (mauve), approximately a 2.7kb portion of pBlueScriptKSII (dark green) and MHV-76 terminal repeats (TR)(grey). Restriction endonuclease digestions sites for *Nhe*I (blue) and *Mfe*I (pink) and predicted fragment sizes are illustrated. The location of the GFP probe (nt 1821-2878 from pHygEGFP), in blue, and 76 probe (nt 9539-10461 from MHV-68), in purple, used in Southern analysis are shown above (Note: this virus was generated and purified by Dr J.Douglas).

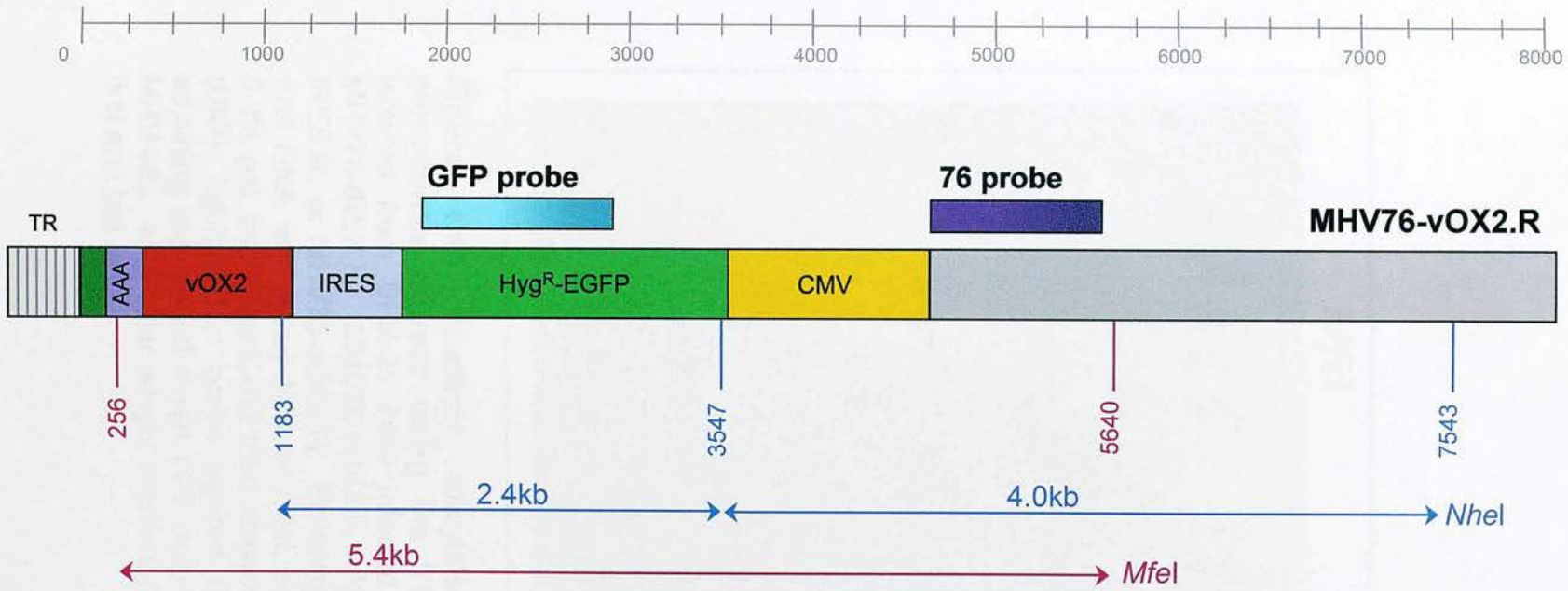

Figure 4.5E Interpretation of the restriction endonuclease map of the left-terminus for the recombinant virus MHV76-vOX2.R for the restriction enzymes *Nhe*I and *Mef*I. A 8kb portion of the left-terminus of the recombinant virus is schematically shown: MHV-76 (grey), CMV (yellow), Hyg^R-EGFP (light green), IRES (light blue), vOX2 (red), polyadenylation (mauve), small portion of pBlueScriptKSII (dark green) and MHV-76 terminal repeats (TR)(grey). Restriction endonuclease digestions sites for *Nhe*I (blue) and *Mfe*I (pink) and predicted fragment sizes are illustrated. The location of the GFP probe (nt 1821-2878 from pHygEGFP), in blue, and 76 probe (nt 9539-10461 from MHV-68), in purple, used in Southern analysis are shown above.

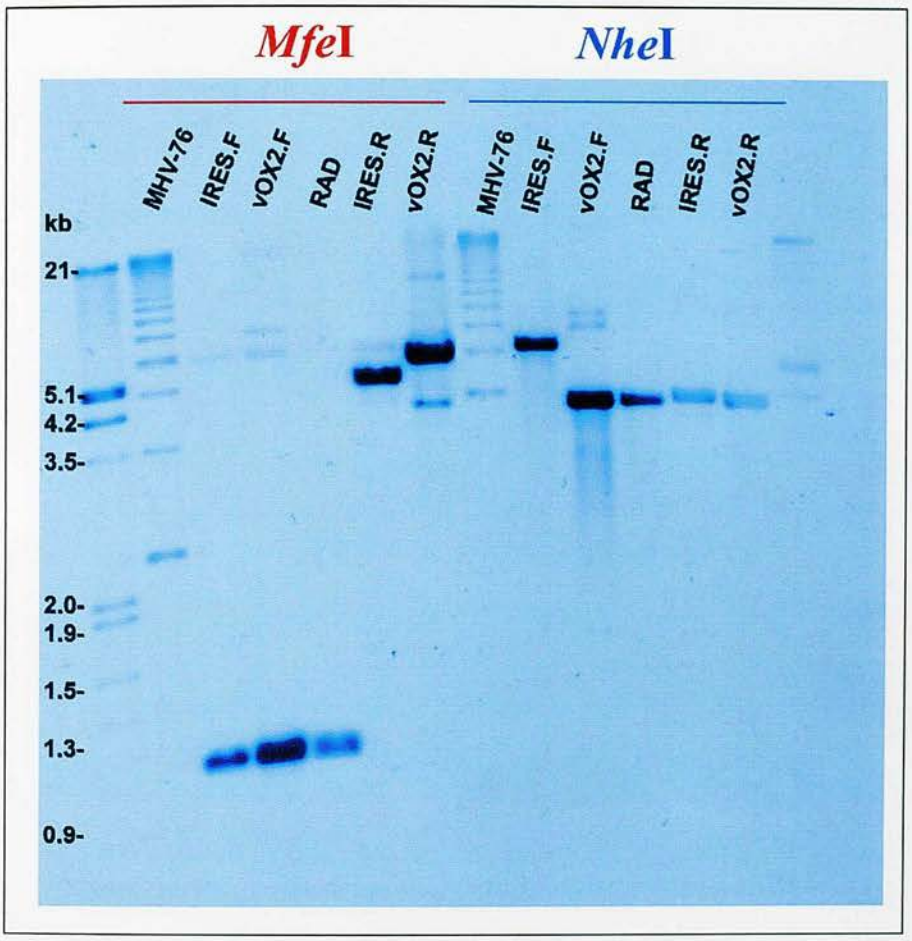

Figure 4.6A Southern anaylsis of MHV-76 and recombinant viruses using the '76' probe. DNA was isolated from BHK-21 cells infected with either MHV-76, MHV76-IRES.F, MHV76-vOX2.F, MHV76-RAD, MHV76-IRES.R, or MHV76-vOX2.R. Following the digestion of 5μg viral DNA with either *Mfe*I or *Nhe*I, samples were run on a 0.8% gel, transferred and then analysed using a digoxigenin (DIG)- hybridisation probe against the region in MHV-76 adjoining the cloned insert ('76' probe; nt 9539-10461 from MHV-68). Molecular weight markers (kb) are included in the first and last lane.

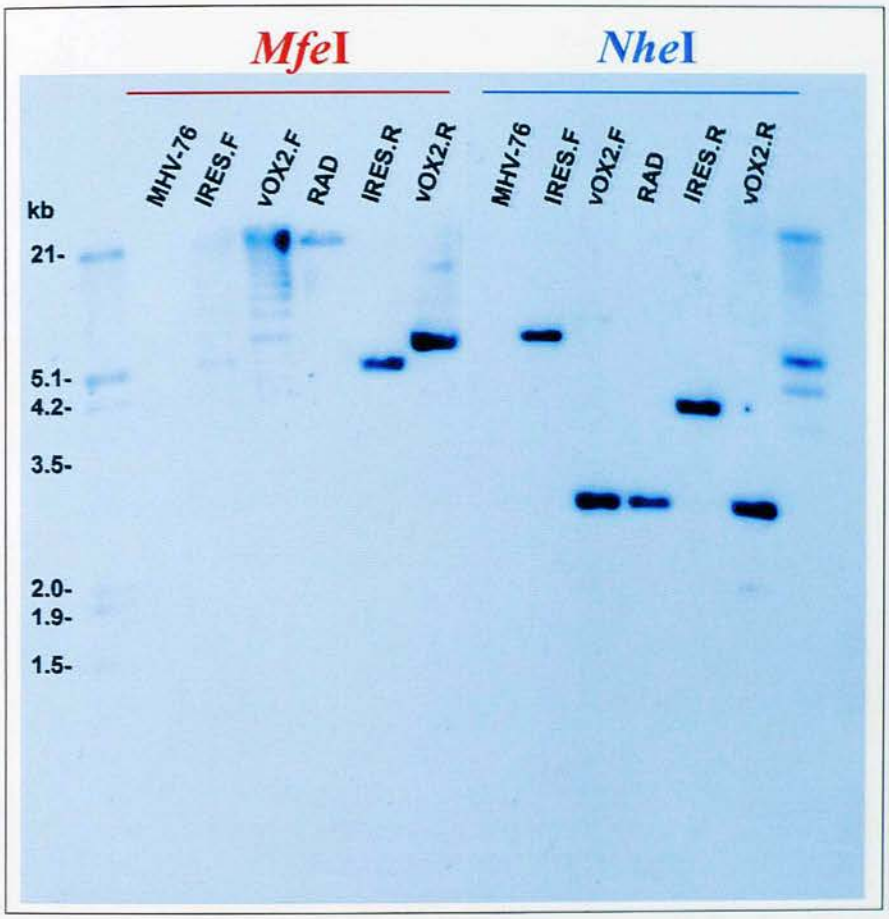

Figure 4.6B Southern anaylsis of MHV-76 and recombinant viruses using the 'GFP' probe. DNA was isolated from BHK-21 cells infected with either MHV-76, MHV76-IRES.F, MHV76-vOX2.F, MHV76-RAD, MHV76-IRES.R, or MHV76-vOX2.R. Following the digestion of 5μg viral DNA with either *Mfe*I or *Nhe*I, samples were run on a 0.8% gel, transferred and then analysed using a digoxigenin (DIG)- hybridisation probe against the EGFP region within the cloned insert ('GFP' probe; nt1821-2878 from pHygEGFP). Molecular weight markers (kb) are included in the first and last lane.

Some other samples also displayed a small number of non-specific bands. When directly compared with the predicted sizes of bands, all non-specific bands were of lesser intensity and were not believed to be significant. Additionally, some non-specific hybridisation may be the result of fragments of DNA that were not fully digested, and thus appear as larger bands than those predicted.

Southern analysis of the wild-type virus (MHV-76) yielded the expected laddering effect with both restriction enzymes, when probed with the '76' probe (Figure 4.5A). As expected, the 'GFP' probe did not hybridise with viral DNA from MHV-76 (Figure 4.6B).

4.4 *In vitro* growth studies

To investigate whether the inclusion of vOX2 or any of the selection markers resulted in an altered replication phenotype *in vitro*, all recombinant viruses were compared with MHV-76 during a single round (MOI=5) (Figure 4.7) and multiple rounds (MOI=0.05) (Figure 4.8) of replication in BHK-21 cells, respectively called a single-step and multi-step growth curve (see 2.3.6). The data from the single- and multi-step growth curves demonstrate that most (MHV76-vOX2.F, MHV76-vOX2.R, MHV76-IRES.F and MHV76-IRES.R) of the viruses replicate with similar kinetics to the wild-type virus, MHV-76. Therefore, it can be inferred that neither vOX2 nor any of the selection markers have any influence on *in vitro* replication or cell-cell spread.

However, when compared with both MHV-76 and MHV76-vOX2.F, the MHV76-RAD virus did display attenuated properties in both the single- and multi-step growth curves (Figures 4.7 and 4.8). As attenuation is present in both growth curves, it is assumed that this result is due to a mutation(s) elsewhere in the virus and not due to the direct mutation made within the RGD site of vOX2. As the RGD motif is associated with cell adhesion, theoretically a mutation generating a non-functional RAD site could potentially affect cell-to-cell spread of the virus and therefore would be expected to have no effect in a single-step growth curve. Consequently, due to an unidentified mutation in this virus, it was decided that the MHV76-RAD virus would not be used in any further experiments.

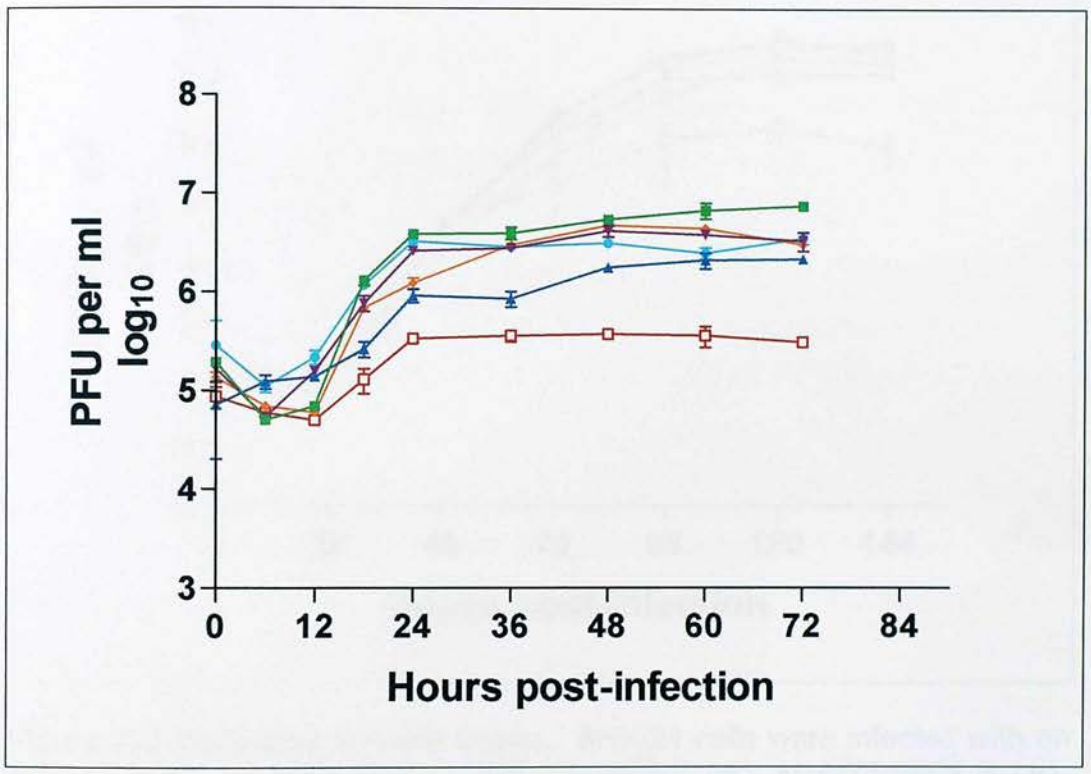

Figure 4.7 Single-Step Growth Curve. BHK-21 cells were infected with an MOI of 5 with MHV-76 (■), MHV76-IRES.F (▲), MHV76-IRES.R (▼), MHV76-vOX2.F (♦), MHV76-vOX2.R (●), or MHV76-RAD (□). Values plotted are mean of two samples per time point, with each sample titrated in duplicate. Data points shown represent the virus titre $\log_{10} \pm$ standard error.

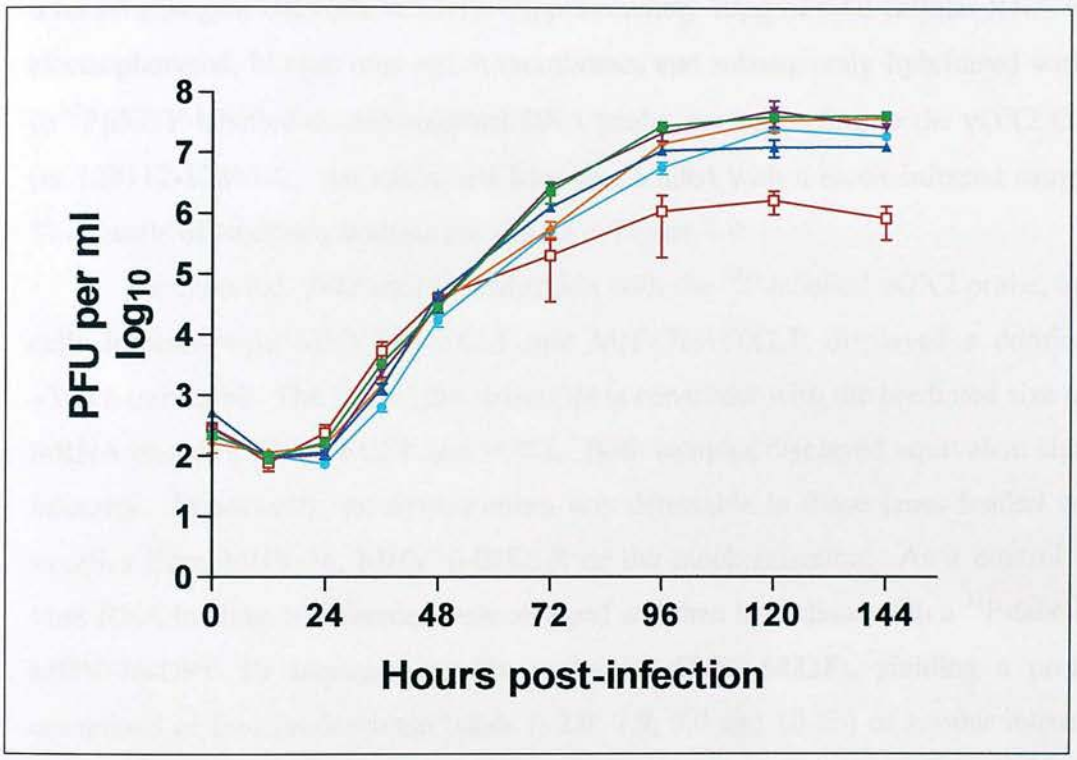

Figure 4.8 Multi-Step Growth Curve. BHK-21 cells were infected with an MOI of 0.05 with MHV-76 (■), MHV76-IRES.F (▲), MHV76-IRES.R (▼), MHV76-vOX2.F (♦), MHV76-vOX2.R (●), or MHV76-RAD (□). Values plotted are mean of two samples per time point, with each sample titrated in duplicate. Data points shown represent the virus titre $\log_{10} \pm$ standard error.

4.5 Transcriptional expression of the recombinant viruses

To verify transcription of the vOX2 ORF, Northern blot analysis was performed on RNA samples extracted from BHK cells infected with the recombinant viruses. BHK-21 cells were infected overnight with either MHV-76, MHV76-IRES.F, MHV76-vOX2.F or MHV76-vOX2.R at a multiplicity of infection (MOI) of 5, before the infected cells were harvested and total RNA extracted using an Rneasy mini kit (Qiagen, UK) (see 2.5.1.1). Approximately 10μg of total cellular RNA was electrophoresed, blotted onto nylon membranes and subsequently hybridised with a [α^{32}P]dCTP-labelled double-stranded DNA probe, corresponding to the vOX2 ORF (nt 128112-128930). An additional lane was loaded with a mock-infected sample. The results of Northern analysis are shown in Figure 4.9.

As expected, following hybridisation with the ^{32}P-labelled vOX2 probe, only cells infected with MHV76-vOX2.F and MHV76-vOX2.R displayed a dominant ~3.7kb transcript. The size of this transcript is consistent with the predicted size of a mRNA encoding Hyg^{R}-EGFP and vOX2. Both samples displayed equivalent signal intensity. Importantly, no hybridisation was detectable in those lanes loaded with samples from MHV-76, MHV76-IRES.R or the mock infection. As a control for viral RNA loading, membranes were stripped and then hybridised with a ^{32}P-labelled MHV-76-ORF 50 sequence-specific probe (nt 68483-68838), yielding a profile comprised of four predominant bands (~2.0, 2.9, 5.0 and 10-kb) of similar intensity in all samples, with the exception of the mock-infection. This expression pattern is consistent with previous observations of ORF 50 transcription (Liu *et al.*, 2000; Wu *et al.*, 2001). Thus, Northern analysis shows that vOX2 is abundantly expressed along with the other selection markers (Hyg^{R}-EGFP) *in vitro* in both MHV76-vOX2.F and MHV76-vOX2.R.

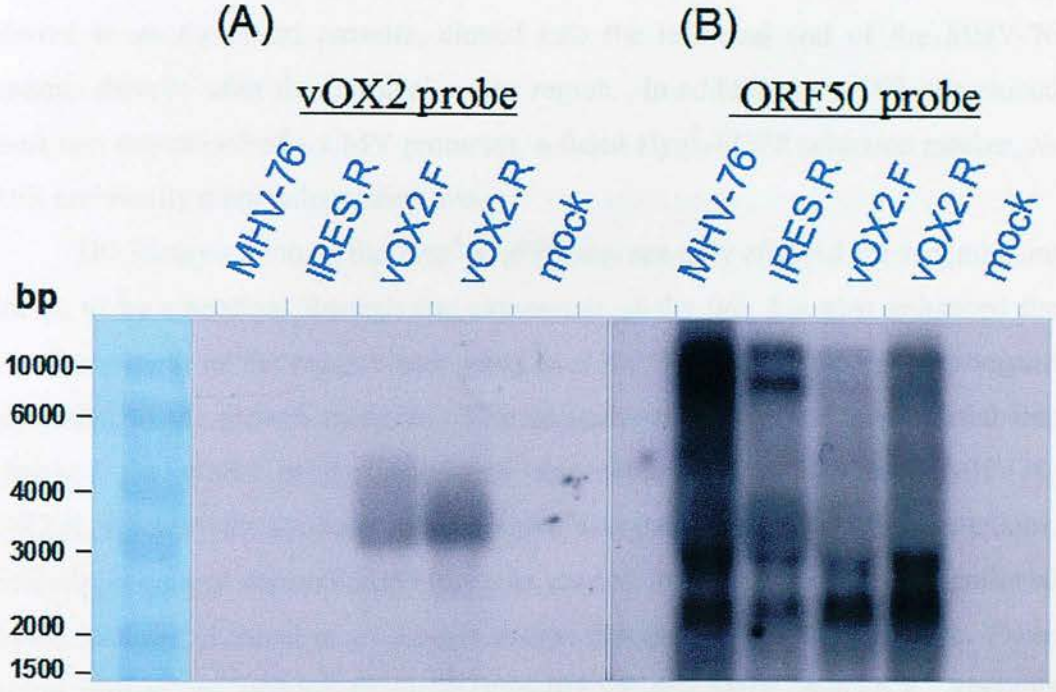

Figure 4.9 Northern analysis of vOX2 transcription by MHV-76 and recombinant viruses. RNA was isolated from BHK-21 cells infected with an MOI of 5 with MHV-76, MHV76-IRES.R, MHV76-vOX2.F or MHV76-vOX2.R, and a mock infection. Samples were analysed by Northern blot on a 1% formaldehyde gel, and successively hybridized with an [α^{32}P]dCTP-labelled probe spanning the (A) vOX2 region (nt 128113-128930 in KSHV) and then spanning the (B) ORF 50 (nt 68483-68838 in MHV-68). The molecular weight marker was stained with Coomassi Blue, shown on the left of the autoradiograph.

4.6 Discussion

These results describe the cloning strategy, generation and purification of several recombinant viruses containing the vOX2 ORF and selection markers, hygromycin (Hyg^R) and EGFP, and relevant control viruses. All recombinant viruses were generated by homologous recombination and the genes of interest, commonly referred to as the insert cassette, cloned into the left-hand end of the MHV-76 genome, directly after the terminal repeat region. In addition to vOX2, the cloned insert was comprised of a CMV promoter, a fused Hyg^R-EGFP selection marker, an IRES and finally a polyadenylation site.

The incorporation of the Hyg^R-EGFP gene not only allowed the recombinant viruses to be visualised through the expression of the *gfp*, but also enhanced the selective growth of the recombinant virus over the wild type virus, as hygromycin was added to the growth medium. Two recombinant viruses were generated that contained the vOX2 gene; these were termed MHV76-vOX2.F and MHV76-vOX2.R, whereby the identical insert cassette was incorporated in both orientations. Similarly, a control recombinant virus was created for each of the afore mentioned viruses, and are identical in all aspects except that they lack the vOX2 gene. These control viruses are referred to as MHV76-IRES.F and MHV76-IRES.R. Attempts were made to generate further controls where homologous recombination was used to create revertant viruses, i.e. re-form wild-type viruses from the recombinant viruses. This form of control virus would ensure that any phenotypic results observed were due to the inserted genes and not due to a mutation elsewhere in the virus. Various techniques were attempted but with no success. It was therefore decided that the generation of two independent viruses (i.e. the forward and reverse) and suitable control recombinant viruses would be adequate. In addition, another virus was created that contained a mutation in the RGD motif within the vOX2 gene. The RGD sequence was changed to a non-functional RAD, with the intention of using this virus to determine whether the RGD motif was used; this virus was termed MHV76-RAD.

All recombinant viruses were purified by limiting dilution and plaque purification and screened by PCR analysis for a minimum of four rounds. After the viruses were found to be pure isolates by PCR (see Table 4.1), the genomic

structures of the samples were further verified by Southern blot analysis (Figures 4.6A and B). All viruses yield profiles similar to those predicted, although partial digestion and use of the DIG-hybridisation method are believed to be the reason for the small amount of non-specific hybridisation. Southern analysis also confirmed that all isolates were pure and free of the wild-type virus, as in a couple of circumstances viral isolates thought to be pure by PCR analysis were found to be contaminated with a small amount of MHV-76. Further rounds of purification, often including an agarose overlay, resulted in the enrichment of the recombinant virus and complete loss of the wild-type virus; this was again verified by southern analysis.

Preliminary characterisation studies performed on all of the recombinant viruses have shown that most of the viruses replicate *in vitro* with similar kinetics to the wild-type virus MHV-76. However, one virus that showed attenuated properties in both the one-step and multi-step growth curve was MHV76-RAD. This virus was identical in all aspects to MHV76-vOX2.F with one small mutation made in the RGD motif within vOX2. It is thought the debilitating effect seen during its replication *in vitro* was not a direct result of the mutation made in the vOX2 ORF but most likely due to an unseen mutation elsewhere in the genome; primarily because the RGD motif is associated with cell adhesion, attenuation in replication during the multi-step growth curve could be explained, but not attenuation during one round of replication i.e. the single-step growth curve. Thus the MHV76-RAD recombinant virus was not included in any further experiments and unfortunately due to time constraints no attempts were made to try and generate a new version of this virus.

Finally, Northern blot analysis was performed to ensure transcription of the inserted genes. As it is clearly evident that the Hyg^R-EGFP ORF is expressed, a ^{32}P-dCTP probe was only generated to hybridise to the vOX2 ORF. Following the infection of BHK-21 cells with the recombinant viruses, RNA was isolated and MHV76-vOX2.F and MHV76-vOX2.R were both found to be expressing the vOX2 ORF. All viruses were probed against another gene within the virus, ORF50, as a positive control.

These results have outlined the production of several recombinant viruses possessing the KSHV vOX2 ORF and relevant control recombinant viruses. *In vitro* analysis reveals that neither the vOX2 gene nor any of the other insert genes enhance

or attenuate replication of the virus *in vitro*. Unfortunately the MHV76-RAD recombinant virus, generated to study the RGD motif, displayed attenuated properties resulting in the discontinued use of this virus in further studies. However, the remaining recombinant viruses generated (MHV76-vOX2.F, MHV76-vOX2.R, MHV76-IRES.F, and MHV76-IRES.R) need to be further characterised and analysed in order to study the properties of the vOX2 ORF *in vivo*. Data describing *in vivo* studies is detailed in the following chapters.

Chapter Five: *In Vivo* Studies using BALB/c Mice

Chapter 5: Animal Model Studies using BALB/c Mice

Following the purification and *in vitro* analysis of the recombinant viruses, the next stage was to study viral replication and pathogenesis *in vivo*. Female BALB/c mice, 4-6 weeks old, were infected intranasally with 4 $x10^5$ PFU of virus (MHV-76, MHV76-IRES.F, MHV76-IRES.R, MHV76-vOX2.F or MHV76-vOX2.R). Lung, spleen and MLN samples were removed at a variety of time-points and analysed for the presence of virus and other resultant pathogenic effects.

5.1 Lytic Replication

5.1.1 Viruses in the lung

5.1.1.1 Replication in the lung

In the initial experiment, BALB/c mice were infected with MHV-76 and recombinant viruses: MHV76-IRES.R, MHV76-vOX2.F or MHV76-vOX2.R. Viral titres in the lung were assessed at days 5, 10, 14 and 21 post-infection (p.i.) by plaque assay (see 2.3.4). Productive virus was only detected on day 5 p.i., with both the recombinant viruses encoding vOX2, MHV76-vOX2.F and MHV76-vOX2.R, having significantly higher levels (up to 10-fold) than the wild-type virus MHV-76 and the control recombinant virus MHV76-IRES.R (Figure 5.1A) (Day 5 lung titre: MHV76-vOX2.F vs. MHV76-IRES.R ; $P < 0.001$ and MHV76-vOX2.R vs MHV76-IRES.R; $p<0.001$).

This experiment was repeated and productive virus measured at earlier time-points, including days 3, 5, 7 and 9 p.i. (Experiment 2). For all viruses, peak viral titres were observed 5 days p.i. and viral clearance by day 9 p.i. (Figure 5.1B). Both MHV76-vOX2.F and MHV76-vOX2.R viral levels were 10-100-fold higher than the control MHV76-IRES.R at days 3 and 5 p.i. (both $p<0.001$) (Figure 5.1C). MHV76-IRES.R viral titres were also lower than the wild-type MHV-76 at all time points (day 5 $p<0.001$).

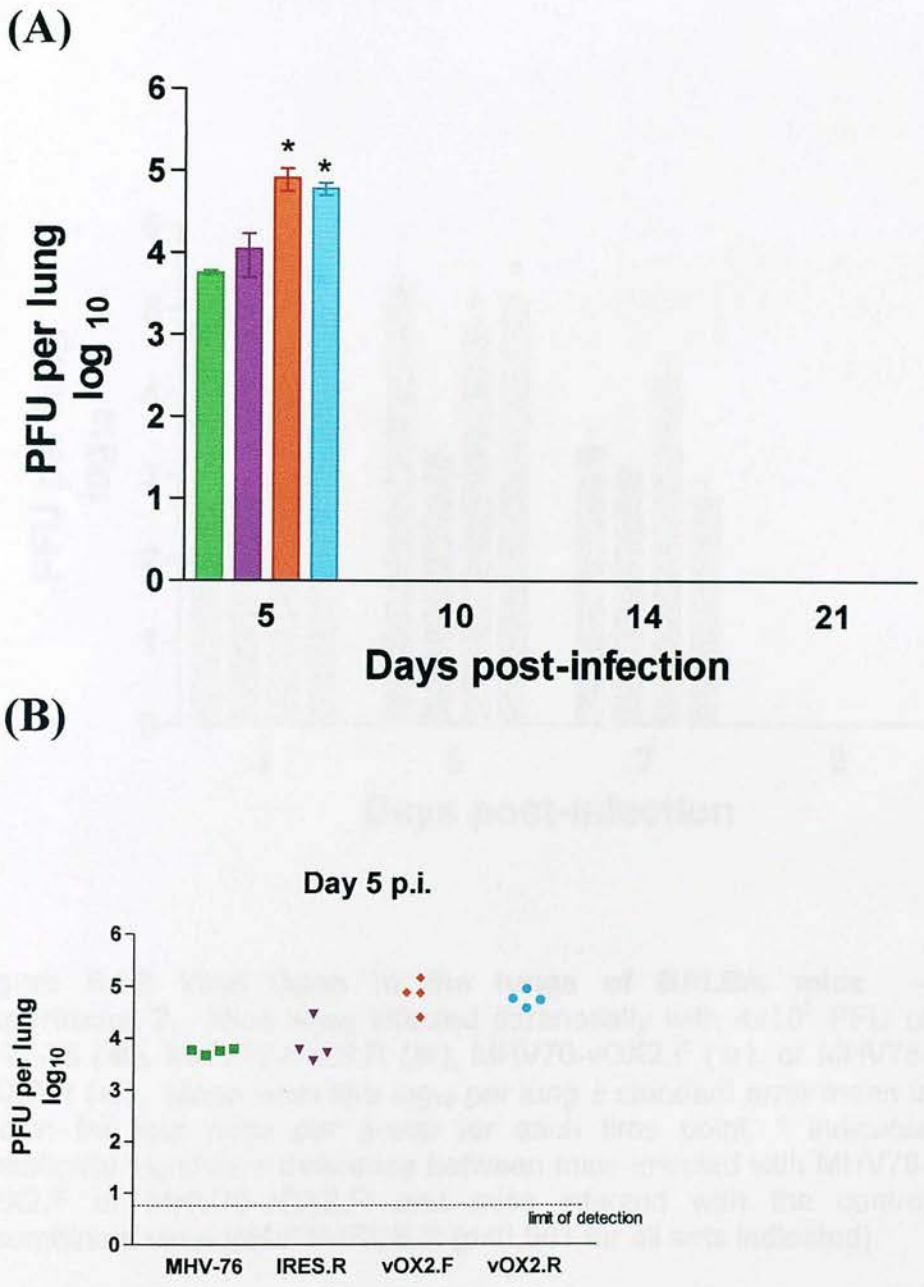

Figure 5.1A Viral titres in the lungs of BALB/c mice – Experiment 1. Mice were infected intranasally with 4 x10^5 PFU of MHV-76 (■), MHV76-IRES.R (■), MHV76-vOX2.F (■), or MHV76-vOX2.R (■). (A) Samples were taken at days 5, 10, 14 and 21 days post-infection. Mean virus titre log_{10} per lung ± standard error mean is shown for four mice per group for each time point. * indicates statistically significant difference between viral titres in mice infected with MHV76-vOX2.F or MHV76-vOX2.R and mice infected with the control recombinant virus MHV76-IRES.R ($p<0.001$ for both sets). (B) Detailed plot of results from 5 days post-infection, where each point is representative of an individual mouse. Dashed line (---) indicates the limit of detection.

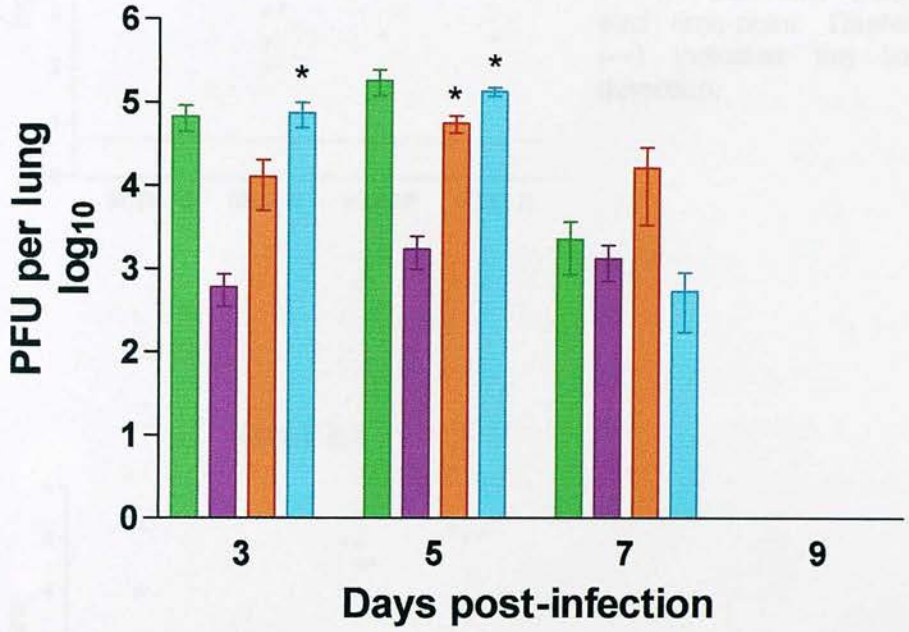

Figure 5.1B Viral titres in the lungs of BALB/c mice – Experiment 2. Mice were infected intranasally with $4x10^5$ PFU of MHV-76 (■), MHV76-IRES.R (■), MHV76-vOX2.F (■), or MHV76-vOX2.R (■). Mean virus titre log_{10} per lung ± standard error mean is shown for four mice per group for each time point. * indicates statistically significant difference between mice infected with MHV76-vOX2.F or MHV76-vOX2.R and mice infected with the control recombinant virus MHV76-IRES.R ($p<0.001$ for all sets indicated).

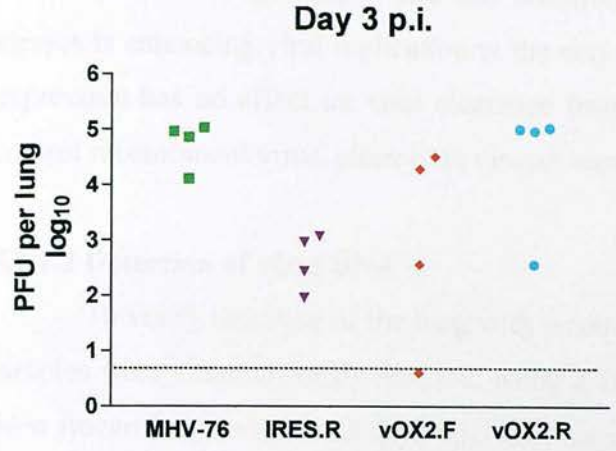

Figure 5.1C Detailed plot of lung titres in BALB/c mice at days 3, 5 and 7 post-infection -Experiment 2. Each point is representative for an individual mouse at each time-point. Dashed line (---) indicates the limit of detection.

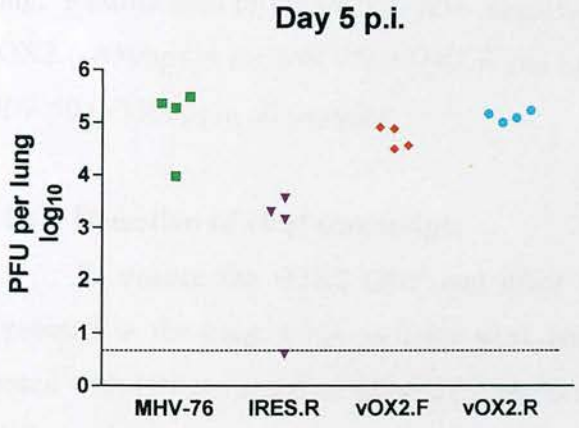

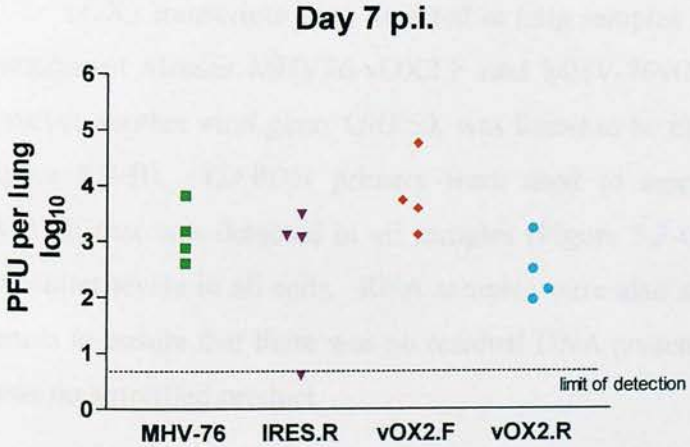

These findings imply that the insertion of vOX2 within the recombinant viruses is enhancing viral replication at the very early time-points. However, vOX2 expression has no effect on viral clearance from the lung when compared with the control recombinant virus, since both viruses were cleared by day 10 p.i.

5.1.1.2 Detection of viral DNA

To verify infection of the lung with recombinant viruses, both DNA and RNA samples were simultaneously isolated, using a QIAGEN RNA/DNA kit (see 2.8.7), from frozen lung samples (5 days p.i., from experiment 2) from mice infected with MHV-76, MHV76-IRES.R, MHV76-vOX2.F and MHV76-vOX2.R. DNA was amplified using the vOX2 primers (vOX-1 and vOX-2), and also using the MHV-76 ORF 50 primers (ORF50-F and ORF50-R) to ensure the presence of virus in the lung. Results seen in Figure 5.2 show amplification of correctly sized sequences for vOX2 (~850bp) in the MHV76-vOX2.F and MHV76-vOX2.R samples only, and for ORF 50 (~350bp) in all samples.

5.1.1.3 Detection of viral transcripts

To ensure the vOX2 ORF and other viral transcripts were actually being expressed in the lung, RNA samples were analysed. Isolated RNA samples were treated with DNase, and then oligo dT primers used to generate cDNA (see 2.5.2 and 2.5.3), which was amplified using a variety of primers, including: vOX2 primers (vOX-1 and vOX-2), ORF 50 primers (ORF50-F and ORF50-R), and GAPDH primers (GAPDH-1 and GAPDH-2).

vOX2 transcripts were detected in lung samples from mice infected with the recombinant viruses MHV76-vOX2.F and MHV-76vOX2.R only (Figure 5.3-A). However another viral gene, ORF50, was found to be expressed in all lung samples (Figure 5.3-B). GAPDH primers were used to amplify a housekeeping gene, GAPDH, that was detected in all samples (Figure 5.3-C); GAPDH is expressed at substantial levels in all cells. RNA samples were also amplified using the GAPDH primers to ensure that there was no residual DNA present; as expected Figure 5.3-D shows no amplified product.

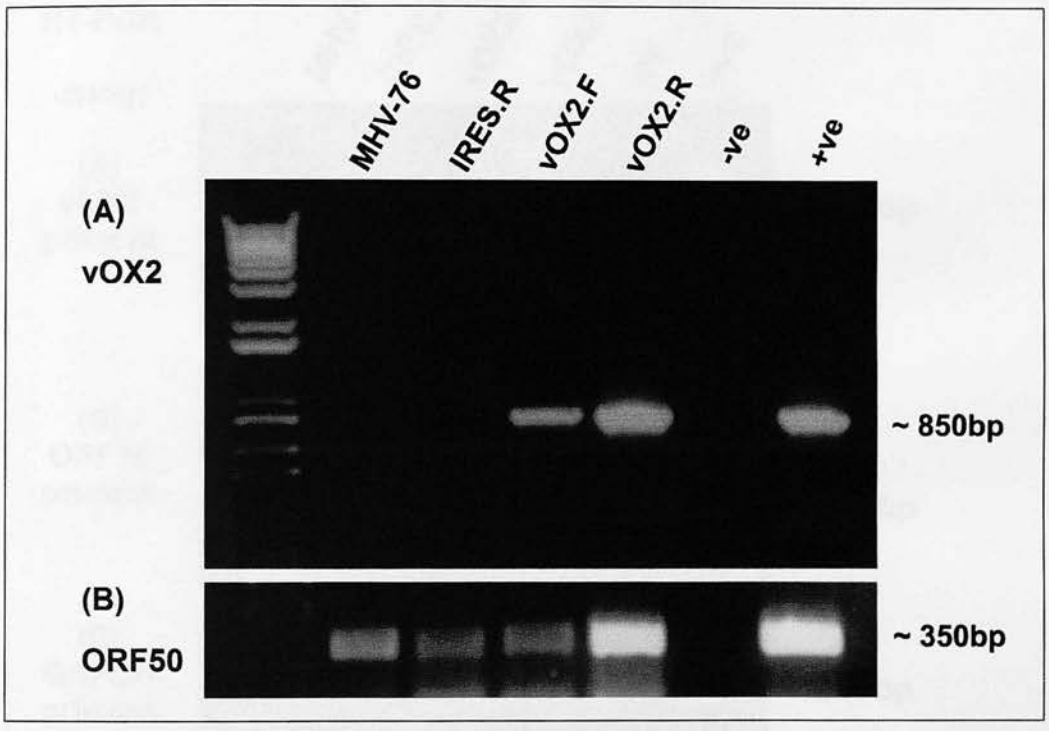

Figure 5.2 Detection of viral DNA in the lungs of BALB/c mice 5 days post-infection. DNA samples were isolated from lung tissue from mice infected with MHV-76, MHV76-IRES.R, MHV76-vOX2.F or MHV76-vOX2.R. DNA samples were amplified using (A) vOX2 primers and (B) ORF 50 primers. PCR products were analysed on a 1.2% agarose gel with a 1Kb+ DNA molecular weight marker (on left hand end). All reactions included the use of dH_20 as a negative control (-ve) and (A) BCBL-1 DNA or (B) MHV-68 DNA as a positive control (+ve).

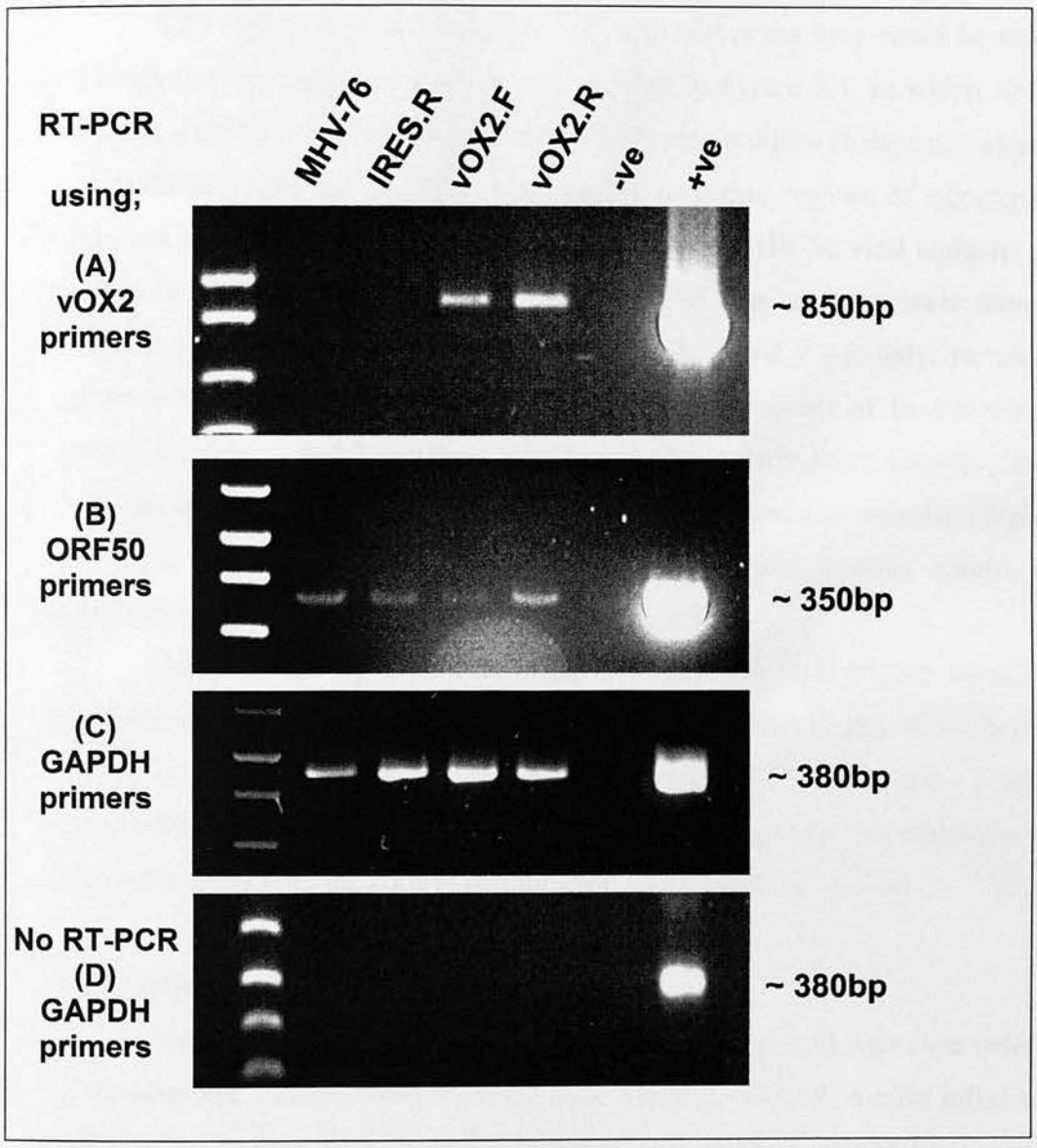

Figure 5.3 Detection of viral transcripts in the lungs of BALB/c mice five days post-infection. RNA samples were isolated from lung tissue from mice infected with MHV-76, MHV76-IRES.R, MHV76-vOX2.F or MHV76-vOX2.R. RNA samples were used in reverse transcriptase reactions using oligo dT primer and the cDNA was amplified by PCR using (A) vOX2 primers, (B) ORF50 primers and (C) GAPDH primers. As an additional negative control, the RNA samples were amplified by PCR using (D) GAPDH primers. PCR products were analysed on a 1.2% agarose gel with a 1Kb+ DNA molecular weight marker (on left hand end). All reactions included a negative control (-ve), dH_20, and positive control (+ve), BCBL1-DNA for (A), MHV-68 DNA for (B), and genomic DNA for (C) and (D).

5.1.1.4 Detection of recombinant viruses in the lung

Cells infected with recombinant viruses within the lung could be visualized through the expression of *gfp*. This is evident in Figure 5.4, in which, following fixation with 4% w/v paraformaldehyde, frozen lung sections (5 days p.i., experiment 2) could be examined for viral infection by detecting regions of *gfp* expression. Sections were also stained for the presence of other MHV-76 viral antigens using a polyclonal MHV-68 antisera. *Gfp* and MHV-76 viral antigens were detected in sections made from lungs samples taken days 3, 5 and 7 p.i. only, no virus was detected in samples taken 9 days p.i. Only minor amounts of fluorescence were visible on days 3 and 7 (images not shown), particularly when directly compared with the levels of *gfp* expression and MHV-76 associated fluorescence displayed 5 days p.i. (Figure 5.4). This further support the lung titration results, where productive viral titres were also seen to peak 5 days p.i.

When comparing the levels of *gfp* and MHV-76 viral antigen expression in the lung sections, the areas infected with MHV76-vOX2.F and MHV76-vOX2.R appear to be more extensive than the control virus, MHV76-IRES.R. These data agree with the 10-100 fold increase in lung titres of the vOX2 recombinant viruses when compared with the control recombinant virus, MHV76-IRES.R.

5.1.1.5 Histology

Following intranasal infection of the mice with the wild-type virus (MHV-76) or recombinant viruses, MHV76-vOX2.F or MHV76-vOX2.R, a mild inflammatory response was observed in haematoxylin and eosin (H&E) stained lung sections 3 days p.i. (Figure 5.5, from experiment 2). This included a small amount of infiltration of inflammatory cells into the perivascular and peribronchial region, and minor vasculitis was observed in the MHV-76 sample. Mice infected with the control recombinant virus, MHV76-IRES.R, showed no indication of an immune response and the section is representative of a healthy/ uninfected lung (Figure 5.5-B). The presence of haemorrhaging in some of the sections is most likely due to the preparation of the sample and not a result of infection with any of the viruses.

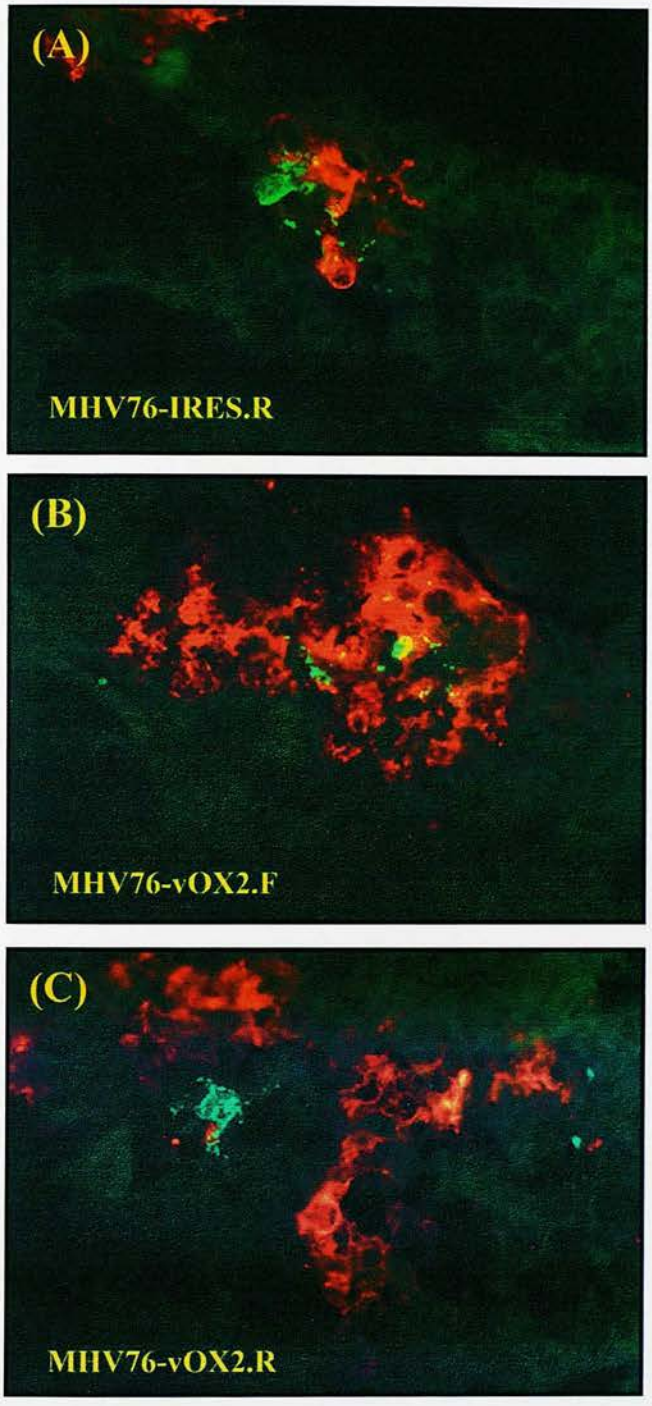

Figure 5.4 Detection of recombinant viruses in the lung. *Gfp* expression from recombinant viruses is visible in frozen lung sections 5 days post-infection, from mice infected with (A) MHV76-IRES.R, (B) MHV76-vOX2.F or (C) MHV76-vOX2.R. Other viral antigens expressed by MHV-76 were also detected when samples were stained using polyclonal anti-MHV-68 antiserum, and then stained with anti-rabbit IgG Alexa Fluor 546 (red). (Samples fixed in 4% (w/v) paraformaldehyde; All images at x 400 magnification)

By day 9 p.i., the inflammatory changes observed during infection with MHV76-vOX2.F and MHV76-vOX2.R were significant, consisting of perivascular, peribronchial and interstitial lymphoid infiltration, with the later being the most severe and involving a greater number of macrophage within the interstitial region (Figure 5.5-G and 5.5-H). Perivascular inflammation and local interstitial wall thickening was visible, but to a lesser degree in the lungs of mice infected with the wild-type virus, MHV-76 (Figure 5.5-E). Mice infected with MHV76-IRES.R showed a minimal amount of immune response at 9 days p.i., including: perivascular inflammation, oedema and minimal interstitial involvement (Figure 5.5 -F).

From these findings, a general grading of severity due to the immune response towards the virus would be as follows: MHV76-vOX2.F & MHV76-vOX2.R > MHV-76 > MHV76-IRES.R.

5.1.1.6 mCD200 expression levels

To investigate if expression levels of mCD200 were down-regulated in the lungs of infected mice, lung sections were stained for the protein. OCT frozen lung sections were fixed with either 4% (w/v) paraformaldehyde (2 hours) or ice-cold methanol/acetone (1:1) (2 minutes). The first attempts were made by staining for mCD200 using a primary antibody from Serotec (rat α mCD200), followed by a secondary antibody from Molecular Probes (goat α rat-AF350 (blue)) (see 2.9.2). This was performed in combination with staining for other viral antigens using the polyclonal anti-MHV-68 sera with goat α rabbit-AF546, as previously described in 5.1.1.4. Theoretically a combination of these two immunostained antigens along with *gfp* expression from the recombinant viruses should be visualized. However after several attempts at optimising staining conditions, mCD200 could not be detected although *gfp* and MHV-76 viral antigens were visualised (data not shown). A variety of other secondary antibodies against the rat α mCD200 and varying dilutions were also tested but with no success (mCD200 expression was detected in the spleen using rabbit α rat-TRITC (red) as the secondary antibody, but mCD200 was not detected in the lung sample; data not shown).

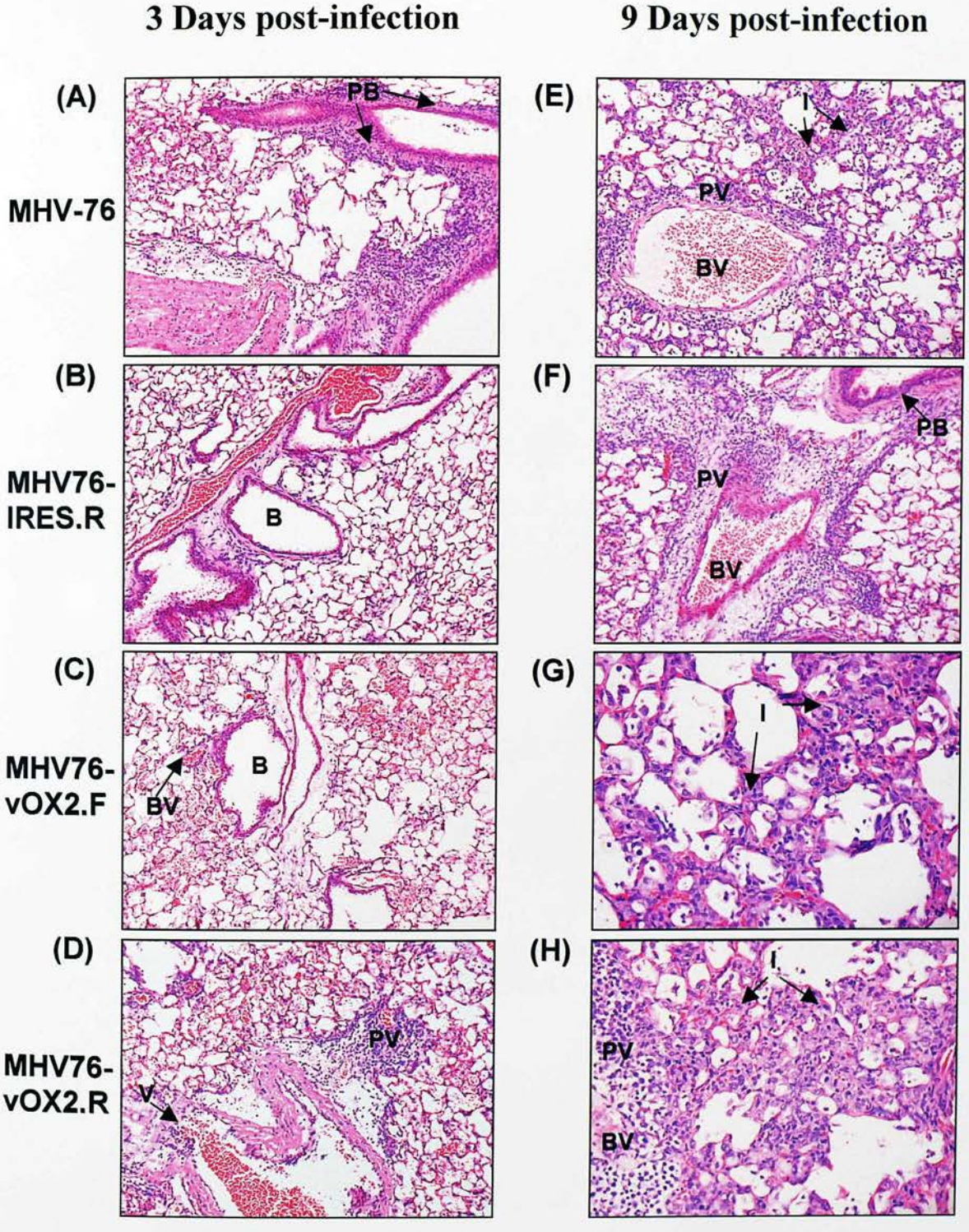

Figure 5.5 Histopathological changes in BALB/c mice lungs. Mice were infected with wild-type MHV-76 and recombinant viruses, MHV76-IRES.R, MHV76-vOX2.F or MHV76-vOX2.R and lung sections stained with haematoxylin and eosin from days 3 (A-D) and 9 (E-H) post-infection (Images A-F original magnification at x100, images G and H at x250; Abbreviations: **B**- bronchiole; **BV**- blood vessel; **I**- interstitial infiltration; **PB**- peri-bronchial inflammation; **PV**- perivascular inflammation; **V**- vasculitis).

5.2 Latency

5.2.1 Viruses in the MLN

Latent viral levels were measured in the MLN from BALB/c mice infected with MHV-76, MHV76-IRES.F and MHV76-vOX2.F, at days 5, 7 and 9 p.i. (Experiment 3). Due to the size of the organ, samples were pooled from 3 to 4 mice per time-point before performing an infective centre assay (see 2.8.3) on approximately 4 $x10^6$ cells. The number of infective centres detected was very low and at most time-points dropped below detectable levels for all viruses (data not shown). These results may not be indicative of the actual viral levels, due to the fact that samples were pooled, identification of MLN difficult, and only a small proportion of cells analysed.

5.2.2 Viruses in the spleen

5.2.2.1 Infective centre assay

The establishment of latency *in vivo* was determined by performing an infective centre assay (see 2.8.3) to detect latently infected splenocytes in mice infected with MHV-76, MHV76-IRES.R, MHV76-vOX2.F and MHV76-vOX2.R. Spleen samples from experiment 1 on days 5, 10, 14 and 21 p.i. were measured. No latent virus was detected at 5 days p.i. Latent MHV-76 was detected at all other time-points and peaked 10 days p.i., when levels varied from approximately 10 to 450 infective centres per spleen (Figure 5.6). The highest amount of latent recombinant virus was detected on day 10 and minimal amounts on day 21 p.i., often with levels nearing the limit of detection (Figure 5.6). These consistently low levels were observed in all mice that were infected with a recombinant virus.

5.2.2.2 Virus-induced splenomegaly

Splenomegaly occurs in mice that have been infected with MHV-68, but this is not a pathogenic effect of MHV-76 infections. To ensure that infection with any of the recombinant viruses did not show this feature, splenocyte numbers were measured at 5, 10, 14 and 21 days p.i. from experiment 1 (see 2.8.3 – splenocytes counted were used to determine the number of splenocytes 10^7 per spleen). A plot of the splenocyte numbers during the specified time-points (Figure 5.7) indicates a

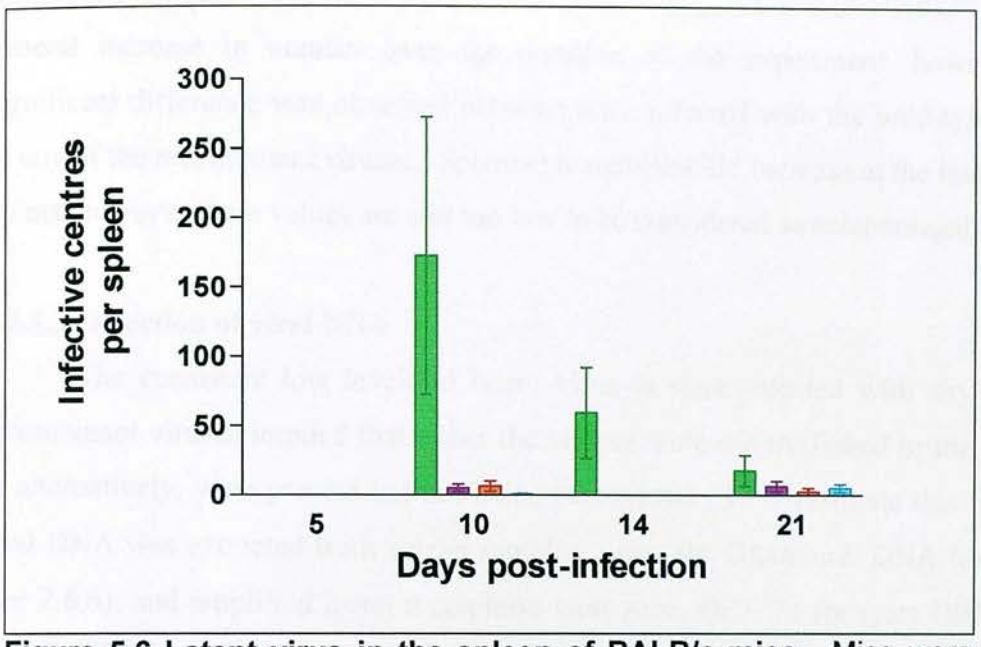

Figure 5.6 Latent virus in the spleen of BALB/c mice. Mice were infected intranasally with $4x10^5$ PFU of MHV-76 (■), MHV76-IRES.R (■), MHV76-vOX2.F (■), or MHV76-vOX2.R (■). Amount of latent virus determined by infective centre assay. Mean infectious centres per spleen ± standard error are shown for four mice per group for each time point.

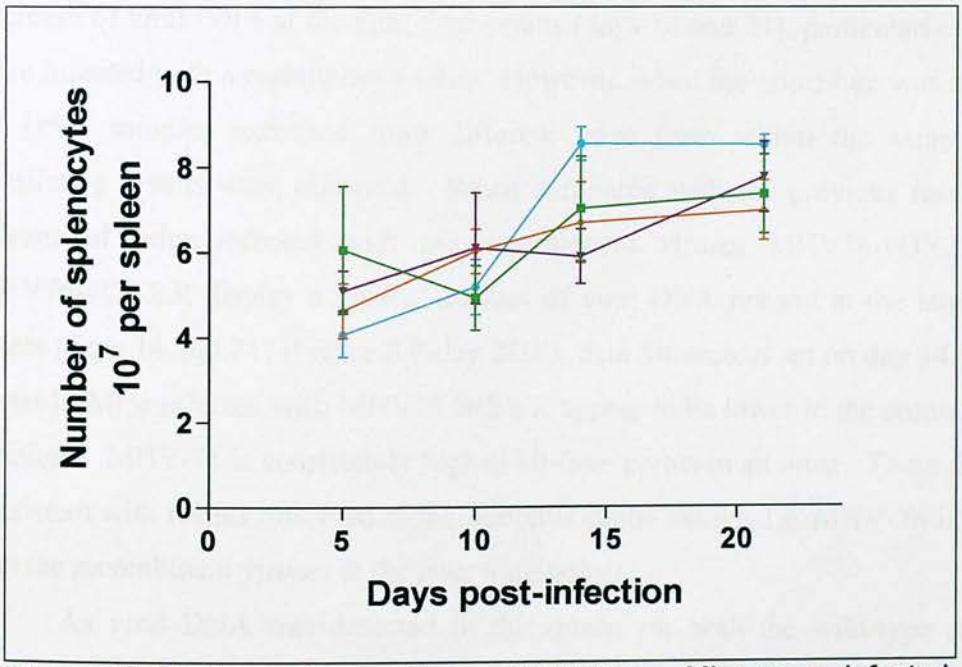

Figure 5.7 Splenocyte numbers of BALB/c. Mice were infected intranasally with $4x10^5$ PFU of MHV-76 (■), MHV76-IRES.R (▼), MHV76-vOX2.F (♦), or MHV76-vOX2.R (●). Number of splenocytes ± standard error is shown for four mice per group for each time point.

general increase in number over the duration of the experiment, however no significant difference was observed between mice infected with the wild-type virus or any of the recombinant viruses. Splenocyte numbers did increase at the later time-points, however these values are still too low to be considered as splenomegaly.

5.2.2.3 Detection of viral DNA

The consistent low levels of latent virus in mice infected with any of the recombinant viruses implied that either the viruses were not trafficked to the spleen or alternatively, were present but not being reactivated. To investigate this further, viral DNA was extracted from spleen samples, using the QIAamp® DNA Mini Kit (see 2.8.6), and amplified using a common viral gene, ORF 74 (primers ORF74-5' and ORF74-3'). Limiting dilution PCR was performed on the extracted DNA (~400ng to 3ng) and detected by southern blot analysis using an ORF 74 probe (nt 68483-68838, from MHV-68).

Initial observations, presented in Figure 5.8, indicate a general trend where all viruses are present at the early time-points (days 5 and 10), followed by a marked decrease of viral DNA at the later time-points (days 14 and 21), particularly in those mice infected with a recombinant virus. However, when the procedure was repeated on DNA samples extracted from different mice from within the same group, conflicting results were observed. When compared with the previous results, the spleens of mice infected with the recombinant viruses MHV76-vOX2.F and MHV76-vOX2.R display a greater amount of viral DNA present at the later time-points (days 14 and 21) (Figure 5.8-day 21(ii), data for second set on day 14 p.i. not shown). Mice infected with MHV76-IRES.R appear to be lower in the second set of reactions. MHV-76 is consistently high at all time-points in all mice. These data are consistent with results observed in the infective centre assays, i.e. MHV-76 is higher than the recombinant viruses at the later time-points.

As viral DNA was detected in the spleen for both the wild-type and the recombinant viruses, it implies that some virus has reached the spleen. These results, however, cannot verify if the virus is intact or if the technique has just detected partial fragments of degraded viral DNA.

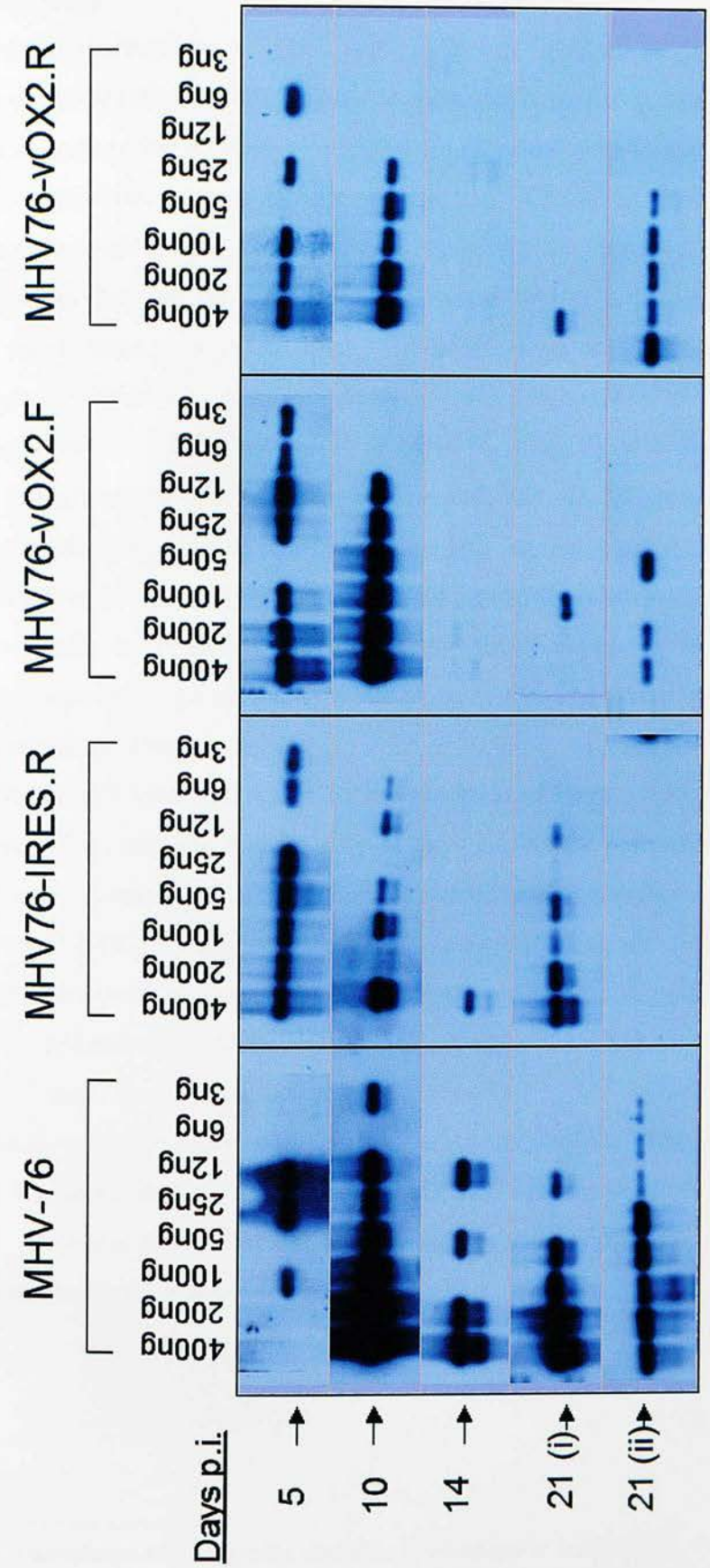

Figure 5.8 Detection of viral DNA in the spleen. BALB/c mice were infected with MHV-76, MHV76-IRES.R, MHV76-vOX2.F, or MHV76-vOX2.R, and spleen samples taken at days 5, 10, 14 and 21 post-infection. Extracted DNA was amplified in limiting dilution PCRs and probed for the ORF 74 product using Southern blot analysis.

5.2.1.4 Histology

Initial observations of H&E stained spleen sections 14 days p.i., found evidence of active inflammation as seen by follicular hyperplasia, with the formation of germinal centres and a minor increase in the marginal zone within the white pulp area in all mice infected with a virus (Figure 5.9). Characteristic features such as mitotic figures and "starry sky" scenarios involving tingible body macrophages[†] were visible in the germinal centres. No germinal centres were detected in spleen sections taken from uninfected mice. In addition to the increased number of lymphocytes within the germinal centres, mice infected with either of the recombinant viruses (MHV76-IRES.R or MHV76-vOX2.F), also displayed a large increase in the number of lymphocytes in the red pulp area (Figure 5.9-C and -D). This is particularly noticeable due to the lymphocytes congregating in the centre of the red pulp area and thus causing a halo effect around the white pulp areas. The red pulp hyperplasia is seemingly a common non-specific response to anything that could cause up-regulation of colony stimulating factors and was only present in the recombinant virus samples.

The lymphocyte aggregates in the red pulp of those mice infected with a recombinant virus, seem to regress after 21 days p.i. but the spleens still possess the germinal centre formations. The germinal centres are also present at day 21 in mice infected with MHV-76 (data not shown). There were no detectable histopathological differences observed between the mice infected with MHV76-vOX2.F and the control recombinant virus, MHV76-IRES.R.

The more severe immune response observed in the spleen of those mice infected with either of the recombinant viruses may explain some of the previous findings, including the low latent viral loads and varying amounts of viral DNA detected. It seems likely that the expression of *gfp* is eliciting a strong immune response against the recombinant viruses.

[†] Tingible macrophages are phagocytic macrophage of apoptotic lymphocytes, filled with nuclear debris. These types of macrophage are particularly noticeable at times of increased proliferation.

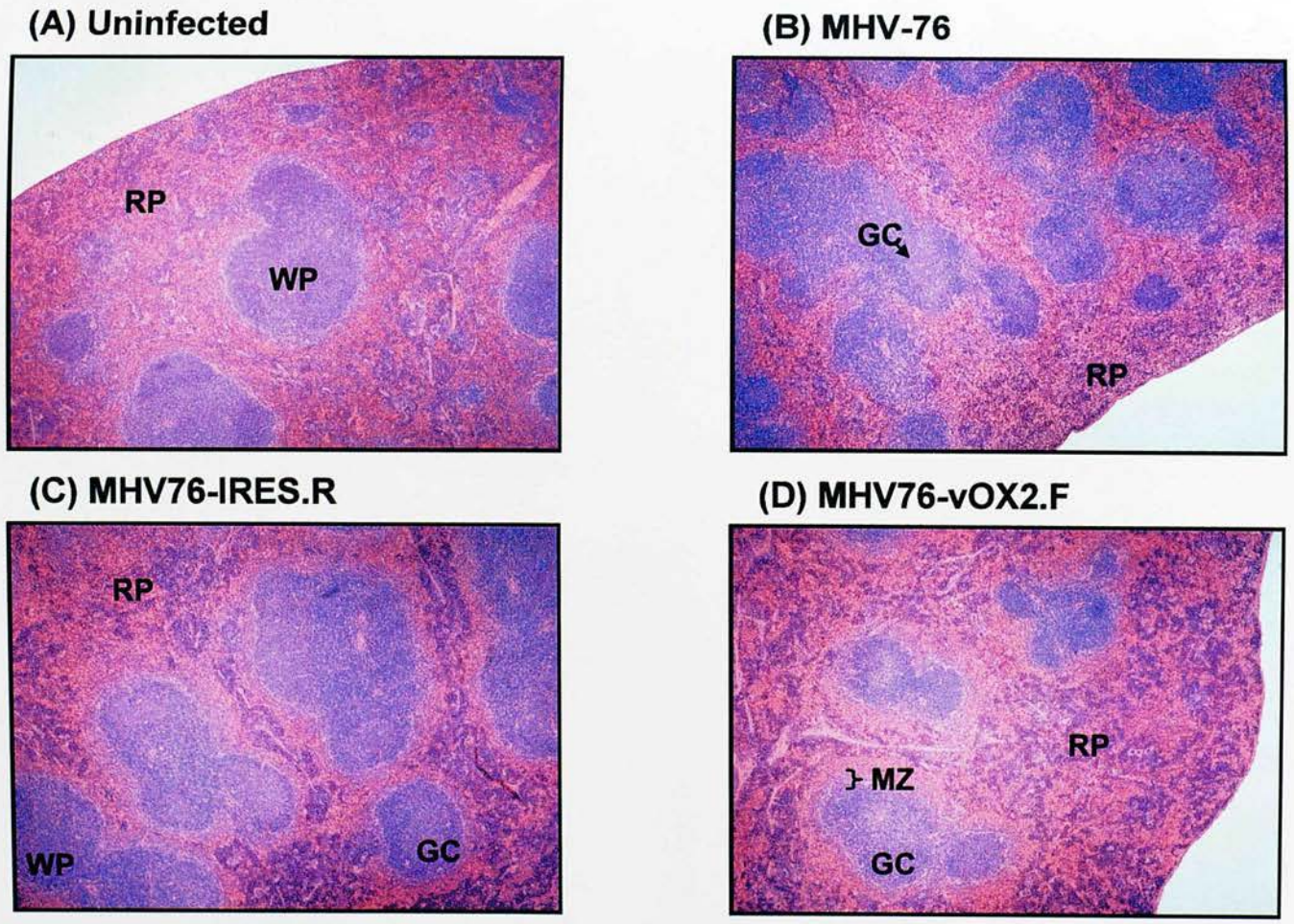

Figure 5.9 Histopathological changes in the spleen. Images of spleen samples (A) uninfected, and infected with (B) MHV-76, (C) MHV76-IRES.R, and (D) MHV76-vOX2.F, 14 days post-infection. Sections are stained with haematoxylin and eosin (Abbreviations : **GC**- germinal center; **MZ**- marginal zone; **RP**- red pulp; **WP**- white pulp. Original magnification approximately x40).

5.2.2.5 Immuno-fluorescent detection of viruses

Frozen sections of spleen samples from mice infected with MHV-76, MHV76-IRES.R, MHV76-vOX2.F, and MHV76-vOX2.R were observed for the expression of *gfp* and immuno-stained for viral antigens from MHV-76, using a polyclonal MHV-68 antisera, at 5, 10, 14 and 21 days p.i. No *gfp* or other viral antigens were detected in any of the spleen samples at any of the time-points (data not shown). These data therefore indicate that no lytic virus was present. It is not known if the GFP gene would be expressed when the recombinant viruses are in a state of latency.

5.3 Discussion

These sets of experiments have been designed to investigate the pathogenesis, lytic and latent states of infection of BALB/c mice with the recombinant viruses generated in chapter four. Two recombinant viruses were created that incorporated the KSHV vOX2 ORF and selection markers into the left-end of the MHV-76 genome; these viruses were termed MHV76-vOX2.F and MHV76-vOX2.R. In addition, two control recombinant viruses were also generated, MHV76-IRES.F and MHV76-IRES.R. *In vitro* analysis showed that all the recombinant viruses replicated with similar kinetics to the wild-type virus MHV-76. The results described in this chapter detail findings following *in vivo* infection.

Following intranasal infection of laboratory mice, the natural route of infection, MHV-76 productively replicates in the lungs. Virally infected cells, predominately macrophage and dendritic cells, are drained to the lymph nodes where latently infected B cells further disseminate the virus to the spleen. vOX2 recombinant virus (MHV76-vOX2.F or MHV76-vOX2.R) replicated to a 10-100 fold higher level in the lungs of BALB/c mice, when directly compared to the control recombinant virus (MHV76-IRES.R).[†] In addition, in the first experiment MHV76-vOX2.F and MHV76-vOX2.R viral levels were higher than the wild-type virus at day 5; levels were more comparable to MHV-76 in the second experiment, with the

[†] MHV76-IRES.R was used as the control recombinant virus in the first two experiments measuring viral replication in the lung, as MHV76-IRES.F was still being generated. An additional experiment was performed using MHV76-IRES.F to verify it had similar properties *in vivo*. The results did show a similar trend to those seen in experiments 1 and 2.

exception of MHV76-vOX2.F on day 7, which was marginally higher than all other viruses. These data suggest that expression of vOX2 enhances viral replication. At all time-points the control recombinant virus displayed lower viral titres than the wild-type virus. One explanation for this is that the selection marker (Hyg^R-EGFP) is attenuating lytic replication within the lung due to an immune response directed against it. It is possible, therefore that vOX2 compensates for this attenuation and allows even more viral replication to occur, surpassing the titres observed for MHV-76.

Cells infected with recombinant viruses could be directly visualised though the expression of the GFP gene. Frozen lung sections taken from the peak time-point (day 5 p.i.), were fixed in paraformaldehyde and then additionally stained for other viral antigens expressed by MHV-76. These findings reflect the previous results, whereby those mice infected with either MHV76-vOX2.F or MHV76-vOX2.R displayed a greater amount of staining for viral antigens co-localising around foci of *gfp*. These data also support the role of vOX2 in allowing an increase in viral replication.

H&E stained lung sections taken from day 3 reveal a mild degree of inflammation in those mice infected with MHV-76, MHV76-vOX2.F or MHV76-vOX2.R. Samples taken at the same time-point from a MHV76-IRES.R infected lung remain healthy in appearance. Interestingly, all groups exhibit a marked increase in inflammation by day 9, the time-point at which viral titres dropped below detectable levels (Figure 5.1B). This could be the point at which any growth advantage provided by vOX2, is overcome by the immune response. This is visible through the increased amount of perivascular, peribronchial and interstitial lymphoid infiltration, which is most evident in mice infected with either MHV76-vOX2.F or MHV76-vOX2.R.

As an additional reassurance that the recombinant viruses possessing vOX2 were infecting the lung, samples of DNA and RNA were simultaneously isolated. Mice infected with MHV76-vOX2.F and MHV76-vOX2.R were positive for vOX2 DNA and mRNA transcripts. Other infected mice were also deemed positive for the presence of viral DNA and mRNA transcripts, i.e. wild-type and control recombinant virus.

In summary, these experiments have shown that the expression of vOX2 enhances viral replication within the lung. It is possible that vOX2 interacts with CD200R expressed on macrophage, resulting in the re-direction, down-regulation or suppression of activation of these cells. This could be the result of inhibiting cytokine production. *In vitro* studies have found that the interaction of a soluble recombinant vOX2 protein with the CD200R resulted in restricting local macrophage activation by inhibiting TNF-α production (Foster-Cuevas *et al.*, 2004). Therefore one could envisage that this temporary suppression of the immune system has provided these recombinant viruses with an advantage allowing more viruses to replicate prior to clearance; this is apparent as data shows productive viral titres to be higher at the early time-points (days 3 to 7 p.i.). However, it is highly likely that the vOX2 protein is only having a local effect as all viruses are cleared from the lung by 9 days p.i. This is also the time point at which histology sections show a more aggressive immune response. Could this be due to the fact that more virus has been generated in the earlier time-points? Further analysis needs to be performed to confirm these findings.

Attempts were made to study mCD200 expression levels in the lungs from virally infected and uninfected mice. It is not known whether mCD200 expression levels decrease at times of pathogenic infection allowing the tightly regulated macrophage to become activated or migrate to the infected sites. Ideally, areas of infected lung would be compared with the local expression of mCD200, however this was not possible, as mCD200 could not be detected in the lung of either infected or uninfected samples by immunostaining. Attempts were also made to use immunostaining to detect macrophage (F4/80) and compare this with infected areas of the lung, but this too was not successful. Further optimisation and an alternative preparation method, such as paraffin fixed sample may be options for future work, as this would be an interesting experiment once optimised.

Studies performed on the MLN were inconclusive. Attempts were made to measure lytic and latent virus in pooled samples of MLN from infected BALB/c mice, but levels were often below the limits of detection. Additionally, *gfp* expression, from the recombinant viruses, was not detected in frozen sections taken from infected MLN samples.

Conflicting results were obtained when the latent viral loads within the spleen were measured. Initial findings suggested that unlike the wild-type virus MHV-76, the recombinant viruses weren't efficiently establishing latency; this was either due to the virus' inability to re-activate or alternatively, not being trafficked to the spleen. To investigate this further, DNA samples were extracted from spleen samples and analysed for the presence of viral DNA using a highly sensitive technique. This entailed a single round of limiting dilution PCR of a single viral gene, ORF 74, followed by southern blot analysis, where samples were probed for the ORF 74 product (Figure 5.8). Using this method viral DNA was detected in the spleens at early time points (days 5 and 10), but much reduced levels (compared with MHV-76) were found at later time points (days 14 and 21). However, it cannot be determined whether this method is detecting whole virus or partial fragments of DNA, which have been degraded by the immune system. Further evidence of a strong immune response against the recombinant viruses in the spleen is noticeable when studying H&E sections. It appears that all recombinant viruses, including the control virus (MHV76-IRES.R), triggered responses. Therefore, the inability to efficiently establish latency is probably not due to vOX2 but most likely to the Hyg^R-EGFP gene within the insert cassette. Previous studies have also reported problems with the incorporation of selection markers, such as GFP, into MHV-68 recombinant viruses (Clambey *et al.*, 2002; Adler *et al.*, 2000). Investigation on the state of latency was not initially considered to be a priority, primarily because the gene of interest, vOX2, is naturally expressed during lytic replication of KSHV. Further studies could be performed on a recombinant MHV-76 virus generated without the Hyg^R-EGFP selection marker, or alternatively, infection via the intra-peritoneal cavity; past studies have suggested that this route of infection may effect the establishment of latency and reactivation (Clambey *et al.*, 2000).

To summarise these findings, the incorporation of the vOX2 ORF into MHV-76 enhances viral replication in the lung. This is likely to be the result of the expression of vOX2 suppressing local macrophage activation or re-directing their migration. This has allowed a greater number of recombinant viruses to replicate before clearance by the immune system.

Chapter Six: CD200 Knock-Out Animal Studies using C57BL/6 Mice

Chapter 6: CD200 knock-out *in vivo* studies using C57BL/6 mice

It was throughout the duration of this research that other groups performed the majority of investigations on both the cellular and murine CD200 homologues. Before this time, information was very limited and it was only in 2000 that the CD200-receptor (CD200R) was identified (Wright *et al.*, 2000). Later in 2003, Wright *et al.*, discovered that the human CD200 (hCD200) protein was not only able to interact with the human CD200-receptor (hCD200R) but also with the murine and rat receptors, mCD200R and rCD200R. More recently the viral homologue (vOX2) has also been found to bind to hCD200R with virtually identical kinetics to the hCD200:hCD200R interaction (Foster-Cuevas *et al.*, 2004).

The role of mCD200 in the control of myeloid-derived cells, has been revealed through the use of transgenic mice. In 2000, Professor Neil Barclay's group at Oxford University, along with DNAX Research Institute of Molecular and Cellular Biology in California generated CD200 gene-targeted mice using C57BL/6 embryonic stem cells[f], referred to as CD200$^{-/-}$ mice. These mice were normal in all aspects of behaviour, appearance, life-span and breeding, with the exception of harbouring increased levels of macrophages and granulocytes. Initial experiments mimicking autoimmune encephalomyelitis (EAE) and arthritis (CIA) in these knock-out mice, verified an important immuno-regulatory role between CD200 and its receptor (Hoek *et al.*, 2000).

Following the kind donation of several mating pairs of these CD200$^{-/-}$ mice by Professor Neil Barclay, further studies could be performed combining infection of these transgenic mice with recombinant viruses possessing a viral homologue of the knocked-out gene. However, prior to these experiments, all procedures first needed to be performed on wild-type mice from the same genetic background, i.e. C57BL/6$^{(+/+)}$.

In both sets of experiments, groups of mice (wild-type C57BL/6$^{(+/+)}$ or CD200$^{(-/-)}$ C57BL/6) were sex and age (4-7 weeks old) matched as best as possible,

[f] The *Nco*I fragment (within the V-like Ig domain) was replaced with a PGK-neo^{R} cassette and used to generate a C57BL/6 CD200$^{-/-}$ breeding colony. Supplementary details can be found in the paper by Hoek *et al.*, 2000.

into groups that were infected with $4x10^5$ PFU of either MHV-76, MHV76-vOX2.F or MHV76-IRES.F. Groups of wild-type mice consisted of four mice per virus. In the first experiment using the CD200$^{-/-}$ mice groups were made up of three mice (data not shown) and six in the follow-up experiment. Lung samples were measured for levels of productive virus (see 2.8.4) and analysed for pathogenesis.

6.1 Productive viral titres in wild-type C57BL/6$^{(+/+)}$

Initial observations of productive viral titres in the lungs of wild-type C57BL/6$^{(+/+)}$ indicated a similar trend to that depicted in the BALB/c mice (Figure 6.1A); peak infection was observed on day 5 p.i. and all viruses were cleared by day 9 p.i. (data not shown for day 9). Detailed analysis of the plots (Figure 6.1B) show equal amounts of all viruses at day 3, with marginally lower levels of MHV76-IRES.F on days 5 and 7 when compared with MHV-76 and MHV76-vOX2.F. There is no significant difference between viral titres of MHV76-IRES.F and MHV76-vOX2.F at any time point.

6.2 Productive viral titres in CD200$^{-/-}$ C57BL/6 mice

The initial experiment using the CD200$^{-/-}$ mice, involved measuring productive virus levels in the lung of mice infected with either MHV76-IRES.F or MHV76-vOX2.F. Only three mice were examined at days 3, 5 and 7 p.i. (data not shown). A similar trend, with a peak at day 5 was observed, however as on days 3 and 7 p.i. two of the three mice were below the limit of detection no conclusive results could be derived. This same experiment was repeated using six mice per time-point per virus, and mice were infected with MHV-76, MHV76-IRES.F or MHV76-vOX2.F.

The viral titres in the lung from days 3, 5 and 7 p.i. are illustrated in Figure 6.2A with the same trend observed (titres peaking 5 days p.i.). However, in contrast with all previous experiments, the average viral titre of mice infected with MHV76-IRES.F surpassed those levels measured in mice infected with MHV76-vOX2.F at all time-points, with the difference on day 5 being statistically significant ($p<0.001$). Detailed plots show tight clusters (Figure 6.2B) and the most prominent difference between the two recombinant viruses is visible 5 days p.i.

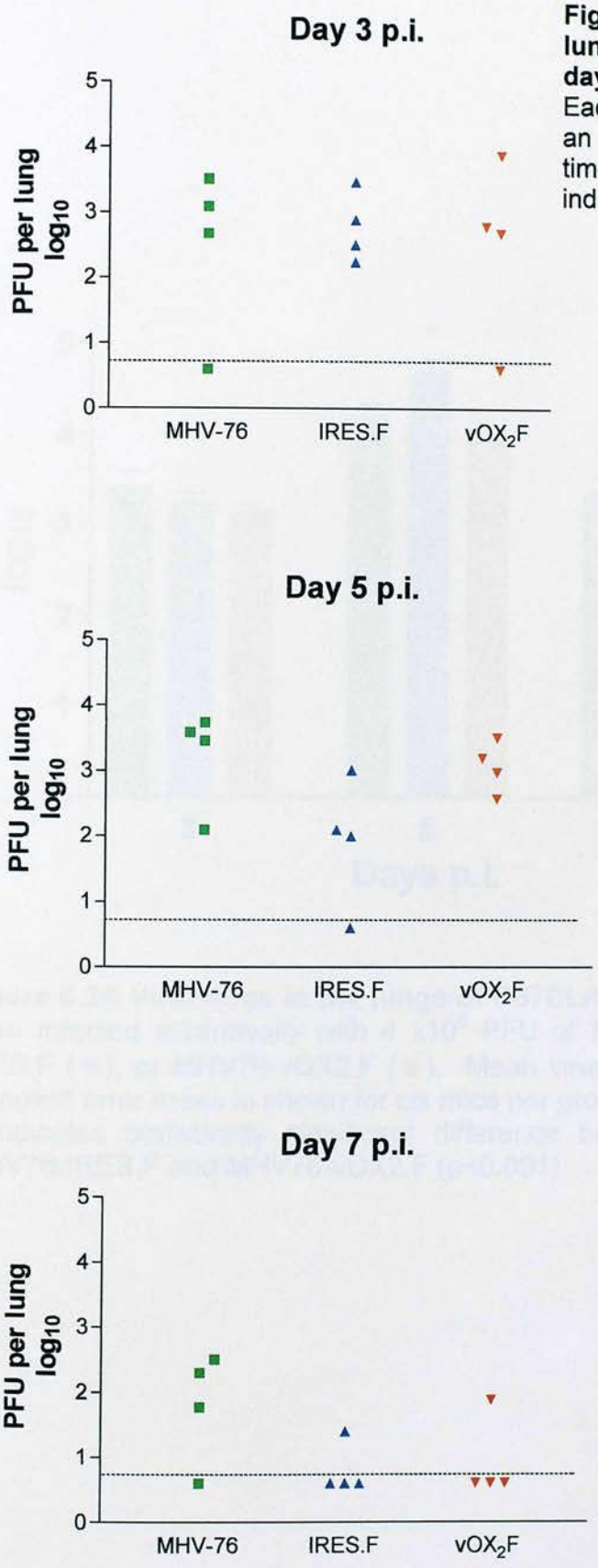

Figure 6.1B Detailed plot of lung titres in C57BL/6 mice at days 3, 5 and 7 post-infection. Each point is representative for an individual mouse at each time-point. Dashed line (---) indicates the limit of detection.

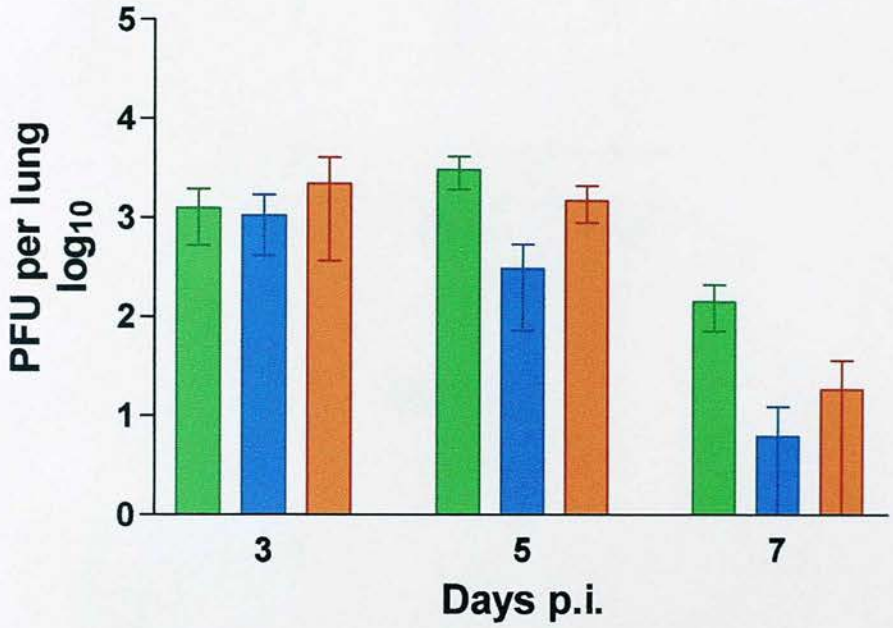

Figure 6.1A Viral titres in the lungs of C57BL/6 mice (wild-type). Mice were infected intranasally with 4 x10^5 PFU of MHV-76 (■), MHV76-IRES.F (■), or MHV76-vOX2.F (■). Mean virus titre log_{10} per lung ± standard error mean is shown for four mice per group for each time point.

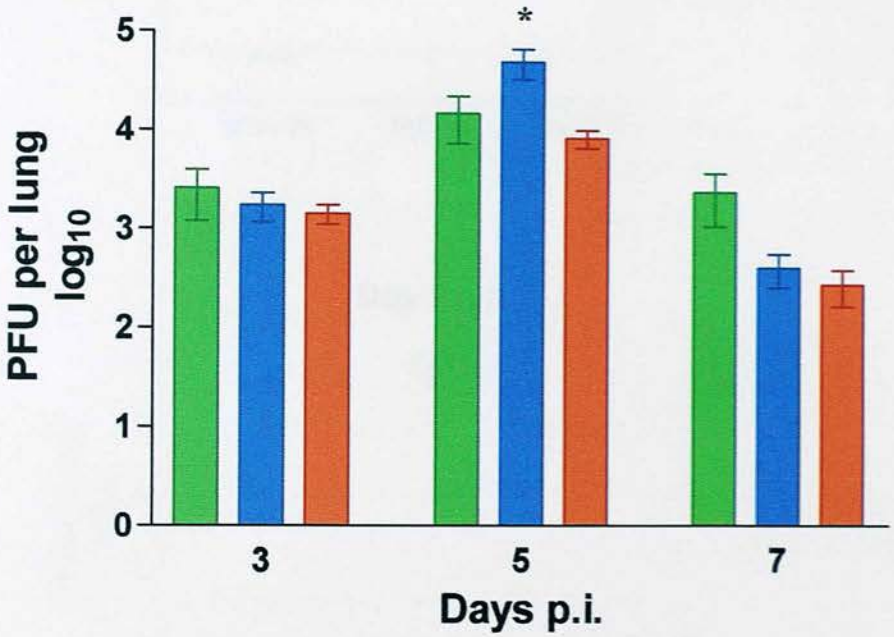

Figure 6.2A Viral titres in the lungs of C57BL/6 CD200$^{-/-}$ mice. Mice were infected intranasally with 4 x10^5 PFU of MHV-76 (■), MHV76-IRES.F (■), or MHV76-vOX2.F (■). Mean virus titre log_{10} per lung ± standard error mean is shown for six mice per group for each time point. * indicates statistically significant difference between viral titres of MHV76-IRES.F and MHV76-vOX2.F ($p<0.001$)

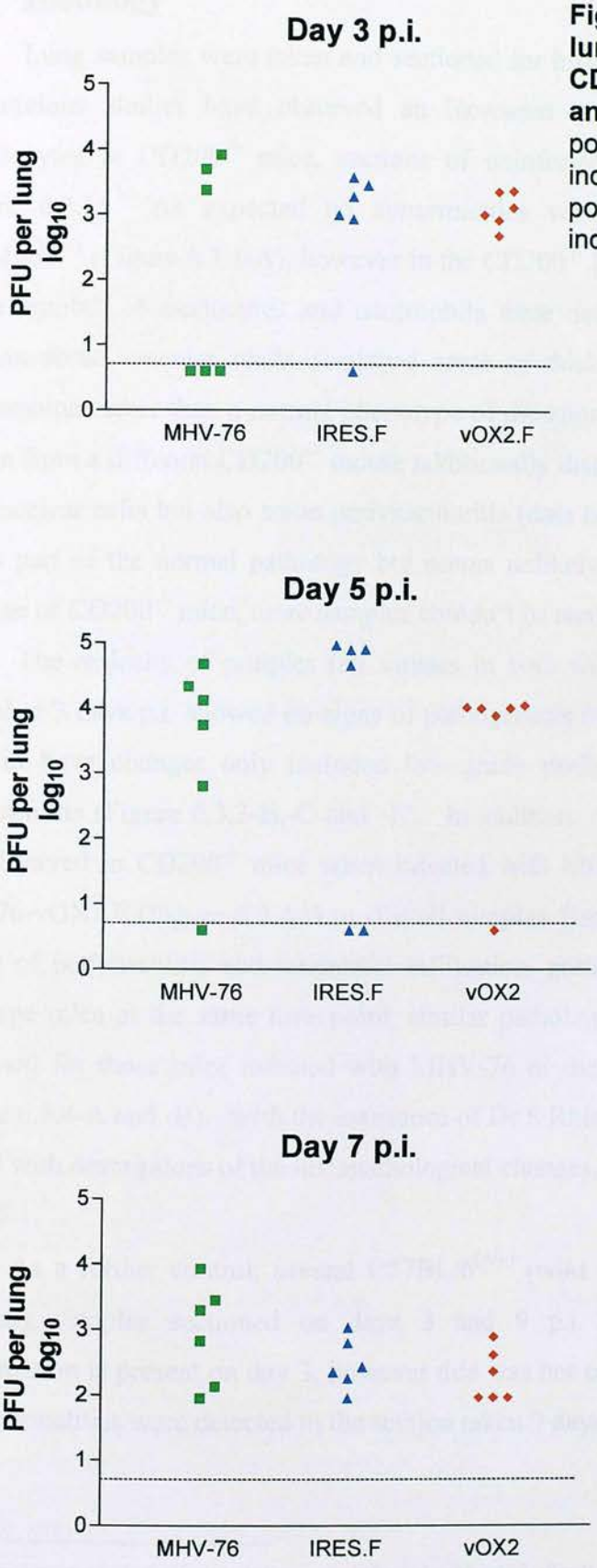

Figure 6.2B Detailed plot of lung titres in C57BL/6 CD200$^{-/-}$ mice at days 3, 5 and 7 post-infection. Each point is representative for an individual mouse at each time-point. Dashed line (---) indicates the limit of detection.

6.3 Histology

Lung samples were taken and sectioned for histological analysis (see 2.8.8). As previous studies have observed an increased number of macrophages and granulocytes in CD200$^{-/-}$ mice, sections of uninfected lungs were first assessed (Figure 6.3.1). As expected no abnormalities was detected in the wild-type C57BL/6$^{(+/+)}$ (Figure 6.3.1-A), however in the CD200$^{-/-}$ lung section a slight increase in the number of monocytes and neutrophils were detected (Figure 6.3.1-B). In addition some vascular walls displayed areas of thickening; this may be due to hypertension rather than a normal phenotype of the knock-out mouse. Another lung section from a different CD200$^{-/-}$ mouse additionally displayed increased numbers of mononuclear cells but also some perivascularitis (data not shown). It is not clear if this is part of the normal pathology but seems unlikely. Unfortunately due to the shortage of CD200$^{-/-}$ mice, more samples couldn't be analysed.

The majority of samples (all viruses in both wild-type and CD200$^{-/-}$ mice) viewed at 3 days p.i. showed no signs of pathogenesis (Figure 6.3.3); those samples that did have changes only included low grade peribronchial inflammation and perivasculitis (Figure 6.3.3-B,-C and -E). In addition, on day 9 p.i. little variation was observed in CD200$^{-/-}$ mice when infected with MHV-76, MHV76-IRES.F, or MHV76-vOX2.F (Figure 6.3.4-D to -F); all samples displayed a moderate to severe degree of perivasculitis and interstitial infiltration, particularly monocytes. In the wild-type mice at the same time-point, similar pathology was evident, but slightly decreased for those mice infected with MHV-76 or the control recombinant virus (Figure 6.3.4-A and -B). With the assistance of Dr S Rhind, these sections have been graded with descriptions of the histopathological changes, the data are summarised in Table 6.1.

As a further control, several C57BL/6$^{(+/+)}$ (wild type) were mock infected[f] and lung samples sectioned on days 3 and 9 p.i. Very mild perivascular inflammation is present on day 3, however this was not considered to be significant. No abnormalities were detected in the section taken 9 days p.i. (Figure 6.3.2).

[f] In replacement of viral aliquots mice were infected with 40µl of cell (BHK-21) lysate (prepared in the same method as virus samples).

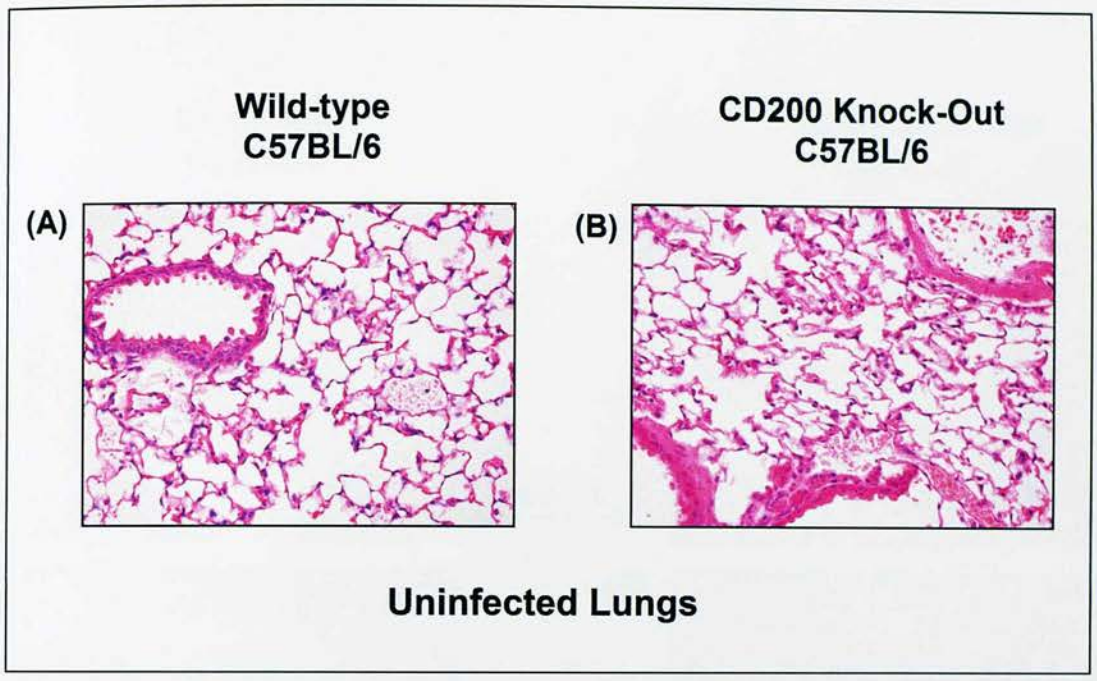

Figure 6.3.1 Histology section of uninfected lungs from the wild-type and CD200$^{-/-}$ C57BL/6 mice. Lung sections were stained with haematoxylin and eosin (Images original magnification at x250).

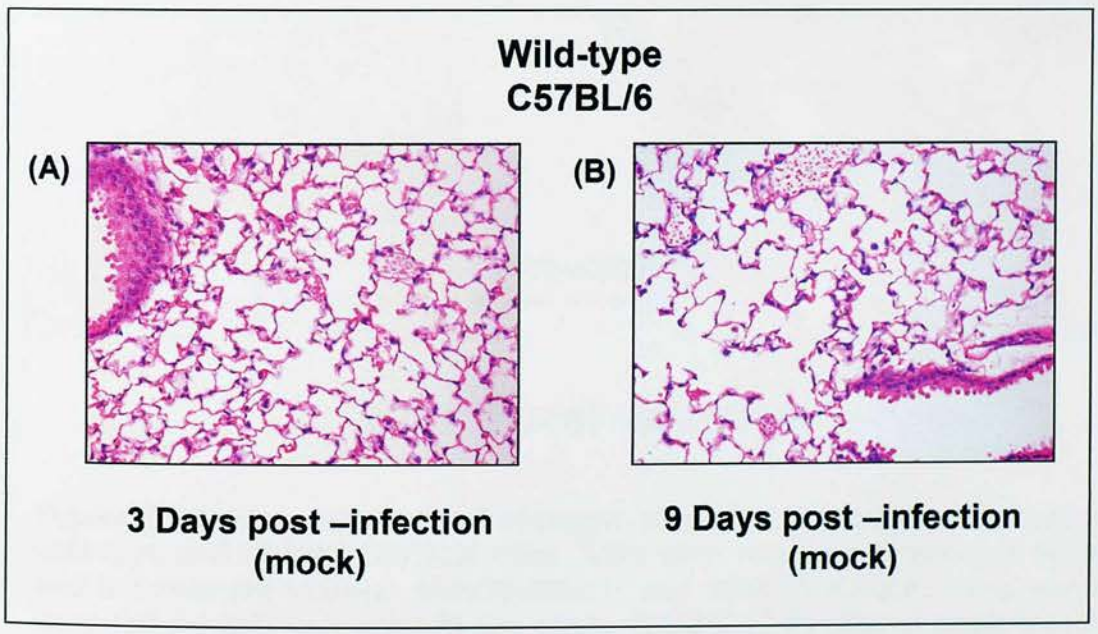

Figure 6.3.2 Histology section of mock-infected lungs 3 and 9 days post-infection from the wild-type C57BL/6 mice. Mice were infected with diluted BHK-21 cell lysate. Lung sections were stained with haematoxylin and eosin (Images original magnification at x250).

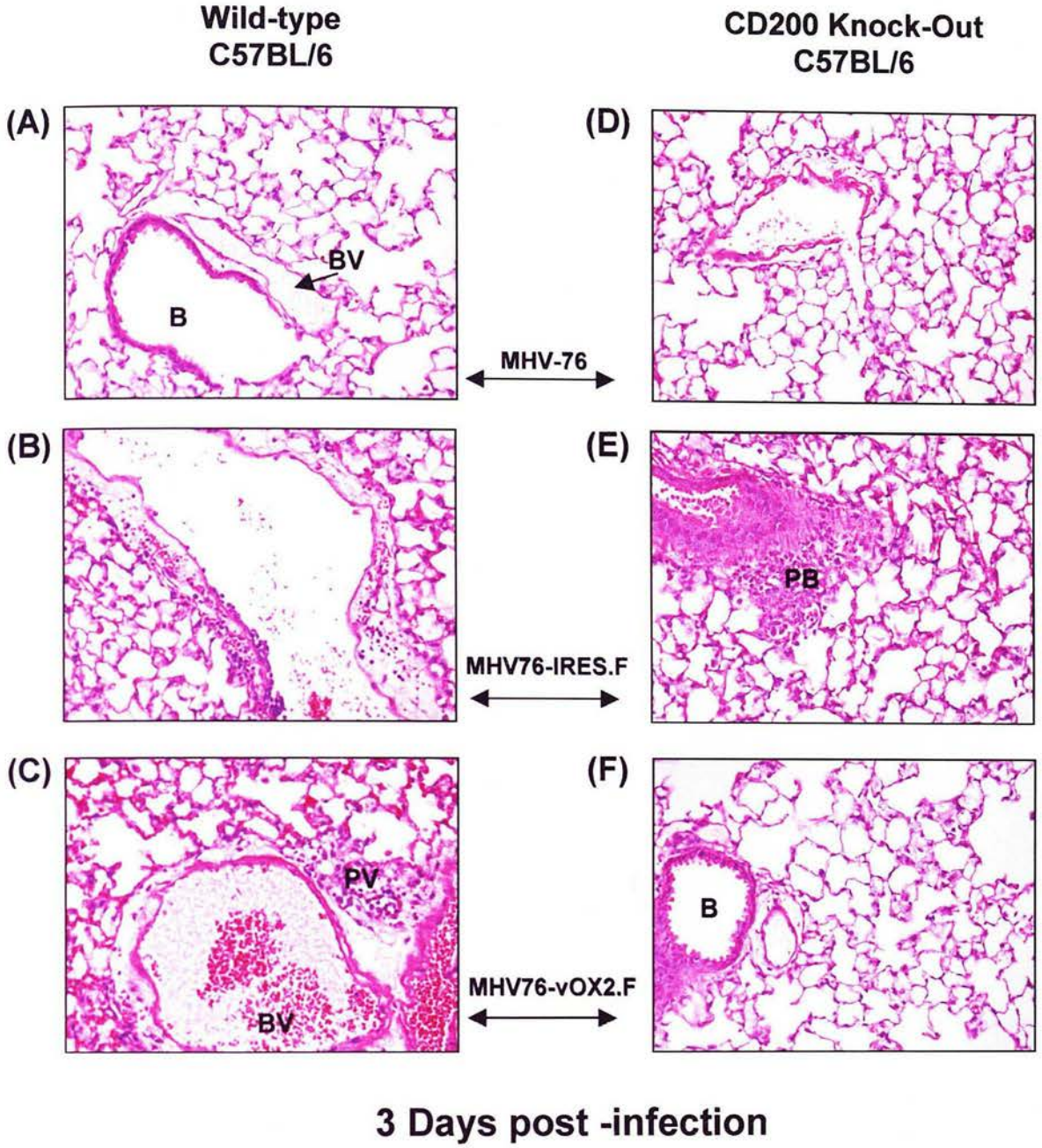

Figure 6.3.3 Histopathological changes observed 3 days post-infection in wild-type and CD200$^{-/-}$ C57BL/6 mice. Mice were infected with wild-type MHV-76 and recombinant viruses, MHV76-IRES.F and MHV76-vOX2.F. Lung sections were stained with haematoxylin and eosin (Images (A-F) original magnification at x250; Abbreviations: **B**- bronchial; **BV**- blood vessel; **PB**- peri-bronchial inflammation; **PV**- perivascular inflammation).

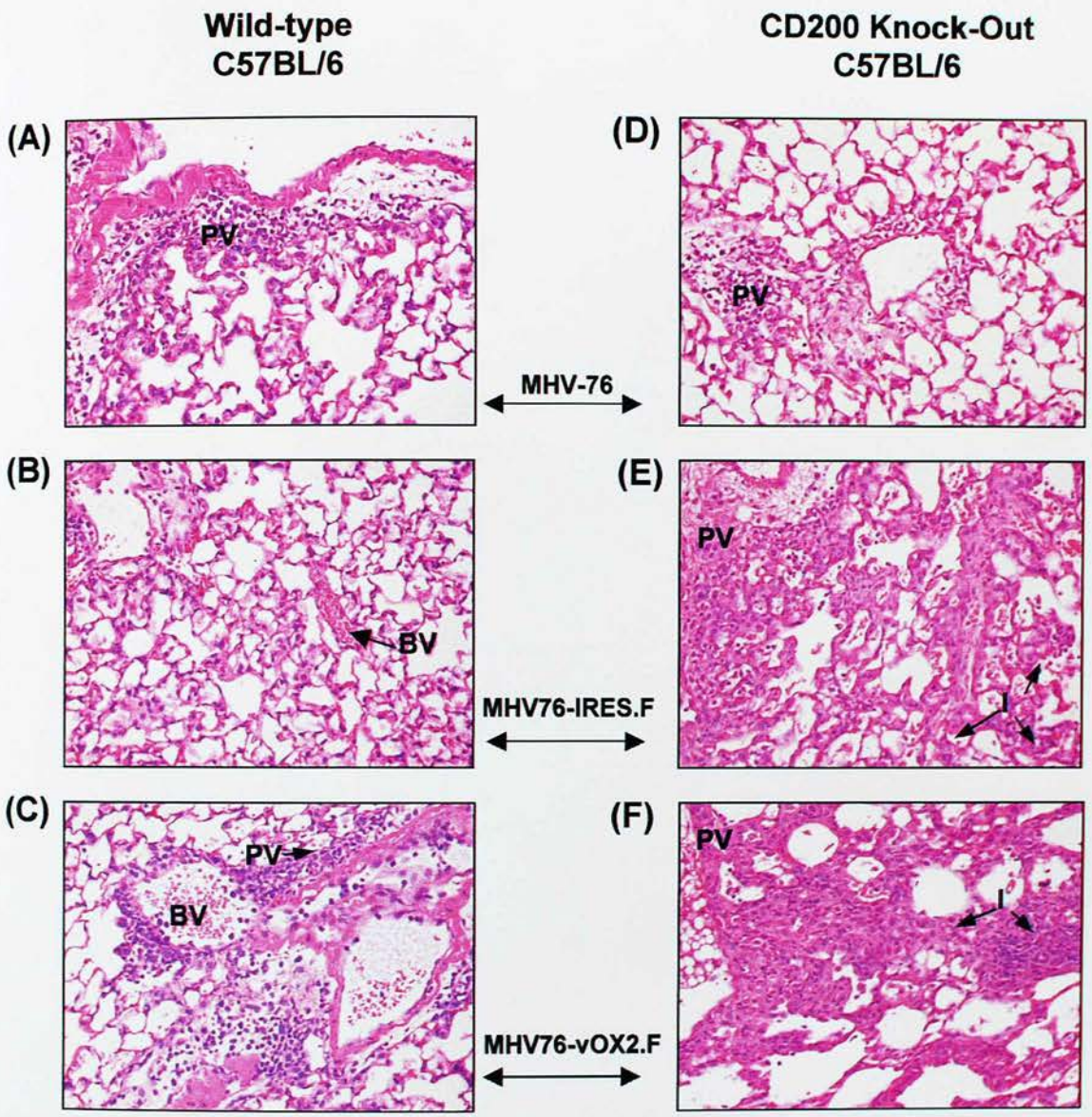

Figure 6.3.4 Histopathological changes observed 9 days post-infection in wild-type and CD200$^{-/-}$ C57BL/6 mice. Mice were infected with wild-type MHV-76 and recombinant viruses, MHV76-IRES.F and MHV76-vOX2.F. Lung sections were stained with haematoxylin and eosin (Images (A-F) original magnification at x250; Abbreviations: **BV**- blood vessel; **I**- interstitial infiltration; **PB**- peri-bronchial inflammation; **PV**- perivascular inflammation).

Table 6.1 Summary of histopathological changes observed in wild-type and CD200$^{-/-}$ C57BL/6 mouse lung sections three and nine days post-infection with MHV-76, MHV76-IRES.F or MHV76-vOX2.F.

	DAY 3		DAY 9	
	Wild-type C57BL/6	**Knock-out** CD200$^{-/-}$ C57BL/6	**Wild-type** C57BL/6	**Knock-out** CD200$^{-/-}$ C57BL/6
MHV-76	no abnormalities detected	no abnormalities detected	perivasculitis, focal interstitial infiltrates (mononuclear) ++	perivasculitis, focal interstitial infiltrates ++
MHV76-IRES.F	low grade peribronchial inflammation, perivasculitis +/++	low grade peribronchial inflammation, perivasculitis around large vessels +	mild perivasculitis, focal interstitial infiltrates ++	perivasculitis, extensive areas of interstitial infiltrates +++
MHV76-vOX2.F	v.mild perivasculitis, occasional foci of interstitial inflammation -/+	no abnormalities detected	perivasculitis, focal interstitial infiltrates +++	perivasculitis, extensive areas of interstitial infiltrates +++

*Sections have been graded by Dr S Rhind; grading varies between no abnormalities (-) to +++ (most severe) as observed within these group of samples.

6.4 Expression of mCD200 and mCD200R (RT-PCT)

Samples of mRNA were isolated from the blood (PBMCs), liver, lung, spleen and MLN from both the wild-type and CD200$^{-/-}$ C57BL/6 mice to study expression levels of the mCD200R and mCD200 genes in the transgenic mice. The SIGMA messenger RNA micro isolation kit (see 2.5.1.2) was utilised for the direct isolation of mRNA from the above-mentioned samples. Following the generation of cDNA by use of the Invitrogen Thermoscript RT-PCR system (used oligo(dT) primers; see 2.5.3) and degradation of DNA (see 2.5.2), cDNA (3µl) was amplified for mCD200, mCD200R and GAPDH, as a positive control (Primers used: mCD200= mCD200-5'+mCD200-3'; mCD200R= mCD200R-5'+mCD200R-3'; GAPDH= GAPDH-1 +GAPDH-2; see Appendix 2). Photographs of the amplified products are shown in Figure 6.4. In the wild-type mice, with the exception of the MLN sample, where the GAPDH control PCR indicated there were low levels of substrate, all other samples were positive for both mCD200 and mCD200R. In contrast, the CD200$^{-/-}$ mice samples were all negative for mCD200 and positive for mCD200R, most at levels similar to the wild-type mice. mCD200R levels are slightly higher in the CD200$^{-/-}$ PBMC sample.

As an additional control, samples of DNase treated mRNA were directly amplified using the same GAPDH primers to ensure no residual DNA was present; no amplification was detected in any of the samples.

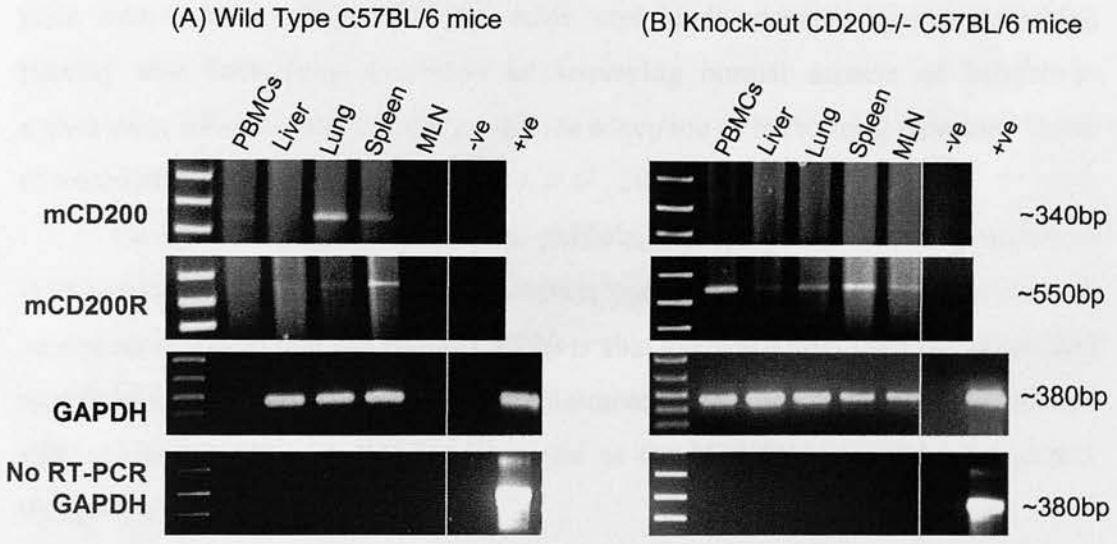

Figure 6.4 Amplification of mRNA extracted from organ samples taken from wild-type and CD200$^{-/-}$ C57BL/6 mice. mRNA samples were extracted from fresh samples of PBMCs, liver, lung, spleen and MLN taken from both the (A) wild-type and (B) CD200$^{-/-}$ knock-out C57BL/6 mice. Once mRNA was isolated, cDNA was generated and used in RT-PCR using primers for the generation of mCD200, mCD200R and GAPDH. Samples of mRNA were directly amplified using the GAPDH primers to ensure no DNA was present. Amplified products were analysed on a 1.5% agarose gel and ran with a 1Kb+ DNA molecular weight marker (on left hand end). All reactions included the use of dH_20 as a negative control (-ve) and genomic DNA as a positive control (+ve) in both GAPDH reactions.

6.5 Discussion

Previous *in vivo* studies (chapter 5) have implied that vOX2 may be responsible for assisting in evading the immune response and enhancing viral replication during acute infection in the lung. To further investigate the role of vOX2 and the possible pathway utilised to gain this advantage, CD200$^{-/-}$ transgenic mice were used. These CD200$^{-/-}$ mice were kindly donated by Professor Neil Barclay and have been described as displaying normal aspects of behaviour, appearance, life-span and breeding, with the exception of harbouring increased levels of macrophages and granulocytes (Hoek *et al.*, 2000).

To date there has been no data published studying the direct interaction of vOX2 with the mouse CD200R. However, one could assume this is possible, as studies have shown that the human CD200 is able to engage with both the mouse and rat CD200R (Wright *et al.*, 2003). Furthermore, vOX2 has been found to interact with the hCD200R with the same kinetics as the hCD200:hCD200R engagement (Foster-Cuveas *et al.*, 2004).

The current belief is that CD200 is able to govern the local macrophage population through the direct cell surface engagement via the CD200-receptor. Thus in mice lacking the CD200 gene (CD200$^{-/-}$ knock-out), an increased number of activated macrophages are seen. This poses the question, is vOX2 able to replace the missing endogenous CD200 and mimic a regulatory control on the local macrophage population? The experiments performed in this chapter were aimed at answering this question.

Before proceeding with studies using the CD200$^{-/-}$ mice, viral titres were first measured in the lung from the wild-type strain of C57BL/6 mice. This experiment is a repeat of those previously performed in BALB/c mice (see 5.1.1). One immediate difference noticeable is the overall decrease in viral titres; the average value is approximately 100-fold lower in C57BL/6 mice compared with those measured in BALB/c mice. Differences in immune response and susceptibility to MHV-68 infection in C57BL/6 and BALB/c mice has previously been reported (Weinberg *et al.*, 2004). As the overall values were lower and group size relatively low, comparison between the groups was difficult. The wild-type mice infected with vOX2-recombinant virus (MHV76-vOX2.F) yield marginally higher titres than those

infected with the control recombinant virus (MHV76-IRES.F), but these were not statistically significant. A trend similar to previous *in vivo* studies was observed whereby the lung titres of the majority of viruses peak 5 days p.i. This trend was also visible in the CD200$^{-/-}$ mice. Differences in the MHV76-vOX2.F and MHV76-IRES.F viral titres were negligible on days 3 and 7, in the CD200$^{-/-}$ mice. Whereas on day 5, viral titres were significantly higher for the control recombinant virus compared to the virus containing vOX2 ($p<0.001$).

As previous studies (Hoek *et al.*, 2000; Broderick *et al.*, 2002) have reported an increase number of macrophages in the CD200$^{-/-}$ mice, uninfected lungs sections were examined. Histological examinations of the lung sections confirmed a slight increase in the number of macrophages in the CD200$^{-/-}$ mice compared to the wild-type C57BL/6 mice. In addition, the lungs from mock-infected C57BL/6 mice[ƒ] were examined on days 3 and 9 p.i.; a very mild inflammatory response was detected in some sites 3 days p.i., however no abnormalities were detected 9 days p.i. Thus confirming that any pathogenesis seen in virally infected samples is likely to be the direct result of the virus and not the preparation media.

The pathology observed in the lung histology sections on days 3 and 9 p.i. is reflected in the viral titres[†]. A summary of these findings is outlined in Table 6.1. After 3 days p.i. most samples show little if any evidence of inflammation, however on day 9 all samples in both the wild-type and knock-out mice show greater areas of perivasculitis and monocyte infiltration within the interstitial regions. Wild-type mice infected with MHV76-vOX2.F displayed a more severe immune response than those mice infected with MHV-76 or MHV76-IRES.F (9 days p.i.). However, due to the limitation on the number of mice available, only one lung sample per time point per virus was studied, therefore making it difficult to determine if these images represent normal statistical variation of the phenotype or a genuine inter-group difference.

[ƒ] C57BL/6 mice were infected with a preparation of cell (BHK-21) lysate made in the same manner as all virus samples. CD200$^{-/-}$ knock-out mice were not mock-infected due to a limitation on the number of mice available.

[†] Based on the previous findings in BALB/c mice (see Chapter 5) and due to the limited number of CD200$^{-/-}$ mice available, histological samples were only taken at the most extreme time-points, days 3 and 9 post-infection.

Unfortunately these data have not been able to confirm the role of vOX2 and the complexity of the CD200$^{-/-}$ mice phenotype, i.e. increased number of macrophages, complicates analysis of the results. However, several scenarios could exist.

- ***Scenario A***

In the event that vOX2 is not able to engage with the mCD200R, viral titres in the CD200$^{-/-}$ mice should either be identical to those seen in the wild-type mice, or an across the board decrease in viral titres (for all viruses) should be observed, resulting from rapid clearance by the more abundant macrophages.

- ***Scenario B***

Assuming vOX2 is able to engage with the mCD200R and down-regulate or re-direct locally activated macrophage, this would allow increased viral replication and be reflected in higher viral titres and perhaps less evidence of inflammation at the earlier time-points.

- ***Scenario C***

Again, assuming vOX2 is able to engage with the mCD200R and down-regulate or re-direct locally activated macrophage, the increased number of macrophages present at the initial stages of acute infection could negate the advantage vOX2 provides during viral replication. This would be reflected by the viral titres of MHV76-vOX2.F dropping to the levels of MHV76-IRES.F and the generation of an immune response also more similar to the control recombinant virus.

Due to the large number of varying factors, arriving at a conclusion from these results is difficult. However, scenario A can be excluded as a possibility as the trend observed in the wild-type mice is not the same in the CD200$^{-/-}$ mice. In the CD200$^{-/-}$ mice, the viral titres of the MHV76-vOX2.F are equal or lower than the control recombinant virus, MHV76-IRES.F. Furthermore, scenario B is also unlikely. In the CD200$^{-/-}$ mice, viral titres are not higher for the vOX2- recombinant

virus and the degree of inflammation in the histological samples is comparable with that seen in the wild-type mice.

From these limited results it seems likely that these data reflect scenario C, i.e. in the wild-type mice, expression of vOX2 provided a small advantage during viral replication but this is lost in the CD200$^{-/-}$ mice. Higher titres of productive virus, particularly on day 5, and a more severe inflammatory response observed in the histological section are seen in those wild-type mice infected with the vOX2 recombinant virus. However, in the CD200$^{-/-}$ mice, the vOX2-recombinant viruses have lost the advantage gained through the expression of vOX2. This is most likely due to the vast number of activated macrophage present at the earlier stages. In the CD200$^{-/-}$ mice the MHV76-vOX2.F titres are lower than the recombinant virus at all time-points measured and both histological samples from the MHV76-vOX2.F and MHV76-IRES.F infected mice were graded with equal severity. These data would suggest that vOX2 (and possibly CD200) is unable to down-regulate previously activated macrophage, but is capable of blocking the activation of unstimulated macrophage. This is reflected in both the viral titres and histopathological samples.

Various tissue samples from wild-type and CD200$^{-/-}$ mice were examined for the expression of mCD200 and mCD200R. As expected, all samples in the CD200$^{-/-}$ mice were negative for mCD200, whereas in the wild-type mice only the spleen, lung, liver and PBMCs tested positive for mCD200. All samples from both the wild-type and CD200$^{-/-}$ mice were positive for mCD200R with similar low expression levels, with the exception of the wild-type MLN sample, which obviously had lower levels of RNA to start with (this is evident by the faint GAPDH band yielded compared with the other samples). This experiment was performed to investigate whether expression levels of mCD200R varied between the wild-type and CD200$^{-/-}$ mice, and from these preliminary findings most samples seem to be expressing similar levels. However, the PBMC sample from the CD200$^{-/-}$ mice does appear to be slightly more intense compared with the other samples; this may be due to the increased numbers of circulating macrophage. Further investigation using a more sensitive method such as immuno-histochemistry staining or reverse-transcriptase real time PCR would need to be performed to confirm any conclusions.

In summary, these data imply that in the CD200$^{-/-}$ mice, recombinant viruses encoding the vOX2 ORF have lost the ability to enhance viral replication previously seen during infection of wild-type mice. This is most likely a result of the phenotype of these CD200$^{-/-}$ mice, which harbour increased numbers of activated macrophages.

Chapter Seven: Conclusions

Chapter 7: Conclusions

The results presented in this thesis demonstrate that the KSHV vOX2 protein is involved in an immunomodulating role. The precise mechanism is not known but it is likely to involve evasion of immune clearance by mimicking the endogenous protein (CD200). It is possible that the vOX2 protein is engaging with the CD200-receptor (CD200R) and either maintaining the down-regulatory signal or re-directing the migration of local CD200R-expressing cells. This would provide an environment whereby the virus could replicate to higher titres.

The vOX2 protein is expressed during lytic KSHV infection and is located on the surface of the cell in the form of an IgSF protein. The protein is highly glycosylated and is structurally similar to other IgSF proteins, containing the common V/C2 set arrangement; the glycosylated extracellular domains are approximately 40kDa in size. Most of these findings are in accord with those published by Chung *et al.* 2002, although their predicted role of vOX2's involvement as a pro-inflammatory signal, differs to the findings reported here.

Primarily due to the restricted host range of KSHV, studies on the closely related murid herpesviruses have been undertaken to better understand the pathogenesis of many human herpesviruses. One virus in particular that has been studied in depth because of its similarities in pathogenesis to human gamma-herpesviruses is the murine gammaherpesvirus-68 (MHV-68). Furthermore, a natural deletion mutant of this virus, MHV-76, has provided an opportunity to generate recombinant murine gammaherpesviruses to aid in the study of unique genes. The KSHV vOX2 ORF and selection markers (Hyg^R-EGFP) were expressed in an MHV-76 genomic background to create a novel gain-of-function recombinant virus, MHV76-vOX2. The studies detailed within this thesis not only describe the generation of these recombinant viruses but also the ability of the virus to replicate *in vitro* with similar kinetics to the wild-type virus, MHV-76. In addition, *in vivo* analysis has demonstrated that those recombinant viruses encoding the vOX2 ORF have enhanced viral replication at early times post-infection in the lung. The advantage provided by vOX2 is most likely due to its ability to mimic the host CD200 by maintaining the down-regulatory status of the local macrophage, as illustrated in the diagrams in Figures 7.1 and 7.2.

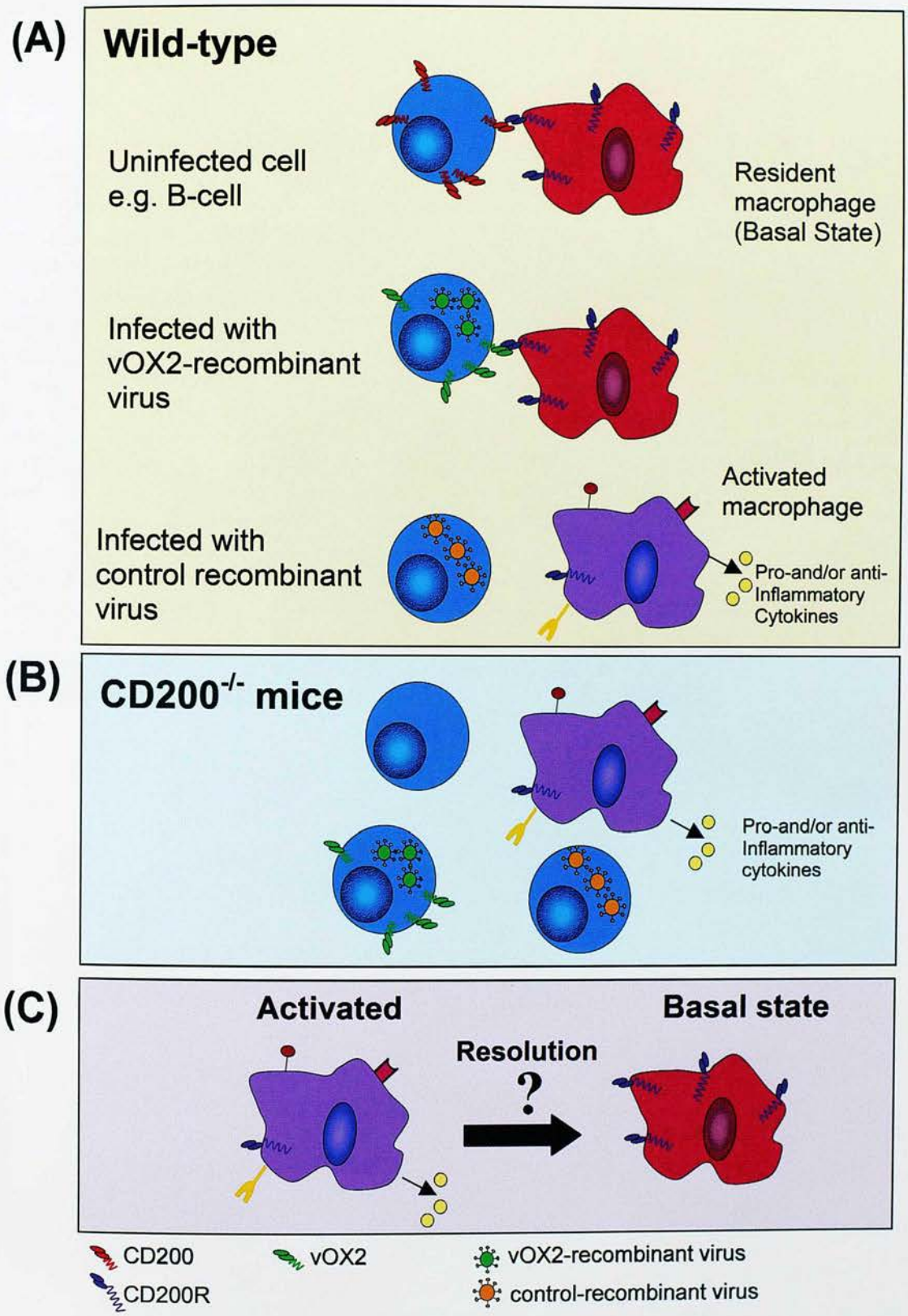

Figure 7.1 Macrophage activation and interaction with virally-infected cells. Detailed legend on following page.

Figure 7.1 Macrophage activation and interaction with virally-infected cells. Resident macrophage populations in different organs such as avelolar macrophages (lung), Kupffer cells (liver) and microglia (CNS) adapt to their local microenvironment and undergo local activation in response to various inflammatory and immune stimuli. (A) Resident macrophage express the CD200R which is able to engage with the CD200 IgSF protein, expressed on the surface of a wide variety of cell types, including B-cells, T-cells, some dendritic cells, neurons, vascular endothelium and some smooth muscle. This engagement is thought to be partly responsible for maintaining the basal state of the local macrophage; we speculate that CD200 expression is down-regulated following viral infection of a cell. It is likely that the viral homologue of the CD200 protein, KSHV vOX2, is also able to interact with the cellular CD200R and in turn maintain the suppressive signal received by the resident macrophage. This does not occur in situations whereby the same cell type (e.g. B-cell) is infected with a different virus, such as the control recombinant virus (i.e. without vOX2). These infected cells trigger the immune response and enhance recruitment of activated macrophage. (B) In $CD200^{-/-}$ mice, the phenotype is different from wild-type mice; the $CD200^{-/-}$ mice have increased numbers of only activated macrophage. (C) At present it is still not clear how the CD200:CD200R engagement is restored upon resolution of infection.

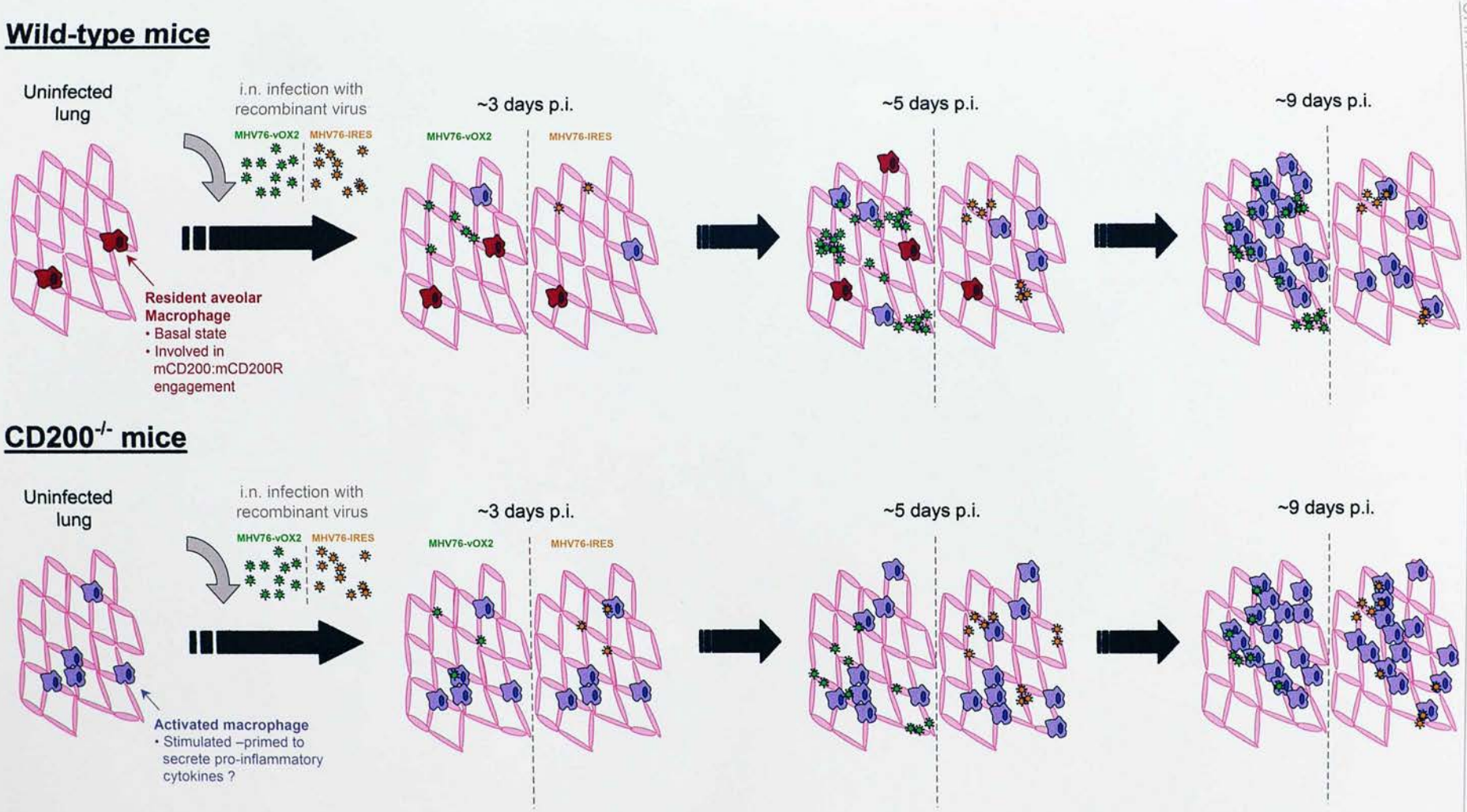

Figure 7.2 Theoretical course of infection and pathogenesis occurring in the lung of wild-type and CD200$^{-/-}$ mice following intranasal inoculation with a MHV-76 recombinant virus encoding the vOX2 ORF or a control recombinant virus. Detailed legend on the following page.

Figure 7.2 Theoretical courses of infection and pathogenesis occurring in the lung of wild-type and CD200$^{-/-}$ mice following intranasal inoculation with a MHV-76 recombinant virus encoding the vOX2 ORF or a control recombinant virus. In the wild-type mice, prior to infection, there are only a limited number of macrophage present. These are commonly known as the resident alveolar macrophage (pink) and are typically in a resting state (unstimulated), partially due to the down-regulatory signal received via the CD200:CD200R interaction. Following infection with a recombinant virus encoding the KSHV vOX2 ORF (a viral homologue of CD200) or a control recombinant virus (i.e. without vOX2), some of the resident macrophage become activated (purple). This results in the secretion of pro-inflammatory cytokines and recruitment of circulating macrophage. However, this is delayed in those mice infected with the vOX2-recombinant virus; the vOX2 protein replaces the down-regulated CD200 and maintains the suppressive signal on the local macrophage via the vOX2:CD200R interaction, thus allowing the virus to survive and replicate. Viral replication peaks at approximately 5 days post-infection for both viruses, although as more of the vOX2-recombinant virus was able to replicate this resulted in a greater influx of macrophages and other inflammatory cells (~9 days p.i.) compared to the control recombinant virus.

The normal phenotype of CD200$^{-/-}$ mice is similar to the wild-type mice with one major difference; all macrophage are in an activated state and more numerous. The vOX2-recombinant virus has no added advantage in this model, as the numbers of macrophages present are too high and already in an activated state; therefore able to recruit more inflammatory cells faster. Both viruses replicate at a similar rate, and both also yield a similar immune response, resulting in inflammation and viral clearance by approximately 9 days post-infection.

It is speculated that once CD200-expressing cells have become infected with a virus, expression of CD200 is down-regulated leading to a loss of the suppressive signal received by the local macrophage. It is the loss of this signal that contributes to the macrophage becoming activated and ultimately recruiting more circulating inflammatory cells. It is likely that vOX2 is compensating for the down-regulated CD200 and delaying the influx of inflammatory cells and allowing the virus to replicate to higher titres. These higher viral titres ultimately lead to an increased inflammatory response (see Figure 7.2). Preliminary *in vivo* studies using $CD200^{-/-}$ mice further supported this theory, as the enhanced viral replication gained by the vOX2-recombinant virus is lost. This was possibly due to the increased number of activated macrophages present from the initial point of infection, resulting in a more rapid clearance of the virus. Further studies regarding both CD200 and CD200R expression patterns during viral infection would not only greatly assist in understanding the control mechanism of macrophage but also the immunomodulating role of vOX2. Additionally, if CD200 and vOX2 have the ability to maintain the basal state of local macrophage, how is resolution restored? (see Figure 7.1). The process by which this occurs is still unknown, however the identification of the CD200 protein and its receptor is still very recent and there are still many aspects relating to their interaction that need to be investigated.

As our understanding of the control of macrophage via the CD200:CD200R interaction has increased, so has the importance of viral homologues of the CD200 protein. As mentioned earlier, a variety of viruses encode a homologue of CD200, seemingly picked-up during viral evolution and aiding in viral fitness. The results within this thesis further support the theory that the KSHV vOX2 protein plays an immunomodulating role by evading immune clearance and ultimately assisting in viral pathogenesis, a theory similarly presented by Foster-Cuveas *et al.*, 2004.

The precise involvement of macrophages in KSHV pathogenesis is not fully understood. However, like MHV-68, KSHV is able to infect macrophage and may use this as for viral dissemination (Blasig *et al.*, 1997; Cornali *et al.*, 1996). Furthermore, macrophages may play a more pivotal role in the formation of KS lesions. KS is a highly angioproliferative disease requiring inflammatory cytokines for the formation of the lesions. In particular the infiltration of $CD8^{+}$ T cells and

$CD14^+/CD68^+$ monocytes-macrophages producing high levels of γ-interferon (γIFN) further promote the formation of KS spindle cells with angiogenic phenotypes (Fiorelli *et al.*, 1998; Sirianni *et al.*, 1998).

The requirement for macrophages during the development of KS lesions is contradictory to our hypothesis that KSHV's vOX2 is involved in evading clearance by macrophages by prolonging their non-activated state. However, we speculate that the role of vOX2 is more crucial during primary infection with KSHV. Most aspects of primary infection with KSHV are unknown, but analogy with primary infection by other γ-herpesviruses leads us to believe that following initial infection of B-cells, clonal expansion occurs followed by the dissemination of virus and establishment of latency. We speculate that it is during this stage of infection that the proposed role of vOX2 comes into effect. The expression of vOX2 during primary infection will ultimately assist in allowing the virus to replicate and establish latency.

Previous studies have reported that expression of vOX2 is significantly induced (up to 168-fold) during lytic replication of KSHV in PEL cell lines (Jenner *et al.*, 2001; Paulose-Murphy *et al.*, 2001). More interestingly, the vOX2 transcript is detectable on a minor population of unstimulated PEL cells. Is it possible that a small subset of lytic cells, within a predominate latent infection, are able to prohibit an immune response against these virally infected cells? Further studies on gene expression profiles in PEL, KS lesions and asymptomatic KSHV positive individuals would generate a better understanding with respect to the involvement of vOX2 in KSHV pathogenesis.

The overall results in this thesis have revealed an important immuno-regulatory role for the KSHV vOX2 protein. If vOX2 does indeed have the ability to suppress activation of local macrophage, this finding would be paramount in KSHV pathogenesis, and perhaps all other viruses encoding CD200-homologues.

Future Work

The studies described within this thesis are preliminary experiments designed to investigate the role of the KSHV-vOX2 protein. Although many of these studies suggest that vOX2 may play an important immuno-regulatory role during viral pathogenesis, there are still several aspects and additional details that could be further investigated. The two main areas on which to focus in the future include protein interaction studies and further *in vivo* analysis of infection with the recombinant viruses.

One of the most useful tools in this study and any future work would be the generation and use of an antibody against vOX2. This antibody would not only allow protein interaction (e.g. with CD200R and CD200R-expressing cells) to be studied *in vitro* but also *in vivo*. A closer examination of the cell types in the vicinity of infected cells during infection with the recombinant viruses would also be advantageous. In particular the earlier time points (those between the initial point of infection and five days post-infection) need to be further scrutinized, as it is most likely that the maximum effect of vOX2 expression is occurring during these early stages of infection.

Ultimately future studies should also focus on other viral-CD200 homologues and explore whether these proteins play a similar role.

References

Adler, H., Messerle, M., Wagner, M., and Koszinowski, U.H. (2000) Cloning and mutagenesis of the murine gammaherpesvirus 68 genome as an infectious bacterial artificial chromosome. *J Virol* **74**: 6964-6974.

Akula, S.M., Pramod, N.P., Wang, F.Z., and Chandran, B. (2001) Human herpesvirus 8 envelope-associated glycoprotein B interacts with heparan sulfate-like moieties. *Virology* **284**: 235-249.

Akula, S.M., Pramod, N.P., Wang, F.Z., and Chandran, B. (2002) Integrin alpha3beta1 (CD 49c/29) is a cellular receptor for Kaposi's sarcoma-associated herpesvirus (KSHV/HHV-8) entry into the target cells. *Cell* **108**: 407-419.

Akula, S.M., Naranatt, P.P., Walia, N.S., Wang, F.Z., Fegley, B., and Chandran, B. (2003) Kaposi's sarcoma-associated herpesvirus (human herpesvirus 8) infection of human fibroblast cells occurs through endocytosis. *J Virol* **77**: 7978-7990.

Albrecht, J., Nicholas, J., Biller, D., cameron, K., Biesinger, B., Newman, C., Wittmann, S., Craxton, M., Coleman, H., Fleckenstein, B., and Honess, R. (1992) Primary structure of the Herpesvirus saimiri genome. *Journal of Virology* **66**: 5047-5058.

Altschul, S.F., Gish, W., Miller, W., Myers, E.W., and Lipman, D.J. (1990) Basic local alignment search tool. *J Mol Biol* **215**: 403-410.

Aoki, Y., Jaffe, E.S., Chang, Y., Jones, K., Teruya-Feldstein, J., Moore, P.S., and Tosato, G. (1999) Angiogenesis and hematopoiesis induced by Kaposi's sarcoma-associated herpesvirus-encoded interleukin-6. *Blood* **93**: 4034-4043.

Armstrong, R., Imrey, P., Lye, M., Armstrong, M., Yu, M., and Sani, S. (1998) Nasopharyngeal carcinoma in Malaysian Chinese: salted fish and other dietary exposures. *International Journal of Cancer* **77**: 228-235.

Arvanitakis, L., Mesri, E.A., Nador, R.G., Said, J.W., Asch, A.S., Knowles, D.M., and Cesarman, E. (1996) Establishment and characterization of a primary effusion (body cavity- based) lymphoma cell line (BC-3) harboring kaposi's sarcoma-associated herpesvirus (KSHV/HHV-8) in the absence of Epstein-Barr virus. *Blood* **88**: 2648-2654.

Arvanitakis, L., Geras-Raaka, E., Varma, A., Gershengorn, M.C., and Cesarman, E. (1997) Human herpesvirus KSHV encodes a constitutively active G-protein- coupled receptor linked to cell proliferation. *Nature* **385**: 347-350.

Arvin, A. (2001) Varicella-Zoster Virus. In *Fields Virology*. Vol. 2. Straus, S.E. (ed): Lipincott Williams and Wilkins, pp. 2731-2767.

Ashkenazi, A., and Dixit, V.M. (1998) Death receptors: signaling and modulation. *Science* **281**: 1305-1308.

Baer, R., Bankier, A., and Biggine, M. (1984) DNA sequence and expression of the B95-8 Epstein-Barr virus genome. *Nature* **310**: 207-211.

Bais, C., Santomasso, B., Coso, O., Arvanitakis, L., Raaka, E.G., Gutkind, J.S., Asch, A.S., Cesarman, E., Gershengorn, M.C., Mesri, E.A., and Gerhengorn, M.C. (1998) G-protein-coupled receptor of Kaposi's sarcoma-associated herpesvirus is a viral oncogene and angiogenesis activator. *Nature* **391**: 86-89.

Ballestas, M.E., Chatis, P.A., and Kaye, K.M. (1999) Efficient persistence of extrachromosomal KSHV DNA mediated by latency- associated nuclear antigen. *Science* **284**: 641-644.

Ballestas, M.E., and Kaye, K.M. (2001) Kaposi's sarcoma-associated herpesvirus latency-associated nuclear antigen 1 mediates episome persistence through cis-acting terminal repeat (TR) sequence and specifically binds TR DNA. *J Virol* **75**: 3250-3258.

Barclay, A.N. (1981) Different reticular elements in rat lymphoid tissue identified by localization of Ia, Thy-1 and MRC OX 2 antigens. *Immunology* **44**: 727-736.

Barclay, A.N., and Ward, H.A. (1982) Purification and chemical characterisation of membrane glycoproteins from rat thymocytes and brain, recognised by monoclonal antibody MRC OX 2. *Eur J Biochem* **129**: 447-458.

Barclay, A.N., Wright, G.J., Brooke, G., and Brown, M.H. (2002) CD200 and membrane protein interactions in the control of myeloid cells. *Trends Immunol* **23**: 285-290.

Baxt, B., and Becker, Y. (1990) The effect of peptides containing the arginine-glycine-aspartic acid sequence on the adsorption of foot-and-mouth disease virus to tissue culture cells. *Virus Genes* **4**: 73-83.

Bieleski, L., and Talbot, S.J. (2001) Kaposi's sarcoma-associated herpesvirus vCyclin open reading frame contains an internal ribosome entry site. *J Virol* **75**: 1864-1869.

Biesinger, B., Muller-Fleckenstein, I., Simmer, B., Lang, G., Wittmann, S., Platzer, E., Desrosiers, R., and Fleckenstein, B. (1992) Stable growth transformation of human T lymphocytes by Herpesvirus saimiri. *Proc. Natl. Acad. Sci. USA* **89**: 3116-3119.

Birkmann, A., Mahr, K., Ensser, A., Yaguboglu, S., Titgemeyer, F., Fleckenstein, B., and Neipel, F. (2001) Cell surface heparan sulfate is a receptor for human herpesvirus 8 and interacts with envelope glycoprotein K8.1. *J Virol* **75**: 11583-11593.

Blackbourn, D.J., and Levy, J.A. (1997) Human herpesvirus 8 in semen and prostate. *Aids* **11**: 249-250.

Blackbourn, D.J., Lennette, E., Klencke, B., Moses, A., Chandran, B., Weinstein, M., Glogau, R.G., Witte, M.H., Way, D.L., Kutzkey, T., Herndier, B., and Levy, J.A. (2000) The restricted cellular host range of human herpesvirus 8. *Aids* **14**: 1123-1133.

Blasig, C., Zietz, C., Haar, B., Neipel, F., Esser, S., Brockmeyer, N.H., Tschachler, E., Colombini, S., Ensoli, B., and Sturzl, M. (1997) Monocytes in Kaposi's sarcoma lesions are productively infected by human herpesvirus 8. *J Virol* **71**: 7963-7968.

Blaskovic, D., Strancekova, M., Svobodova, J., and Mistrikova, J. (1980) Isolation of five strains of herpesviruses from two species of free living rodents. *Acta Virologica* **24**: 468.

Bornhorst, J.A., and Falke, J.J. (2000) Purification of proteins using polyhistidine affinity tags. *Methods Enzymol* **326**: 245-254.

Borriello, F., Lederer, J., Scott, S., and Sharpe, A.H. (1997) MRC OX-2 defines a novel T cell costimulatory pathway. *J Immunol* **158**: 4548-4554.

Boshoff, C., Schulz, T.F., Kennedy, M.M., Graham, A.K., Fisher, C., Thomas, A., McGee, J.O., Weiss, R.A., and O'Leary, J.J. (1995) Kaposi's sarcoma-associated herpesvirus infects endothelial and spindle cells. *Nat Med* **1**: 1274-1278.

Boshoff, C., Gao, S.J., Healy, L.E., Matthews, S., Thomas, A.J., Coignet, L., Warnke, R.A., Strauchen, J.A., Matutes, E., Kamel, O.W., Moore, P.S., Weiss, R.A., and Chang, Y. (1998) Establishing a KSHV+ cell line (BCP-1) from peripheral blood and characterizing its growth in Nod/SCID mice. *Blood* **91**: 1671-1679.

Boshoff, C., and Chang, Y. (2001) Kaposi's sarcoma-associated herpesvirus: a new DNA tumor virus. *Annu Rev Med* **52**: 453-470.

Boshoff, C., and Weiss, R.A. (2001) Epidemiology and pathogenesis of Kaposi's sarcoma-associated herpesvirus. *Philos Trans R Soc Lond B Biol Sci* **356**: 517-534.

Boulanger, M.J., Chow, D.C., Brevnova, E., Martick, M., Sandford, G., Nicholas, J., and Garcia, K.C. (2004) Molecular mechanisms for viral mimicry of a human cytokine: activation of gp130 by HHV-8 interleukin-6. *J Mol Biol* **335**: 641-654.

Brinkmann, M.M., Glenn, M., Rainbow, L., Kieser, A., Henke-Gendo, C., and Schulz, T.F. (2003) Activation of mitogen-activated protein kinase and NF-kappaB pathways by a Kaposi's sarcoma-associated herpesvirus K15 membrane protein. *J Virol* **77**: 9346-9358.

Broderick, C., Hoek, R.M., Forrester, J.V., Liversidge, J., Sedgwick, J.D., and Dick, A.D. (2002) Constitutive retinal CD200 expression regulates resident microglia and activation state of inflammatory cells during experimental autoimmune uveoretinitis. *Am J Pathol* **161**: 1669-1677.

Browne, H., Bell, S., Minson, T., and Wilson, D. (1996) An Endoplasmic Reticulum-Retained Herpes Simplex Virus Glycoprotein H is Absent from Secreted Virions: Evidence for Reenvelopment during Egress. *Journal of Virology* **70**: 4311-4316.

Bukovsky, A., Presl, J., Zidovsky, J., and Mancal, P. (1983) The localization of Thy-1.1, MRC OX 2 and Ia antigens in the rat ovary and fallopian tube. *Immunology* **48**: 587-596.

Bukovsky, A., Presl, J., and Zidovsky, J. (1984) Association of some cell surface antigens of lymphoid cells and cell surface differentiation antigens with early rat pregnancy. *Immunology* **52**: 631-640.

Burkhardt, A.L., Bolen, J.B., Kieff, E., and Longnecker, R. (1992) An Epstein-Barr virus transformation-associated membrane protein interacts with src family tyrosine kinases. *J Virol* **66**: 5161-5167.

Burkitt, D. (1962) A children's cancer dependentupon climatic factors. *Nature* **194**: 232-234.

Burton, E.A., Hong, C.S., and Glorioso, J.C. (2003) The stable 2.0-kilobase intron of the herpes simplex virus type 1 latency-associated transcript does not function as an antisense repressor of ICP0 in nonneuronal cells. *J Virol* **77**: 3516-3530.

Burysek, L., Yeow, W.S., Lubyova, B., Kellum, M., Schafer, S.L., Huang, Y.Q., and Pitha, P.M. (1999) Functional analysis of human herpesvirus 8-encoded viral interferon regulatory factor 1 and its association with cellular interferon regulatory factors and p300. *J Virol* **73**: 7334-7342.

Calderwood, M.A., Hall, K.T., Matthews, D.A., and Whitehouse, A. (2004) The herpesvirus saimiri ORF73 gene product interacts with host-cell mitotic chromosomes and self-associates via its C terminus. *J Gen Virol* **85**: 147-153.

Cameron, C., Hota-Mitchell, S., Chen, L., Barrett, J., Cao, J.X., Macaulay, C., Willer, D., Evans, D., and McFadden, G. (1999) The complete DNA sequence of myxoma virus. *Virology* **264**: 298-318.

Cannon, M., Philpott, N.J., and Cesarman, E. (2003) The Kaposi's sarcoma-associated herpesvirus G protein-coupled receptor has broad signaling effects in primary effusion lymphoma cells. *J Virol* **77**: 57-67.

Cesarman, E., Mesri, E.A., and Gershengorn, M.C. (2000) Viral G protein-coupled receptor and Kaposi's sarcoma: a model of paracrine neoplasia? *J Exp Med* **191**: 417-422.

Cha, T., Tom, E., Kemble, G., Duke, G., Mocarski, E.S., and Spaete, R.R. (1996) Human Cytomegalovirus clinical isolates carry at least 19 genes not found in laboratory strains. *Journal of Virology* **70**: 78-83.

Chadburn, A., Cesarman, E., Nador, R.G., Liu, Y.F., and Knowles, D.M. (1997) Kaposi's sarcoma-associated herpesvirus sequences in benign lymphoid proliferations not associated with human immunodeficiency virus. *Cancer* **80**: 788-797.

Chang, J.Y., Wang, S., Hung, C.C., Tsai, T.F., and Hsiao, C.H. (2002) Multiple Epstein-Barr virus-associated subcutaneous angioleiomyomas in a patient with acquired immunodeficiency syndrome. *Br J Dermatol* **147**: 563-567.

Chang, Y., Cesarman, E., Pessin, M.S., Lee, F., Culpepper, J., Knowles, D.M., and Moore, P.S. (1994) Identification of herpesvirus-like DNA sequences in AIDS-associated Kaposi's sarcoma. *Science* **266**: 1865-1869.

Chapman, A., Rickinson, A., Thomas, W., Jarrett, R., Crocker, J., and Lee, S. (2001) Epstein-Barr virus-specific cytotoxic T lymphocyte responses in the blood and tumor site of Hodgkin's disease patients: Implications for a T-cell-based therapy. *Cancer Research* **61**: 6129-6226.

Chee, M., and Barrell, B. (1990) Herpesviruses: a study of parts. *Trends Genet* **6**: 86-91.

Cheng, E.H., Nicholas, J., Bellows, D.S., Hayward, G.S., Guo, H.G., Reitz, M.S., and Hardwick, J.M. (1997) A Bcl-2 homolog encoded by Kaposi sarcoma-associated virus, human herpesvirus 8, inhibits apoptosis but does not heterodimerize with Bax or Bak. *Proc Natl Acad Sci U S A* **94**: 690-694.

Cho, Y., Ramer, J., Rivailler, P., Quink, C., Garber, R.L., Beier, D.R., and Wang, F. (2001) An Epstein-Barr-related herpesvirus from marmoset lymphomas. *Proc Natl Acad Sci U S A* **98**: 1224-1229.

Choi, J., Ishido, S., and Jung, J. (2000a) The collagen repeat sequence is determinant of the degree of Herpesvirus saimiri STP transforming activity. *Journal of Virology* **74**: 8102-8110.

Choi, J., Means, R.E., Damania, B., and Jung, J.U. (2001) Molecular piracy of Kaposi's sarcoma associated herpesvirus. *Cytokine Growth Factor Rev* **12**: 245-257.

Choi, J.K., Lee, B.S., Shim, S.N., Li, M., and Jung, J.U. (2000b) Identification of the novel K15 gene at the rightmost end of the Kaposi's sarcoma-associated herpesvirus genome. *J Virol* **74**: 436-446.

Chung, Y.H., Means, R.E., Choi, J.K., Lee, B.S., and Jung, J.U. (2002) Kaposi's sarcoma-associated herpesvirus OX2 glycoprotein activates myeloid-lineage cells to induce inflammatory cytokine production. *J Virol* **76**: 4688-4698.

Cinquina, C.C., Grogan, E., Sun, R., Lin, S.F., Beardsley, G.P., and Miller, G. (2000) Dihydrofolate reductase from Kaposi's sarcoma-associated herpesvirus. *Virology* **268**: 201-217.

Clambey, E.T., Virgin, H.W.t., and Speck, S.H. (2000) Disruption of the murine gammaherpesvirus 68 M1 open reading frame leads to enhanced reactivation from latency. *J Virol* **74**: 1973-1984.

Clambey, E.T., Virgin, H.W.t., and Speck, S.H. (2002) Characterization of a spontaneous 9.5-kilobase-deletion mutant of murine gammaherpesvirus 68 reveals tissue-specific genetic requirements for latency. *J Virol* **76**: 6532-6544.

Clark, D.A., Ding, J.W., Yu, G., Levy, G.A., and Gorczynski, R.M. (2001a) Fgl2 prothrombinase expression in mouse trophoblast and decidua triggers abortion but may be countered by OX-2. *Mol Hum Reprod* **7**: 185-194.

Clark, D.A., Yu, G., Levy, G.A., and Gorczynski, R.M. (2001b) Procoagulants in fetus rejection: the role of the OX-2 (CD200) tolerance signal. *Semin Immunol* **13**: 255-263.

Clark, D.A., Keil, A., Chen, Z., Markert, U., Manuel, J., and Gorczynski, R.M. (2003) Placental trophoblast from successful human pregnancies expresses the tolerance signaling molecule, CD200 (OX-2). *Am J Reprod Immunol* **50**: 187-195.

Clark, M.J., Gagnon, J., Williams, A.F., and Barclay, A.N. (1985) MRC OX-2 antigen: a lymphoid/neuronal membrane glycoprotein with a structure like a single immunoglobulin light chain. *Embo J* **4**: 113-118.

Cocchi, F., Menotti, L., Mirandola, P., Lopez, M., and Campadelli-Fiume, G. (1998) The ectodomain of a novel member of the immunoglobulin subfamily related to the poliovirus receptor has the attributes of a bona fide receptor for herpes simplex virus types 1 and 2 in human cells. *J Virol* **72**: 9992-10002.

Cohrs, R.J., Barbour, M., and Gilden, D.H. (1996) Varicella-zoster virus (VZV) transcription during latency in human ganglia: detection of transcripts mapping to genes 21, 29, 62, and 63 in a cDNA library enriched for VZV RNA. *J Virol* **70**: 2789-2796.

Corbellino, M., Bestetti, G., Galli, M., and Parravicini, C. (1996) Absence of HHV-8 in prostate and semen. *N Engl J Med* **335**: 1237; author reply 1238-1239.

Cornali, E., Zietz, C., Benelli, R., Weninger, W., Masiello, L., Breier, G., Tschachler, E., Albini, A., and Sturzl, M. (1996) Vascular endothelial growth factor regulates angiogenesis and vascular permeability in Kaposi's Sarcoma. *American Journal of Pathology* **149**: 1851-1869.

Coscoy, L., and Ganem, D. (2000) Kaposi's sarcoma-associated herpesvirus encodes two proteins that block cell surface display of MHC class I chains by enhancing their endocytosis. *Proc Natl Acad Sci U S A* **97**: 8051-8056.

Damania, B., Choi, J.K., and Jung, J.U. (2000) Signaling activities of gammaherpesvirus membrane proteins. *J Virol* **74**: 1593-1601.

Davison, A.J. (2002) Evolution of the herpesviruses. *Vet Microbiol* **86**: 69-88.

de Thoisy, B., Pouliquen, J.F., Lacoste, V., Gessain, A., and Kazanji, M. (2003) Novel gamma-1 herpesviruses identified in free-ranging new world monkeys (golden-handed tamarin [Saguinus midas], squirrel monkey [Saimiri sciureus], and white-faced saki [Pithecia pithecia]) in French Guiana. *J Virol* 77: 9099-9105.

Deiss, L.P., and Frenkel, N. (1986) Herpes simplex virus amplicon: cleavage of concatemeric DNA is linked to packaging and involves amplification of the terminally reiterated a sequence. *J Virol* **57**: 933-941.

Desrosiers, R.C., Sasseville, V.G., Czajak, S.C., Zhang, X., Mansfield, K.G., Kaur, A., Johnson, R.P., Lackner, A.A., and Jung, J.U. (1997) A herpesvirus of rhesus monkeys related to the human Kaposi's sarcoma-associated herpesvirus. *J Virol* **71**: 9764-9769.

Diamond, C., Brodie, S.J., Krieger, J.N., Huang, M.L., Koelle, D.M., Diem, K., Muthui, D., and Corey, L. (1998) Human herpesvirus 8 in the prostate glands of men with Kaposi's sarcoma. *J Virol* **72**: 6223-6227.

Dick, A.D., Broderick, C., Forrester, J.V., and Wright, G.J. (2001) Distribution of OX2 antigen and OX2 receptor within retina. *Invest Ophthalmol Vis Sci* **42**: 170-176.

Dick, A.D., Carter, D., Robertson, M., Broderick, C., Hughes, E., Forrester, J.V., and Liversidge, J. (2003) Control of myeloid activity during retinal inflammation. *J Leukoc Biol* **74**: 161-166.

Dittmer, D., Lagunoff, M., Renne, R., Staskus, K., Haase, A., and Ganem, D. (1998) A cluster of latently expressed genes in Kaposi's sarcoma-associated herpesvirus. *J Virol* **72**: 8309-8315.

Djerbi, M., Screpanti, V., Catrina, A.I., Bogen, B., Biberfeld, P., and Grandien, A. (1999) The inhibitor of death receptor signaling, FLICE-inhibitory protein defines a new class of tumor progression factors. *J Exp Med* **190**: 1025-1032.

Douglas, J., Dutia, B., Rhind, S., Stewart, J.P., and Talbot, S.J. (2004) Expression in a recombinant murid herpesvirus 4 reveals the in vivo transforming potential of the K1 open reading frame of Kaposi's sarcoma-associated herpesvirus. *J Virol* **78**: 8878-8884.

Duboise, S., Guo, J., Czajak, S., Desrosiers, R., and Jung, J. (1998) STP and Tip are essential for Herpesvirus saimiri oncogenicity. *Journal of Virology* **72**: 1308-1313.

Dupin, N., Fisher, C., Kellam, P., Ariad, S., Tulliez, M., Franck, N., van Marck, E., Salmon, D., Gorin, I., Escande, J.P., Weiss, R.A., Alitalo, K., and Boshoff, C. (1999) Distribution of human herpesvirus-8 latently infected cells in Kaposi's sarcoma, multicentric Castleman's disease, and primary effusion lymphoma. *Proc Natl Acad Sci U S A* **96**: 4546-4551.

Dupin, N., Diss, T.L., Kellam, P., Tulliez, M., Du, M.Q., Sicard, D., Weiss, R.A., Isaacson, P.G., and Boshoff, C. (2000) HHV-8 is associated with a plasmablastic variant of Castleman disease that is linked to HHV-8-positive plasmablastic lymphoma. *Blood* **95**: 1406-1412.

Duro, D., Schulze, A., Vogt, B., Bartek, J., Mittnacht, S., and Jansen-Durr, P. (1999) Activation of cyclin A gene expression by the cyclin encoded by human herpesvirus-8. *J Gen Virol* **80 (Pt 3)**: 549-555.

Ebrahimi, B., Dutia, B.M., Roberts, K.L., Garcia-Ramirez, J.J., Dickinson, P., Stewart, J.P., Ghazal, P., Roy, D.J., and Nash, A.A. (2003) Transcriptome profile of murine gammaherpesvirus-68 lytic infection. *J Gen Virol* **84**: 99-109.

Efstathiou, S., Ho, Y.M., Hall, S., Styles, C.J., Scott, S.D., and Gompels, U.A. (1990a) Murine herpesvirus 68 is genetically related to the gammaherpesviruses Epstein-Barr virus and herpesvirus saimiri. *J Gen Virol* **71 (Pt 6)**: 1365-1372.

Efstathiou, S., Ho, Y.M., and Minson, A.C. (1990b) Cloning and molecular characterization of the murine herpesvirus 68 genome. *J Gen Virol* **71 (Pt 6)**: 1355-1364.

Ejercito, P.M., Kieff, E.D., and Roizman, B. (1968) Characterization of herpes simplex virus strains differing in their effects on social behaviour of infected cells. *J Gen Virol* **2**: 357-364.

Ellis, M., Chew, Y.P., Fallis, L., Freddersdorf, S., Boshoff, C., Weiss, R.A., Lu, X., and Mittnacht, S. (1999) Degradation of p27(Kip) cdk inhibitor triggered by Kaposi's sarcoma virus cyclin-cdk6 complex. *Embo J* **18**: 644-653.

Elward, K., and Gasque, P. (2003) "Eat me" and "don't eat me" signals govern the innate immune response and tissue repair in the CNS: emphasis on the critical role of the complement system. *Mol Immunol* **40**: 85-94.

Epstein, M., Achong, B., and Barr, Y. (1965) Morphological and biological studies on a virus in cultured lympoblasts from Burkitt's lymphoma. *Journal of Experimental Medicine* **121**: 761-770.

Evans, T.J., Farrell, P.J., and Swaminathan, S. (1996) Molecular genetic analysis of Epstein-Barr virus Cp promoter function. *J Virol* **70**: 1695-1705.

Everly, D.N., Jr., Feng, P., Mian, I.S., and Read, G.S. (2002) mRNA degradation by the virion host shutoff (Vhs) protein of herpes simplex virus: genetic and biochemical evidence that Vhs is a nuclease. *J Virol* **76**: 8560-8571.

Feng, P., Everely, D., and Read, S. (2001) mRNA Decay during Herpesvirus Infections: Interaction between a Putative Viral Nuclease and a Cellular Translation Factor. *Journal of Virology* **75**: 10272-10280.

Fickenscher, H., Biesinger, B., Knappe, A., and Wittmann, S. (1996) Regulation of the Herpesvirus saimiri oncogene *stp*C, similar to that of T-cell activation genes, in growth-transformed human T lymphocytes. *Journal of Virology* **70**: 6012-6019.

Fickenscher, H., and Fleckenstein, B. (2001) Herpesvirus saimiri. *Phil. Tans. R. Soc. Lond. B* **356**: 545-567.

Fingeroth, J.D., Weis, J.J., Tedder, T.F., Strominger, J.L., Biro, P.A., and Fearon, D.T. (1984) Epstein-Barr virus receptor of human B lymphocytes is the C3d receptor CR2. *Proc Natl Acad Sci U S A* **81**: 4510-4514.

Fiorelli, V., Gendelman, R., Sirianni, M.C., Chang, H.K., Colombini, S., Markham, P.D., Monini, P., Sonnabend, J., Pintus, A., Gallo, R.C., and Ensoli, B. (1998) gamma-Interferon produced by CD8+ T cells infiltrating Kaposi's sarcoma induces spindle cells with angiogenic phenotype and synergy with human immunodeficiency virus-1 Tat protein: an immune response to human herpesvirus-8 infection? *Blood* **91**: 956-967.

Flano, E., Kim, I.J., Moore, J., Woodland, D.L., and Blackman, M.A. (2003) Differential gamma-herpesvirus distribution in distinct anatomical locations and cell subsets during persistent infection in mice. *J Immunol* **170**: 3828-3834.

Flint, S.J., Enquist, L.W., Krug, R.M., Racaniello, V.R., and Skalka, A.M. (2000) *Principles of Virology-Molecular Biology, Pathogeneis and Control*: ASM Press.

Flore, O., Rafii, S., Ely, S., O'Leary, J.J., Hyjek, E.M., and Cesarman, E. (1998) Transformation of primary human endothelial cells by Kaposi's sarcoma-associated herpesvirus. *Nature* **394**: 588-592.

Foster-Cuevas, M., Wright, G.J., Puklavec, M.J., Brown, M.H., and Barclay, A.N. (2004) Human herpesvirus 8 K14 protein mimics CD200 in down-regulating macrophage activation through CD200 receptor. *J Virol* **78**: 7667-7676.

Fox, G., Parry, N.R., Barnett, P.V., McGinn, B., Rowlands, D.J., and Brown, F. (1989) The cell attachment site on foot-and-mouth disease virus includes the amino acid sequence RGD (arginine-glycine-aspartic acid). *J Gen Virol* **70 (Pt 3)**: 625-637.

Friborg, J., Jr., Kong, W.P., Flowers, C.C., Flowers, S.L., Sun, Y., Foreman, K.E., Nickoloff, B.J., and Nabel, G.J. (1998) Distinct biology of Kaposi's sarcoma-associated

herpesvirus from primary lesions and body cavity lymphomas. *J Virol* **72**: 10073-10082.

Friborg, J., Jr., Kong, W., Hottiger, M.O., and Nabel, G.J. (1999) p53 inhibition by the LANA protein of KSHV protects against cell death. *Nature* **402**: 889-894.

Fruh, K., Ahn, K., Djaballah, H., Sempe, P., van Endert, P.M., Tampe, R., Peterson, P.A., and Yang, Y. (1995) A viral inhibitor of peptide transporters for antigen presentation. *Nature* **375**: 415-418.

Gaidano, G., Pastore, C., Gloghini, A., Canzonieri, V., Capello, D., Franceschi, S., Saglio, G., and Carbone, A. (1997) Genetic heterogeneity of AIDS-related small non-cleaved cell lymphoma. *Br J Haematol* **98**: 726-732.

Gaidano, G., Capello, D., Cilia, A.M., Gloghini, A., Perin, T., Quattrone, S., Migliazza, A., Lo Coco, F., Saglio, G., Ascoli, V., and Carbone, A. (1999) Genetic characterization of HHV-8/KSHV-positive primary effusion lymphoma reveals frequent mutations of BCL6: implications for disease pathogenesis and histogenesis. *Genes Chromosomes Cancer* **24**: 16-23.

Gangappa, S., van Dyk, L.F., Jewett, T.J., Speck, S.H., and Virgin, H.W.t. (2002) Identification of the in vivo role of a viral bcl-2. *J Exp Med* **195**: 931-940.

Gao, S.J., Boshoff, C., Jayachandra, S., Weiss, R.A., Chang, Y., and Moore, P.S. (1997) KSHV ORF K9 (vIRF) is an oncogene which inhibits the interferon signaling pathway. *Oncogene* **15**: 1979-1985.

Garber, A.C., Shu, M.A., Hu, J., and Renne, R. (2001) DNA binding and modulation of gene expression by the latency-associated nuclear antigen of Kaposi's sarcoma-associated herpesvirus. *J Virol* **75**: 7882-7892.

Garber, D.A., Beverley, S.M., and Coen, D.M. (1993) Demonstration of circularization of herpes simplex virus DNA following infection using pulsed field gel electrophoresis. *Virology* **197**: 459-462.

Garber, D.A., Schaffer, P.A., and Knipe, D.M. (1997) A LAT-associated function reduces productive-cycle gene expression during acute infection of murine sensory neurons with herpes simplex virus type 1. *J Virol* **71**: 5885-5893.

Godden-Kent, D., Talbot, S.J., Boshoff, C., Chang, Y., Moore, P., Weiss, R.A., and Mittnacht, S. (1997) The cyclin encoded by Kaposi's sarcoma-associated herpesvirus stimulates cdk6 to phosphorylate the retinoblastoma protein and histone H1. *J Virol* **71**: 4193-4198.

Gompels, U.A., and Kasolo, F.C. (1996) HHV-8 serology and Kaposi's sarcoma. *Lancet* **348**: 1587-1588.

Gong, M., Ooka, T., Matsuo, T., and Kieff, E. (1987) Epstein-Barr virus glycoprotein homologous to herpes simplex virus gB. *J Virol* **61**: 499-508.

Gong, M., and Kieff, E. (1990) Intracellular trafficking of two major Epstein-Barr virus glycoproteins, gp350/220 and gp110. *J Virol* **64**: 1507-1516.

Gorczynski, L., Chen, Z., Hu, J., Kai, Y., Lei, J., Ramakrishna, V., and Gorczynski, R.M. (1999a) Evidence that an OX-2-positive cell can inhibit the stimulation of type 1 cytokine production by bone marrow-derived B7-1 (and B7-2)-positive dendritic cells. *J Immunol* **162**: 774-781.

Gorczynski, R.M., Chen, Z., Fu, X.M., and Zeng, H. (1998) Increased expression of the novel molecule OX-2 is involved in prolongation of murine renal allograft survival. *Transplantation* **65**: 1106-1114.

Gorczynski, R.M., Cattral, M.S., Chen, Z., Hu, J., Lei, J., Min, W.P., Yu, G., and Ni, J. (1999b) An immunoadhesin incorporating the molecule OX-2 is a potent immunosuppressant that prolongs allo- and xenograft survival. *J Immunol* **163**: 1654-1660.

Gorczynski, R.M., Cohen, Z., Fu, X.M., and Lei, J. (1999c) Anti-rat OX-2 blocks increased small intestinal transplant survival after portal vein immunization. *Transplant Proc* **31**: 577-578.

Gorczynski, R.M., Bransom, J., Cattral, M., Huang, X., Lei, J., Xiaorong, L., Min, W.P., Wan, Y., and Gauldie, J. (2000a) Synergy in induction of increased renal allograft survival after portal vein infusion of dendritic cells transduced to express TGFbeta and IL-10, along with administration of CHO cells expressing the regulatory molecule OX-2. *Clin Immunol* **95**: 182-189.

Gorczynski, R.M., Chen, Z., Clark, D.A., Hu, J., Yu, G., Li, X., Tsang, W., and Hadidi, S. (2000b) Regulation of gene expression of murine MD-1 regulates subsequent T cell activation and cytokine production. *J Immunol* **165**: 1925-1932.

Gorczynski, R.M., Chen, Z., Kai, Y., and Lei, J. (2000c) Evidence for persistent expression of OX2 as a necessary component of prolonged renal allograft survival following portal vein immunization. *Clin Immunol* **97**: 69-78.

Gorczynski, R.M., Yu, K., and Clark, D. (2000d) Receptor engagement on cells expressing a ligand for the tolerance-inducing molecule OX2 induces an immunoregulatory population that inhibits alloreactivity in vitro and in vivo. *J Immunol* **165**: 4854-4860.

Gorczynski, R.M. (2001) Transplant tolerance modifying antibody to CD200 receptor, but not CD200, alters cytokine production profile from stimulated macrophages. *Eur J Immunol* **31**: 2331-2337.

Gorczynski, R.M., Chen, Z., Hu, J., Kai, Y., and Lei, J. (2001a) Evidence of a role for CD200 in regulation of immune rejection of leukaemic tumour cells in C57BL/6 mice. *Clin Exp Immunol* **126**: 220-229.

Gorczynski, R.M., Chen, Z., Yu, K., and Hu, J. (2001b) CD200 immunoadhesin suppresses collagen-induced arthritis in mice. *Clin Immunol* **101**: 328-334.

Gorczynski, R.M., Chen, Z., Lee, L., Yu, K., and Hu, J. (2002a) Anti-CD200R ameliorates collagen-induced arthritis in mice. *Clin Immunol* **104**: 256-264.

Gorczynski, R.M., Hadidi, S., Yu, G., and Clark, D.A. (2002b) The same immunoregulatory molecules contribute to successful pregnancy and transplantation. *Am J Reprod Immunol* **48**: 18-26.

Gorczynski, R.M., Hu, J., Chen, Z., Kai, Y., and Lei, J. (2002c) A CD200FC immunoadhesin prolongs rat islet xenograft survival in mice. *Transplantation* **73**: 1948-1953.

Gorczynski, R.M., Chen, Z., Kai, Y., Wong, S., and Lee, L. (2004) Induction of tolerance-inducing antigen-presenting cells in bone marrow cultures in vitro using monoclonal antibodies to CD200R. *Transplantation* **77**: 1138-1144.

Gradoville, L., Gerlach, J., Grogan, E., Shedd, D., Nikiforow, S., Metroka, C., and Miller, G. (2000) Kaposi's sarcoma-associated herpesvirus open reading frame 50/Rta protein activates the entire viral lytic cycle in the HH-B2 primary effusion lymphoma cell line. *J Virol* **74**: 6207-6212.

Grandadam, M., Dupin, N., Calvez, V., Gorin, I., Blum, L., Kernbaum, S., Sicard, D., Buisson, Y., Agut, H., Escande, J.P., and Huraux, J.M. (1997) Exacerbations of clinical symptoms in human immunodeficiency virus type 1-infected patients with multicentric Castleman's disease are associated with a high increase in Kaposi's sarcoma herpesvirus DNA load in peripheral blood mononuclear cells. *J Infect Dis* **175**: 1198-1201.

Granzow, H., Klupp, B.G., Fuchs, W., Veits, J., Osterrieder, N., and Mettenleiter, T.C. (2001) Egress of alphaherpesviruses: comparative ultrastructural study. *J Virol* **75**: 3675-3684.

Grubman, M.J., and Baxt, B. (2004) Foot-and-mouth disease. *Clin Microbiol Rev* **17**: 465-493.

Grundhoff, A., and Ganem, D. (2001) Mechanisms governing expression of the v-FLIP gene of Kaposi's sarcoma-associated herpesvirus. *J Virol* **75**: 1857-1863.

Haddad, R.S., and Hutt-Fletcher, L.M. (1989) Depletion of glycoprotein gp85 from virosomes made with Epstein-Barr virus proteins abolishes their ability to fuse with virus receptor-bearing cells. *J Virol* **63**: 4998-5005.

Hall, K.T., Giles, M.S., Goodwin, D.J., Calderwood, M.A., Carr, I.M., Stevenson, A.J., Markham, A.F., and Whitehouse, A. (2000) Analysis of gene expression in a human cell line stably transduced with herpesvirus saimiri. *J Virol* **74**: 7331-7337.

Haque, T., Wilkie, G., Taylor, C., Amlot, P., Murad, P., Iley, A., Dombagoda, D., Britton, K., Swerdlow, A., and Crawford, D. (2002) Treatment of Epstein-Barr-virus-positive post-transplantation lymphoproliferative disease with partly HLA-matched allogeneic cytotoxic T cells. *Lancet* **360**: 436.

Harada, S., and Kieff, E. (1997) Epstein-Barr virus nuclear protein LP stimulates EBNA-2 acidic domain- mediated transcriptional activation. *J Virol* **71**: 6611-6618.

Harley, C.A., Dasgupta, A., and Wilson, D.W. (2001) Characterization of herpes simplex virus-containing organelles by subcellular fractionation: role for organelle acidification in assembly of infectious particles. *J Virol* **75**: 1236-1251.

Hatzivassiliou, E., Miller, W., Raab-Traub, N., Kieff, E., and Mosialos, G. (1998) A Fusion of the EBV Latent Membrane Protein-1 (LMP1) Transmembrane Domains to the CD40 Cytoplasmic Domain Is Similar to LMP1 in Constitutive Activation of Epidermal Growth Factor Receptor Expression, Nuclear Factor-κB, and Stress-Activated Protein Kinase. *Journal of Immunology* **160**: 1116-1121.

Hayward, G.S. (1999) KSHV strains: the origins and global spread of the virus. *Semin Cancer Biol* **9**: 187-199.

Hengge, U.R., Ruzicka, T., Tyring, S.K., Stuschke, M., Roggendorf, M., Schwartz, R.A., and Seeber, S. (2002a) Update on Kaposi's sarcoma and other HHV8 associated diseases. Part 2: pathogenesis, Castleman's disease, and pleural effusion lymphoma. *Lancet Infect Dis* **2**: 344-352.

Hengge, U.R., Ruzicka, T., Tyring, S.K., Stuschke, M., Roggendorf, M., Schwartz, R.A., and Seeber, S. (2002b) Update on Kaposi's sarcoma and other HHV8 associated diseases. Part 1: epidemiology, environmental predispositions, clinical manifestations, and therapy. *Lancet Infect Dis* **2**: 281-292.

Hill, A., Jugovic, P., York, I., Russ, G., Bennink, J., Yewdell, J., Ploegh, H., and Johnson, D. (1995) Herpes simplex virus turns off the TAP to evade host immunity. *Nature* **375**: 411-415.

Hirayama, T., and Ito, Y. (1981) A new view of the etiology of nasopharyngeal carcinoma. *Prev Med* **10**: 614-622.

Ho, H.H., Du, D., and Gershengorn, M.C. (1999) The N terminus of Kaposi's sarcoma-associated herpesvirus G protein-coupled receptor is necessary for high affinity chemokine binding but not for constitutive activity. *J Biol Chem* **274**: 31327-31332.

Ho, M., Miller, G., Atchison, R.W., Breinig, M.K., Dummer, J.S., Andiman, W., Starzl, T.E., Eastman, R., Griffith, B.P., Hardesty, R.L., and et al. (1985) Epstein-Barr virus infections and DNA hybridization studies in posttransplantation lymphoma and lymphoproliferative lesions: the role of primary infection. *J Infect Dis* **152**: 876-886.

Hochuli, E., Bannwarth, W., Dobeli, H., Gentz, R., and Stuber, D. (1988) Genetic approach to facilitate purification of recombinant proteins with a novel chelate adsorbent. *Bio/Technology* **6**: 1321-1325.

Hoek, R.M., Ruuls, S.R., Murphy, C.A., Wright, G.J., Goddard, R., Zurawski, S.M., Blom, B., Homola, M.E., Streit, W.J., Brown, M.H., Barclay, A.N., and Sedgwick, J.D. (2000) Down-regulation of the macrophage lineage through interaction with OX2 (CD200). *Science* **290**: 1768-1771.

Hoischen, S.H., Vollmer, P., Marz, P., Ozbek, S., Gotze, K.S., Peschel, C., Jostock, T., Geib, T., Mullberg, J., Mechtersheimer, S., Fischer, M., Grotzinger, J., Galle, P.R., and Rose-John, S. (2000) Human herpes virus 8 interleukin-6 homologue triggers gp130 on neuronal and hematopoietic cells. *Eur J Biochem* **267**: 3604-3612.

Hynes, R.O. (1987) Integrins: a family of cell surface receptors. *Cell* **48**: 549-554.

Hynes, R.O. (1992) Integrins: versatility, modulation, and signaling in cell adhesion. *Cell* **69**: 11-25.

Hynes, R.O. (1999) Cell adhesion: old and new questions. *Trends Cell Biol* **9**: M33-37.

Inoue, N., Winter, J., Lal, R.B., Offermann, M.K., and Koyano, S. (2003) Characterization of entry mechanisms of human herpesvirus 8 by using an Rta-dependent reporter cell line. *J Virol* **77**: 8147-8152.

Irmler, M., Thome, M., Hahne, M., Schneider, P., Hofmann, K., Steiner, V., Bodmer, J.L., Schroter, M., Burns, K., Mattmann, C., Rimoldi, D., French, L.E., and Tschopp, J. (1997) Inhibition of death receptor signals by cellular FLIP. *Nature* **388**: 190-195.

Ishido, S., Wang, C., Lee, B.S., Cohen, G.B., and Jung, J.U. (2000) Downregulation of major histocompatibility complex class I molecules by Kaposi's sarcoma-associated herpesvirus K3 and K5 proteins. *J Virol* **74**: 5300-5309.

Ishiyama, T., Koike, M., Nakamura, S., Kakimoto, T., Akimoto, Y., and Tsuruoka, N. (1996) Interleukin-6 receptor expression in the peripheral B cells of patients with multicentric Castleman's disease. *Ann Hematol* **73**: 179-182.

Jacoby, M.A., Virgin, H.W.t., and Speck, S.H. (2002) Disruption of the M2 gene of murine gammaherpesvirus 68 alters splenic latency following intranasal, but not intraperitoneal, inoculation. *J Virol* **76**: 1790-1801.

Jayachandra, S., Low, K.G., Thlick, A.E., Yu, J., Ling, P.D., Chang, Y., and Moore, P.S. (1999) Three unrelated viral transforming proteins (vIRF, EBNA2, and E1A) induce the MYC oncogene through the interferon-responsive PRF element by using different transcription coadaptors. *Proc Natl Acad Sci U S A* **96**: 11566-11571.

Jenner, R.G., Alba, M.M., Boshoff, C., and Kellam, P. (2001) Kaposi's sarcoma-associated herpesvirus latent and lytic gene expression as revealed by DNA arrays. *J Virol* **75**: 891-902.

Jin, L., Peng, W., Perng, G., Brick, D., Nesburn, A., Jones, C., and Wechsler, S. (2003) Identification of Herpes Simplex Virus Type 1 Latency-Associted Transcript that both Inhibit Apoptosis and Enhace the Spontaneous Reactivation Phenotype. *Journal of Virology* **77**: 6556-6561.

Jones, D., Ballestas, M.E., Kaye, K.M., Gulizia, J.M., Winters, G.L., Fletcher, J., Scadden, D.T., and Aster, J.C. (1998) Primary-effusion lymphoma and Kaposi's sarcoma in a cardiac-transplant recipient. *N Engl J Med* **339**: 444-449.

Jung, J.U., Trimble, J.J., King, N.W., Biesinger, B., Fleckenstein, B.W., and Desrosiers, R.C. (1991) Identification of transforming genes of subgroup A and C strains of Herpesvirus saimiri. *Proc Natl Acad Sci U S A* **88**: 7051-7055.

Jung, J.U., and Desrosiers, R.C. (1995) Association of the viral oncoprotein STP-C488 with cellular ras. *Mol Cell Biol* **15**: 6506-6512.

Jussila, L., Valtola, R., Partanen, T.A., Salven, P., Heikkila, P., Matikainen, M.T., Renkonen, R., Kaipainen, A., Detmar, M., Tschachler, E., Alitalo, R., and Alitalo, K. (1998) Lymphatic endothelium and Kaposi's sarcoma spindle cells detected by antibodies against the vascular endothelial growth factor receptor-3. *Cancer Res* **58**: 1599-1604.

Kanda, K., Decker, T., Aman, P., Wahlstrom, M., von Gabain, A., and Kallin, B. (1992) The EBNA2-related resistance towards alpha interferon (IFN-alpha) in Burkitt's

lymphoma cells effects induction of IFN-induced genes but not the activation of transcription factor ISGF-3. *Mol Cell Biol* **12**: 4930-4936.

Kanegane, H., Yachie, A., Miyawaki, T., and Tosato, G. (1998) EBV-NK cells interactins and lymphoproliferative disorders. *Leuk Lymphoma* **29**: 491-498.

Kao, P.N., Chen, L., Brock, G., Ng, J., Kenny, J., Smith, A.J., and Corthesy, B. (1994) Cloning and expression of cyclosporin A- and FK506-sensitive nuclear factor of activated T-cells: NF45 and NF90. *J Biol Chem* **269**: 20691-20699.

Kaposi, M. (1872) Idiopathic multiple pigmented sarcoma of the skin. *Arch Dermatol Syphil* **4**: 265-273.

Kara, P.D., Afonso, C.L., Wallace, D.B., Kutish, G.F., Abolnik, C., Lu, Z., Vreede, F.T., Taljaard, L.C., Zsak, A., Viljoen, G.J., and Rock, D.L. (2003) Comparative sequence analysis of the South African vaccine strain and two virulent field isolates of Lumpy skin disease virus. *Arch Virol* **148**: 1335-1356.

Katano, H., and Sata, T. (2000) Human herpesvirus 8 virology, epidemiology and related diseases. *Jpn J Infect Dis* **53**: 137-155.

Katano, H., Sato, Y., and Sata, T. (2001) Expression of p53 and human herpesvirus-8 (HHV-8)-encoded latency-associated nuclear antigen with inhibition of apoptosis in HHV-8-associated malignancies. *Cancer* **92**: 3076-3084.

Kennedy, P.G., Barrass, J.D., Graham, D.I., and Clements, G.B. (1990) Studies on the pathogenesis of neurological diseases associated with Varicella-Zoster virus. *Neuropathol Appl Neurobiol* **16**: 305-316.

Kilger, E., Kieser, A., Baumann, M., and Hammerschmidt, W. (1998) Epstein-Barr virus-mediated B-cell proligeration is dependent upon latent membrane protein1, which stimulates an activated CD40 receptor. *The EMBO* **16**: 1700-1709.

Kilpatrick, D.R., and Rouhandeh, H. (1985) Cloning and physical mapping of Yaba monkey tumor virus DNA. *Virology* **143**: 399-406.

Kim, I.J., Flano, E., Woodland, D.L., Lund, F.E., Randall, T.D., and Blackman, M.A. (2003) Maintenance of long term gamma-herpesvirus B cell latency is dependent on CD40-mediated development of memory B cells. *J Immunol* **171**: 886-892.

Kitagawa, N., Goto, M., Kurozumi, K., Maruo, S., Yasukawa, M., Hino, K., Suzuki, T., Todo, S., and Takada, K. (2000) Epstein-Barr virus-encoded poly(A)$^-$ RNA supports Burkitt's Lymphoma growth through interleukin-10 induction. *The EMBO Journal* **19**: 6742-6750.

Kledal, T.N., Rosenkilde, M.M., Coulin, F., Simmons, G., Johnsen, A.H., Alouani, S., Power, C.A., Luttichau, H.R., Gerstoft, J., Clapham, P.R., Clark-Lewis, I., Wells, T.N., and Schwartz, T.W. (1997) A broad-spectrum chemokine antagonist encoded by Kaposi's sarcoma-associated herpesvirus. *Science* **277**: 1656-1659.

Kliche, S., Nagel, W., Kremmer, E., Atzler, C., Ege, A., Knorr, T., Koszinowski, U., Kolanus, W., and Haas, J. (2001) Signaling by human herpesvirus 8 kaposin A through direct membrane recruitment of cytohesin-1. *Mol Cell* **7**: 833-843.

Komano, J., Sugiura, M., and Takada, K. (1998) Epstein-Barr virus contributes to the malignant phenotype and to apoptosis resistance in Burkitt's Lymphpma cell line Akata. *Journal of Virology* **72**: 9150-9156.

Komano, J., Mauro, S., Kurozumi, K., Oda, T., and Takada, K. (1999) Oncogenic role of Epstein-Barr virus-encoded RNAs in Burkitt's lymphoma cell line Akata. *Journal of Virology* **73**: 9827-9831.

Komatsu, T., Ballestas, M.E., Barbera, A.J., Kelley-Clarke, B., and Kaye, K.M. (2004) KSHV LANA1 binds DNA as an oligomer and residues N-terminal to the oligomerization domain are essential for DNA binding, replication, and episome persistence. *Virology* **319**: 225-236.

Krithivas, A., Young, D.B., Liao, G., Greene, D., and Hayward, S.D. (2000) Human herpesvirus 8 LANA interacts with proteins of the mSin3 corepressor complex and negatively regulates Epstein-Barr virus gene expression in dually infected PEL cells. *J Virol* **74**: 9637-9645.

Kyte, J., and Doolittle, R.F. (1982) A simple method for displaying the hydropathic character of a protein. *J Mol Biol* **157**: 105-132.

Lackner, C.A., and Condit, R.C. (2000) Vaccinia virus gene A18R DNA helicase is a transcript release factor. *J Biol Chem* **275**: 1485-1494.

Laemmli, U.K. (1970) Cleavage of structural proteins during the assembly of the head of the bacteriophage T4. *Nature* **277**: 680-685.

Lagunoff, M., and Roizman, B. (1994) Expression of a herpes simplex virus 1 open reading frame antisense to the g1 34.5 gene and transcibed by an RNA 3' coterminal with the unspliced latency-associted transcript. *Journal of Virology* **71**: 1019-1024.

Lagunoff, M., Majeti, R., Weiss, A., and Ganem, D. (1999) Deregulated signal transduction by the K1 gene product of Kaposi's sarcoma-associated herpesvirus. *Proc Natl Acad Sci U S A* **96**: 5704-5709.

Laman, H., Coverley, D., Krude, T., Laskey, R., and Jones, N. (2001) Viral cyclin-cyclin-dependent kinase 6 complexes initiate nuclear DNA replication. *Mol Cell Biol* **21**: 624-635.

Lee, B.J., Koszinowski, U.H., Sarawar, S.R., and Adler, H. (2003) A gammaherpesvirus G protein-coupled receptor homologue is required for increased viral replication in response to chemokines and efficient reactivation from latency. *J Immunol* **170**: 243-251.

Lee, B.S., Alvarez, X., Ishido, S., Lackner, A.A., and Jung, J.U. (2000) Inhibition of intracellular transport of B cell antigen receptor complexes by Kaposi's sarcoma-associated herpesvirus K1. *J Exp Med* **192**: 11-21.

Lee, D.M., Friend, D.S., Gurish, M.F., Benoist, C., Mathis, D., and Brenner, M.B. (2002) Mast cells: a cellular link between autoantibodies and inflammatory arthritis. *Science* **297**: 1689-1692.

Lee, H., Guo, J., Li, M., Choi, J.K., DeMaria, M., Rosenzweig, M., and Jung, J.U. (1998a) Identification of an immunoreceptor tyrosine-based activation motif of K1 transforming protein of Kaposi's sarcoma-associated herpesvirus. *Mol Cell Biol* **18**: 5219-5228.

Lee, H., Veazey, R., Williams, K., Li, M., Guo, J., Neipel, F., Fleckenstein, B., Lackner, A., Desrosiers, R.C., and Jung, J.U. (1998b) Deregulation of cell growth by the K1 gene of Kaposi's sarcoma- associated herpesvirus. *Nat Med* **4**: 435-440.

Lee, H.J., Essani, K., and Smith, G.L. (2001) The genome sequence of Yaba-like disease virus, a yatapoxvirus. *Virology* **281**: 170-192.

Levitskaya, J., Coram, M., Levitsky, V., Imreh, S., Steigerwald-Mullen, P.M., Klein, G., Kurilla, M.G., and Masucci, M.G. (1995) Inhibition of antigen processing by the internal repeat region of the Epstein-Barr virus nuclear antigen-1. *Nature* **375**: 685-688.

Levitskaya, J., Sharipo, A., Leonchiks, A., Ciechanover, A., and Masucci, M. (1997) Inhibition of ubiquitin/proteasome-dependent protein degradation by the Gly-Ala repeat domain of the Epstein-Barr virus nuclear antigen1. *Proc. Nat. Acad. Sci. USA* **94**: 12616-12621.

Li, H., Wang, H., and Nicholas, J. (2001) Detection of direct binding of human herpesvirus 8-encoded interleukin-6 (vIL-6) to both gp130 and IL-6 receptor (IL-6R) and identification of amino acid residues of vIL-6 important for IL-6R-dependent and -independent signaling. *J Virol* **75**: 3325-3334.

Li, M., Lee, H., Yoon, D.W., Albrecht, J.C., Fleckenstein, B., Neipel, F., and Jung, J.U. (1997) Kaposi's sarcoma-associated herpesvirus encodes a functional cyclin. *J Virol* **71**: 1984-1991.

Li, M., Lee, H., Guo, J., Neipel, F., Fleckenstein, B., Ozato, K., and Jung, J.U. (1998) Kaposi's sarcoma-associated herpesvirus viral interferon regulatory factor. *J Virol* **72**: 5433-5440.

Li, M., Damania, B., Alvarez, X., Ogryzko, V., Ozato, K., and Jung, J.U. (2000) Inhibition of p300 histone acetyltransferase by viral interferon regulatory factor. *Mol Cell Biol* **20**: 8254-8263.

Lim, C., Sohn, H., Gwack, Y., and Choe, J. (2000) Latency-associated nuclear antigen of Kaposi's sarcoma-associated herpesvirus (human herpesvirus-8) binds ATF4/CREB2 and inhibits its transcriptional activation activity. *J Gen Virol* **81**: 2645-2652.

Longnecker, R., Druker, B., Roberts, T.M., and Kieff, E. (1991) An Epstein-Barr virus protein associated with cell growth transformation interacts with a tyrosine kinase. *J Virol* **65**: 3681-3692.

Longnecker, R. (2000) Epstein-Barr virus latency: LMP2, a regulator or means for Epstein-Barr virus persistence? *Adv Cancer Res* **79**: 175-200.

Lu, S., Day, N., Degos, L., Lepage, V., Wang, P., Chan, S., Simons, M., McKnight, B., Easton, D., Zeng, Y., and de-The, G. (1990) Linkage of nasopharyngeal carcinoma sussceptibility locus to the HLA regions. *Nature* **346**: 470-471.

Mabit, H., Nakano, M., Prank, U., Saam, B., Dohner, K., Sodeik, B., and Greber, U. (2002) Intact Microtubules Support Adenovirus and HErpes Simplex Virus Infection. *Journal of Virology* **76**: 9962-9971.

Macrae, A., Dutia, B., Milligan, S., Brownstein, D., Allen, D., Mistrikova, J., and Davison, A. (2001a) Anlysis of a novel strain of murine gammaherpesvirus reveals a genomic locus important for acute pathogenesis. *Journal of Virology* **75**: 5315-5327.

Macrae, A.I., Dutia, B.M., Milligan, S., Brownstein, D.G., Allen, D.J., Mistrikova, J., Davison, A.J., Nash, A.A., and Stewart, J.P. (2001b) Analysis of a novel strain of murine gammaherpesvirus reveals a genomic locus important for acute pathogenesis. *J Virol* **75**: 5315-5327.

Macrae, A.I. (2002) Studies on the contribution of the left unique region of the genome to Murine Gammaherpesviru-68 pathogenesis. In *Department of Veterinary Pathology* Edinburgh: University of Edinburgh, pp. 356.

Macrae, A.I., Usherwood, E.J., Husain, S.M., Flano, E., Kim, I.J., Woodland, D.L., Nash, A.A., Blackman, M.A., Sample, J.T., and Stewart, J.P. (2003) Murid herpesvirus 4 strain 68 M2 protein is a B-cell-associated antigen important for latency but not lymphocytosis. *J Virol* **77**: 9700-9709.

Macsween, K., and Crawford, D. (2003) Epstein-Barr virus- recent advances. *The LANCET Infectious Diseases* **3**: 131-140.

Mann, D.J., Child, E.S., Swanton, C., Laman, H., and Jones, N. (1999) Modulation of p27(Kip1) levels by the cyclin encoded by Kaposi's sarcoma-associated herpesvirus. *Embo J* **18**: 654-663.

Mannick, J.B., Cohen, J.I., Birkenbach, M., Marchini, A., and Kieff, E. (1991) The Epstein-Barr virus nuclear protein encoded by the leader of the EBNA RNAs is important in B-lymphocyte transformation. *J Virol* **65**: 6826-6837.

Lu, S., Day, N., Degos, L., Lepage, V., Wang, P., Chan, S., Simons, M., McKnight, B., Easton, D., Zeng, Y., and de-The, G. (1990) Linkage of nasopharyngeal carcinoma sussceptibility locus to the HLA regions. *Nature* **346**: 470-471.

Mabit, H., Nakano, M., Prank, U., Saam, B., Dohner, K., Sodeik, B., and Greber, U. (2002) Intact Microtubules Support Adenovirus and HErpes Simplex Virus Infection. *Journal of Virology* **76**: 9962-9971.

Macrae, A., Dutia, B., Milligan, S., Brownstein, D., Allen, D., Mistrikova, J., and Davison, A. (2001a) Anlysis of a novel strain of murine gammaherpesvirus reveals a genomic locus important for acute pathogenesis. *Journal of Virology* **75**: 5315-5327.

Macrae, A.I., Dutia, B.M., Milligan, S., Brownstein, D.G., Allen, D.J., Mistrikova, J., Davison, A.J., Nash, A.A., and Stewart, J.P. (2001b) Analysis of a novel strain of murine gammaherpesvirus reveals a genomic locus important for acute pathogenesis. *J Virol* **75**: 5315-5327.

Macrae, A.I. (2002) Studies on the contribution of the left unique region of the genome to Murine Gammaherpesviru-68 pathogenesis. In *Department of Veterinary Pathology* Edinburgh: University of Edinburgh, pp. 356.

Macrae, A.I., Usherwood, E.J., Husain, S.M., Flano, E., Kim, I.J., Woodland, D.L., Nash, A.A., Blackman, M.A., Sample, J.T., and Stewart, J.P. (2003) Murid herpesvirus 4 strain 68 M2 protein is a B-cell-associated antigen important for latency but not lymphocytosis. *J Virol* **77**: 9700-9709.

Macsween, K., and Crawford, D. (2003) Epstein-Barr virus- recent advances. *The LANCET Infectious Diseases* **3**: 131-140.

Mann, D.J., Child, E.S., Swanton, C., Laman, H., and Jones, N. (1999) Modulation of p27(Kip1) levels by the cyclin encoded by Kaposi's sarcoma-associated herpesvirus. *Embo J* **18**: 654-663.

Mannick, J.B., Cohen, J.I., Birkenbach, M., Marchini, A., and Kieff, E. (1991) The Epstein-Barr virus nuclear protein encoded by the leader of the EBNA RNAs is important in B-lymphocyte transformation. *J Virol* **65**: 6826-6837.

Martinez-Guzman, D., Rickabaugh, T., Wu, T.T., Brown, H., Cole, S., Song, M.J., Tong, L., and Sun, R. (2003) Transcription program of murine gammaherpesvirus 68. *J Virol* **77**: 10488-10503.

Mayama, S., Cuevas, L.E., Sheldon, J., Omar, O.H., Smith, D.H., Okong, P., Silvel, B., Hart, C.A., and Schulz, T.F. (1998) Prevalence and transmission of Kaposi's sarcoma-associated herpesvirus (human herpesvirus 8) in Ugandan children and adolescents. *Int J Cancer* **77**: 817-820.

McCaughan, G.W., Clark, M.J., and Barclay, A.N. (1987a) Characterization of the human homolog of the rat MRC OX-2 membrane glycoprotein. *Immunogenetics* **25**: 329-335.

McCaughan, G.W., Clark, M.J., Hurst, J., Grosveld, F., and Barclay, A.N. (1987b) The gene for MRC OX-2 membrane glycoprotein is localized on human chromosome 3. *Immunogenetics* **25**: 133-135.

McGeoch, D.J., and Davison, A.J. (1999) The descent of human herpesvirus 8. *Semin Cancer Biol* **9**: 201-209.

McMaster, W.R., and Williams, A.F. (1979) Identification of Ia glycoproteins in rat thymus and purification from rat spleen. *Eur J Immunol* **9**: 426-433.

Medveczky, M., Szomolanyi, E., Hesselton, R., DeGrand, D., Geck, P., and Medveczky, P. (1989) Herpesvirus saimiri strains from three DNA subgroups have different oncogenic potentials inthe New Zealand white rabbits. *Journal of Virology* **63**: 3601-3611.

Medveczky, P., Szomolanyi, E., Desrosiers, R.C., and Mulder, C. (1984) Classification of herpesvirus saimiri into three groups based on extreme variation in a DNA region required for oncogenicity. *J Virol* **52**: 938-944.

Mesri, E.A. (1999) Inflammatory reactivation and angiogenicity of Kaposi's sarcoma-associated herpesvirus/HHV8: a missing link in the pathogenesis of acquired immunodeficiency syndrome-associated Kaposi's sarcoma. *Blood* **93**: 4031-4033.

Miles, S.A., Rezai, A.R., Salazar-Gonzalez, J.F., Vander Meyden, M., Stevens, R.H., Logan, D.M., Mitsuyasu, R.T., Taga, T., Hirano, T., Kishimoto, T., and et al. (1990) AIDS

Kaposi sarcoma-derived cells produce and respond to interleukin 6. *Proc Natl Acad Sci U S A* **87**: 4068-4072.

Miller, G., Heston, L., Grogan, E., Gradoville, L., Rigsby, M., Sun, R., Shedd, D., Kushnaryov, V.M., Grossberg, S., and Chang, Y. (1997) Selective switch between latency and lytic replication of Kaposi's sarcoma herpesvirus and Epstein-Barr virus in dually infected body cavity lymphoma cells. *J Virol* **71**: 314-324.

Minson, A.C., Davison, A., Eberle, R., Desroisiers, R.C., Fleckenstein, B., McGeoch, D.J., Pellet, P.E., Roizman, B., and Studdert, M.J. (2000) Family Herpesviridae. In *Virus Taxonomy*. Wickner, R.B. (ed). San Diego: Academic Press, pp. 203 - 225.

Molden, J., Chang, Y., You, Y., Moore, P.S., and Goldsmith, M.A. (1997) A Kaposi's sarcoma-associated herpesvirus-encoded cytokine homolog (vIL-6) activates signaling through the shared gp130 receptor subunit. *J Biol Chem* **272**: 19625-19631.

Molesworth, S., Lake, C., Borza, C., Turk, S., and Hutt-Fletcher, L. (2000) Epstein-Barr virus gH is essential for penetration of B cells but also plays a role in attachment of virus to epithelial cells. *Journal of Virology* **74**: 6324-6332.

Montgomery, R., Warner, M., Lum, B., and Spear, P. (1996) Herpes Simplex Virus-1 Entry into Cells Mediated by Novel Member of the TNF/NGF Receptor Family. *Cell* **87**: 427-436.

Moore, A.Y., and Chang, A.C. (2001) Kaposi's Sarcoma-Associated Herpesvirus. In *Fields Virology*. Vol. 2. Straus, S.E. (ed): Lipincott Williams and Wilkins, pp. 2803-2833.

Moore, P.S., Kingsley, L.A., Holmberg, S.D., Spira, T., Gupta, P., Hoover, D.R., Parry, J.P., Conley, L.J., Jaffe, H.W., and Chang, Y. (1996) Kaposi's sarcoma-associated herpesvirus infection prior to onset of Kaposi's sarcoma. *Aids* **10**: 175-180.

Moorman, N.J., Willer, D.O., and Speck, S.H. (2003) The gammaherpesvirus 68 latency-associated nuclear antigen homolog is critical for the establishment of splenic latency. *J Virol* **77**: 10295-10303.

Moses, A.V., Fish, K.N., Ruhl, R., Smith, P.P., Strussenberg, J.G., Zhu, L., Chandran, B., and Nelson, J.A. (1999) Long-term infection and transformation of dermal microvascular endothelial cells by human herpesvirus 8. *J Virol* **73**: 6892-6902.

Mossman, K., Sherburne, R., Lavery, C., Duncan, J., and Smiley, J. (2000) Evidence the Herpes Simplex Virus VP16 is Required for Viral Egress Downstream of the Initial Envelopment Event. *Journal of Virology* **74**: 6287-6299.

Mueller, N., Evans, A., Harris, N., Comstock, G., Jellum, E., Magnus, K., Orentreich, N., Polk, B., and Vogelman, J. (1989) Hodgkin's disease and Epstein-Barr virus. Altered antibody pattern before diagnosis. *New England Journal of Medicine* **320**: 689-695.

Muralidhar, S., Pumfery, A.M., Hassani, M., Sadaie, M.R., Kishishita, M., Brady, J.N., Doniger, J., Medveczky, P., and Rosenthal, L.J. (1998) Identification of kaposin (open reading frame K12) as a human herpesvirus 8 (Kaposi's sarcoma-associated herpesvirus) transforming gene. *J Virol* **72**: 4980-4988.

Muralidhar, S., Veytsmann, G., Chandran, B., Ablashi, D., Doniger, J., and Rosenthal, L.J. (2000) Characterization of the human herpesvirus 8 (Kaposi's sarcoma-associated herpesvirus) oncogene, kaposin (ORF K12). *J Clin Virol* **16**: 203-213.

Murphy, P.M. (2001) Viral exploitation and subversion of the immune system through chemokine mimicry. *Nat Immunol* **2**: 116-122.

Nador, R.G., Cesarman, E., Chadburn, A., Dawson, D.B., Ansari, M.Q., Sald, J., and Knowles, D.M. (1996) Primary effusion lymphoma: a distinct clinicopathologic entity associated with the Kaposi's sarcoma-associated herpes virus. *Blood* **88**: 645-656.

Nakamura, H., Li, M., Zarycki, J., and Jung, J.U. (2001) Inhibition of p53 tumor suppressor by viral interferon regulatory factor. *J Virol* **75**: 7572-7582.

Nanbo, A., Inoue, K., Adachi-Takasawa, K., and Takada, K. (2002) Epstein-Barr virus RNA confers resistance to interferon-α-induced apoptosis in Burkitt's lymphoma. *The EMBO Journal* **21**: 954-965.

Nash, A.A., Dutia, B.M., Stewart, J.P., and Davison, A.J. (2001) Natural history of murine gamma-herpesvirus infection. *Philos Trans R Soc Lond B Biol Sci* **356**: 569-579.

Nathan, C., and Muller, W.A. (2001) Putting the brakes on innate immunity: a regulatory role for CD200? *Nat Immunol* **2**: 17-19.

Neipel, F., Albrecht, J.C., and Fleckenstein, B. (1998) Human herpesvirus 8--the first human Rhadinovirus. *J Natl Cancer Inst Monogr*: 73-77.

Nicholas, J., Ruvolo, V.R., Burns, W.H., Sandford, G., Wan, X., Ciufo, D., Hendrickson, S.B., Guo, H.G., Hayward, G.S., and Reitz, M.S. (1997) Kaposi's sarcoma-associated human herpesvirus-8 encodes homologues of macrophage inflammatory protein-1 and interleukin-6. *Nat Med* **3**: 287-292.

Nicholls, J., Agathanggelou, A., Fung, K., Xiangguo, Z., and Niedobitek, G. (1997) The association of squamous cell carcinomas of the nasopharynx with Epstein-Barr virus shows geographical variation reminiscent of Burkitt's lymphoma. *Journal of Pathology* **183**: 164-168.

Nickoloff, B.J., and Griffiths, C.E. (1989) The spindle-shaped cells in cutaneous Kaposi's sarcoma. Histologic simulators include factor XIIIa dermal dendrocytes. *Am J Pathol* **135**: 793-800.

Niedobitek, G., Agathanggelou, A., Herbst, H., Whitehead, L., Wright, D.H., and Young, L.S. (1997) Epstein-Barr virus (EBV) infection in infectious mononucleosis: virus latency, replication and phenotype of EBV-infected cells. *J Pathol* **182**: 151-159.

Niller, H., Salamon, D., Ilg, K., Koroknai, A., Banati, F., Bauml, G., Rucker, O., Schwarzmann, F., Wolf, H., and Minarovits, J. (2003) The in vivo binding site for oncoprotein c-Myc in the prooter for Epstein-Barr virus (EBV) encoding RNA (EBER) 1 suggests a specific role for EBV in lymphomagenesis. *Med Sci Monit* **9**: 1-9.

Ojala, P.M., Tiainen, M., Salven, P., Veikkola, T., Castanos-Velez, E., Sarid, R., Biberfeld, P., and Makela, T.P. (1999) Kaposi's sarcoma-associated herpesvirus-encoded v-cyclin triggers apoptosis in cells with high levels of cyclin-dependent kinase 6. *Cancer Res* **59**: 4984-4989.

Ojala, P.M., Yamamoto, K., Castanos-Velez, E., Biberfeld, P., Korsmeyer, S.J., and Makela, T.P. (2000) The apoptotic v-cyclin-CDK6 complex phosphorylates and inactivates Bcl-2. *Nat Cell Biol* **2**: 819-825.

Osborne, J., Moore, P.S., and Chang, Y. (1999) KSHV-encoded viral IL-6 activates multiple human IL-6 signaling pathways. *Hum Immunol* **60**: 921-927.

Parker, B., Bankier, A., Satchwell, S., Barrell, B., and Farrell, P. (1990) Sequence and transcription of Raji Epstein-Barr virus DNA spanning the B95-8 deletion region. *Virology* **179**: 339-346.

Parravicini, C., Chandran, B., Corbellino, M., Berti, E., Paulli, M., Moore, P.S., and Chang, Y. (2000) Differential viral protein expression in Kaposi's sarcoma-associated herpesvirus-infected diseases: Kaposi's sarcoma, primary effusion lymphoma, and multicentric Castleman's disease. *Am J Pathol* **156**: 743-749.

Parry, C.M., Simas, J.P., Smith, V.P., Stewart, C.A., Minson, A.C., Efstathiou, S., and Alcami, A. (2000) A broad spectrum secreted chemokine binding protein encoded by a herpesvirus. *J Exp Med* **191**: 573-578.

Pauk, J., Huang, M.L., Brodie, S.J., Wald, A., Koelle, D.M., Schacker, T., Celum, C., Selke, S., and Corey, L. (2000) Mucosal shedding of human herpesvirus 8 in men. *N Engl J Med* **343**: 1369-1377.

Paulose-Murphy, M., Ha, N.K., Xiang, C., Chen, Y., Gillim, L., Yarchoan, R., Meltzer, P., Bittner, M., Trent, J., and Zeichner, S. (2001) Transcription program of human herpesvirus 8 (kaposi's sarcoma- associated herpesvirus). *J Virol* **75**: 4843-4853.

Peng, W., Henderson, G., Perng, G., Nesburn, A., Wechsler, S., and Jones, C. (2003) The Gene that Encodes the Herpes Simplex Virus Type 1 Latency-Associated Transcript Influences the Accumulation of Transcripts (Bcl-x_L and Bcl-x_s) that Encode Apoptotic Regulatory Proteins. *Journal of Virology* **77**: 10714-10718.

Penn, I., and Porat, G. (1995) Central nervous system lymphomas in organ allograft recipients. *Transplantation* **59**: 240-244.

Pertel, P.E. (2002) Human herpesvirus 8 glycoprotein B (gB), gH, and gL can mediate cell fusion. *J Virol* **76**: 4390-4400.

Piolot, T., Tramier, M., Coppey, M., Nicolas, J.C., and Marechal, V. (2001) Close but distinct regions of human herpesvirus 8 latency-associated nuclear antigen 1 are responsible for nuclear targeting and binding to human mitotic chromosomes. *J Virol* **75**: 3948-3959.

Platt, G.M., Simpson, G.R., Mittnacht, S., and Schulz, T.F. (1999) Latent nuclear antigen of Kaposi's sarcoma-associated herpesvirus interacts with RING3, a homolog of the Drosophila female sterile homeotic (fsh) gene. *J Virol* **73**: 9789-9795.

Ploegh, H., and Watts, C. (1998) Antigen recognition. *Curr Opin Immunol* **10**: 57-58.

Poole, L.J., Zong, J.C., Ciufo, D.M., Alcendor, D.J., Cannon, J.S., Ambinder, R., Orenstein, J.M., Reitz, M.S., and Hayward, G.S. (1999) Comparison of genetic variability at multiple loci across the genomes of the major subtypes of Kaposi's sarcoma-associated herpesvirus reveals evidence for recombination and for two distinct types of open reading frame K15 alleles at the right-hand end. *J Virol* **73**: 6646-6660.

Preston, S., Wright, G.J., Starr, K., Barclay, A.N., and Brown, M.H. (1997) The leukocyte/neuron cell surface antigen OX2 binds to a ligand on macrophages. *Eur J Immunol* **27**: 1911-1918.

Radkov, S.A., Kellam, P., and Boshoff, C. (2000) The latent nuclear antigen of Kaposi sarcoma-associated herpesvirus targets the retinoblastoma-E2F pathway and with the oncogene Hras transforms primary rat cells. *Nat Med* **6**: 1121-1127.

Ragoczy, T., Heston, L., and Miller, G. (1998) The Epstein-Barr Virus Rta Protein Activted Lytic Cycle Genes and Can Disrupt Latency in B lymphocytes. *Journal of Virology* **72**: 7978-7984.

Renne, R., Blackbourn, D., Whitby, D., Levy, J., and Ganem, D. (1998) Limited transmission of Kaposi's sarcoma-associated herpesvirus in cultured cells. *J Virol* **72**: 5182-5188.

Rickinson, A., and Kieff, E. (2001) Epstein-Barr Virus. In *Fields Virology*. Vol. 2. Straus, S.E. (ed): Lipincott Williams and Wilkins, pp. 2575-2627.

Roizman, B., and Knipe, D.M. (2001) Herpes simplex viruses and their replication. In *Fields Virology*. Vol. 2. Straus, S.E. (ed): Lipincott Williams and Wilkins, pp. 2399-2459.

Roizman, B., and Pellett, P.E. (2001) The Family *Herpesviridae*: A Brief Introduction. In *Fields Virology*. Vol. 2. Straus, S.E. (ed): Lippincott Williams & Wilkins, pp. 2381 - 2397.

Rooney, C., Smith, C., Ng, C., Loftin, S., Sixbey, J., Gan, Y., Srivastava, D., Bowman, L., Krance, R., Brenner, M., and Heslop, H. (1998) Infusion of cytotoxic T cells for the prevention and treatment of Epstein-Barr virus-induced lymphoma in allogeneic transplant recipients. *Blood* **92**: 1549-1555.

Roskrow, M., Suzuki, N., Gan, Y., Sixbey, J., Ng, C., Kimbrough, S., Hudson, M., Brenner, M., Heslop, H., and Rooney, C. (1998) Epstein-Barr Virus (EBV)-specific cytotoxic T lymphocytes for the treatment of patients with EBV-positive relapsed Hodgkin's disease. *Blood* **91**: 2925-2934.

Roy, D.J., Ebrahimi, B.C., Dutia, B.M., Nash, A.A., and Stewart, J.P. (2000) Murine gammaherpesvirus M11 gene product inhibits apoptosis and is expressed during virus persistence. *Arch Virol* **145**: 2411-2420.

Russo, J.J., Bohenzky, R.A., Chien, M.C., Chen, J., Yan, M., Maddalena, D., Parry, J.P., Peruzzi, D., Edelman, I.S., Chang, Y., and Moore, P.S. (1996) Nucleotide sequence of the Kaposi sarcoma-associated herpesvirus (HHV8). *Proc Natl Acad Sci U S A* **93**: 14862-14867.

Sadler, R., Wu, L., Forghani, B., Renne, R., Zhong, W., Herndier, B., and Ganem, D. (1999) A complex translational program generates multiple novel proteins from the latently expressed kaposin (K12) locus of Kaposi's sarcoma-associated herpesvirus. *J Virol* **73**: 5722-5730.

Sarid, R., Sato, T., Bohenzky, R.A., Russo, J.J., and Chang, Y. (1997) Kaposi's sarcoma-associated herpesvirus encodes a functional bcl-2 homologue. *Nat Med* **3**: 293-298.

Sarid, R., Flore, O., Bohenzky, R.A., Chang, Y., and Moore, P.S. (1998) Transcription mapping of the Kaposi's sarcoma-associated herpesvirus (human herpesvirus 8) genome in a body cavity-based lymphoma cell line (BC-1). *J Virol* **72**: 1005-1012.

Sarid, R., Wiezorek, J.S., Moore, P.S., and Chang, Y. (1999) Characterization and cell cycle regulation of the major Kaposi's sarcoma-associated herpesvirus (human herpesvirus 8) latent genes and their promoter. *J Virol* **73**: 1438-1446.

Schafer, A., Lengenfelder, D., Grillhosl, C., Wieser, C., Fleckenstein, B., and Ensser, A. (2003) The latency-associated nuclear antigen homolog of Herpesvirus saimiri inhibits lytic virus replication. *Journal of Virology* **77**: 5911-5925.

Scholle, F., Longnecker, R., and Raab-Traub, N. (1999) Epithelial cell adhesion to extracellular matrix proteins induces tyrosine phosphorylation of the Epstein-Barr virus latent membrane protein 2: a role for C-terminal Src kinase. *J Virol* **73**: 4767-4775.

Schulz, T.F. (1998) Kaposi's sarcoma-associated herpesvirus (human herpesvirus-8). *J Gen Virol* **79 (Pt 7)**: 1573-1591.

Searles, R.P., Bergquam, E.P., Axthelm, M.K., and Wong, S.W. (1999) Sequence and genomic analysis of a Rhesus macaque rhadinovirus with similarity to Kaposi's sarcoma-associated herpesvirus/human herpesvirus 8. *J Virol* **73**: 3040-3053.

Secor, V.H., Secor, W.E., Gutekunst, C.A., and Brown, M.A. (2000) Mast cells are essential for early onset and severe disease in a murine model of multiple sclerosis. *J Exp Med* **191**: 813-822.

Selvarajah, S. (2001) Early events following Murine Gammaherpesvirus (MHV-68) infection. In *Department of Veterinary Pathology* Edinburgh: University of Edinburgh, pp. 135.

Seo, T., Lee, D., Lee, B., Chung, J.H., and Choe, J. (2000) Viral interferon regulatory factor 1 of Kaposi's sarcoma-associated herpesvirus (human herpesvirus 8) binds to, and inhibits transactivation of, CREB-binding protein. *Biochem Biophys Res Commun* **270**: 23-27.

Seo, T., Park, J., Lee, D., Hwang, S.G., and Choe, J. (2001) Viral interferon regulatory factor 1 of Kaposi's sarcoma-associated herpesvirus binds to p53 and represses p53-dependent transcription and apoptosis. *J Virol* **75**: 6193-6198.

Shapiro, I.M., Volsky, D.J., Saemundsen, A.K., Anisimova, E., and Klein, G. (1982) Infection of the human T-cell-derived leukemia line Molt-4 by Epstein-Barr virus (EBV): induction of EBV-determined antigens and virus reproduction. *Virology* **120**: 171-181.

Sharp, T.V., Wang, H.W., Koumi, A., Hollyman, D., Endo, Y., Ye, H., Du, M.Q., and Boshoff, C. (2002) K15 protein of Kaposi's sarcoma-associated herpesvirus is latently expressed and binds to HAX-1, a protein with antiapoptotic function. *J Virol* **76**: 802-816.

Shieh, M.T., WuDunn, D., Montgomery, R.I., Esko, J.D., and Spear, P.G. (1992) Cell surface receptors for herpes simplex virus are heparan sulfate proteoglycans. *J Cell Biol* **116**: 1273-1281.

Simas, J.P., and Efstathiou, S. (1998) Murine gammaherpesvirus 68: a model for the study of gammaherpesvirus pathogenesis. *Trends Microbiol* **6**: 276-282.

Sirianni, M.C., Vincenzi, L., Fiorelli, V., Topino, S., Scala, E., Uccini, S., Angeloni, A., Faggioni, A., Cerimele, D., Cottoni, F., Aiuti, F., and Ensoli, B. (1998) gamma-Interferon production in peripheral blood mononuclear cells and tumor infiltrating lymphocytes from Kaposi's sarcoma patients: correlation with the presence of human herpesvirus-8 in peripheral blood mononuclear cells and lesional macrophages. *Blood* **91**: 968-976.

Sitas, F., Carrara, H., Beral, V., Newton, R., Reeves, G., Bull, D., Jentsch, U., Pacella-Norman, R., Bourboulia, D., Whitby, D., Boshoff, C., and Weiss, R. (1999) Antibodies against human herpesvirus 8 in black South African patients with cancer. *N Engl J Med* **340**: 1863-1871.

Skepper, J., Whiteley, A., Browne, H., and Minson, A. (2001) Herpes Simplex Virus Nucleocapsids Mature to Progeny Virions by an Envelopment -> Deenvelopment -> Renevelopment Pathway. *Journal of Virology* **75**: 5697-5702.

Smith, P., Coletta, P., Markham, A., and Whitehouse, A. (2001) In vivo episomal maintenance of a herpesvirus saimiri-based gene delivery vector. *Gene Therapy* **8**: 1762-1769.

Soulier, J., Grollet, L., Oksenhendler, E., Cacoub, P., Cazals-Hatem, D., Babinet, P., d'Agay, M.F., Clauvel, J.P., Raphael, M., Degos, L., and et al. (1995) Kaposi's sarcoma-associated herpesvirus-like DNA sequences in multicentric Castleman's disease. *Blood* **86**: 1276-1280.

Staskus, K.A., Zhong, W., Gebhard, K., Herndier, B., Wang, H., Renne, R., Beneke, J., Pudney, J., Anderson, D.J., Ganem, D., and Haase, A.T. (1997) Kaposi's sarcoma-associated herpesvirus gene expression in endothelial (spindle) tumor cells. *J Virol* **71**: 715-719.

Staskus, K.A., Sun, R., Miller, G., Racz, P., Jaslowski, A., Metroka, C., Brett-Smith, H., and Haase, A.T. (1999) Cellular tropism and viral interleukin-6 expression distinguish human herpesvirus 8 involvement in Kaposi's sarcoma, primary effusion lymphoma, and multicentric Castleman's disease. *J Virol* **73**: 4181-4187.

Stevenson, A., Frolova-Jones, E., Hall, K., Kingsey, S., Markham, A., Whitehouse, A., and Meredith, D. (2000) A herpevirus saimir-bases gene therapy vector with potential for use in cancer immunotherapy. *Cancer Gene Therapy* **7**: 1077-1085.

Stewart, J.P., Janjua, N.J., Pepper, S.D., Bennion, G., Mackett, M., Allen, T., Nash, A.A., and Arrand, J.R. (1996) Identification and characterization of murine gammaherpesvirus 68 gp150: a virion membrane glycoprotein. *J Virol* **70**: 3528-3535.

Stewart, J.P., Usherwood, E.J., Ross, A., Dyson, H., and Nash, T. (1998) Lung epithelial cells are a major site of murine gammaherpesvirus persistence. *J Exp Med* **187**: 1941-1951.

Sturzl, M., Brandstetter, H., and Roth, W.K. (1992) Kaposi's sarcoma: a review of gene expression and ultrastructure of KS spindle cells in vivo. *AIDS Res Hum Retroviruses* **8**: 1753-1763.

Sturzl, M., Blasig, C., Schreier, A., Neipel, F., Hohenadl, C., Cornali, E., Ascherl, G., Esser, S., Brockmeyer, N.H., Ekman, M., Kaaya, E.E., Tschachler, E., and Biberfeld, P. (1997) Expression of HHV-8 latency-associated T0.7 RNA in spindle cells and endothelial cells of AIDS-associated, classical and African Kaposi's sarcoma. *Int J Cancer* **72**: 68-71.

Sturzl, M., Hohenadl, C., Zietz, C., Castanos-Velez, E., Wunderlich, A., Ascherl, G., Biberfeld, P., Monini, P., Browning, P.J., and Ensoli, B. (1999a) Expression of K13/v-FLIP gene of human herpesvirus 8 and apoptosis in Kaposi's sarcoma spindle cells. *J Natl Cancer Inst* **91**: 1725-1733.

Sturzl, M., Wunderlich, A., Ascherl, G., Hohenadl, C., Monini, P., Zietz, C., Browning, P.J., Neipel, F., Biberfeld, P., and Ensoli, B. (1999b) Human herpesvirus-8 (HHV-8) gene expression in Kaposi's sarcoma (KS) primary lesions: an in situ hybridization study. *Leukemia* **13 Suppl 1**: S110-112.

Su , Z., Peluso, M., Raffegerst, S., Schendel, D., and Roskrow, M. (2001) The generation of LMP2a-specific cytotoxic T lymphocytes for the treatment of patients with Epstein-Barr virus-positive Hodgkin disease. *European Journal of Immunology* **31**: 947-958.

Sugden, B., Phelps, M., and Domoradzki, J. (1979) Epstein-Barr virus DNA is amplified in transformed lymphocytes. *Journal of Virology* **31**: 590-595.

Sun, R., Lin, S.F., Staskus, K., Gradoville, L., Grogan, E., Haase, A., and Miller, G. (1999) Kinetics of Kaposi's sarcoma-associated herpesvirus gene expression. *J Virol* **73**: 2232-2242.

Sunil-Chandra, N.P., Efstathiou, S., Arno, J., and Nash, A.A. (1992) Virological and pathological features of mice infected with murine gamma-herpesvirus 68. *J Gen Virol* **73**: 2347-2356.

Sunil-Chandra, N.P., Arno, J., Fazakerley, J., and Nash, A.A. (1994) Lymphoproliferative disease in mice infected with murine gammaherpesvirus 68. *Am J Pathol* **145**: 818-826.

Swanton, C., Mann, D.J., Fleckenstein, B., Neipel, F., Peters, G., and Jones, N. (1997) Herpes viral cyclin/Cdk6 complexes evade inhibition by CDK inhibitor proteins. *Nature* **390**: 184-187.

Talbot, S., and Whitby, D. (1999) Kaposi's sarcoma and Human Herpesvirus-8. In *HIV and the New Viruses*. Weiss, A. and Dalgliesh, A. (eds): Academic Press, England, pp. 359-384.

Talbot, S.J., Weiss, R.A., Kellam, P., and Boshoff, C. (1999) Transcriptional analysis of human herpesvirus-8 open reading frames 71, 72, 73, K14, and 74 in a primary effusion lymphoma cell line. *Virology* **257**: 84-94.

Tanner, J.E., and Alfieri, C. (2001) The Epstein-Barr virus and post-transplant lymphoproliferative disease: interplay of immunosuppression, EBV, and the immune system in disease pathogenesis. *Transpl Infect Dis* **3**: 60-69.

Thomas, J., Hotchin, N., Allday, M., Amlot, P., Rose, M., Yacoub, M., and Crawford, D. (1990) Immunohistology of Epstein-Barr virus-associted antigens in B cell disorders from immunocomprised individuals. *Transplantation* **49**: 944-953.

Thomas, R.K., Re, D., Wolf, J., and Diehl, V. (2004) Part I: Hodgkin's lymphoma--molecular biology of Hodgkin and Reed-Sternberg cells. *Lancet Oncol* **5**: 11-18.

Thomkinson, B., and Kieff, E. (1992) Use of Second-site homologous recombination to demonstrate that Epstein-Barr virus nuclear protein 3B is not important for lymphocyte infection or growth transformation in vitro. *Journal of Virology* **66**: 2893-2903.

Thorley-Lawson, D.A., and Babcock, G.J. (1999) A model for persistent infection with Epstein-Barr virus: The stealth virus of human B cells. *Life Sciences* **65**: 1433-1453.

Thornberry, N.A., and Lazebnik, Y. (1998) Caspases: enemies within. *Science* **281**: 1312-1316.

Tierney, R.J., Steven, N., Young, L.S., and Rickinson, A.B. (1994) Epstein-Barr virus latency in blood mononuclear cells: analysis of viral gene transcription during primary infection and in the carrier state. *J Virol* **68**: 7374-7385.

Tomescu, C., Law, W.K., and Kedes, D.H. (2003) Surface downregulation of major histocompatibility complex class I, PE-CAM, and ICAM-1 following de novo infection of endothelial cells with Kaposi's sarcoma-associated herpesvirus. *J Virol* **77**: 9669-9684.

Townsley, A.C., Dutia, B.M., and Nash, A.A. (2004) The m4 gene of murine gammaherpesvirus modulates productive and latent infection in vivo. *J Virol* **78**: 758-767.

Tulman, E.R., Afonso, C.L., Lu, Z., Zsak, L., Kutish, G.F., and Rock, D.L. (2001) Genome of lumpy skin disease virus. *J Virol* **75**: 7122-7130.

Usherwood, E.J., Ross, A.J., Allen, D.J., and Nash, A.A. (1996) Murine gammaherpesvirus-induced splenomegaly: a critical role for CD4 T cells. *J Gen Virol* **77**: 627-630.

van der Merwe, P.A., McPherson, D.C., Brown, M.H., Barclay, A.N., Cyster, J.G., Williams, A.F., and Davis, S.J. (1993) The NH2-terminal domain of rat CD2 binds rat CD48 with a low affinity and binding does not require glycosylation of CD2. *Eur J Immunol* **23**: 1373-1377.

Verbeke, C., Wenthe, U., Bergler, W., and Zentgraf, H. (2000) Characterization of the expanded T cell population ininfectious mononucleosis: apoptosis, expression of apoptosis-related genes, and Epstein-Barr virus (EBV) status. *Clinical Experimental Immunology* **120**: 294-300.

Verma, S.C., and Robertson, E.S. (2003) ORF73 of herpesvirus Saimiri strain C488 tethers the viral genome to metaphase chromosomes and binds to cis-acting DNA sequences in the terminal repeats. *J Virol* **77**: 12494-12506.

Veronese, M., Veronesi, A., D'Andrea, E., Del Mistro, A., Indraccolo, S., Mazza, M., Mion, M., Zamarchi, R., Menin, C., and Panozzo, M. (1992) Lympoproliferative disease in human peripheral blood mononuclear cell-injected SCID mice. I.T lymphocyte requirement for B cell tumor generation. *Journal of Experimental Medicine* **176**: 1763-1667.

Verzijl, D., Fitzsimons, C.P., Van Dijk, M., Stewart, J.P., Timmerman, H., Smit, M.J., and Leurs, R. (2004) Differential activation of murine herpesvirus 68- and Kaposi's sarcoma-associated herpesvirus-encoded ORF74 G protein-coupled receptors by human and murine chemokines. *J Virol* **78**: 3343-3351.

Vieira, J., Huang, M.L., Koelle, D.M., and Corey, L. (1997) Transmissible Kaposi's sarcoma-associated herpesvirus (human herpesvirus 8) in saliva of men with a history of Kaposi's sarcoma. *J Virol* **71**: 7083-7087.

Vieites, J.M., de la Torre, R., Ortega, M.A., Montero, T., Peco, J.M., Sanchez-Pozo, A., Gil, A., and Suarez, A. (2003) Characterization of human cd200 glycoprotein receptor gene located on chromosome 3q12-13. *Gene* **311**: 99-104.

Viejo-Borbolla, A., Kati, E., Sheldon, J.A., Nathan, K., Mattsson, K., Szekely, L., and Schulz, T.F. (2003) A Domain in the C-terminal region of latency-associated nuclear antigen 1 of Kaposi's sarcoma-associated Herpesvirus affects transcriptional activation and binding to nuclear heterochromatin. *J Virol* **77**: 7093-7100.

Virgin, H.W.t., Latreille, P., Wamsley, P., Hallsworth, K., Weck, K.E., Dal Canto, A.J., and Speck, S.H. (1997) Complete sequence and genomic analysis of murine gammaherpesvirus 68. *J Virol* **71**: 5894-5904.

Wang, D., Liebowitz, K., and Kieff, E. (1985) An EBV membrane protein expressed in immortalized lymphocytes transforms established roden cells. *Cell* **43**: 831-840.

Wang, D., Liebowitz, D., Wang, F., Gregory, C., Rickinson, A., Larson, R., Springer, T., and Kieff, E. (1988) Epstein-Barr virus latent infection membrane protein alters the human B- lymphocyte phenotype: deletion of the amino terminus abolishes activity. *J Virol* **62**: 4173-4184.

Wang, F.Z., Akula, S.M., Pramod, N.P., Zeng, L., and Chandran, B. (2001) Human herpesvirus 8 envelope glycoprotein K8.1A interaction with the target cells involves heparan sulfate. *J Virol* **75**: 7517-7527.

Wang, F.Z., Akula, S.M., Sharma-Walia, N., Zeng, L., and Chandran, B. (2003) Human herpesvirus 8 envelope glycoprotein B mediates cell adhesion via its RGD sequence. *J Virol* 77: 3131-3147.

Wang, X., Kenyon, W., Li, Q., Mullberg, J., and Hutt-Fletcher, L. (1998a) Epstein-Barr virus uses different complexes of glycoproteins gH and gL to infect B lymphocytes and epithelial cells. *Journal of Virology* **72**: 5552-5558.

Wang, X., Kenyon, W.J., Li, Q., Mullberg, J., and Hutt-Fletcher, L.M. (1998b) Epstein-Barr virus uses different complexes of glycoproteins gH and gL to infect B lymphocytes and epithelial cells. *J Virol* **72**: 5552-5558.

Wang, X.P., and Gao, S.J. (2003) Auto-activation of the transforming viral interferon regulatory factor encoded by Kaposi's sarcoma-associated herpesvirus (human herpesvirus-8). *J Gen Virol* **84**: 329-336.

Webb, M., and Barclay, A.N. (1984) Localisation of the MRC OX-2 glycoprotein on the surfaces of neurones. *J Neurochem* **43**: 1061-1067.

Weinberg, J.B., Lutzke, M.L., Alfinito, R., and Rochford, R. (2004) Mouse strain differences in the chemokine response to acute lung infection with a murine gammaherpesvirus. *Viral Immunol* **17**: 69-77.

Whiteley, A., Bruun, B., Minson, T., and Browne, H. (1999) Effects of Targeting Herpes Simplex Virus Type 1 gD to the Endoplasmic Reticulum and *trans*-Golgi Network. *Journal of Virology* **73**: 9515-9520.

Whitley, R. (2001) Herpes Simplex Viruses. In *Fields Virology*. Vol. 2. Straus, S.E. (ed): Lipincott Williams and Wilkins, pp. 2461-.

Willer, D.O., McFadden, G., and Evans, D.H. (1999) The complete genome sequence of shope (rabbit) fibroma virus. *Virology* **264**: 319-343.

Woisetschlaeger, M., Jin, X.W., Yandava, C.N., Furmanski, L.A., Strominger, J.L., and Speck, S.H. (1991) Role for the Epstein-Barr virus nuclear antigen 2 in viral promoter switching during initial stages of infection. *Proc Natl Acad Sci U S A* **88**: 3942-3946.

Wright, G.J., Puklavec, M.J., Willis, A.C., Hoek, R.M., Sedgwick, J.D., Brown, M.H., and Barclay, A.N. (2000) Lymphoid/neuronal cell surface OX2 glycoprotein recognizes a novel receptor on macrophages implicated in the control of their function. *Immunity* **13**: 233-242.

Wright, G.J., Jones, M., Puklavec, M.J., Brown, M.H., and Barclay, A.N. (2001) The unusual distribution of the neuronal/lymphoid cell surface CD200 (OX2) glycoprotein is conserved in humans. *Immunology* **102**: 173-179.

Wright, G.J., Cherwinski, H., Foster-Cuevas, M., Brooke, G., Puklavec, M.J., Bigler, M., Song, Y., Jenmalm, M., Gorman, D., McClanahan, T., Liu, M.R., Brown, M.H., Sedgwick, J.D., Phillips, J.H., and Barclay, A.N. (2003) Characterization of the CD200 receptor family in mice and humans and their interactions with CD200. *J Immunol* **171**: 3034-3046.

Wu, F.Y., Ahn, J.H., Alcendor, D.J., Jang, W.J., Xiao, J., Hayward, S.D., and Hayward, G.S. (2001a) Origin-independent assembly of Kaposi's sarcoma-associated herpesvirus DNA replication compartments in transient cotransfection assays and association with the ORF-K8 protein and cellular PML. *J Virol* **75**: 1487-1506.

Wu, T.T., Tong, L., Rickabaugh, T., Speck, S., and Sun, R. (2001b) Function of Rta is essential for lytic replication of murine gammaherpesvirus 68. *J Virol* **75**: 9262-9273.

Wysocka, J., and Herr, W. (2003) The Herpes Simplex Virus VP16-induced complex: The makings of a regulatory switch. *Trends in Biochemical Sciences* **28**.

Yoshizaki, K., Matsuda, T., Nishimoto, N., Kuritani, T., Taeho, L., Aozasa, K., Nakahata, T., Kawai, H., Tagoh, H., Komori, T., and et al. (1989) Pathogenic significance of interleukin-6 (IL-6/BSF-2) in Castleman's disease. *Blood* **74**: 1360-1367.

Zietz, C., Bogner, J.R., Goebel, F.D., and Lohrs, U. (1999) An unusual cluster of cases of Castleman's disease during highly active antiretroviral therapy for AIDS. *N Engl J Med* **340**: 1923-1924.

Zimring, J.C., Goodbourn, S., and Offermann, M.K. (1998) Human herpesvirus 8 encodes an interferon regulatory factor (IRF) homolog that represses IRF-1-mediated transcription. *J Virol* **72**: 701-707.

Zong, J.C., Ciufo, D.M., Alcendor, D.J., Wan, X., Nicholas, J., Browning, P.J., Rady, P.L., Tyring, S.K., Orenstein, J.M., Rabkin, C.S., Su, I.J., Powell, K.F., Croxson, M., Foreman, K.E., Nickoloff, B.J., Alkan, S., and Hayward, G.S. (1999) High-level variability in the ORF-K1 membrane protein gene at the left end of the Kaposi's sarcoma-associated herpesvirus genome defines four major virus subtypes and multiple variants or clades in different human populations. *J Virol* **73**: 4156-4170.

Zou, X., Lu, S., and Liu, B. (1994) Volatile N-nitrosamines and their precursors in Chinese salted fish - possible etological factor for NPC in china. *International Journal of Cancer* **59**: 155-158.